Theses and Dissertations

2017

The Role of Additive and Solvent Coordination in Sm(II) Reactions

Tesia Valeska Chciuk
Lehigh University

Follow this and additional works at: http://preserve.lehigh.edu/etd

Part of the Chemistry Commons

The Role of Additive and Solvent Coordination in Sm(II) Reactions

by

Tesia V. Chciuk

A Dissertation

Presented to the Graduate and Research Committee

of Lehigh University

in Candidacy for the Degree of

Doctor of Philosophy

in

Department of Chemistry

Lehigh University

May 22, 2017

Approved and recommended for acceptance as a dissertation in partial fulfillment of the requirements for the degree of Doctor of Philosophy

Tesia V. Chciuk

The Role of Additive and Solvent Coordination in Sm(II) Reactions

_____

Defense Date

                                        _____

                                        Dr. Robert A. Flowers, II
                                        Dissertation Director

_____

Approved Date

                                        Committee Members:

                                        _____

                                        Dr. Marcos Pires

                                        _____

                                        Dr. Mark Chen

                                        _____

                                        Dr. Stefanie Sharp-Goldman
                                        Outside Committee Member

ACKNOWLEDGMENTS

I'd also like to thank the Pamphilis family for welcoming me in and providing warmth, laughter, and support that I've never experienced before and will never forget.

Of course, I also have to convey my appreciation to the close friends that helped me retain my sanity over the last five years: Michelle Shortell, Tareva Byrd, and Quinn Casey. Thanks for all the laughter, good times, and for listening to me complain about pretty much everything over drinks.

We are nothing without the people that believe in us.

Table of Contents

Chapter 7. Solvent-Dependent Substrate Reduction by {Sm[N(SiMe$_3$)$_2$]$_2$(THF)$_2$}:

Elucidating the Role of Solvent Coordination in Sm(II) Chemistry

LIST OF FIGURES

LIST OF TABLES

LIST OF SCHEMES

List of Abbreviations

Cyclic Voltammetry	CV
Tetrahydrofuran	THF
Acetonitrile	MeCN
Dichloromethane	DCM
Tetra-n-butyl ammonium fluoride	TBAF
Equivalents	equiv
Ethyl acetate	EtOAc
Hexamethylphosphoramide	HMPA
Deuterium oxide	D_2O
Nuclear Magnetic Resonance	NMR
Gas Chromatograph	GC
Mass spectrometer	MS
Ethylene glycol	EG
Isothermal Titration Calorimetry	ITC
Bond Dissociation Free Energy	BDFE
Natural Population Analysis	NPA
Proton Coupled Electron Transfer	PCET

ABSTRACT

The tunable reactivity of Sm(II) has fascinated chemists over the last few decades and has led to a plethora of Sm(II)-based reagent combinations. Although many mechanistic studies have been performed to date, a complete understanding of the principles governing the interaction of Sm(II) with solvent, additive, and substrate has remained evasive. The series of mechanistic studies described in this dissertation were aimed to isolate and observe the role of each individual reaction component. The impact of solvent on the reactivity of Sm(II) was examined by measuring the rate of reduction of a series of substrates in both coordinating and noncoordinating solvents using the highly soluble reductant $\{Sm[N(SiMe_3)_2]_2(THF)_2\}$. When SmI_2 is combined with a proton source, such as water or ethylene glycol, the reagent combination is capable of reducing substrates well outside the reducing power of SmI_2. Until recently, it was proposed that these reactions took place through sequential electron-proton transfer, but recent mechanistic studies have demonstrated that many of these reductions occur through a concerted process of proton-coupled electron-transfer (PCET). Through PCET, high-energy intermediates are bypassed, enabling highly endergonic reactions to proceed. Mechanistic studies were performed to examine the reduction of both coordinating and non-coordinating substrates as well as reductive cyclizations using the SmI_2-H_2O reagent combination and its ability to promote formal hydrogen atom transfer. Then, the use of alternative proton donors was employed to further elucidate the mechanism behind the unique reactivity of H_2O. Finally, using the information gathered from the previous

studies, new reagent combinations have been realized. Ideally, these studies will provide an even more useful reagent for the synthesis of complex organic molecules and contribute to a more complete understanding of the reactivity of low valent metals.

Chapter 1. Introduction to Samarium Chemistry

1.1 Physical Properties Governing the Reactivity of Samarium

Research on the reactivity of samarium (Sm), a rare earth element, has only been underway for about a hundred and fifty years. Although it was first isolated in 1879 by De Boisbaudran and was named for the mineral from which it was obtained, samarskite, it received little attention from the synthetic organic community until work by Henri Kagan.[1] The seminal work of Kagan showed that divalent samarium could be prepared and readily undergoes single electron transfer to transition from the +2 to +3 oxidation state. Since this pioneering work, the reactivity of Sm(II)-complexes has been the subject of many publications and has been applied to many challenging syntheses.

The coordination chemistry of lanthanides is strongly influenced by several important characteristics that differ from transition and main group metals. Lanthanides are considered hard Lewis acids and thus show a strong affinity for hard bases such as H_2O.[2] This Lewis acidity makes samarium highly oxophilic. Additionally, because the valence electrons reside in the 4f orbitals and penetrate the xenon core, they do not overlap with ligand orbitals and thus ligand interactions are governed primarily by steric and electrostatic effects.[3]

Another rationale for the unique chemistry displayed by samarium and other *f*-block elements is a result of the lanthanide contraction, an effective reduction in the Ln^{+3} radii with increasing atomic number. This is a result of poor screening of the nucleus by the f electrons, which results in an increase in the effective nuclear charge and leads to contraction of the atomic radius.[2] In the case of samarium, the divalent cation is

significantly larger than the trivalent cation, and as a result, the coordination sphere of divalent samarium is larger.

1.2 Introduction to Divalent Samarium as a Synthetic Reagent

Employed as a strong single-electron reductant, Sm(II) has been applied to a wide range of reductions and bond-forming reactions over the past 35 years. The most widely-used Sm(II)-based reagent is samarium diiodide (SmI_2). It is generally prepared in one step by combination of elemental samarium metal and iodine at room temperature in THF providing a 0.1 M solution. Since Kagan introduced samarium diiodide to chemists in 1980, it has attained an importance reserved for only select reagents and has led to the generation and use of other Sm(II)-based reagents.[4] While SmI_2 is straightforward to prepare and is relatively soluble in electron donor solvents, there are a number of challenges that face the synthetic community with regard to understanding its unique reactivity.

The distinctive place held by SmI_2 in the arsenal of synthetic chemists is a result of its versatility in mediating numerous fundamentally important transformations in organic synthesis including functional group reductions (alkyl halide, carbonyls and related functional groups), the cross coupling of reducible functional groups (Grignard and Barbier reactions, carbonyl- and alkyl halide-alkene couplings and related cross coupling reactions), and cascade reactions that proceed through free radical and anionic intermediates. As consequence of its versatility, it can be used for the synthesis of a wide range of multifunctional targets. Given the broad utility of the reagent, there are several outstanding reviews on the applications of SmI_2 in synthesis.[5–11]

Although the majority of SmI_2 chemistry is performed in THF, the reagent also has some solubility in MeCN and DME. Though the preparation and use of this reagent requires dry and air-free techniques, most reactions can be performed under mild conditions with short reaction times and good selectivity, making this a powerful reagent for synthetic chemists.

Through the use of additives such as electron donor ligands, proton donors, and inorganic salts, the chemistry of SmI_2 can be modulated to vary the rate, diastereoselectivity, and chemoselectivity of reactions. The influence of these various additive classes and the mechanistic basis for their effects is further discussed in Section 1.3.

1.2.1 Reductions

The majority of reactions utilizing SmI_2 are reductions, but a great range of the reactivity of this reagent is determined by either the presence or absence of additives. The following section includes examples of a wide array of functional groups reducible by SmI_2 with a range of additives.

1.2.1.1 Reduction of Halides

Alkyl halides can be reduced using SmI_2, and enhanced reactivity is achieved with the addition of additives. Kagan showed that SmI_2 alone could reduce alkyl bromides and iodides to the corresponding alkane, while benzylic and allylic halides provided coupled products like the one shown in Scheme 1.1.[4]
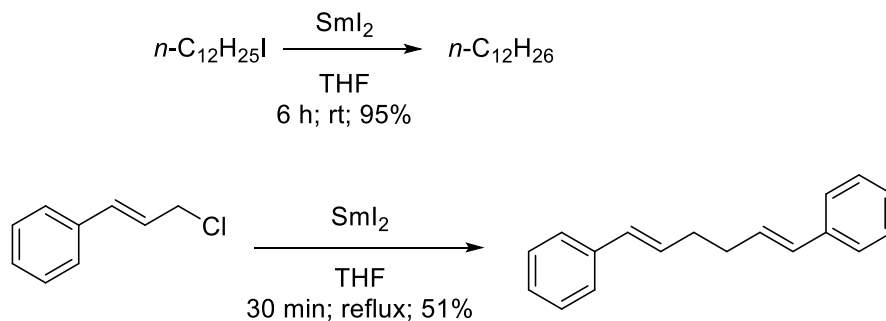
Scheme 1.1 Reduction of alkyl and benzylic halides by SmI_2.

The reduction of carbon-halogen bonds was further examined by Inanaga with the addition of HMPA and a proton donor. With this reagent combination, HMPA acts as an electron donor ligand to produce a stronger Sm(II) reductant. This combination increased the rate of reduction of alkyl iodides and enabled the reduction of unactivated alkyl bromides and some chlorides as exemplified in Scheme 1.2.[12]
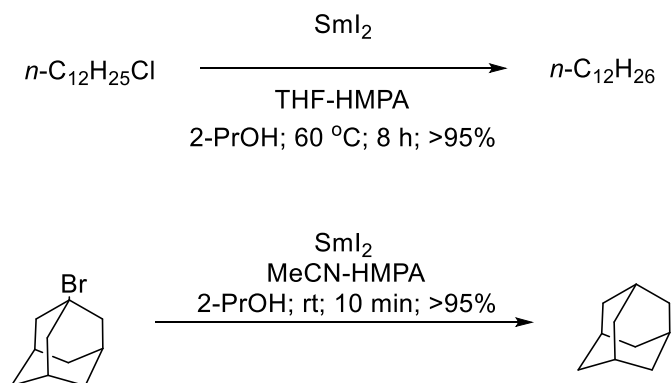
Scheme 1.2 Reduction of alkyl halides by SmI_2.

Hilmersson was able to greatly expand the scope of reducible halides and drastically increase reaction rates through the addition of water and amine additives. Scheme 1.3 shows the fast and high-yielding reduction of benzyl chloride with this

6

combination. This reagent combination has since been found to reduce a wide array of functional groups, some of which are presented in subsequent sections. The formation of the insoluble triethylammonium iodide leads to precipitation and likely acts as a driving force for the reaction. [13]
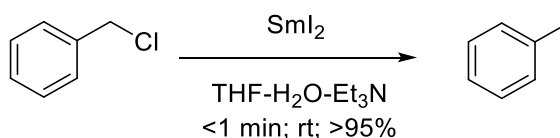
Scheme 1.3 Reduction of benzyl chloride by SmI_2-H_2O-Et_3N.

1.2.1.2 Reduction of Carbon-Carbon Double and Triple Bonds

Kagan discovered that SmI_2 could reduce conjugated double bonds at room temperature. Furthermore, conjugated double bonds could be reduced selectively in the presence of isolated double bonds. The reduction of ethyl cinnamate in Scheme 1.4 shows selectivity for reduction of the double bond in the presence of an ester.
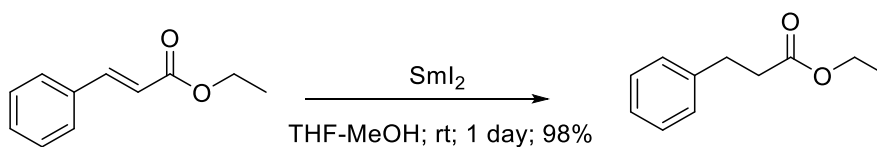
Scheme 1.4 Reduction of ethyl cinnamate by SmI_2.

Although SmI_2 can selectively reduce conjugated olefins slowly, Hilmersson discovered the SmI_2-H_2O-amine combination could perform these transformations rapidly and selectively in the presence of isolated double bonds or even phenyl groups

like those shown in Scheme 1.5. In these examples *N,N,N',N'',N''*-pentamethyldiethylenetriamine (PMDTA) is utilized as the amine additive.
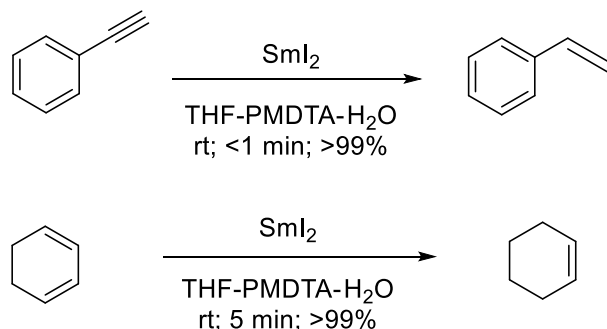
Scheme 1.5 Hilmersson's reduction of conjugated double and triple bonds by SmI_2.

The reduction of arenes by SmI_2 has also been reported by Hilmersson.[14] Using arenes of increasing redox potential, Hilmersson was able to estimate the redox potential of the powerful SmI_2-H_2O-amine combination.
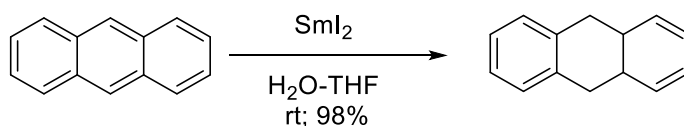
Scheme 1.6 Reduction of anthracene by SmI_2-H_2O-amine.

1.2.1.3 Reduction of Carbon-Oxygen Bonds

Due to its strong oxophilicity, Sm(II) is quite reactive toward oxygen-containing substrates. In his seminal report, Kagan investigated the reduction of aldehydes and ketones as well as the deoxygenation of epoxides, which are both exemplified in Scheme 1.7.[4]

8
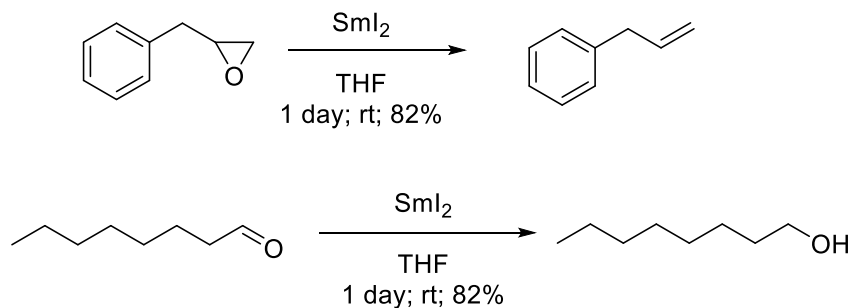
Scheme 1.7 Reduction of C-O bonds by SmI$_2$.

Flowers demonstrated the tunable reactivity of SmI$_2$ through a study of the reduction of β-hydroxyketones carried out in a series of different solvents in Scheme 1.8. When the reduction was carried out in THF and DME, the *syn* diastereomer was the predominant product, however, in MeCN with methanol as a proton donor, the major product was the *anti* diastereomer. [15]
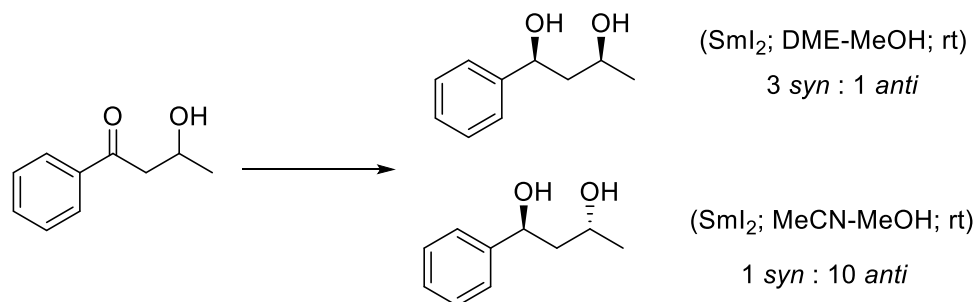
Scheme 1.8 Diastereoselectivity differences obtained in the reduction of β-hydroxyketones.

With the combination of water and amine, challenging reductions such as those of carboxylic acids, esters, and amides can be accomplished, providing the primary alcohol.[16–18] As shown below, Procter was able to show selectivity for the reduction of

the amide functionality in the presence of an amine in the synthesis of Atenolol in Scheme 1.9.[16]
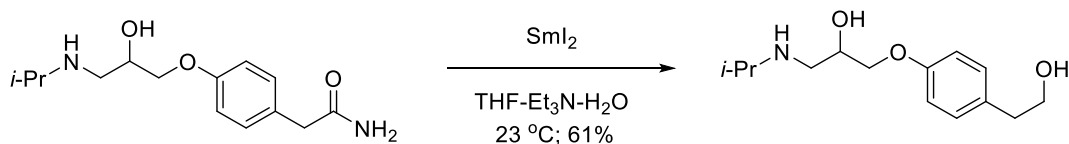
Scheme 1.9 Procter's selective reduction of amide in the presence of an amine.

1.2.1.4 Reduction of Nitriles

The nitrile functional group is an especially challenging functionality to reduce. Successful reduction of this moiety by SmI_2 was reported by Procter. While SmI_2 alone cannot perform this reduction, the SmI_2-H_2O-amine reagent combination can perform the reduction in high yield. Scheme 1.10 shows an example of this reduction to provide the corresponding primary amine product.
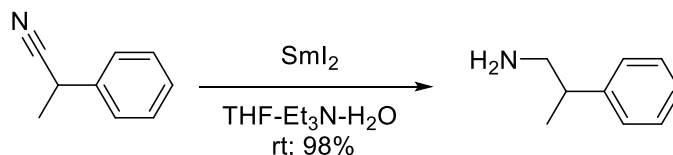
Scheme 1.10 Reduction of nitrile group to primary amine by SmI_2.

1.2.2 Carbon-Carbon Bond-Forming Reactions

SmI_2 has been used for a range of reductive bond-forming reactions due to its ease of use and selectivity. The following sections describe a few of the many coupling reactions to which SmI_2 has been applied.

10

1.2.2.1 Barbier Couplings

The first reported bond-forming reactions executed using SmI_2 were Barbier couplings between alkyl halides and ketones performed by Kagan.[19] Using SmI_2, benzyl bromide and 2-octanone can undergo reductive coupling to provide a tertiary alcohol, which is illustrated in Scheme 1.11.
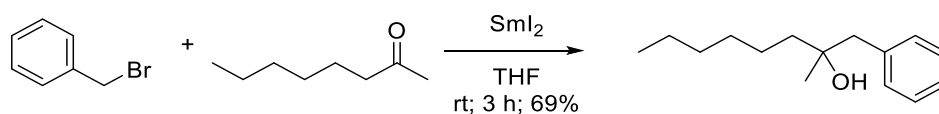
Scheme 1.11 Typical Barbier coupling by SmI_2.

In the absence of additives, the coupling of ketones occurs at a slow rate, but with the addition of HMPA, the alkylation occurs significantly faster. Mechanistic studies by Curran, which were later expanded by Flowers, found that the preferential formation of an organosamarium intermediate of the alkyl halide is a key step in the process of the Barbier coupling with SmI_2-HMPA.[20,21]

The samarium Barbier reaction has been applied to both intermolecular and intramolecular bond-forming. A recent example of an intramolecular Barbier coupling is shown below in which the reaction was applied to the total synthesis of 10-isocyano-4-cadinene by Matsuda and coworkers.[22]
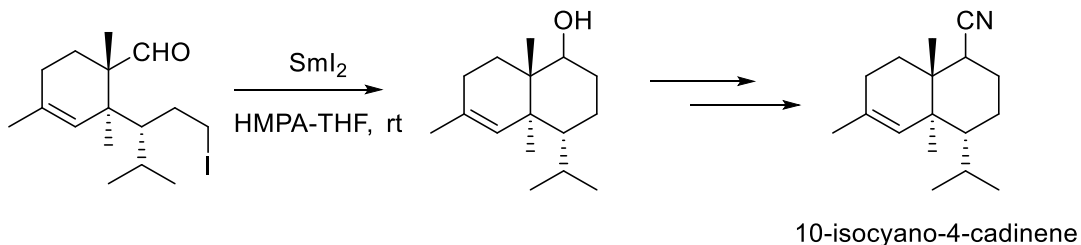
Scheme 1.12 Intramolecular samarium Barbier coupling.

1.2.2.2 Halide-Alkene Couplings

SmI$_2$ can also induce the reductive intramolecular coupling of halides with alkenes. This can be utilized to perform cyclizations such as the spirocyclization of benzamides developed by Tanaka and shown in Scheme 1.13. [23]
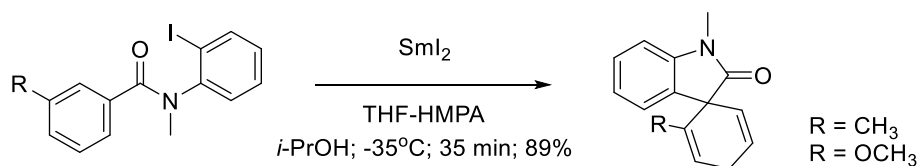
Scheme 1.13 Reductive coupling of aryl halide and alkene with SmI$_2$.

1.2.2.3 Pinacol Couplings

The homocoupling of ketones to provide vicinal alcohols occurs very slowly with SmI$_2$ in THF. Interestingly, with the addition of lithium halide salts, pinacol couplings with SmI$_2$ can be achieved quickly and in high yield. Flowers reported the coupling of cyclohexanone in the presence of lithium chloride or bromide to produce the corresponding pinacol product in minutes(Scheme 1.14). It is proposed that *in situ*

12

formation of SmCl$_2$ and SmBr$_2$, which are stronger but less-soluble reductants, are the source of this enhanced reactivity.[24]
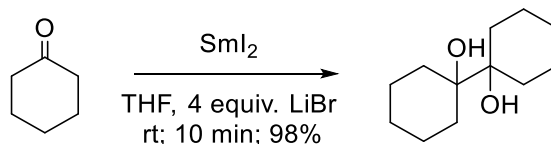
Scheme 1.14 Reductive coupling of cyclohexanone to yield pinacol.

1.2.2.4 Reformatsky Reactions

The Reformatsky reaction, in which a ketone undergoes condensation with an α-halo ester to produce a new carbon-carbon bond, has been applied to a variety of total syntheses. An example of this is depicted in Scheme 1.15 where the use of SmI$_2$ to form new carbocycles through reductive coupling was investigated by Molander.[25]
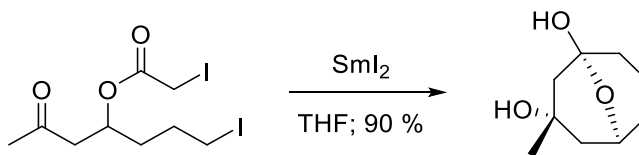
Scheme 1.15 SmI$_2$-induced Reformatsky reaction.

A recent example of a SmI$_2$-promoted intramolecular Reformatsky reaction is found in an intermediate step of the total synthesis of an array of saundersioside analogues, which are proposed to possess antitumor activity. As shown in Scheme 1.16, a seven-membered lactone is formed in good yield with high stereoselectivity, which is proposed to result from the ability of the carbonyl oxygen to coordinate to Sm(II) in the transition state of the stereoselective determining step.[26]

13

(1) SmI$_2$; THF; RT; 89%
(2) SOCl$_2$; Pd/C, Hg; TBAF, THF; 93%
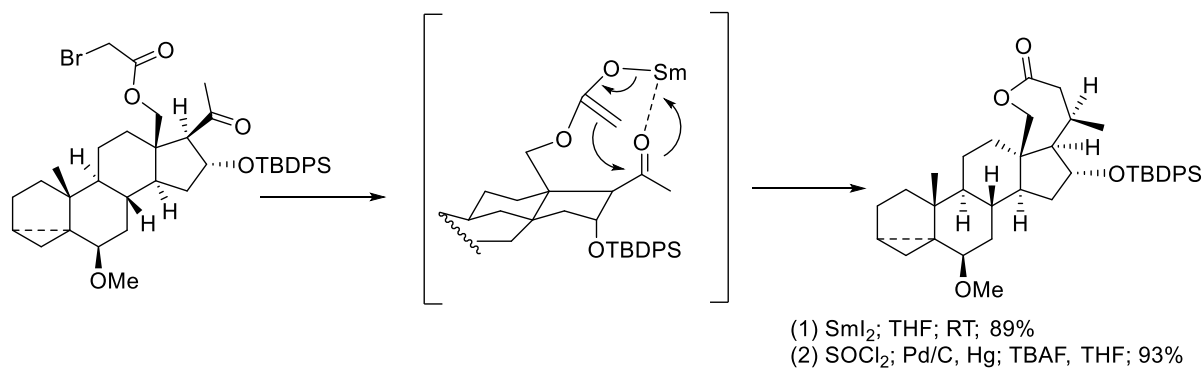
Scheme 1.16 Intramolecular Reformatsky reaction.

1.3. Additives in Sm(II) Chemistry

One of the features of Sm(II) that is apparent from the reactions outlined in the previous section is that additives drive the tunable reactivity that make this a highly useful synthetic reagent. Additives commonly utilized in conjunction with SmI$_2$ and other Sm(II)-based reductants can be classified into three major groups: 1) Lewis bases (HMPA and other electron donor ligands and chelating ethers) 2) proton donors (water, alcohols, and glycols), and 3) inorganic additives (NiI$_2$, FeCl$_3$, LiCl, etc.). In addition, the solvent milieu can also play an important role in the reactivity of Sm(II) reductants, predominantly through changes in the coordination sphere of the metal.

1.3.1 Lewis Bases

Lewis bases containing basic nitrogen and oxygen are often employed to accelerate reactions of SmI$_2$ and other Sm(II)-based reductants. Typically, Lewis base additives act as ligands for Sm(II), accelerating the electron transfer process by making the reagent a stronger reductant or stabilizing the Sm(III) oxidation state.[27–29] More

recently, it has been shown that these additives can also have an impact in post electron transfer steps of reductions or in activating carbon-halide bonds.

1.3.1.1 HMPA

The most commonly utilized Lewis base in reactions with Sm(II) reductants is HMPA. Despite its toxicity and suspected carcinogenicity, HMPA remains the additive of choice in many SmI_2-promoted reductions and bond-forming reactions. It not only exhibits unique behavior as a ligand for Sm(II), but it has synthetic advantages such as its ability to significantly enhance the rate and stereochemical outcome of Sm(II)-mediated bond-forming reactions.[21,30] In some cases, proton donor sources can be employed in place of HMPA to carry out SmI_2 mediated reductions, which has garnered much attention over the last decade.

The potential of the combination of a Sm(II) reductant and HMPA was first realized when Inanaga demonstrated that a range of alkyl and aryl halides can be readily reduced by SmI_2 when HMPA was employed as a cosolvent. It is important to note that this seminal report alerted the synthetic community to the importance of HMPA and its use led to the development of a large number of subsequent reactions.[12] An important example below in Scheme 1.17 highlights the reduction of an aryl halide in the presence of an ester.
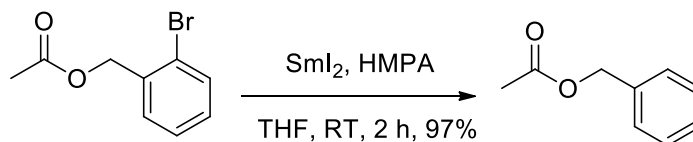
Scheme 1.17 SmI_2-HMPA-induced reduction of aryl halide.

Early work in the Flowers group revealed that the coordination of HMPA to Sm(II) produced a stronger reductant, which was observed even at relatively low concentrations. Table 1.1 illustrates the boost in redox potential experienced by Sm(II) in the presence of HMPA.[28]

Table 1.1. Effect of HMPA concentration on Sm(II) redox potential. [28]

Equivalents of HMPA vs SmI$_2$[a]	Oxidation Potential (V)[b]	ΔE (V)
0	-1.33	0
1	-1.43	0.10
2	-1.46	0.13
3	-1.95	0.62
4	-2.05	0.72
5	-2.05	0.72

[a] [SmI$_2$] = 0.5 mM, [b] vs. Ag/AgNO$_3$ reference electrode in THF.

The role of HMPA in reductions of SmI$_2$ was further examined using kinetic studies. As shown in Table 1.2, the rate of reduction of alkyl iodides was greatly accelerated with the addition of HMPA, which followed the thermodynamic redox potential data provided in Table 1.1. Interestingly, the reduction of a ketone, 2-butanone, did not follow this trend, displaying only a minor rate enhancement. This observed difference was attributed to the difference between outer sphere electron transfer in the reduction of alkyl iodide and inner sphere coordination-dependent electron transfer for the ketone, which is not appreciably enhanced in the sterically-hindered Sm-HMPA complexes.[31]

Table 1.2. Effect of HMPA concentration on the rate of reduction with SmI$_2$. [31]

Sm(II) System	Substrate	k (M^{-1}s^{-1})
SmI$_2$	1-iodobutane	(8 ± 2) x 10^{-4}
[Sm(THF)$_2$(HMPA)$_4$]I$_2$	1-iodobutane	1.0 ± 0.1
[Sm(HMPA)$_6$]I$_2$	1-iodobutane	2.6 ± 0.1
SmI$_2$	2-butanone	(7 ± 3) x 10^{-4}
[Sm(THF)$_2$(HMPA)$_4$]I$_2$	2-butanone	(8 ± 1) x 10^{-3}
[Sm(HMPA)$_6$]I$_2$	2-butanone	(8 ± 1) x 10^{-3}

One of the classic examples of SmI$_2$-HMPA chemistry is the samarium Barbier reaction. Curran and coworkers carried out numerous early mechanistic studies designed to elucidate the mechanism of the samarium Barbier reaction. A series of reactions run under both Barbier and Grignard conditions are shown below in Scheme 1.18. In all cases they found that the product yields and stereoselectivity did not depend on the sequence of reagent and substrate addition, consistent with the formation of an organosamarium intermediate under Barbier conditions.[32]
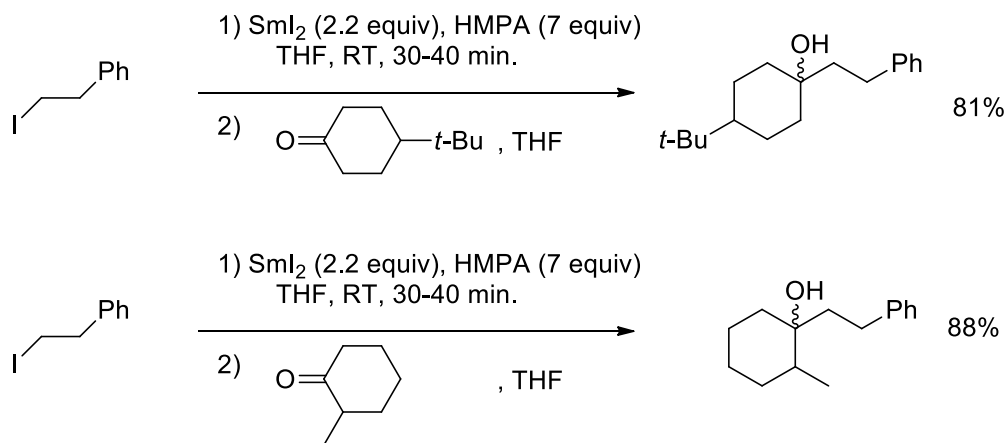
Scheme 1.18 SmI$_2$-HMPA Barbier coupling reaction.

Curran utilized HMPA to cyclize an aryl radical onto a cyclobutene in the total synthesis of Penitrem D as in Scheme 1.19. A range of intramolecular radical cyclizations were carried out in this fashion producing yields ranging from 49-90%. It was also found that the addition of acetone led to coupling onto the cyclobutane, which affords a tertiary alcohol side-chain.[33]

A 73 %   **B** 16 %
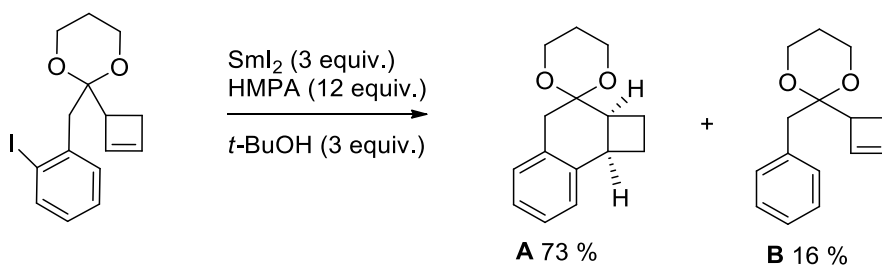
Scheme 1.19 Halide-alkene cyclization induced by SmI$_2$-HMPA.

A number of publications by Tanaka have shown SmI$_2$ in combination with HMPA and a proton donor can be utilized to generate spirocycles. It was found that the spirocyclization of benzamides with electron-donating *o*-methyl or *o*-methoxy substitutions provided high yield as per Scheme 1.20.[23]

89%   9%
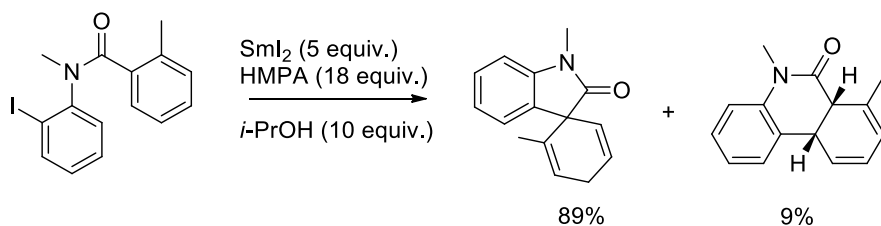
Scheme 1.20 Spirocyclization using SmI$_2$-HMPA by Tanaka.

1.3.1.2 Bis(trimethylsilyl)amide

The Evans group reported on the bulky but highly soluble $Sm(HMDS)_2THF_2$ complex in 1988. Generated from the sodium or potassium salts combined with SmI_2, this reductant is soluble in an even wider array of organic solvents, including nonpolar solvents like hexane. The crystal structure is shown in Figure 1.1, and has two THF molecules coordinated to it, providing additional bulk to the complex.[34]
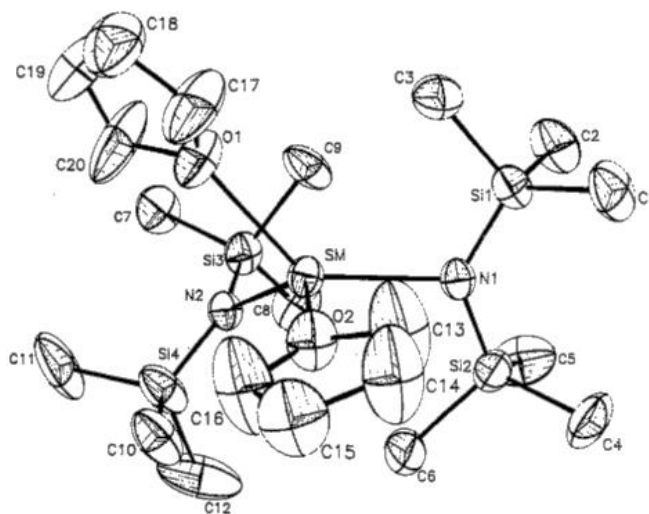
Figure 1.1 X-ray crystal structure of $Sm(HMDS)_2THF_2$. [34]

The redox potential of the complex was determined vs Ag/AgNO3 as -2.1 V, making it a significantly more powerful reductant that SmI_2.[35] The reactivity of this complex was examined by both the Flowers[35,36] and Hilmersson group[37,38] and is further presented in Chapter 7.

1.3.2 Proton Donors

Although proton donors have been utilized in reactions featuring Sm(II) since the early 1980's, the differences in reactivity provided by each proton donor has required

decades of research to unveil. In particular, water has proven to be a versatile additive with key reactivity differences from other proton sources, such as alcohols and glycols.

1.3.2.1 Water

The use of water as an additive for SmI_2 has received a great deal of attention in recent years due to its ability to act not only as a proton donor, but also as a ligand whereby it enhances the reactivity of SmI_2. In an early report by Kagan, the reduction of 2-octanone to 2-octanol was shown to proceed in the presence of small amounts of water over the competing pinacol coupling that occurs in the absence of water as shown in Scheme 1.21. Interestingly, the use of methanol as a proton source instead of water provided a very poor yield, which was an early indication that water provided a unique enhancement to the reactivity of SmI_2.[4]
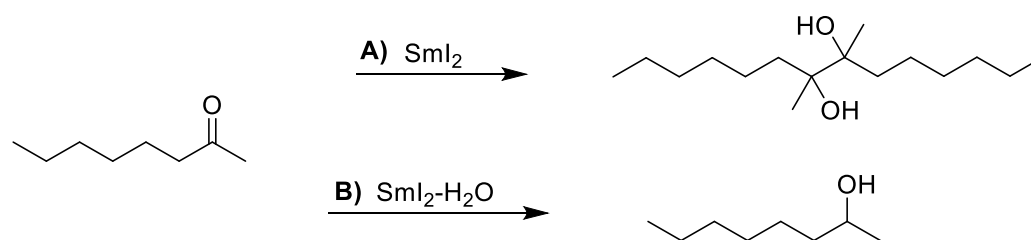
Scheme 1.21 Reduction of 2-octanone to 2-octanol with H_2O (B) instead of pinacol coupling (A).

Studies on this system by Flowers and coworkers established that H_2O coordinates to samarium and displaces coordinated solvent and iodide as shown in the UV-vis spectra in Figure 1.2. [39]
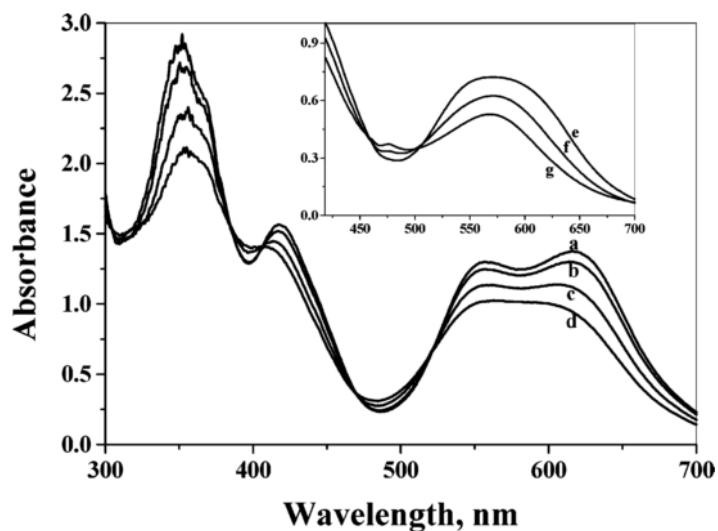
Figure 1.2 Absorption spectra of 2.5 mM SmI$_2$ in the presence of increasing amounts of water. (a) [H$_2$O] = 0.025 M, (b) [H$_2$O] = 0.05 M, (c) [H$_2$O] = 0.125 M, (d) [H$_2$O] = 0.188 M, (e) [H$_2$O] = 0.15 M, (f) [H$_2$O] = 0.3 M, (g) [H$_2$O] = 0.45 M. [39]

Additionally, cyclic voltammetry revealed that the addition of water increases the reduction potential of SmI$_2$ up to -1.9 V(*vs.* Ag/AgNO$_3$).[30,39] This boost in redox potential afforded through the addition of H$_2$O is shown in Figure 1.3, where the rate of reduction of benzyl bromide through rate-limiting electron transfer was enhanced with increasing H$_2$O concentration.[39]
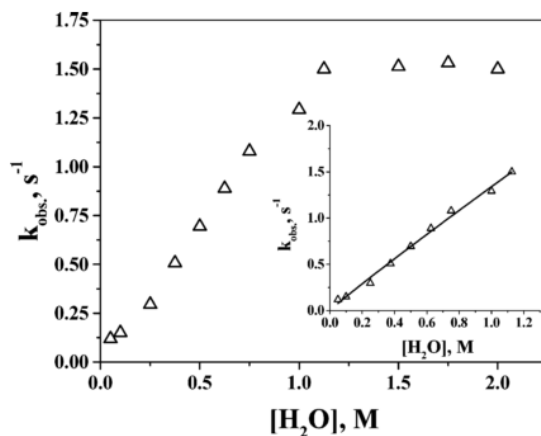
Figure 1.3 Rate of reduction of benzyl bromide by SmI_2 with increasing concentration of H_2O. [39]

Another interesting facet of the reactivity of SmI_2-H_2O is that this system is capable of initiating the reduction and reductive coupling of functional groups that lie well outside the accessible thermodynamic redox potential according to the above cyclic voltammetry study. Many examples of this reactivity have been reported, a significant portion of them by Procter[40–44], one of which is shown in Scheme 1.22. [40]
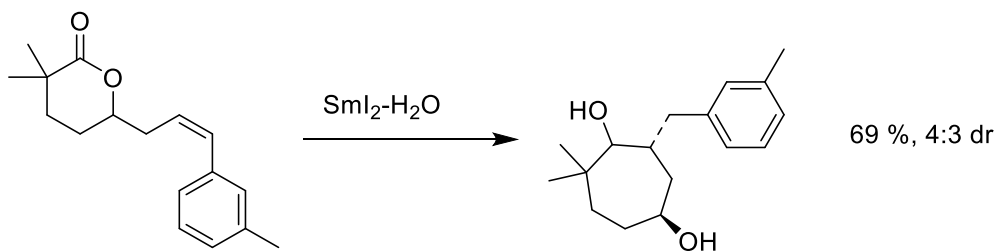
Scheme 1.22 Reductive cyclization of lactone to form cycloheptanediol.

Thus, the use of H_2O provides a more powerful Sm(II)-based reductant with unique reduction and cross-coupling abilities that clearly lacks the toxicity and potential

carcinogenicity of other additives such as HMPA. Although mechanistic studies have examined the reactivity of SmI_2-H_2O, questions still remain about the basis for this unique combination, and are presented in Chapters 2,3,4, and 5.

1.3.2.2 Glycols and Alcohols

The addition of alcohols to SmI_2 reactions was first reported by Kagan. It was found that the addition of alcohols like methanol and *t*-butanol led to lower reaction times and greater yields.[4] Hoz later examined the role of alcohol through UV-Vis, product distribution, and isotopic labelling studies.[45–47] The effect of methanol coordination to SmI_2 is shown in Scheme 1.6, however this change does not occur until significantly higher concentrations than where synthetic conditions typically lie.[45] Typical examples of the use of alcohols as additives are shown in Scheme 1.4 and 1.8. They have shown special utility in combination with HMPA for specific reductive cyclizations.[5,9]
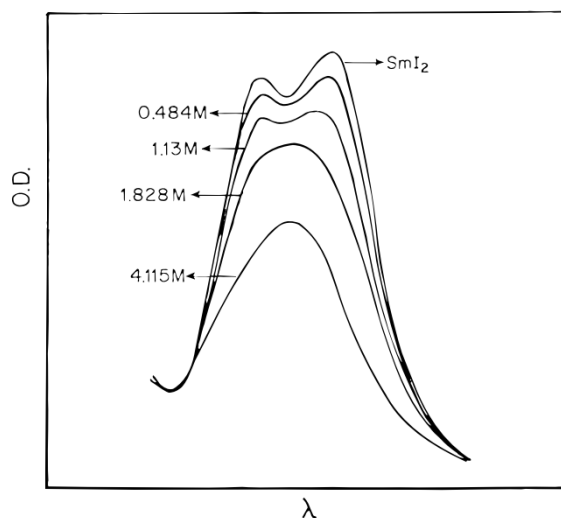
Figure 1.4 Change in UV-vis spectrum of SmI_2 with increasing concentrations of methanol. [45]

In the mechanistic study of the reduction of acetophenone, the Flowers group revealed that the pK_a of an alcohol additive directly correlates to the rate of reduction. In combination with steric effects, this was the first rationalization of the different influences provided by alcohols.[48]

Like water, glycols have also been shown to coordinate to Sm(II), however, because of their ability to coordinate in a multidentate fashion, they exhibit coordinative saturation at much lower concentrations. This multidentate coordination was confirmed by x-ray crystal structure as shown in Figure 1.5 for the complex resulting from diethylene glycol coordination. This structure confirms that iodide is displaced to the outer sphere of the complex upon coordination of glycol.[49]
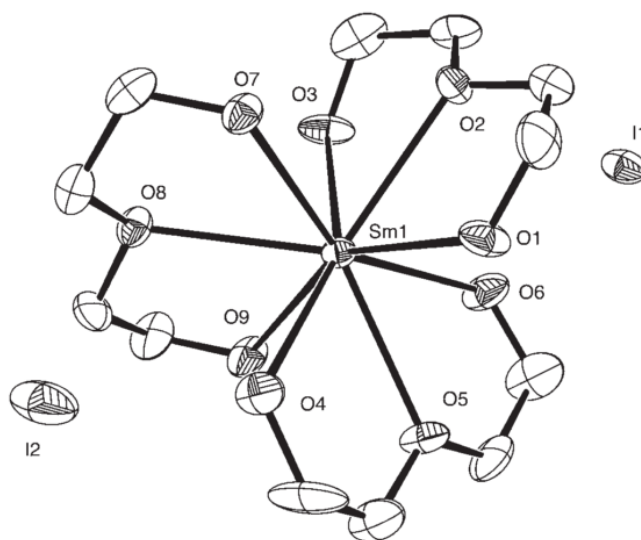
Figure 1.5 X-ray crystal structure of [Sm(dg)$_3$]I$_2$ [49].

The mechanistic difference imparted by glycols compared to water in Sm(II) chemistry is further described in Chapter 3.

1.3.2.3 Samarium-water-amine

Dahlén and Hilmersson were the first to report the combination of water and amine with SmI$_2$ to produce a reductant even more reactive than SmI$_2$ combined with either additive alone.[50] Cyclic voltammetric experiments performed by Flowers and Hilmersson showed that this combination of additives does not significantly alter the redox potential of SmI$_2$.[13] This finding suggests that the mechanism of the reduction is likely more complex than just the production of a more powerful Sm(II)-based reductant. Since its introduction to the synthetic community, this reagent combination has been utilized for many complex transformations and mechanistic studies.[14,51–58] Examples of the reactivity of this reducing system are shown above in Schemes 1.3, 1.5, 1.9, and 1.10.

1.3.3 Inorganic Additives

1.3.3.1 Lithium halide salts

The addition of lithium halide salts (predominantly LiBr and LiCl) has a large effect on the reactivity of SmI$_2$ by displacing the iodide to produce SmBr$_2$ and SmCl$_2$, respectively.[24] Although SmBr$_2$ and SmCl$_2$ have minimal solubility in THF, they have more negative redox potentials than SmI$_2$ and can therefore reduce substrates typically recalcitrant to electron transfer. In situ preparation via the addition of lithium salts allows the reagents prepared by this method to have temporary solubility, at least for the duration of the reaction. As a consequence, the reagents should be used soon after the halide salts are mixed with SmI$_2$.[59] Although the reductants produced throughout this

method do not have the broad applicability of SmI_2-HMPA, they do offer advantages in some intramolecular and cross coupling reactions as well as accelerated pinacol couplings.

Wood and coworkers established that the combination of SmI_2-LiCl containing *t*-butanol as a proton source was effective for the cyclization of an isocyanate onto an α,β-unsaturated ketone to form a spirooxindole.[60] When SmI_2 was employed alone, only a 5 % yield of the product was obtained. However, when 4 equiv of LiCl was added to SmI_2, the intermediate isocyanate was converted to the spiroxindole in a 75% yield as shown below in Scheme 23.
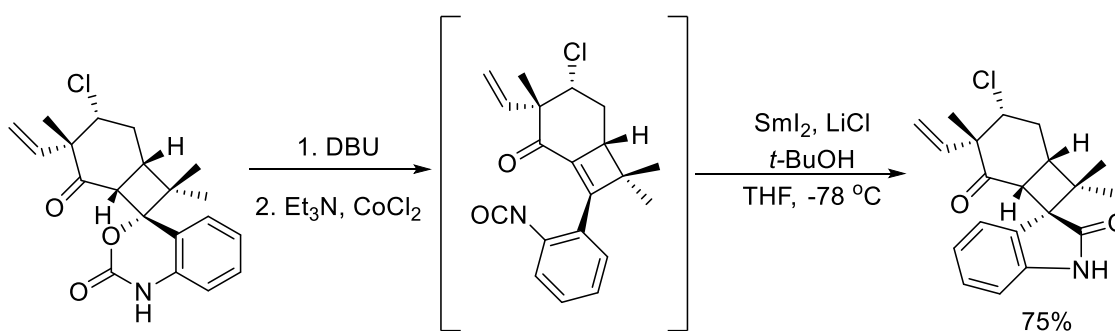
Scheme 1.23. SmI_2-LiCl spirocyclization.

For a thorough discussion of samarium dibromide and dichloride, see Chapter 8.

1.3.3.2 Transition Metal Salts

Catalytic amount of transition metal salts derived from Ni(II), Fe(III), and Cu(II) have been shown to increase the efficiency of SmI_2-mediated reactions. The use of transition metal salts can be traced to the seminal work of Kagan who showed that $FeCl_3$

could be employed to accelerate the coupling of ketones and alkyl iodides as in Scheme 24.[4]
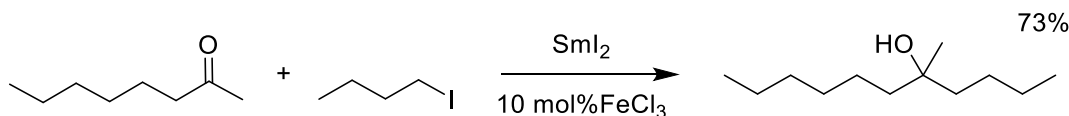
Scheme 1.24. Use of FeCl$_3$ for the coupling of ketone and alkyl iodides by SmI$_2$.

Kagan has shown that in most cases, NiI$_2$ is superior to other transition metal salts.[61] As a consequence of these early studies, NiI$_2$ is utilized in most instances. Although the use of NiI$_2$ in reactions has become routine, its mechanistic role was unknown until the recent work of Flowers who showed that SmI$_2$ reduces Ni(II) to Ni(0) and that Ni-derived intermediates are likely responsible for the progression of events leading to bond formation in the coupling of alkyl halides and ketones.[21]

1.3.4 Solvent

The solubility and reactivity of samarium-based reagents varies widely. There are many instances of key reactivity differences when an alternate solvent is utilized. These examples show the large effects on product identity that occur when changes in solvent structure influence the degree of solvent coordination to samarium.

1.3.4.1 Coordinating Solvents (Other than THF)

1.3.4.1.1 Tetrahydropyran

The ability to prepare SmI$_2$ in tetrahydropyran (THP) was attractive to Kagan due to limitations in THF caused by side-product formation. Reactions using acid chlorides were observed to proceed more cleanly in THP than in THF because the rate of solvent

ring-opening is significantly decreased. It was also discovered that acyl samarium

intermediates were stabilized in THP, meaning these species could be stored for later use.

Thus, α-hydroxyketones could be prepared from acid chloride and ketone combinations

in a straightforward manner as shown in Table 1.3. As evidenced by entries 5 and 6,

cyclohexanoyl chloride and *n*-nonanoyl chloride led to homocoupling of the acyl

samarium species.[62]
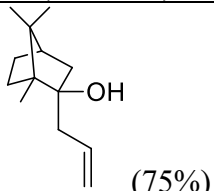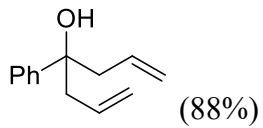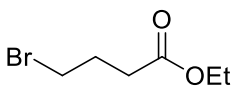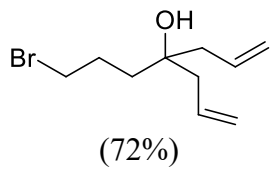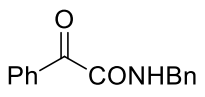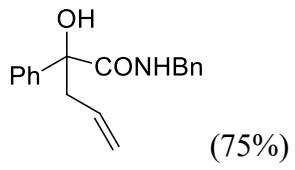
Table 1.3. Coupling of Ketones with Acid Chlorides in THP by SmI_2. [62]
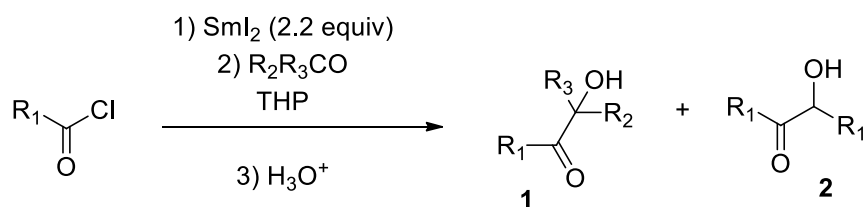
Entry	R_1	R_2	R_3	T (°C)	Yield of 1 (%)	Yield of 2 (%)
1	1-methylcyclohexyl	H	C_2H_5	0	> 95	trace
2	1-methylcyclohexyl	CH_3	C_2H_5	0	94	trace
3	1-adamantyl	CH_3	C_2H_5	-18	> 95	trace
4	1-adamantyl	CH_3	C_2H_5	0	84	16
5	*n*-octyl	H	C_2H_5	-18	0	80
6	cyclohexyl	H	C_2H_5	-18	0	90

Since organosamarium species were previously found to be stabilized in THP, Kagan was able to expand coupling reactions to provide cross-couplings between allyl and benzyl halides with ketones and esters as shown in Table 39.[63,64] A few examples of allylic samarium compounds that were prepared with SmI_2 in THP combined with allyl iodide at reduced temperatures are given in Table 1.4. These organosamarium species eacted readily with a variety of ketones. They were able to provide evidence for the existence of the proposed organosamarium intermediates by isotopic incorporation upon quenching with D_2O.
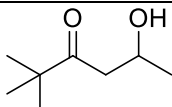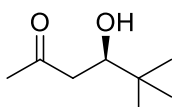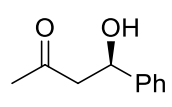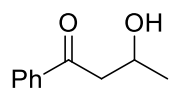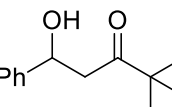
Table 1.4. Reaction of Allylsamarium Diiodide in THP on Various Ketones.[63]

Ketone Substrate	Reaction Time (h)	Allyl iodide: Ketone	Major Product (Yield %)
	0.25	1 : 0.5	(75%)
$PhCO_2C_2H_5$	2	1 : 0.45	(88%)
	1.5	1 : 0.4	(72%)
	2	1 : 0.75	(75%)

1.3.4.1.2 Dimethoxyethane

   Work by Flowers and coworkers has shown that higher diastereoselectivity could be achieved in the reduction of β-hydroxyketones when dimethoxyethane (DME) was utilized as the solvent. With the addition of methanol as a proton source, quantitative yields of reduced product were obtained. The *syn* diastereomer was the preferred product in most instances, as shown in Table 1.5. They were able to compare the reactivity in THF, CH$_3$CN, and DME and were able to show that the diastereoselectivity could easily be manipulated by changing the solvent. [15]

Table 1.5. Diastereoselectivities of β-Hydroxyketone Reductions in DME. [15]

Substrate	syn : anti
	15 : 1
	> 99 : < 1
	< 1 : > 99
	> 99 : < 1
	50 : 50

1.3.4.1.3 Acetonitrile

30

Due to the limited solubility and stability of SmI_2 in acetonitrile, the use of $Sm(OTf)_2$ for reactions in acetonitrile was investigated by Flowers and coworkers. The ketyl-olefin cyclization of 2-but-3-enyl-cyclohexane-1-one was examined to determine if this solvent-reagent combination provided similar reactivity to that of SmI_2 in THF in the presence and absence of additives. Table 1.6 shows that reductive cyclization occurs in the presence of additives to provide good yields and varying diastereoselectivities.[65]

Table 1.6. Reductive cyclization using $Sm(OTF)_2$ in MeCN. [65]
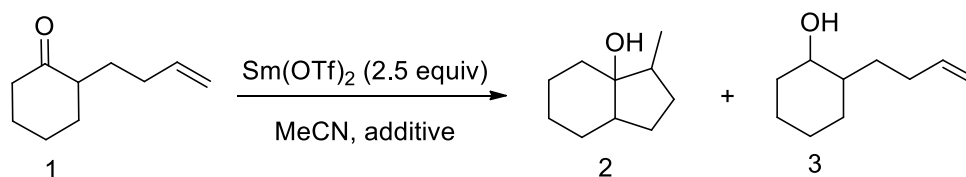
Additive	Equivalents	Time	Yield 2, %	cis: trans	Yield 3, %
None	-	2 days	0	-	-
HMPA	10	10 mins	96 ± 2	1 : 100	< 1
DMPU	10	2 days	72 ± 2	1 : 50	6
DMPU t-BuOH	10 3	12 hours	96 ± 2	1 : 13	< 1

Tani and Kunishima reported the reductive cleavage of an allyloxy group from diallyl acetals with SmI_2 in acetonitrile leading to generation of a carbanion that undergoes 2,3-rearrangement as in Scheme 25.[66] A good yield was achieved under reflux, and interestingly, the addition of HMPA led to poor yield. It is suspected that the observed lower reactivity in THF is a consequence of the coordinating ability of solvent. This explains the high yield in acetonitrile, which does not coordinate as strongly. Under

reflux in MeCN they found no evidence for the formation of 1,2-rearrangement product, which tends to compete with 2,3-rearrangement, providing a new regioselective method for this type of Wittig rearrangement.
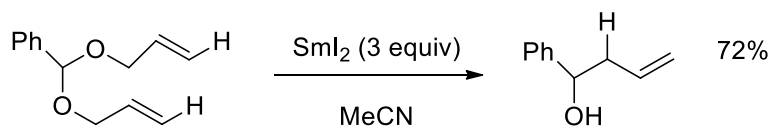
Scheme 1.25 Reductive cleavage of diallyl acetals with SmI_2 in acetonitrile.

The coupling of α-chloro-α,β-unsaturated phenones and aldehydes was studied by Concellón. In THF, the reaction was found to work well with ketones, but not with aldehydes. When solvent was switched from THF to acetonitrile, selectivity was significantly enhanced. Table 1.7 provides a few of the successfully generated products in moderate yield with high selectivity in acetonitrile.[67]

Table 1.7. Coupling of α-Chloro-α,β-Unsaturated Phenones and Aldehydes. [67]
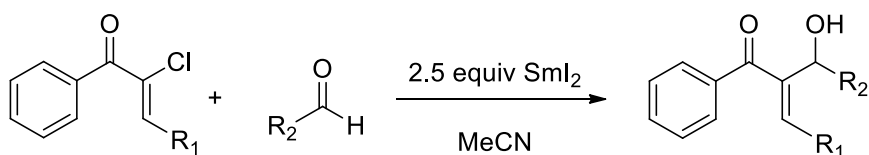
Entry	R_1	R_2	R_3	Yield, %	*Z / E*
1	*n*-C_4H_9	cyclohexyl	H	75	89 / 11
2	cyclohexyl	cyclohexyl	H	52	96.5 / 3.5
3	cyclohexyl	Ph	H	60	96.5 / 3.5
4	cyclohexyl	*n*-C_7H_{15}	H	72	96 / 4

32

1.3.4.2 Non-coordinating Solvents

1.3.4.2.1 Benzene-HMPA

When Barbier reactions with aryl halides are attempted in THF, the resulting intermediate aryl radical abstracts hydrogen from THF to provide reduced product.[12] The use of benzene-HMPA as a solvent system for the coupling of aryl halides with ketones was introduced by Tani.[68] It is proposed that this solvent combination provides a much lower rate of hydrogen atom abstraction so that coupled products are favored. The coupling of iodobenzene with benzyl butyl ketone as in Scheme 1.26 provided 74% yield in ten minutes. A few other aryl iodide and ketone combinations were investigated with fair yields. In a later publication, the reductive coupling of vinyl halides with carbonyls using the Barbier method was also found to proceed smoothly in benzene-HMPA.[69]
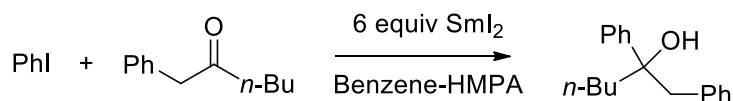
Scheme 1.26 Coupling by SmI$_2$ in benzene-HMPA.

Tani and coworkers reported on the successful coupling of alkynyl iodides with ketones or aldehydes mediated by SmI$_2$ in a mixture of HMPA and benzene.[70] The Barbier method of addition was found to provide the best yields over that of the Grignard-type addition. This provides a unique method for generating propargyl alcohols in good yield and was further studied to provide an expanded scope, which is surveyed in Table 1.8.[71]

Table 1.8. Coupling of Iodoalkynes and Carbonyls in Benzene-HMPA with SmI_2. [71]
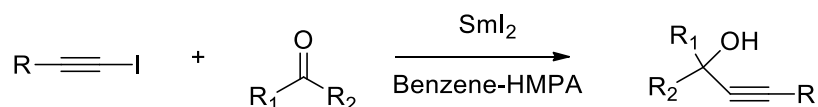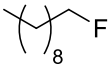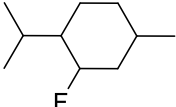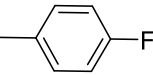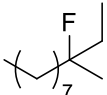
R	Ketone	Yield (%)[a]
$n\text{-}C_8H_{17}$	Bu—C(=O)—Bu	78
$n\text{-}C_8H_{17}$	Ph—CH$_2$—C(=O)—Bu	76
$n\text{-}C_8H_{17}$	$t\text{-}Bu$—(cyclohexanone)=O	76[b]
Ph	Bu—C(=O)—Bu	75
(cyclopentylmethyl)	Bu—C(=O)—Bu	78
$n\text{-}C_8H_{17}$	Ph—CH$_2$—CHO	65

[a] Alkynyl iodide : carbonyl : SmI_2 = 1.0 : 1.5 : 4.0 [b] cis/trans mixture

1.3.4.2.2 Hexanes

Hilmersson found that $Sm[N(SiMe_3)_2]_2$ in hexane could mediate reductive cleavage of the C-F bond where other samarium-solvent-additive combinations failed.[37] By increasing the temperature from ambient to 100 ºC using a microwave cavity, good to excellent yields were obtained in relatively short reaction times. As shown in Table 1.9, primary, secondary, tertiary, and cyclic alkyl fluorides were reduced to their corresponding hydrocarbon in 60 minutes or less. This provided a new method for the cleavage of the infamously strong C-F bond.

Table 1.9. Reductive Defluorination of Alkylfluorides with Sm[N(SiMe$_3$)$_2$]$_2$. [37]

Substrate	Time (min)	Yield (%)[a]
	60	95
	40	90
	60	75[b]
	10	89

[a] 2.5 equivalents of Sm[N(SiMe$_3$)$_2$]$_2$ [b] 10 equivalents of Sm[N(SiMe$_3$)$_2$]$_2$

1.4 Project Goals

Although many clues have been revealed to explain some of the reactivity observed in Sm(II) chemistry, many gaps in our understanding of this versatile reagent still exist. The questions that the work in this dissertation aims to answer are related to the coordination ability of additives, substrate, and solvent: 1) Why does the addition of H$_2$O promote the reduction of substrates well outside the range expected according to redox potential alone? 2) Does H$_2$O provide a unique reactivity because of the way it coordinates to Sm(II) or can alternative coordinating proton donors provide similar reactivity? 3) How does substrate coordination affect the reactivity of SmI$_2$-H$_2$O? 4) With an understanding of how proton donors affect the reactivity of SmI$_2$, are new additives accessible? 5) What is the mechanistic basis for the impact of solvent coordination on the reactivity of Sm(II) 6) Can alternative additives grant access to samarium dihalides and unlock previously unreachable reactivity?

1.5 References

(1)   Boisbaudran, L. de. *Comptes Rendus l'Academie des Sci.* **1879**.

(2)   Kaltsoyannis, N.; Scott, P. *The ƒ Elements*, 1st ed.; Evans, J., Ed.; Oxford University Press: Oxford, UK, 2007.

(3)   Cotton, S. *Lanthanide and Actinide Chemistry*; John Wiley & Sons, Ltd.: Chichester, UK, 2006.

(4)   Girard, P.; Namy, J. L.; Kagan, H. B. *J. Am. Chem. Soc.* **1980**, *102* (8), 2693–2698.

(5)   Szostak, M.; Fazakerley, N. J.; Parmar, D.; Procter, D. J. *Chem. Rev.* **2014**, *114* (11), 5959–6039.

(6)   Gopalaiah, K.; Kagan, H. B. *Chem. Rec.* **2013**, *13* (2), 187–208.

(7)   Kagan, H. B. *Tetrahedron* **2003**, *59* (52), 10351–10372.

(8)   Molander, G. A.; Harris, C. R. *J. Org. Chem.* **1998**, *63* (3), 812–816.

(9)   Nicolaou, K. C.; Ellery, S. P.; Chen, J. S. *Angew. Chemie Int. Ed.* **2009**, *48* (39), 7140–7165.

(10)   Edmonds, D. J.; Johnston, D.; Procter, D. J. *Chem. Rev.* **2004**, *104* (7), 3371–3403.

(11)   Dahlén, A.; Hilmersson, G. *Eur. J. Inorg. Chem.* **2004**, *2004* (17), 3393–3403.

(12)   Inanaga, J.; Ishikawa, M.; Yamaguchi, M. *Chem. Lett.* **1987**, 1485–1486.

(13)   Dahlen, A.; Hilmersson, G.; Knettle, B. W.; Flowers, II, R. A. *J. Org. Chem.* **2003**, *68*, 4870–4875.

(14)   Dahlén, A.; Nilsson, A.; Hilmersson, G. *J. Org. Chem.* **2006**, *71* (4), 1576–1580.

(15)   Chopade, P. R.; Davis, T. A.; Prasad, E.; Flowers, II, R. A. *Org. Lett.* **2004**, *6* (16),

2685–2688.

(16)   Szostak, M.; Spain, M. *J. Am. Chem. Soc.* **2014**, *136*, 2268–2271.

(17)   Szostak, M.; Spain, M.; Procter, D. J. *Org. Lett.* **2012**, *14* (3), 840–843.

(18)   Szostak, M.; Spain, M.; Eberhard, A. J.; Procter, D. J. *J. Org. Chem.* **2014**.

(19)   Girarad, P.; Namy, J.; Kagan, B. *J. Amer. Chem. Soc* **1980**, *102* (8), 2693–2698.

(20)   Curran, D.; Xin, G.; Zhang, W.; Dowd, P. *Tetrahedron* **1997**, *53* (27), 9023–9042.

(21)   Choquette, K. A.; Sadasivam, D. V.; Flowers, II, R. A. *J. Am. Chem. Soc.* **2010**, *132* (49), 17396–17398.

(22)   Nishikawa, K.; Nakahara, H.; Shirokura, Y. *Org. Lett.* **2010**, *12* (5), 904–907.

(23)   Iwasaki, H.; Eguchi, T.; Tsutsui, N.; Ohno, H.; Tanaka, T. *J. Org. Chem.* **2008**, *73* (18), 7145–7152.

(24)   Fuchs, J. R.; Mitchell, M. L.; Shabangi, M.; Flowers, II, R. A. *Tetrahedron Lett.* **1997**, *38* (47), 8157–8158.

(25)   Molander, G. A.; Hue, Y. Le; Brown, G. A. *J. Org. Chem.* **2001**, *66* (13), 4511–4516.

(26)   Cheng, S.-L.; Jiang, X.-L.; Shi, Y.; Tian, W.-S. *Org. Lett.* **2015**, *17*, 2346–2349.

(27)   Farran, H.; Hoz, S. *Org. Lett.* **2008**, *10* (5), 865–867.

(28)   Shabangi, M.; Flowers, II, R. A. *Tetrahedron Lett.* **1997**, *38* (7), 1137–1140.

(29)   Enemærke, R.; Hertz, T.; Skrydstrup, T.; Daasbjerg, K. *Chem. - A Eur. J.* **2000**, *6* (20), 3747–3754.

(30)   Sadasivam, D. V; Teprovich, J. A.; Procter, D. J.; Flowers, II, R. A. *Org. Lett.* **2010**, *12* (18), 4140–4143.

(31)   Prasad, E.; Flowers, II, R. A. *J. Am. Chem. Soc.* **2002**, *124*, 6895–6899.

(32)   Curran, D. P.; Totleben, M. J. *J. Am. Chem. Soc.* **1992**, *114*, 6050–6058.

(33)   Rivkin, A.; González-López de Turiso, F.; Nagashima, T.; Curran, D. P. *J. Org. Chem.* **2004**, *69* (11), 3719–3725.

(34)   Evans, W. J.; Drummond, D. K.; Zhang, H.; Atwood, J. L. *J. Inorg. Chem.* **1988**, *27* (3), 575–579.

(35)   Prasad, E.; Knettle, B. W.; Flowers, II, R. A. *J. Am. Chem. Soc.* **2002**, *124* (49), 14663–14667.

(36)   Prasad, E.; Knettle, B. W.; Flowers, II, R. A. *J. Am. Chem. Soc.* **2004**, *126*, 6891–6894.

(37)   Janjetovic, M.; Träff, A. M.; Ankner, T.; Wettergren, J.; Hilmersson, G. *Chem. Commun. (Camb).* **2013**, *49* (18), 1826–1828.

(38)   Chciuk, T. V; Hilmersson, G.; Flowers, R. A. *J. Org. Chem.* **2014**, *79*, 9441–9443.

(39)   Prasad, E.; Flowers, II, R. A. *J. Am. Chem. Soc.* **2005**, *127* (51), 18093–18099.

(40)   Parmar, D.; Price, K.; Spain, M.; Matsubara, H.; Bradley, P. A.; Procter, D. J. *J. Am. Chem. Soc.* **2011**, *133*, 2418–2420.

(41)   Yalavac, I.; Lyons, S. E.; Webb, M. R.; Procter, D. J. *Chem. Commun.* **2014**, *50*, 12863–12866.

(42)   Szostak, M.; Spain, M.; Procter, D. J. *J. Am. Chem. Soc.* **2014**, *136* (23), 8459–8466.

(43)   Johnston, D.; McCusker, C. M.; Procter, D. J. *Tetrahedron Lett.* **1999**, *40*, 4913–4916.

(44)   Szostak, M.; Spain, M.; Procter, D. J. *Nat. Protoc.* **2012**, *7* (5), 970–977.

(45)   Yacovan, A.; Hoz, S. *J. Am. Chem. Soc.* **1996**, *118* (11), 261–262.

(46)   Amiel-levy, M.; Hoz, S. *J. Am. Chem. Soc.* **2009**, *131*, 8280–8284.

(47)   Upadhyay, S. K.; Hoz, S. *J. Org. Chem.* **2011**, *76* (5), 1355–1360.

(48)   Chopade, P. R.; Prasad, E.; Flowers, II, R. A. *J. Am. Chem. Soc.* **2004**, *126* (1), 44–45.

(49)   Teprovich, J. A.; Balili, M. N.; Pintauer, T.; Flowers, II, R. A. *Angew. Chem. Int. Ed. Engl.* **2007**, *46* (43), 8160–8163.

(50)   Dahlén, A.; Hilmersson, G. *Tetrahedron Lett.* **2002**, *43*, 7197–7200.

(51)   Dahlén, A.; Sundgren, A.; Lahmann, M.; Oscarson, S.; Hilmersson, G. *Org. Lett.* **2003**, *5* (22), 4085–4088.

(52)   Dahlen, A.; Hilmersson, G. *Tetrahedron Lett.* **2003**, *44*, 2661–2664.

(53)   Davis, T. A.; Chopade, P. R.; Hilmersson, G.; Flowers, II, R. A. *Org. Lett.* **2005**, *7* (1), 119–122.

(54)   Ankner, T.; Hilmersson, G. *Org. Lett.* **2009**, *11* (3), 503–506.

(55)   Ankner, T.; Hilmersson, G. *Tetrahedron* **2009**, *65* (52), 10856–10862.

(56)   Szostak, M.; Sautier, B.; Spain, M.; Procter, D. *Org. Lett.* **2014**, *16*, 1092–1095.

(57)   Szostak, M.; Spain, M.; Eberhart, A. J.; Procter, D. J. *J. Org. Chem.* **2014**, *79* (24), 11988–12003.

(58)   Szostak, M.; Spain, M.; Procter, D. J. *Chem. - A Eur. J.* **2014**, *20* (15), 4222–4226.

(59)   Miller, R. S.; Sealy, J. M.; Shabangi, M.; Kuhlman, M. L.; Fuchs, J. R.; Flowers, II, R. A. *J. Am. Chem. Soc.* **2000**, *122*, 7718–7722.

(60) Reisman, S. E.; Ready, J. M.; Weiss, M. M.; Hasuoka, A.; Hirata, M.; Tamaki, K.; Ovaska, T. V.; Smith, C. J.; Wood, J. L. *J. Am. Chem. Soc.* **2008**, *130* (6), 2087–2100.

(61) Machrouhi, F.; Hamann, B.; Namy, J.-L.; Kagan, H. B. *Synlett* **1996**, *1996* (7), 633–634.

(62) Namy, J.-L.; Colomb, M.; Kagan, H. B. *Tetrahedron Lett.* **1994**, *35* (11), 1723–1726.

(63) Hamann-Gaudinet, B.; Namy, J.-L.; Kagan, H. B. *Tetrahedron Lett.* **1997**, *38* (37), 6585–6588.

(64) Hamann-Gaudinet, B.; Namy, J.-L.; Kagan, H. B. *J. Organomet. Chem.* **1998**, *567* (1–2), 39–47.

(65) Maisano, T.; Tempest, K. E.; Sadasivam, D. V; Flowers, II, R. A. *Org. Biomol. Chem.* **2011**, *9* (6), 1714–1716.

(66) Hioki, K.; Kono, K.; Tani, S.; Kunishima, M. *Tetrahedron Lett.* **1998**, *39* (29), 5229–5232.

(67) Concellón, J. M.; Bernad, P. L.; Huerta, M.; Garcia-Granda, S.; Diaz, M. R. *Chem. - A Eur. J.* **2003**, *9*, 5343–5347.

(68) Kunishima, M.; Hioki, K.; Kono, K.; Sakuma, T.; Tani, S. *Chem. Pharm. Bull. (Tokyo).* **1994**, *42* (10), 2190–2192.

(69) Kunishima, M.; Yoshimura, K.; Nakata, D.; Hioki, K.; Tani, S. *Chem. Pharm. Bull. (Tokyo).* **1999**, *47* (8), 1196–1197.

(70) Kunishima, M.; Tanaka, S.; Kono, K.; Hioki, K.; Tani, S. *Tetrahedron Lett.* **1995**,

36 (21), 3707–3710.

(71)   Kunishima, M.; Nakata, D.; Tanaka, S.; Hioki, K.; Tani, S. *Tetrahedron* **2000**, *56* (51), 9927–9935.

Chapter 2. Proton-Coupled Electron-Transfer in the Reduction of Arenes by SmI$_2$-H$_2$O

2.1 Background and Significance

2.1.1 The Role of Water in SmI$_2$ Reductions

The complex role of water in Sm-induced reductions has been a topic of interest since Kagan's initial report of enhanced product yield through the addition of proton donors.[1] The addition of water and alcohols to SmI$_2$ in THF has a significant impact on the selectivity and reactivity of the reagent.[2,3] A wide range of highly selective reductions and reductive coupling reactions have been carried out with high efficiency.[4] In each case, the effectiveness of the approach is dependent on proton donor concentration, competition for Sm(II) coordination between substrate, proton donor, and other reaction components. Functional group reductions and bond-forming reactions initiated by SmI$_2$-proton donor systems are complicated by the interplay between proton donor coordination to Sm(II) and their ability to donate a proton through cleavage of the O-H bond. Given this, proton donors employed in SmI$_2$ reactions are distinguished by those which have favorable steric and electronic properties that lead to a high affinity for Sm(II) (water, methanol, glycols) and those that do not (phenol, 2,2,2,-trifluoroethanol, t-butanol, etc.).[5,6]

Among Sm(II)-proton donor systems, those that employ water or coordinating proton donors are the most effective at reducing substrates typically recalcitrant to reduction through electron transfer.[3,4] The seminal work of Curran and Hasegawa demonstrated that water addition to SmI$_2$ accelerated the rate of functional group

reduction and they proposed that the effectiveness of the reducing system was a consequence of water coordination to Sm(II).[7] This hypothesis was later confirmed by Hoz and Flowers.[5,6,8–11] The mechanistic impact of proton donors on reductions involving SmI_2 have been subject to many studies over the last decade, but explanations for some observations have remained elusive, particularly with regard to the ability of SmI_2 to reduce substrates that lie well outside the expected range based on redox potentials alone.

2.1.2 Use of Arenes for Estimating Limiting Reducing Power

For the last few decades, the reduction of aromatic hydrocarbons has been used to estimate the limits of the reactivity of lanthanide metals toward organic substrates. Chauvin and coworkers were the first to show that SmI_2 could reduce anthracene to 9,10-dihydroanthracene as illustrated in Scheme 2.1, which has a reduction potential of 1.98 V vs. standard calomel electrode (SCE), but was ineffective in the reduction of arenes with higher reduction potentials.[12] The observed reactivity of SmI_2 toward anthracene is in contrast to the directly measured reduction potential of SmI_2 of -1.33 V vs Ag/AgCl measured by cyclic voltammetry by Flowers[13], but a thorough explanation of the discontinuity observed between observed reducing power and measured redox potential has not been forthcoming.

$E_{1/2}$ = -1.98 V
vs SCE
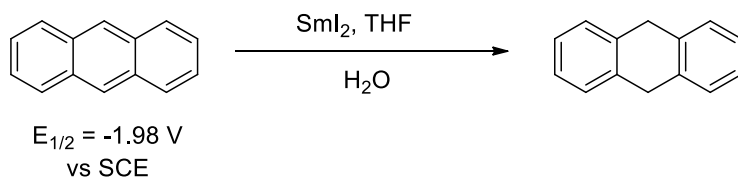
Scheme 2.1. Reduction of anthracene by SmI_2-H_2O.

Despite this discrepancy, arenes have been considered ideal model systems for determining the effective reduction potential of a reducing agent, primarily due to the large range of reduction potentials they span in addition to the absence of polar atoms such as oxygen that can promote coordination and thereby promote inner-sphere reactivity.

Although SmI_2 was shown to have a higher upper limit of reactivity than its reduction potential suggested, the reduction of arenes has continued to serve as a means of characterizing the reducing ability of many lanthanide-based reagent combinations. For instance, Hilmersson reduced a series of aromatic hydrocarbons spanning a large range of redox potentials to elucidate the limiting reducing power of the SmI_2-H_2O-amine and YbI_2-H_2O-amine reagent systems, which are too unstable to measure directly with cyclic voltammetry.[14] Successive experiments utilizing arenes as a method for estimating the reducing power of other Sm-based reagent combinations were performed by Procter.[15]

The generally-accepted mechanism through which the reduction of arenes is expected to proceed with SmI_2 is that of repeated sequential electron transfer (ET) and proton transfer (PT). As shown in Scheme 2.2, this stepwise mechanism mirrors that of other arene reductions with alkali metals such as the Birch reduction, and proceeds through a series of anionic intermediates.[14]
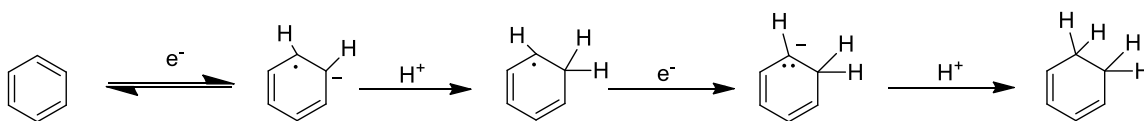
Scheme 2.2. Typical stepwise mechanism for the reduction of an unsaturated hydrocarbon.

Therefore, since arenes lack coordinating functionalities and are expected to proceed through a simple stepwise reduction mechanism, they are ideal model substrates for examination of the role of H_2O in a Sm-induced reduction. Additionally, understanding the mechanism through which they are reduced will conclusively confirm or deny whether they can be used to accurately estimate the redox potential of SmI_2-H_2O and other reduction systems.

2.1.2 Reduction of Alkyl Halides by SmI_2

The reduction of alkyl halides by SmI_2 and SmI_2-H_2O is a fairly well-understood mechanism, but a direct comparison under similar conditions to the reduction of an arene has not been previously reported. The generally-accepted mechanism of reduction of an alkyl or benzyl halide by SmI_2-H_2O is that of rate-limiting dissociative electron transfer as in Scheme 2.3.[11,16,17] By comparing and contrasting kinetic experiments for the reduction of an alkyl halide and an arene performed under similar conditions, the mechanism of the reduction of an arene can be elucidated.

$$I_2(H_2O)_n\text{-}Sm^{II} \ + \ I\diagup\!\!\diagdown C_{11}H_{23} \ \rightleftharpoons \ \left[I_2(H_2O)_n\text{-}Sm^{II}\text{-}\text{-}I\diagup\!\!\diagdown C_{11}H_{23} \right]^{\ddagger}$$

$$\downarrow$$

$$I_3(H_2O)_n\text{-}Sm^{III} \ + \ {}^{\bullet}\diagdown C_{11}H_{23} \ \xrightarrow{\ H^+\ } \ C_{12}H_{26}$$
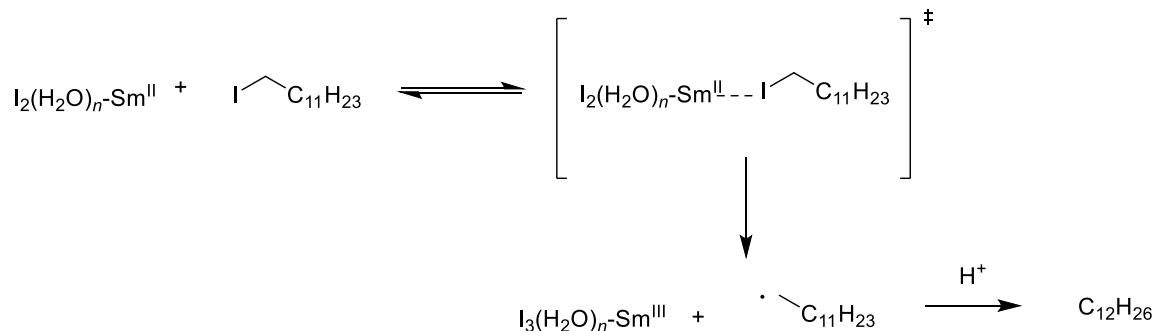
Scheme 2.3. Typical mechanism for the reduction of an alkyl halide (1-iodododecane) by $SmI_2\text{-}H_2O$.

The work in this chapter examines the role of water in the reduction of two non-coordinating substrates to compare and contrast the mechanism of reduction for each. The reduction of anthracene is compared to 1-iodododecane, which is known to reduce through a dissociative electron transfer mechanism, to reveal that water has a significantly greater impact on the rate of reduction of anthracene. This is attributed to the ability of H_2O to promote a proton-coupled electron-transfer (PCET) reduction of anthracene that enhances the reactivity of Sm(II) by bypassing a high-energy intermediate and provides an explanation for the discrepancy between the measured reduction potential and limit of reactivity observed in this area for decades.

2.2 Experimental Details

2.2.1 Materials

Samarium powder was purchased from Acros Organics. SmI_2 was generated by the standard method of samarium metal combined with iodine in THF and allowed to stir for a period of at least 4 hours. Iodometric titrations were performed to verify concentration of

SmI$_2$. Anthracene was purchased from Alfa Aesar. 1-Iodododecane was purchased from VWR. All other chemicals were used without further purification. Substrates were stored over sieves and deoxygenated prior to use. Tetrahydrofuran was purified by a solvent purification system (Innovative Technology Inc.; MA). H$_2$O, D$_2$O, methanol, and 2,2,2-trifluoroethanol were deoxygenated by bubbling through with argon overnight.

2.2.2 Instrumentation

Proton NMR spectra were recorded on a Bruker 500 MHz spectrometer in CDCl$_3$. Carbon NMR were performed at 125 MHz in CDCl$_3$. GC-MS analyses were done with an HP 5890 Series II Gas Chromatograph with an HP Mass Selector Detector. GC analyses were done using a Shimadzu Gas Chromatograph GC-14B with biphenyl standard. Kinetic experiments were performed with a computer-controlled SX.18 MV stopped-flow spectrophotometer (Applied Photophysics Ltd. Surrey, UK). The kinetic solutions were injected separately into the stopped-flow system from airtight Hamilton syringes prepared in a glove box. The cell block and the drive syringes of the stopped flow reaction analyzer were flushed a minimum of three times with dry, deoxygenated THF to make the system anaerobic. Between each experiment, the cell block was washed with dilute HNO$_3$ (2x), DI H$_2$O (3x), and THF (3x) before additional anhydrous deoxygenated THF washes (3x). The reaction rates were determined from the decay of SmI$_2$ at 560 nm.

2.2.3 Methods

2.2.3.1 General Procedure for Synthetic-Scale and GC-Yield SmI$_2$-H$_2$O Reductions

2.2.3.1.1 Procedure for GC Yields

Inside an Ar glove box, the quantity of substrate (9 mg anthracene, 0.05 mmol or 75 µL

iodododecane, 0.304 mmol) given above was combined with 2.5 equiv of 0.1 M SmI_2 in a vial with a magnetic stirrer. Following dissolution, the proton donor (100 equiv H_2O vs SmI_2) was diluted in 5 mL THF and added dropwise. The reaction was left until the mixture became colorless and a white precipitate formed. The vial was removed from the box and THF was removed via rotary evaporation. Product was extracted for GC yield with biphenyl-containing hexanes after quenching with 0.1 M HCl solution.

2.2.3.1.2 Work-up Procedure for Isolated Products

The above procedure was scaled up (100 mg anthracene and 100 μL 1-iodododecane). Each product was extracted using hexanes and washed with 0.1 M HCl and water. The organic layer was then treated with saturated aqueous sodium thiosulfate, and then brine. The remaining solution was then dried with magnesium sulfate, filtered, and then the solvent was removed by rotary evaporation. The resulting products were then placed under a high vacuum system to ensure complete removal of solvent. 9,10-Dihydroanthracene and dodecane were analyzed by GC-MS and NMR.

2.2.3.2 General Procedure for SmI_2-H_2O Stopped-Flow Kinetic Studies

Kinetic experiments were performed with a computer-controlled SX.18 MV stopped-flow spectrophotometer (Applied Photophysics Ltd. Surrey, UK). The SmI_2, substrate, and water solutions were injected separately into the stopped-flow system from airtight Hamilton syringes prepared in a glove box. The cell block and the drive syringes of the stopped flow reaction analyzer were flushed a minimum of three times with dry, degassed THF to make the system anaerobic. The reaction rates were determined from the decay of SmI_2 at 560 nm. Unless specified otherwise, all kinetic measurements for the reduction of anthracene were

carried out at 25 $^{\circ}$C and reductions of 1-iodododecane at 35 $^{\circ}$C.

2.2.3.3 General Procedure for SmI$_2$-H$_2$O UV-vis Studies

Spectra were obtained using the Spectra setting on the stopped-flow spectrophotometer. One solution of SmI$_2$ was generated for one syringe to remain at a constant concentration while concentration of additive/s or substrate was changed in the other syringe. All spectra were measured at 25 $^{\circ}$C.

2.3 Results and Discussion

To study the mechanism of the reduction of anthracene and compare it to 1-iodododecane, kinetic and thermodynamic experiments including rate order, kinetic isotope, bulk protonation, activation parameter studies were carried out primarily using stopped-flow spectrophotometry.

2.3.1 Kinetic Analysis for the Reduction of 1-Iodododecane

2.3.1.1 Kinetic Order Experiments

To determine the order of each component of the reaction, rates were measured under pseudo-first order conditions. The order for each component was determined independently. The rate order of SmI$_2$ was determined using fractional times method. The rate order of 1-iodododecane was determined with a fixed concentration of H$_2$O where the order of H$_2$O was 2 to remain at a synthetically-relevant proton donor concentration. Similar to previous studies on the mechanistic role of water, an increasing in rate corresponding to saturation was obtained as in Figure 2.1.
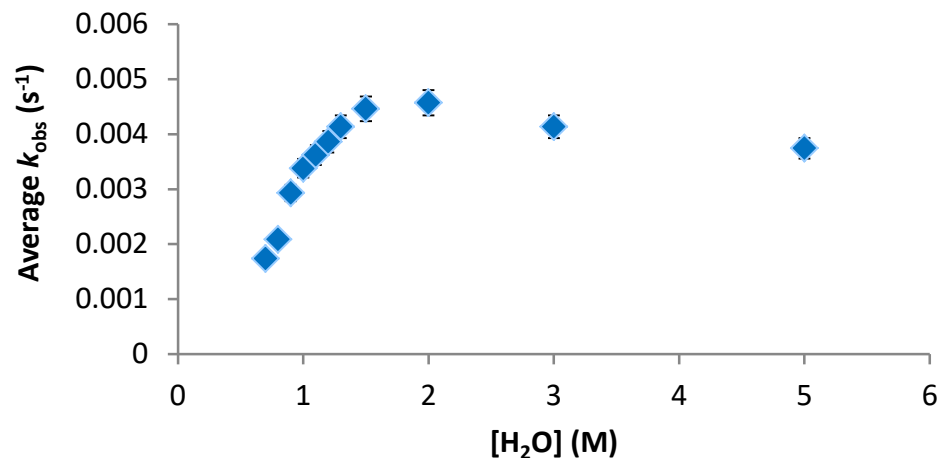
Figure 2.1. Influence of $[H_2O]$ on the rate of reduction of 100 mM 1-iodododecane by 10 mM SmI_2.

Table 2.1. Rate data for the reduction of 1-Iodododecane by SmI_2-H_2O.

Reaction Component	Rate Order
SmI_2	1^a
1-Iodododecane	1.1 ± 0.1^b
Water	$2 \pm 0.1 \ (0\text{-}1.2 \text{ M})^c$

Conditions: [a]Fractional times method. 10 mM SmI_2, 100 mM 1-iodododecane, 0.7- 1.2 M H_2O. [b]10 mM SmI_2, 100-300 mM 1-iodododecane, 1 M H_2O. [c] 10 mM SmI_2, 100 mM 1-iodododecane, 0-1.75M H_2O. The rate orders are the average of 3 independent experiments.

2.3.1.2 Activation Parameters

Activation parameters for the reduction of 1-iodododecane were determined by measuring the rate of reduction with fixed concentrations of all components over a range of 30 °C and preparing an Eyring plot to solve for each parameter.
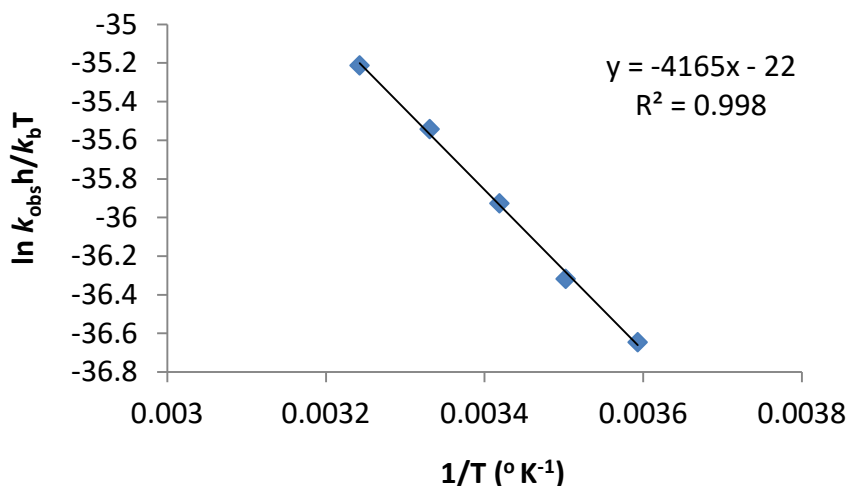
Figure 2.2. Erying plot for the rate of reduction of 100 mM 1-iodododecane by 10 mM SmI$_2$ and 1 M H$_2$O from 5-35 $^\circ$C.

Table 2.2. Activation parameters for the reduction of 1-Iodododecane by SmI$_2$-H$_2$O.

$\Delta H^\ddagger$ (kcal/mol)	$\Delta S^\ddagger$ (cal/mol*K)	$\Delta G^\ddagger$ (kcal/mol)	E_a (kcal/mol)
8.6 ± 1	-42 ± 1	21 ± 1	9.2 ± .2

Conditions: 10 mM SmI$_2$ and 100 mM 1-iodododecane in THF. The activation parameters are the average of 3 independent experiments from 5-35 $^\circ$C and are reported as ± σ. [a]Obtained from $\ln(k_{obs}h/k$T)- $\Delta H^\ddagger$/RT + $\Delta S^\ddagger$/R. [b]Calculated from $\Delta G^\ddagger = \Delta H^\ddagger$-T$\Delta S^\ddagger$.

2.3.1.3 Proposed Mechanism

The proposed mechanism of reduction for 1-iodododecane is consistent with other studies on the reduction of alkyl halides by SmI$_2$. The rate of reduction is consistent with the difference in thermodynamic redox potentials and is enhanced by the increase in redox potential as water is added.[11,18] This data is consistent with the reduction proceeding through a dissociative electron transfer as described above in Scheme 2.3.

51

2.3.2 Kinetic Analysis for the Reduction of Anthracene

2.3.2.2 Pseudo-First Order Rate Data

The rate of reduction of anthracene was examined using pseudo-first order conditions. The first variable examined was the influence of water. Increasing the concentration of water led to a significant increase in the rate of reduction by over an order of magnitude, as shown in Figure 2.3.
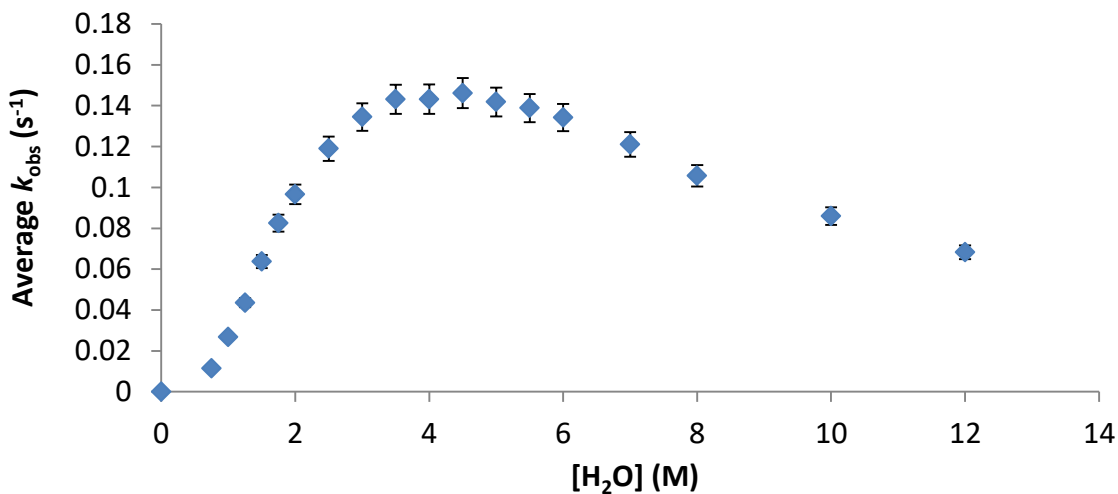
Figure 2.3. Influence of [H_2O] on the rate of reduction of 100 mM anthracene by 10 mM SmI$_2$.

The rate order of water varies with concentration, but is second order in the typical range of concentrations utilized in synthetic reactions. Another interesting aspect of the data is that water has a detrimental effect on rate at very high concentrations. This suggests that water must be displaced to allow substrate access to the metal center for reduction to occur.

Since the order of water was 2 in the typical range of synthetic conditions, subsequent experiments to examine the role of other components were performed with

100 equivalents of water to maintain consistency and are provided in Table 2.3. Additional kinetic order experiments revealed that the rate order of anthracene and SmI_2 were both approximately 1. First order in anthracene and samarium is consistent with rate-limiting electron transfer from samarium to substrate, as expected. The higher order obtained for water at synthetically-relevant concentrations suggests a complex role for water.

Table 2.3. Rate data for the reduction of anthracene by SmI_2-H_2O.

Reaction Component	Rate Order
SmI_2	1[a]
Anthracene	0.9 ± 0.1[b]
Water	2.0 ± 0.1 (0-1.75 M)

Conditions: [a]Fractional times method. 10 mM SmI_2, 100 mM anthracene, 0.75-2M H_2O. [b]5 mM SmI_2, 60-100 mM anthracene, 500 mM H_2O. [c]10 mM SmI_2, 100 mM anthracene, 0-1.75M H_2O. The rate orders are the average of 3 independent experiments.

2.3.2.3 Kinetic Isotope Effect

The rate of reduction of anthracene was measured with a range of concentrations of both H_2O and D_2O to determine whether protonation was involved in the rate-limiting step. Figure 2.4 shows that the rate of reduction with D_2O is consistently lower and as seen in the inset, the k_H/k_D is consistently around 1.7.
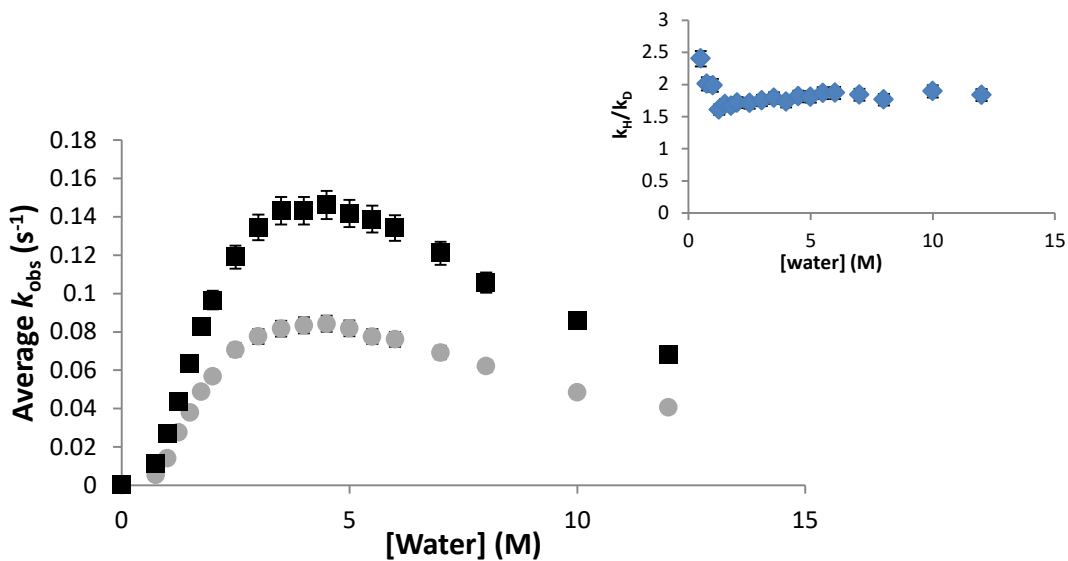
Figure 2.4. Comparison of the rates of reduction of anthracene with SmI_2-H_2O (■) and SmI_2-D_2O (●). Inset: k_H/k_D plot vs. [water].

Because D_2O and H_2O molecules are significantly different in size and the chemistry of Sm(II) is strongly influenced by sterics, the coordination of H_2O and D_2O to Sm(II) were compared using UV-vis to determine if the observed kinetic isotope effect was a result of differences in coordination. As shown in Figure 2.5, the influence of H_2O compared to D_2O on the spectrum of SmI_2 appears nearly identical, and thus it is unlikely that the observed kinetic isotope effect is a consequence of coordination differences.
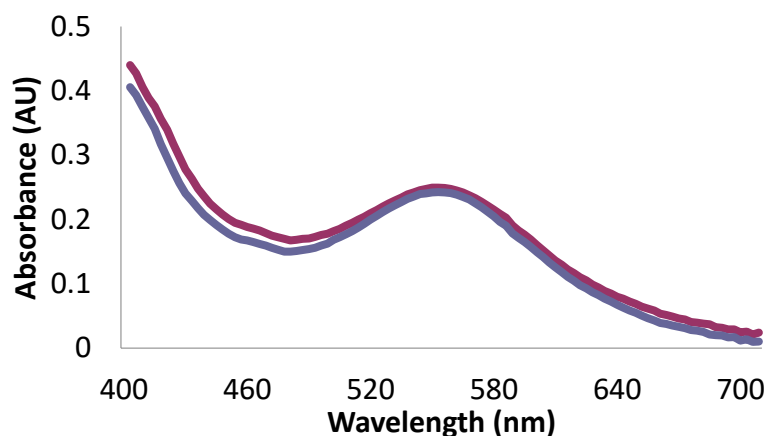
Figure 2.5. Comparison of the visible spectrum of SmI$_2$-H$_2$O (magenta) and SmI$_2$-D$_2$O (purple) at 5 mM SmI$_2$.

For this case, the k_H/k_D determined for the reduction of anthracene is a primary isotope effect. A k_H/k_D value greater than unity is typically indicative of a rate-limiting proton transfer event. From a classical perspective, when this study is combined with the activation parameters displayed in Table 2.4 below, this data is consistent with a highly ordered early transition state where very little O-H(D) bond cleavage has occurred and very little C-H(D) bond formation has taken place in the activated complex. In this case, the isotope effect is predicted to be small since the zero point vibrational energy differences for H and D between the reactant and transition state are small. This offers an explanation for the low but still primary isotope effect and suggests that protonation is an important aspect of the mechanism.

2.3.2.4 Activation Parameters

The activation parameters were determined by measuring the rate of reduction under constant concentrations over a range of temperatures. To be consistent with

synthetically-relevant conditions, 1 M H_2O was used, the point at which the order of water is 2. The very small enthalpy of activation suggests that the transition state has very little bond reorganization, which suggests the transition state closely resembles the starting materials. There is also a very large negative entropy of activation value, which is consistent with a highly-ordered transition state.

Table 2.4. Calculated activation parameters for the reduction of anthracene by SmI_2-H_2O.

$\Delta H^{\ddagger}$ (kcal/mol)	$\Delta S^{\ddagger a}$ (cal/mol*K)	$\Delta G^{\ddagger a}$ (kcal/mol)	E_a^{b} (kcal/mol)
0.1	-64.1	19.24	0.74

Conditions: 10 mM SmI_2 and 100 mM anthracene in THF. The activation parameters are the average of 3 independent experiments from 20-40 °C and are reported as ±σ. [a]Obtained from $\ln(k_{obs}h/kT)$- $\Delta H^{\ddagger}/RT$ + $\Delta S^{\ddagger}/R$. [b]Calculated from $\Delta G^{\ddagger}$= $\Delta H^{\ddagger}$-$T\Delta S^{\ddagger}$.

2.3.2.5 Bulk Protonation Study

In a previous study, the Hoz group proposed that two modes of proton transfer could be discerned: protonation arising from coordinated proton donor and that of bulk protonation. The highly acidic but non-coordinating proton donor, 2,2,2-trifluoroethanol (TFE) was used as a bulk source of protons in the reduction of 1,1-diaryl-2,2-dicyanoethylene to distinguish between these two types of protonation.[9] Using this approach, if protonation of anthracene arose from the bulk solution rather than from metal-coordinated water, the presence of a more acidic non-coordinating proton source would increase the rate of reduction. For this experiment, the rate of reduction with water was compared to that of an equal concentration mixture of TFE and water. Figure 2.6 indicates that there is a negative rather than positive effect on the rate of reduction in the

presence of TFE, which suggests bulk protonation is not occurring and is therefore not enhanced in the presence of TFE.
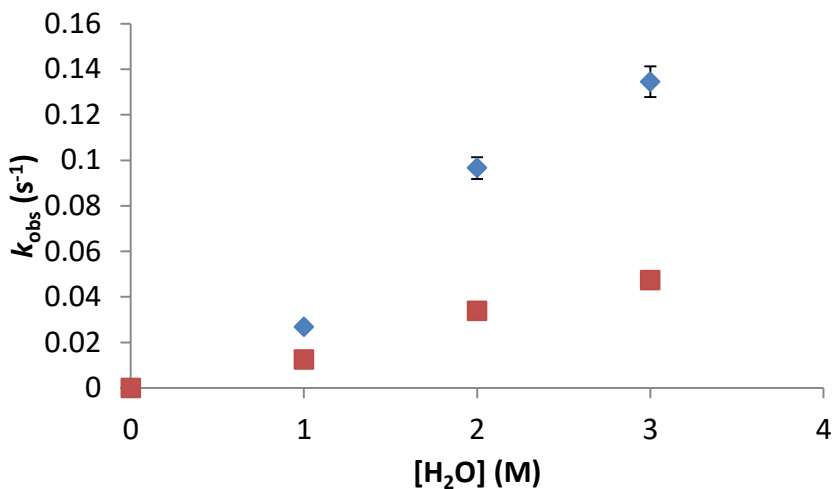
Figure 2.6. Plot of k_{obs} vs. [H_2O] for the reduction of 100 mM anthracene in the presence of an equal concentration of TFE and water (■) and with only water (◆).

2.3.2.6 Proposed Mechanism

Although the stepwise mechanism provided in Scheme 2.2 was the expected mode of reduction with SmI_2-H_2O, the experimental data is consistent with an alternative mechanism. Experimental data including kinetic isotope effect, activation parameters, and bulk protonation experiments supported simultaneous proton and electron transfer, which is indicative of a transition state such as the one shown in Scheme 2.4.
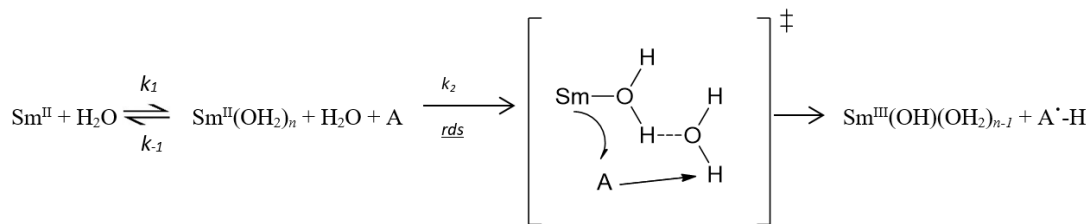
Scheme 2.4. Proposed mechanism for the reduction of anthracene by SmI_2-H_2O.

2.3.2.7 Steady-State Approximation

To further investigate the feasibility of a coupled electron and proton transfer, the steady-state approximation was applied to derive a rate expression. Based on the above proposed mechanism, the empirical rate expression can be expressed as Equation 2.1.

$$-d[Sm^{II}] = k_2[Sm(H_2O)][H_2O][A]$$
$$\overline{\phantom{-d[Sm^{II}]}}$$
$$dt \qquad\qquad\qquad\qquad\qquad\qquad\qquad\qquad (2.1)$$

If the steady state approximation is assumed for $Sm(H_2O)$:

$$-d[Sm(H_2O)_n] = k_1[Sm^{II}][H_2O]-k_{-1}[Sm(H_2O)_n]-k_2[Sm(H_2O)_n][H_2O][A]= 0$$
$$\overline{}$$
$$dt$$

The concentration of $Sm(H_2O)_n$ can be assumed to be equal to:

$$[Sm(H_2O)_n] = \frac{k_1[Sm^{II}][H_2O]}{k_{-1} + k_2[H_2O][A]}$$

Substituted into the rate expression yields:

$$-d[Sm^{II}]/dt = \frac{k_1k_2[Sm^{II}][H_2O][H_2O][A]}{k_{-1} + k_2[H_2O][A]}$$

The contribution from the slow step, $k_2[H_2O][A]$, is assumed to be small and provides:

$$-d[Sm^{II}] = K_1k_2[Sm^{II}][H_2O]^2[A] \qquad\qquad\qquad (2.2)$$
$$\overline{\phantom{-d[Sm^{II}]}}$$
$$dt$$

Therefore, both empirical (**Equation 2.1**) and steady-state derived (**Equation 2.2**) rate laws are consistent with the involvement of proton and electron transfer in the rate-limiting step.

2.3.2.8 Proton-Coupled Electron-Transfer as a Mechanism

It is important to consider the present results in the context of earlier studies of the Sm(II)-water system and classic studies on proton transfer to arene radical anions. Previous studies have demonstrated that water has a high affinity for Sm(II).[5,6,19,20] Coordination of water to the Lewis acidic Sm increases the acidity of the O-H bond.[21] Concomitant with this process, the ease of oxidation of Sm(II) is enhanced by producing a more powerful reductant.[11] In other words, as water coordinates to Sm(II) a more powerful reductant is formed in concert with a better proton donor.

This simultaneous increase in Lewis acidity and decrease in ligand pK_a has been observed for other metal-ligand complexes as well.[22–25] In a well-characterized example, the Kovacs group showed the effects of the individual electron and proton transfer on the Lewis acidity and reducing power of an Fe(II)-H_2O complex ($[Fe^{II}(O^{Me2}N_4(tren))(H_2O)]^+$), as shown in the thermochemical cycle in Figure 2.7.[22] In this example, the transfer of a proton from Fe(II)-H_2O (**I**) leads to a stronger reductant(**III**), although the initial transfer of the proton is more difficult to achieve than the alternative stepwise process where an electron is transferred at a lower potential(**II**) but leads to a lowering of the pK_a. By undergoing concomitant proton and electron transfer, the bond dissociation free energy (BDFE) of the metal-bound water is significantly lowered, providing a more facile reduction through a formal hydrogen atom transfer (HAT). This data clearly showed that the coordination of H_2O to a low valent metal favors a coupled electron and proton transfer process because it increases the reducing power of the metal while simultaneously increasing the Lewis acidity and weakening the O-H bond.[22] Unfortunately, since a measure of the pK_a's of H_2O bound to

Sm^{II} and Sm^{III} are not readily accessible at this time, a similar thermochemical cycle cannot be fully calculated, although an analogous series of relationships would be expected for Sm-bound H$_2$O.
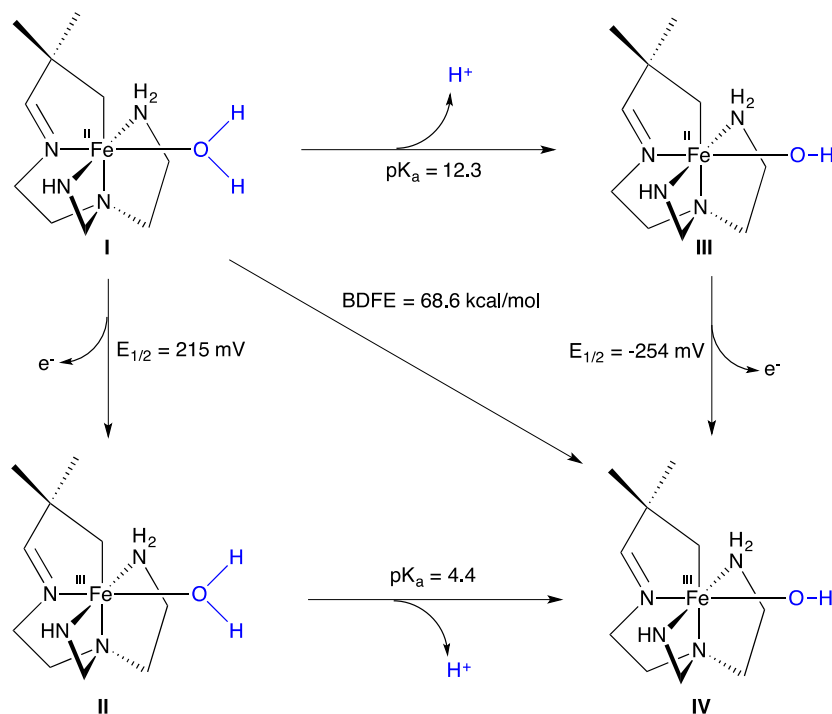
Figure 2.7. Thermochemical cycle for ([Fe^{II}(O^{Me2}N$_4$(tren))(H$_2$O)]$^+$). [22]

In addition to work on Sm(II)-water complexes, there is a great deal of classic work on the protonation of anthracene radical anions by water and other proton donors.[26–29] An early report by Bank found that protonation of the sodium-generated anthracene radical anion by water in THF occurred through water bound to the sodium countercation.[26]

In light of the data and framework from previous studies, the question that arises is: What is the procession of events that leads to the initial electron and proton transfer in the reduction of anthracene by Sm(II)-water? To answer this question, it is useful to keep

a number of points in mind: 1) SmI_2 is incapable of reducing anthracene in the absence

of water. 2) Addition of successive amounts of water to SmI_2 in THF likely drives

coordination, resulting in the formation of a Sm(II)-water complex. 3) Reduction of

anthracene initiates with amounts of water well below that required to influence the

reducing power of SmI_2. 4) The rate order of water is 2 and the KIE experiment

provided a k_H/k_D of 1.7. 5) The rate law describing the reduction provides the

stoichiometry of the activated complex relative to reactants but only the transition state

for the rate-limiting step can be probed with any certainty.[21]

Given the points above, there are several possible events that can occur in the

initial electron-proton transfer from the Sm(II)-H_2O complex to anthracene: 1) A rate-

limiting electron transfer (ET) followed by a proton transfer (PT);[30] 2) An ET followed

by a rate-limiting PT, or 3) a PCET. The key difference between the two stepwise

mechanisms (1 and 2) and 3 is whether the electron and proton are transferred

sequentially or in one kinetic step.

In a classic review, Mayer notes that it is a common supposition that stepwise

transfers of a proton and electron are favored over a concerted PCET, but this intuition is

incorrect in most cases since ΔG is always lower for PCET than ΔG for the initial PT or

ET.[31] Although sequential ET-PT is the accepted process in the chemistry of Sm(II)

reductions and reductive couplings, bond-weakening processes are extremely common in

the PCET literature for a wide range of complexes that lead to significant weakening of

N-H and O-H bonds.[32–38] In the present case, concerted transfer of a proton and electron

from Sm(II)-H_2O to anthracene is thermodynamically equivalent to a hydrogen atom

transfer between the same reactants, which as a consequence provides information about changes in the homolytic bond dissociation energy of the O-H bond of water upon binding to samarium.

2.3.2.9 Bond-Weakening Implication

A thermochemical analysis of the data allows for the calculation of the bond-weakening of bound water to SmI_2. The bond dissociation energy (BDE) of the O-H bond of water is 117.6 kcal/mol.[39]   However, the BDE of the initial radical formed via hydrogen atom transfer to anthracene is comparably weak, with a value of 44.9 kcal/mol.[40] This analysis demonstrates that the BDE of the O-H bond in the Sm(II)-H_2O complex is decreased by at least 72.7 kcal/mol.
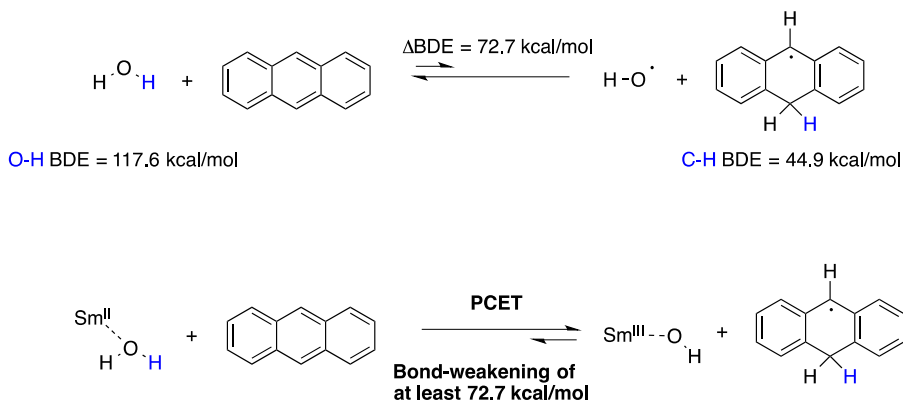
Figure 2.8. Explanation of the bond-weakening of water bound to samarium derived from the reduction of anthracene.

Bond weakening of water is well precedented in the literature. In the pioneering work of Wood and Renaud, it was shown that borane-water or borane-alcohol complexes could be used as H-atom donors to radicals.[41,42] In 1997, Stack demonstrated that

coordination of alcohols to non-heme iron models of lipoxygenases significantly reduces the O-H bond strength of the bound ligand.[43] More recently, experiments by Cuerva and coworkers revealed that water bound to $Cp_2Ti^{III}Cl$ decreased the O-H BDE by approximately 60 kcal/mol.[44,45] As a consequence, Ti^{III}-water complexes serve as efficient H-atom donors for alkyl radicals. These findings were exploited in elegant work by Knowles in the development of a catalytic bond-weakening protocol for the conjugate amination.[46] In each of the examples cited above, bond weakening is significant but the decrease in the O-H bond of the Sm(II)-H_2O complex of at least 72.7 kcal/mol derived from the analysis shown in Figure 2.7, is the largest reported to date. It should also be noted that although this bond-weakening is quite large, it is merely an example and does not necessarily represent the upper limit of this effect.

2.3.3. Comparison of 1-Iodododecane to Anthracene

The results of these kinetic experiments are consistent with other reports that examined the mechanism of reduction of alkyl halides with this system, but the advantage of these experiments is that they were carried out under identical conditions, which allowed for the first direct comparison of an arene and alkyl halide reduction. As is evident in Figure 2.8, the impact of water on the rate of the reduction of anthracene is significantly greater than that of 1-iodododecane.

63
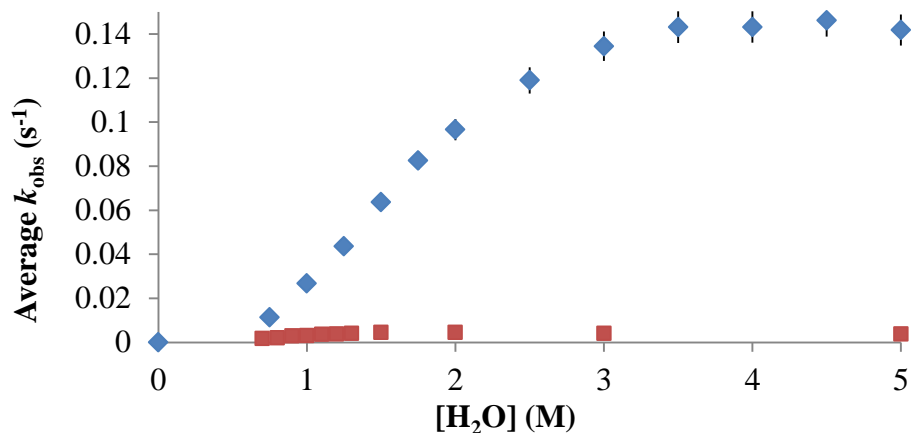
Figure 2.9 Comparison of the influence of water on the reduction of anthracene (◆) and 1-iodododecane (■).

The large difference in rates is a consequence of the difference in the proposed mechanisms for each. Since experimental data suggests that anthracene is reduced through a concerted PCET, high-energy intermediates are bypassed; as a result, the reduction of anthracene is more facile than the electron transfer that occurs in the reduction of an alkyl halide even though, as shown in Scheme 2.5, the reduction of anthracene should be a more endothermic process. This large observed difference in substrates provides further support for the proposed mechanism of PCET for the reduction of anthracene.

$\Delta G^{\circ} = 25$ kcal/mol

SmI$_2$ + [anthracene]

$E_{1/2} = -0.89$ V vs SCE

$E_{1/2} = -1.98$ V vs SCE

$\Delta G^{\circ} = 0.2$ kcal/mol

SmI$_2$ + C$_{12}$H$_{25}$-I $\longrightarrow$ SmI$_3$ + $^{\bullet}$C$_{12}$H$_{25}$

$E_{1/2} = -0.89$ V vs SCE

$E_{1/2} = -0.9$ V vs SCE
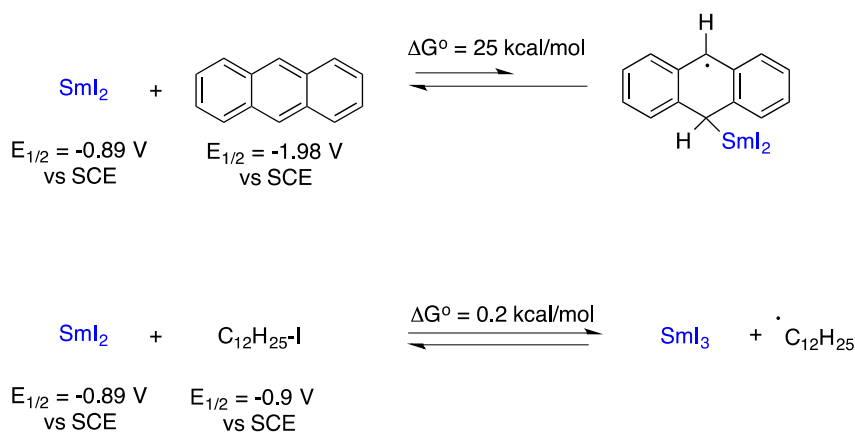
Scheme 2.5 Comparison of the relative reduction potentials and resulting ΔG values for the reduction of 1-iodododecane and anthracene.

2.4 Conclusions

Overall, the collection of studies and experimental work described herein support a PCET for the reduction of anthracene by SmI$_2$ containing water in concentrations of that are typically employed in reductions. Although the majority of the work described above is focused within this modest concentration range, it is useful to consider why higher concentrations of water lead to saturation and eventual inverse order of the proton donor. As higher concentrations of water are added, THF and iodide are displaced from the coordination sphere of Sm(II) and replaced by water.[20] Once Sm(II) is saturated, additional water is likely to hydrogen bond in the second coordination sphere. Second sphere interactions are recognized to be of importance to rare earth-mediated reactions.[47] In the present case, anthracene would have to displace water in the second coordination sphere leading to a change in the mechanism where water displacement is likely rate-limiting. A caveat with this hypothesis is the fact that as high amounts of water are added

to THF, the solvent polarity changes significantly and as a consequence may impact the mechanism of ET.[48,49]

One final point to consider is whether arenes are a suitable measure of the redox potential of Sm(II)-H_2O or other coordinating proton donor systems. Classic studies on the reduction of arenes by rare-earth reductants in the absence of any additive showed that arene dimerization occurred through radical-radical coupling.[50,51] The present study shows that SmI_2 alone is incapable of reducing anthracene and that the reduction initiates at concentrations of water below the level where it impacts the reducing power of Sm(II) and is inhibited at higher concentrations where the proton donor has a maximal impact on the redox potential of the metal. Additionally, the concerted nature of the ET-PT makes estimation of the redox potential tenuous at best. Given this, these results suggest that arenes are not an ideal indicator of redox potential for SmI_2-water systems given the mechanistic complexity of the reaction.

The results described in this chapter show that the reduction of an arene by SmI_2 containing modest concentrations of water proceeds through a highly-ordered transition state where the initial transfer of an electron and proton proceed through PCET. The kinetic and thermodynamic data contrast strongly with the electron transfer process observed for the reduction of 1-iodododecane. The complexity of the reduction resulting from PCET shows that care should be employed when interpreting deuterium isotope effects or mechanisms deduced from empirical models based on knowledge of ground state reductants and reaction products alone. Although the studies presented herein reveal the complexity of arene reduction by Sm(II)-water, these results may have an

important impact for the reduction of other functional groups and the exploration of the bond-weakening that results from coordination to low valent metals as well. This is especially important for carbonyls and related functional groups that are commonly present in SmI_2-H_2O reactions and are likely to compete with water for coordination to Sm(II), a concept which is further explored in the following chapters.

2.5 References

(1)   Girard, P.; Namy, J. L.; Kagan, H. B. *J. Am. Chem. Soc.* **1980**, *102* (8), 2693–2698.

(2)   Szostak, M.; Spain, M.; Parmar, D.; Procter, D. J. *Chem. Commun.* **2012**, *48*, 330–346.

(3)   Dahlén, A.; Hilmersson, G. *Eur. J. Inorg. Chem.* **2004**, *2004* (17), 3393–3403.

(4)   Chciuk, T. V.; Flowers, II, R. A. In *Science of Synthesis*; Marek, I., Ed.; Georg Thieme Verlag KG: Stuttgart, 2016; pp 177–261.

(5)   Yacovan, A.; Hoz, S. *J. Am. Chem. Soc.* **1996**, *118* (11), 261–262.

(6)   Chopade, P. R.; Prasad, E.; Flowers, II, R. A. *J. Am. Chem. Soc.* **2004**, *126* (1), 44–45.

(7)   Hasegawa, E.; Curran, D. P. *J. Org. Chem.* **1993**, *58*, 5008–5010.

(8)   Tarnopolsky, A.; Hoz, S. *J. Am. Chem. Soc.* **2007**, *129* (11), 3402–3407.

(9)   Tarnopolsky, A.; Hoz, S. *Org. Biomol. Chem.* **2007**, *5*, 3801–3804.

(10)   Amiel-levy, M.; Hoz, S. *J. Am. Chem. Soc.* **2009**, *131*, 8280–8284.

(11)   Prasad, E.; Flowers, II, R. A. *J. Am. Chem. Soc.* **2005**, *127* (51), 18093–18099.

(12)   Chauvin, Y.; Olivier, H.; Saussine, L. *Inorganica Chim. Acta* **1989**, *161* (1), 45–

47.

(13) Shabangi, M.; Flowers, II, R. A. *Tetrahedron Lett.* **1997**, *38* (7), 1137–1140.

(14) Dahlén, A.; Nilsson, A.; Hilmersson, G. *J. Org. Chem.* **2006**, *71* (4), 1576–1580.

(15) Szostak, M.; Spain, M.; Procter, D. J. *J. Org. Chem.* **2014**, *79* (6), 2522–2537.

(16) Andrieux, C. P.; Gallardo, I.; Saveant, J. M. *J. Am. Chem. Soc.* **1989**, *111* (5), 1620–1626.

(17) Andrieux, C. P.; Gorande, A. L.; Savéant, J.-M. *J. Am. Chem. Soc.* **1992**, *114* (17), 6892–6904.

(18) Prasad, E.; Flowers, II, R. A. *J. Am. Chem. Soc.* **2002**, *124*, 6895–6899.

(19) Teprovich, J. A.; Balili, M. N.; Pintauer, T.; Flowers, II, R. A. *Angew. Chem. Int. Ed. Engl.* **2007**, *46* (43), 8160–8163.

(20) Sadasivam, D. V; Teprovich, J. A.; Procter, D. J.; Flowers, II, R. A. *Org. Lett.* **2010**, *12* (18), 4140–4143.

(21) Neverov, A. A.; Gibson, G.; Brown, R. S. *Inorg. Chem.* **2003**, *42* (1), 228–234.

(22) Brines, L. M.; Coggins, M. K.; Poon, P. C. Y.; Toledo, S.; Kaminsky, W.; Kirk, M. L.; Kovacs, J. A. *J. Am. Chem. Soc.* **2015**, *137* (6), 2253–2264.

(23) Mayer, J. M.; Rhile, I. J. *Biochim. Biophys. Acta - Bioenerg.* **2004**, *1655* (1–3), 51–58.

(24) Warren, J. J.; Mayer, J. M. *J. Am. Chem. Soc.* **2011**, *133* (22), 8544–8551.

(25) Mayer, J. M. *J. Phys. Chem. Lett.* **2011**, *2*, 1481–1489.

(26) Bank, S.; Bockrath, B. *J. Am. Chem. Soc.* **1972**, *94*, 6076–6083.

(27) Minnich, E. R.; Long, L. D.; Ceraso, M.; Dye, J. L. *J. Am. Chem. Soc.* **1973**, *95*

(4), 1061–1070.

(28)   Papadakis, N.; Dye, J. L. *J. Phys. Chem.* **1978**, *82* (10), 1111–1114.

(29)   Nielsen, M. F.; Ingold, K. U. *J. Am. Chem. Soc.* **2006**, *128* (4), 1172–1182.

(30)   Szostak, M.; Spain, M.; Procter, D. J. *J. Org. Chem.* **2014**, *79* (6), 2522–2537.

(31)   Mayer, J. M. *Annu. Rev. Phys. Chem.* **2004**, *55*, 363–390.

(32)   Roth, J. P.; Mayer, J. M. *Inorg. Chem.* **1999**, *38* (12), 2760–2761.

(33)   Manner, V. W.; Mayer, J. M. *J. Am. Chem. Soc.* **2009**, *131* (29), 9874–9875.

(34)   Fang, H. Y.; Ling, Z.; Lang, K.; Brothers, P. J.; de Bruin, B.; Fu, X. F. *Chem. Sci.* **2014**, *5* (3), 916–921.

(35)   Wu, A.; Mayer, J. M. *J. Am. Chem. Soc.* **2008**, *130* (44), 14745–14754.

(36)   Wu, A.; Masland, J.; Swartz, R. D.; Kaminsky, W.; Mayer, J. M. *Inorg. Chem.* **2007**, *46* (26), 11190–11201.

(37)   Milsmann, C.; Semproni, S. P.; Chirik, P. J. *J. Am. Chem. Soc.* **2014**, *136* (34), 12099–12107.

(38)   Estes, D. P.; Grills, D. C.; Norton, J. R. **2014**, *4*, 4–7.

(39)   Ruscic, B.; Wagner, A. F.; Harding, L. B.; Asher, R. L.; Feller, D.; Dixon, D. A.; Peterson, K. A.; Song, Y.; Qian, X.; Ng, C. Y.; Liu, J.; Chen, W.; Schwenke, D. W. *J. Phys. Chem. A* **2002**, *106* (11), 2727–2747.

(40)   Stein, S. E.; Brown, R. L. *J. Am. Chem. Soc.* **1991**, *113* (3), 787–793.

(41)   Spiegel, D. A.; Wiberg, K. B.; Schacherer, L. N.; Medeiros, M. R.; Wood, J. L. *J. Am. Chem. Soc.* **2005**, *127* (36), 12513–12515.

(42)   Pozzi, D.; Scanlan, E. M.; Renaud, P. *J. Am. Chem. Soc.* **2005**, *127* (41), 14204–

14205.

(43)   Jonas, R. T.; Stack, T. D. P. *J. Am. Chem. Soc.* **1997**, *119*, 8566–8567.

(44)   Cuerva, J. M.; Campaña, A. G.; Justicia, J.; Rosales, A.; Oller-López, J. L.; Robles, R.; Cárdenas, D. J.; Buñuel, E.; Oltra, J. E. *Angew. Chemie - Int. Ed.* **2006**, *45* (33), 5522–5526.

(45)   Paradas, M.; Campaña, A. G.; Jiménez, T.; Robles, R.; Oltra, J. E.; Buñuel, E.; Justicia, J.; Cárdenas, D. J.; Cuerva, J. M. *J. Am. Chem. Soc.* **2010**, *132* (36), 12748–12756.

(46)   Tarantino, K. T.; Miller, D. C.; Callon, T. A; Knowles, R. R. *J. Am. Chem. Soc.* **2015**, *137*, 6440–6443.

(47)   Robinson, J. R.; Gordon, Z.; Booth, C. H.; Carroll, P. J.; Walsh, P. J.; Schelter, E. J. *J. Am. Chem. Soc.* **2013**, *135* (50), 19016–19024.

(48)   Chciuk, T. V; Hilmersson, G.; Flowers, R. A. *J. Org. Chem.* **2014**, *79*, 9441–9443.

(49)   Chopade, P. R.; Davis, T. A.; Prasad, E.; Flowers, II, R. A. *Org. Lett.* **2004**, *6* (16), 2685–2688.

(50)   Evans, W. J.; Gonzales, S. L.; Ziller, J. W. *J. Am. Chem. Soc.* **1994**, *116* (6), 2600–2608.

(51)   Fedushkin, I. L.; Bochkarev, M. N.; Dechert, S.; Schumann, H. *Chem. - A Eur. J.* **2001**, *7* (16), 3558–3563.

Chapter 3. Glycols as Hydrogen Atom Transfer Promoters in Reactions by SmI$_2$

3.1 Background and Significance

3.1.1 Use of Chelating Alcohols in Synthetic SmI$_2$ Reductions

Coordinating alcohols have been employed to enhance the reaction rate and act as a proton source in SmI$_2$ reactions over the past twenty years.[1–5] One attractive aspect of their use is that in many cases they can be utilized as an acceptable alternative to water, which is especially useful when working under anhydrous conditions or with water-sensitive substrates. Typical alcohols for these applications can include methanol, 2,2,2-trifluoroethanol (TFE), *t*-butanol, isopropanol, ethylene glycol (eg), and diethylene glycol (dg).

In some cases, however, glycols have shown unique reactivity. For example, Procter showed that 6-substituted uracils could be synthesized from barbituric acid derivatives using SmI$_2$ combined with eg, as in Scheme 3.1, and it was found that the addition of water instead led to an alternative mechanism that yielded 5-substituted product through a 1,2-reduction. The difference in product distribution and mechanism was explained by eg-assisted dehydration followed by a 1,2 shift of the isobutyl moiety that occurs as a result of steric congestion and suggests that this reagent combination has potential for high chemoselectivity in other instances as well.[6]
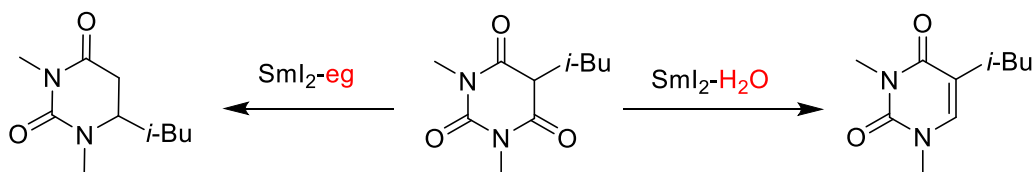
Scheme 3.1 The difference in product distribution in the reduction of barbituric acids between water and eg.

3.1.2 Mechanistic Studies of SmI$_2$-Alcohol Systems

The Hoz group was the first to show a strong reactivity difference between alcohols that coordinate to samarium and those that do not. Using a competition experiment between a diphenyl olefin and its deactivated anisyl counterpart, the product distributions arising from the combination of SmI$_2$ with methanol, isopropanol, and trifluoroacetic acid (TFA) were compared as in Scheme 3.2. At low concentrations of proton source, a high degree of selectivity toward reduction of the diphenyl substrate was observed with isopropanol and methanol but not for TFA. These results suggested that at low concentrations of methanol and isopropanol, protonation occurred from within a metal-coordinated alcohol complex to promote reduction of the diphenyl substrate before equilibration with the anisyl substrate could occur.[1] This work was later revisited with kinetic experiments that were consistent with a stepwise electron-transfer followed by a proton-transfer process [5]. Therefore, despite the fact that both substrates were activated for electron transfer because of the high degree of conjugation, the proton source led to a high degree of selectivity.

X= H (Diphenyl)
X= OMe (Anisyl)
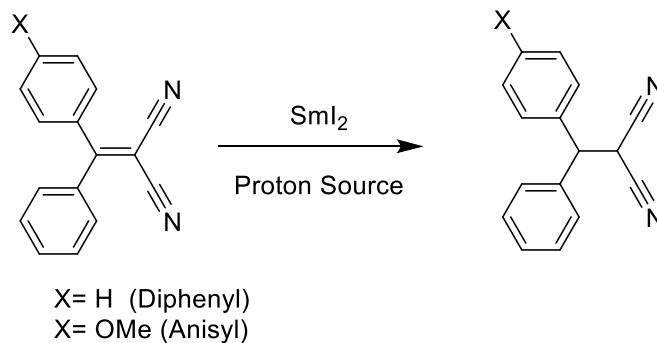
Scheme 3.2 Hoz's competition experiment in the reduction of an olefin by SmI_2-alcohols.

The first mechanistic study on the role of glycols in reductions of SmI_2 was undertaken by the Hilmersson group, using 3-heptanone as a model substrate and with methanol, ethylene glycol monomethyl ether (egme), eg, dg, triethylene glycol, and tetraethylene glycol. [3]
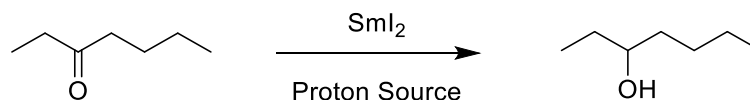
Scheme 3.3 Reduction of 3-heptanone by SmI_2.

The kinetic experiments revealed that the number of ethereal oxygens played a central role in the ability of a glycol to provide rate enhancement. The greatest rate enhancement for the reduction of 3-heptanone was observed with dg and was approximately 255 times that of SmI_2 alone. In the case of tetraglycol, it was surmised that too many coordinated oxygens saturated the coordination sphere of the metal and as a result, it only had a modest effect on the rate of reduction. It was also noted that monomethyl ethers of the corresponding glycols were not as effective as their parent glycol. These initial experiments revealed the delicate balance between coordination and saturation that dominates the reactivity of SmI_2. [3]

Mechanistic work in the Flowers group has also provided important information about the relative reactivity of different proton donors and their affinity for samarium. A direct relationship appears to exist between both the acidity (pK_a) of the proton donor and the steric hindrance near its oxygen with the observed rate of reduction of acetophenone in Figure 3.1. Similar to Hilmersson's observations, a strong difference appears between

those alcohols that coordinate strongly and those that do not. Interestingly, the rate of reduction with water is an outlier in this instance and does not appear to fit the linear acidity-rate correlation.[7]
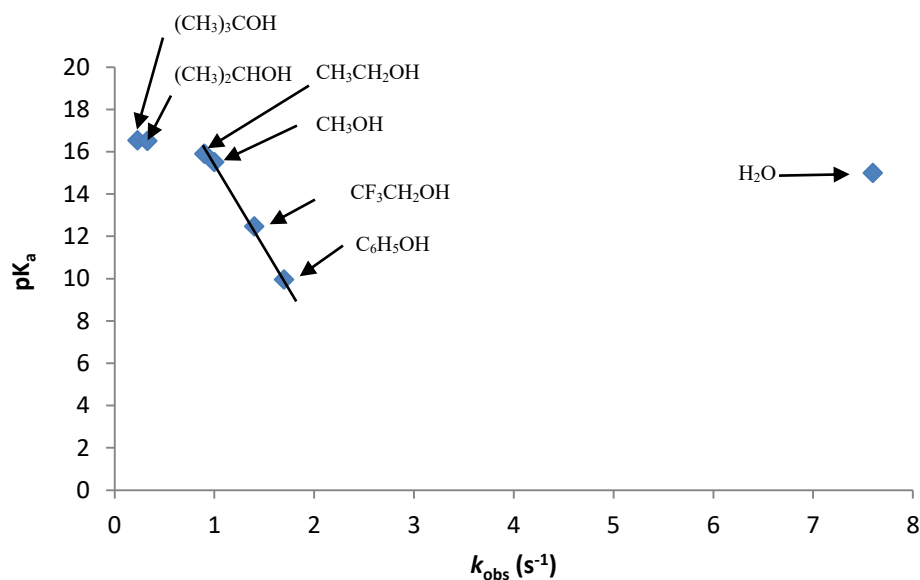
Figure 3.1 Relationship between k_{obs} and pK_a in the reduction of acetophenone. [7]

The significant difference in coordination behavior that was observed between glycols and their monomethyl ethers has previously been demonstrated by UV-vis as well. Much higher concentrations of dgme were required to perturb the characteristic absorption of SmI_2 at 560 and 620 nm than with dg. Additionally, Sm-glycol crystal structures generated by excess addition of glycol to SmI_2 have shown that glycols are able to displace the iodine ions to the outer sphere of the metal, as displayed in Figure 3.2.[2]
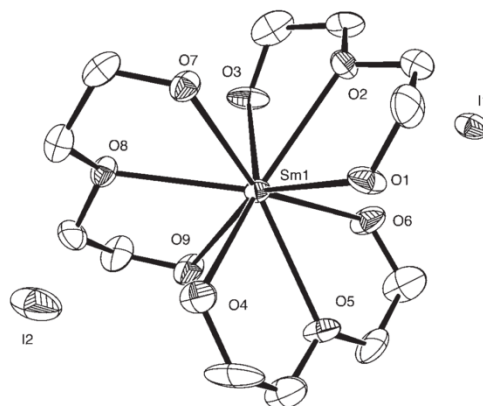
Figure 3.2 Crystal structure of $[Sm(dg)_3]I_2$. [2]

Therefore, the previous work in this area has shown that glycols have a high affinity for Sm(II) and lead to enhanced reaction rate, but this strong coordination can be disrupted by the addition of methyl moietys on to the alcohol.

3.1.3 Project Goals

The work outlined in Chapter 2 revealed the ability of water to act as a hydrogen atom transfer (HAT) promoter in the reduction of anthracene. Proton donors that do not have a high affinity for Sm(II), such as methanol, are ineffective for arene reduction.[8] Since initial studies in Chapter 2 showed that the affinity of water for Sm(II) is critical, it raises several important questions: 1) Does the combination of SmI_2 and water provide a unique combination for HAT to substrates? 2) Can high affinity proton donors be used in place of water to promote reductions? 3) Is there a relationship between proton donor affinity for Sm(II) and initial HAT to substrate? The studies described in this chapter are designed to answer these important questions. Overall, the experiments presented are

consistent with previous work and demonstrate that strong proton donor coordination to Sm(II) is a prerequisite for reduction through PCET.

To examine the importance of the proton donor coordination to Sm(II), several proton donors were chosen: dg, diethylene glycol monomethyl ether (dgme), eg, egme, water, and TFE. Proton donors such as dg, eg, and water are known to coordinate strongly to Sm(II), and the monomethyl ethers dgme and egme were chosen since the replacement of a hydroxyl proton with a methyl group has a deleterious impact on the affinity of proton donors for Sm(II).[2,3] The proton donor TFE does not coordinate to Sm(II), even at high concentrations.[4,5,9] Anthracene and benzyl chloride were chosen as substrates since studies would not be complicated by competition with proton donors for coordination sites on Sm(II). Additionally, benzyl chloride has lower redox potential and is reduced through a rate-limiting dissociative electron transfer[10], whereas the reduction of anthracene is highly endergonic and has been shown to be reduced through a PCET by Sm(II)-water[11](Scheme 3.4). If proton donor coordination is important for PCET from a Sm(II) donor complex, high affinity donors would be expected to have a larger relative impact on the rate of reduction of anthracene than benzyl chloride.
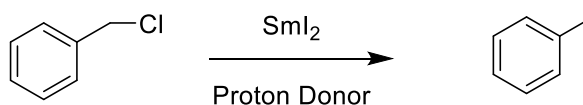
$E_{1/2}$ = -0.73 V
vs SCE in MeCN
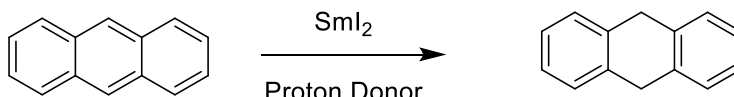
$E_{1/2}$ = -1.98 V vs SCE

Scheme 3.4 Ease of reduction of benzyl chloride and anthracene by SmI_2-proton donor.

3.2 Experimental Details

3.2.1 Materials

Samarium powder was purchased from Acros Organics. SmI_2 was generated by the standard method of samarium metal combined with iodine in THF and allowed to stir for at least 4 hours. Iodometric titrations were performed to verify the concentration of SmI_2. Anthracene was purchased from Alfa Aesar. Benzyl chloride was purchased from VWR and vacuum distilled to ensure purity. All other chemicals were verified by ^1H NMR and used without further purification. Benzyl chloride and proton donors were stored over sieves and deoxygenated prior to use. Inhibitor-free tetrahydrofuran was purified by a Solvent Purification system (Innovative Technology Inc.; MA).

3.2.2 Instrumentation

Proton NMR spectra were recorded on a Bruker 500 MHz spectrometer in $CDCl_3$. Carbon NMR were performed at 125 MHz in $CDCl_3$. GC-MS analyses were done with an HP 5890 Series II Gas Chromatograph with an HP Mass Selector Detector. GC analyses were performed using a Shimadzu Gas Chromatograph GC-14B with biphenyl standard. Kinetic experiments were performed with a computer-controlled SX.18 MV stopped-flow spectrophotometer (Applied Photophysics Ltd. Surrey, UK). The kinetic solutions were injected separately into the stopped-flow system from airtight Hamilton syringes prepared in a glove box. The cell block and the drive syringes of the stopped flow reaction analyzer were flushed a minimum of three times with dry, deoxygenated THF to make the system anaerobic. Between each experiment, the cell block was washed with dilute HNO_3 (2x), DI

H$_2$O (3x), and THF (3x) before additional anhydrous deoxygenated THF washes (3x). The reaction rates were determined from the decay of SmI$_2$ at 560 nm. ITC data was obtained using a MicroCal VP-ITC. The glycol IR experiment was carried out using a Mettler-Toledo's ReactIR 15 fitted with DiComp probe and running iCIR software 4.3 SP1.

3.2.3 Methods

3.2.3.1 General Procedure for Synthetic-Scale Reductions

3.2.3.1.1 Procedure for the Reduction of Anthracene

Inside an Ar glove box, 50 mg of anthracene was dissolved in 2.5 eq (vs anthracene) of 0.1 M SmI$_2$ in THF. Following dissolution, the desired glycol (10 eq vs Sm) was dissolved in 1 mL THF (vs. SmI$_2$) and added dropwise to the reaction. The reaction was left until the mixture became colorless and a white precipitate formed or for 24 hours if color loss did not occur. The round bottom flask was removed from the box and quenched with air and 0.1 M HCl. 9,10-Dihydroanthracene was extracted using DCM and washed with water. The organic layer was then treated with saturated aqueous sodium thiosulfate, and then brine. The remaining solution was then dried with magnesium sulfate, filtered and then solvent was removed by rotary evaporation. The resulting product was then placed under a high vacuum system to ensure complete removal of solvent. 9,10-Dihydroanthracene was analyzed by ^{1}H and ^{13}C NMR.

3.2.3.1.2 Procedure for the Reduction of Benzyl Chloride

Inside an Ar glove box, 50 µL of benzyl chloride (0.435 mmol) was dissolved in 2.5 eq (vs. benzyl chloride) of 0.1 M SmI$_2$ in THF. Following dissolution, the desired glycol (10 eq vs Sm) was dissolved in 1 mL THF (vs. SmI$_2$) and added dropwise to the reaction. The

reaction was left until the mixture became colorless and a white precipitate formed or for 24 hours if color loss did not occur. The round bottom flask was removed from the box and quenched with air and 0.1M HCl. Toluene was extracted using diethyl ether. The organic layer was then treated with saturated aqueous sodium thiosulfate, and then brine. The remaining solution was then dried with magnesium sulfate, filtered and then solvent was removed by rotary evaporation. Toluene product was verified by ^{1}H and ^{13}C NMR.

3.2.3.2 General Procedure for SmI$_2$-H$_2$O Stopped-Flow Kinetic Studies

Kinetic experiments were performed with a computer-controlled SX.18 MV stopped-flow spectrophotometer (Applied Photophysics Ltd. Surrey, UK). The SmI$_2$, substrate, and water solutions were injected separately into the stopped-flow system from airtight Hamilton syringes prepared in a glove box. The cell block and the drive syringes of the stopped flow reaction analyzer were flushed a minimum of three times with dry, degassed THF to make the system anaerobic. The reaction rates were determined from the decay of SmI$_2$ at 560 nm. Unless specified otherwise, all kinetic measurements for the reductions were carried out at 25 $^{\circ}$C unless otherwise stated.

3.2.3.3 General Procedure for SmI$_2$ Isothermal Titration Calorimetry (ITC)

All titrations were performed at 25 °C with 3 mM SmI$_2$ in the cell and 90 mM glycol solution in the syringe. The syringe volume was 250 μL while the cell volume was 1.4 mL. The cell was first deoxygenated by flushing with argon for at least 15 minutes. All solutions were prepared in an argon glove box and SmI$_2$ solutions were transported in airtight BD syringes and injected into the cell. Over the course of the experiment, 140 injections of 2 μL glycol solution were injected over 4 s with a 180 s delay between injections. Following each

titration experiment, the glycol was injected into THF to obtain a heat of dilution. The heat of dilution for the glycols and SmI_2 were all close to zero.

3.3 Results and Discussion

To study the mechanism of Sm-induced reduction with different coordinating and non-coordinating proton donors, kinetic and thermodynamic experiments including rate order, kinetic isotope, bulk protonation, and activation parameter studies were carried out primarily using stopped-flow spectrophotometry. Additionally, relative affinity for samarium was determined using isothermal titration calorimetry and infrared (IR) spectroscopy experiments.

3.3.1 Analysis of Additive Affinity

3.3.1.1 Glycol Conformation Determination by IR

Although it has generally been assumed that glycols bind to samarium in a multidentate fashion, the only evidence to suggest this to date has arisen from crystal structure data. Although the single crystal x-ray structures of organometallic complexes can provide a great deal of useful information, care must be exercised in their interpretation and application to complexes in solution since crystallization can drive coordination that may not be truly representative of the solution as a consequence of solvent evaporation. With this in mind, the bidentate coordination of eg was examined using infrared spectroscopy (IR).

A glycol conformation IR experiment was carried out using a Mettler-Toledo's ReactIR 15 fitted with DiComp probe and running iCIR software 4.3 SP1. A two necked round bottom flask was equipped with a stir bar and was fixed to the ReactIR probe. The

flask was flushed with argon and an argon background (256 scans) was obtained. Then 11.5 mL of THF was added through a rubber septum into the flask and a solvent reference was taken. To this, 1.25 mL of eg was added and the spectrum was monitored between 1160 and 780 wavenumbers. Next, 4.5 mL of 0.1 M SmI_2 was added to the flask. Once a shift was observed, an additional 25 equivalents vs SmI_2 (1.25 mL) of eg was added. The resulting spectrum is reported below in Figure 3.3.
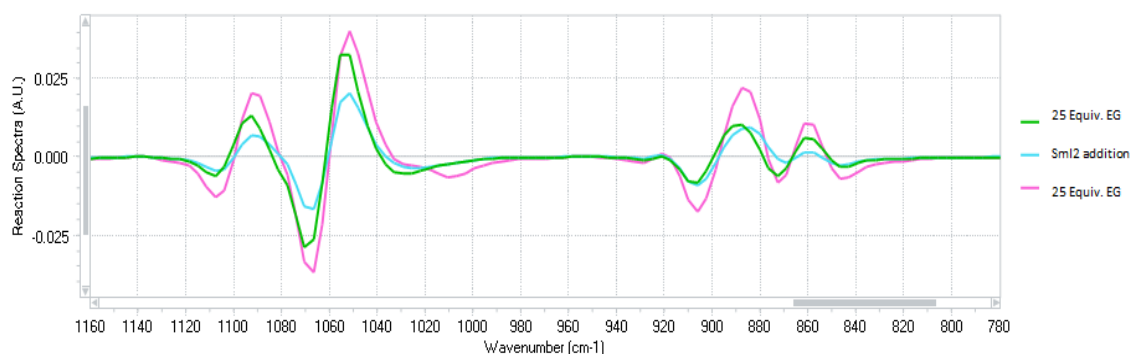
Figure 3.3 Shift in CH_2 wag frequencies to lower wavenumbers upon addition of SmI_2.

Previous work probing the coordination behavior of glycols has suggested that upon coordination to first row transition and alkaline earth metal cations, changes in the force constants occur to produce a shift in the stretching frequencies of glycols to lower wavenumbers.[12] This is consistent with the above observation where the peaks at 1090, 1055, 890, and 860 cm^{-1} undergo a shift to lower wavenumber upon the addition of SmI_2. The frequencies at 890 and 860 cm^{-1} have been assigned to the *gauche* CH_2 rocking vibration, and have previously been observed to shift to lower wavenumbers upon bidentate coordination to cobalt and nickel cations in solution.[13,14] When excess eg was added, a shift in these peaks back to the original wavenumbers consistent with free solution eg was observed. Therefore, this experiment further confirms bidentate

coordination of glycol to samarium and is consistent with the previously determined crystal structures for Sm-glycols.

3.3.1.2 Glycol Binding Affinity by Isothermal Titration Calorimetry

To examine the impact of proton donor affinity for SmI_2 isothermal titration calorimetry (ITC) was employed. As displayed in Figure 3.4, increasing amounts of proton donor were titrated into SmI_2 in THF to produce an isotherm describing the binding affinity for each proton donor.
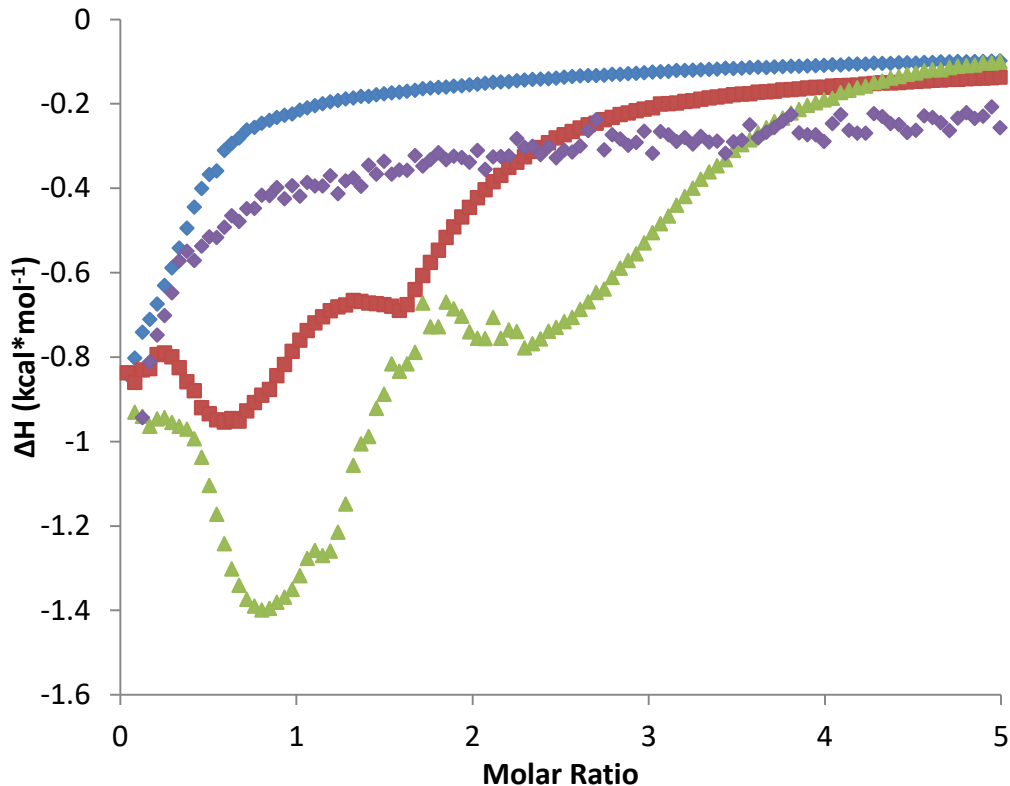
Figure 3.4 ITC binding isotherms for the addition of 2 µL aliquots of 90 mM egme (◆), dgme (◆), eg(■), and dg (▲) to SmI_2 (1.4 mL, 3 mM) in THF.

It was expected that a mathematical fit of the data could determine the solution stoichiometry of Sm(II)-proton donors since the stoichiometry of the SmI_2-dg and SmI_2-dgme complexes are known from X-ray crystal structures.[2] A caveat with this supposition is that X-ray structures were obtained from the slow evaporation of solvent from solutions of proton donors and SmI_2, creating an environment that may not represent the structures in relatively dilute solutions (< 0.1 M) of Sm(II)-glycol complexes. Several attempts were made to fit the data, but all fits provided a significant amount of error. Qualitatively, the data clearly show that the interaction of eg and dg with SmI_2 are distinct from egme and dgme. The binding isotherms for egme and dgme are consistent with low affinity coordination, whereas the data for eg and dg are consistent with higher affinity binding. Furthermore, the parabolic shape in the initial portion of the eg and dg binding isotherms are consistent with systems where a higher affinity binding site has a less exothermic enthalpy change than the lower binding affinity sites.[15] It can be inferred that the less exothermic coordination of eg and dg is a consequence of the displacement of iodide from the inner sphere of Sm(II) upon addition of these additives.[16] Regardless of the complexity of observing proton donor coordination to SmI_2, UV-vis studies on these additives clearly show the same trends, providing affinities that follow the trend dg >eg >H_2O >>dgme >egme.

3.3.2 Kinetic Analysis for the Reduction of Benzyl Chloride

3.3.2.1 Influence of Proton Donors

To determine the order of each component of the reaction using stopped-flow spectrophotometry, rates were measured under pseudo-first order conditions. The order

for each component was determined independently. The rate order of SmI$_2$ was determined by the method of fractional times. The rate order of benzyl chloride was determined at a fixed concentration of ethylene glycol where the order of ethylene glycol was 2 to remain at synthetically-relevant proton donor concentration. Like the observations detailed in Chapter 2, water and other coordinating proton donors showed saturation behavior corresponding to a plateau in rate at high concentrations.
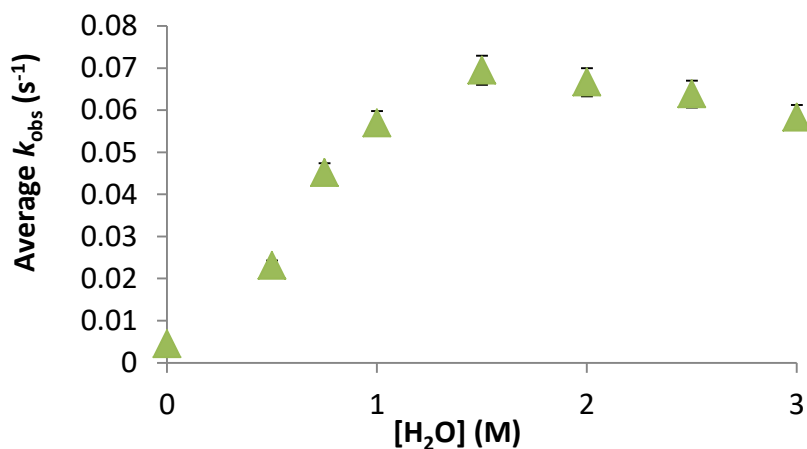
Figure 3.5 Rates of reduction of benzyl chloride with increasing concentration of water.
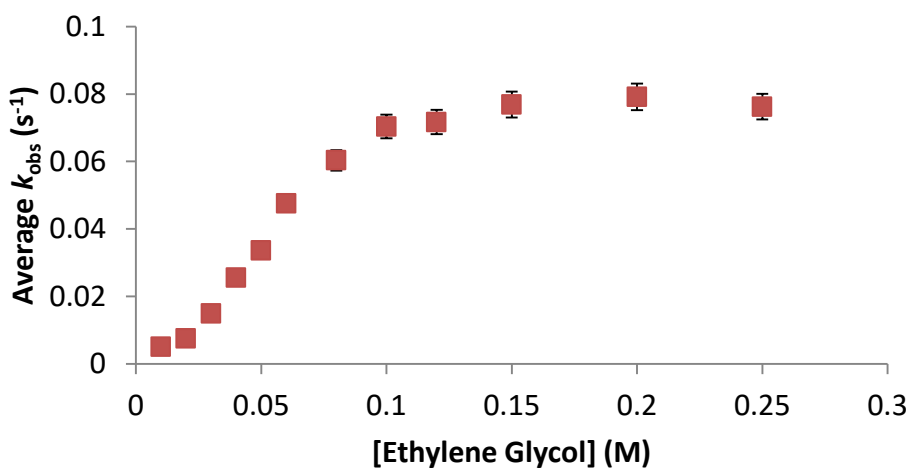
Figure 3.6 Rates of reduction of benzyl chloride with increasing concentration of eg.
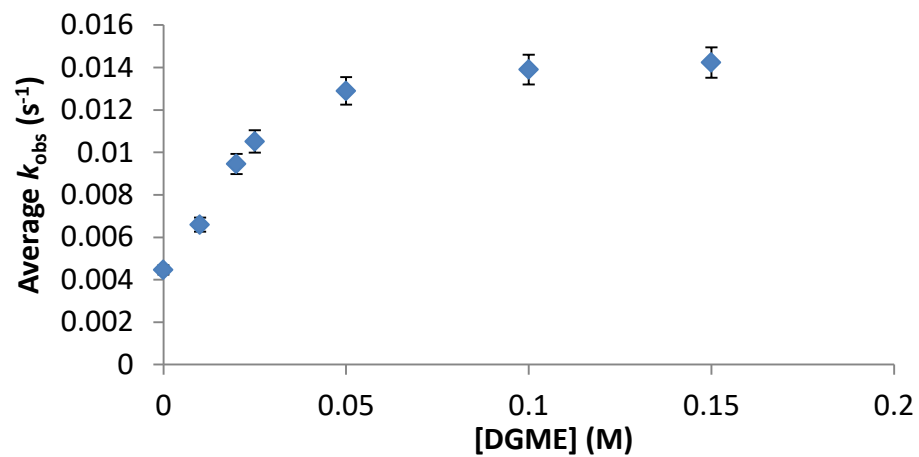
Figure 3.7 Rates of reduction of benzyl chloride with increasing concentration of dgme.
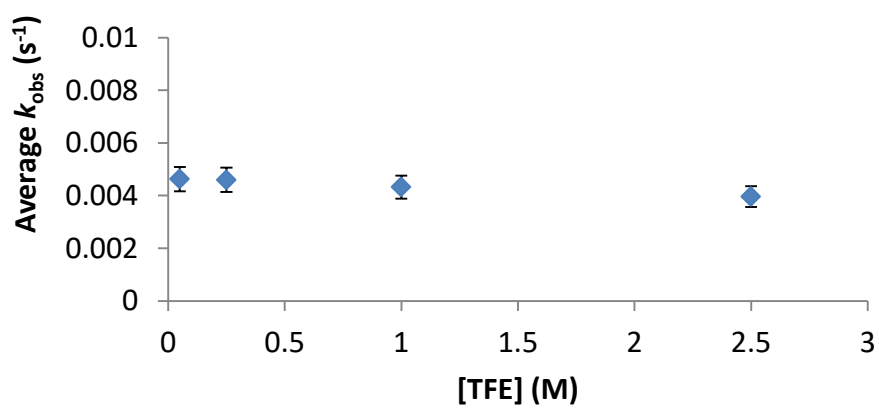
Figure 3.8 Rates of reduction of benzyl chloride with increasing concentration of TFE.

85
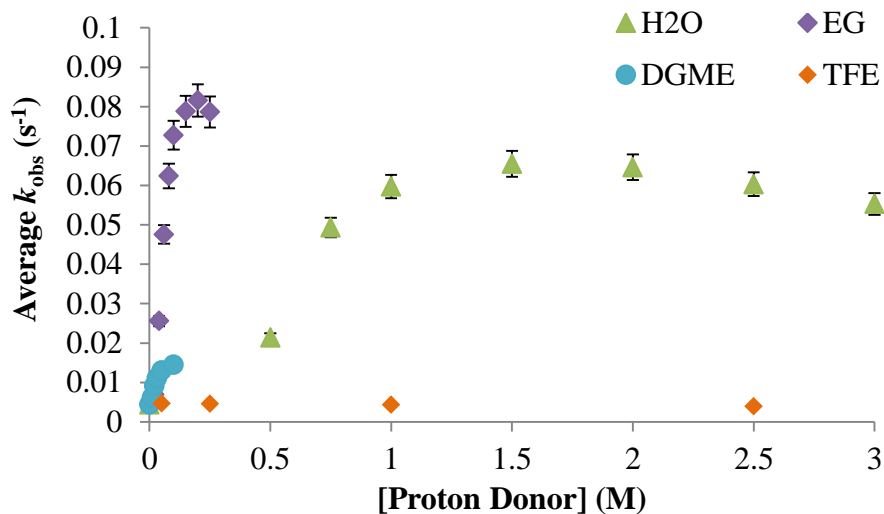
Figure 3.9 Comparison of relative reduction rates of 100 mM benzyl chloride by 10 mM SmI$_2$ as a function of proton donor concentration.

It is evident from Figure 3.9 that although each proton donor that coordinates to samarium provides a rate enhancement, not all glycols provide the same degree of rate enhancement. As expected, the monomethyl derivatives do not provide the same degree of rate enhancement as the methyoxy glycols.

Table 3.1 Rate Orders for the reduction of benzyl chloride by SmI$_2$.

Reaction Component	Rate Order
SmI$_2$	1[a]
Benzyl Chloride	1.1 ± 0.1[b]

Conditions: [a]Fractional times method. [b]10 mM SmI$_2$, 100-300 mM benzyl chloride, 0.05 M eg. The rate orders are the average of 3 independent experiments.

The rate order of SmI$_2$ and benzyl chloride are both unity, which supports the expected mechanism of rate-limiting dissociative electron transfer. The order of proton donor is highly dependent on the identity of the donor, with highly coordinating proton

donors such as water and ethylene glycol second order at synthetically relevant low concentrations. TFE appears to have a zero-order dependence, which is consistent with its lack of coordination and therefore lack of involvement in the rate-limiting step.

3.3.2.2 Kinetic Isotope Effect

The kinetic isotope study was performed using equimolar quantities of degassed eg and egD$_2$ (DO(CH$_2$)$_2$OD) where the concentration was varied from 0.01 – 1 M. The concentration of benzyl chloride was maintained at 100 mM and SmI$_2$ was maintained at 10 mM. The experiment was also performed with D$_2$O and H$_2$O to compare and determine whether protonation was involved in the rate-limiting step for either proton donor.
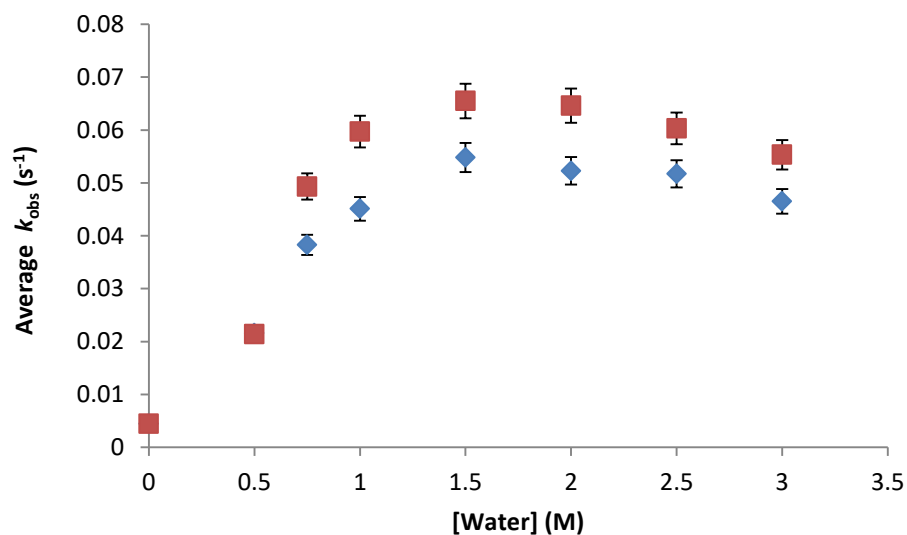
Figure 3.10 Rates of reduction of benzyl chloride with increasing concentrations of H$_2$O (■) and D$_2$O(◆).
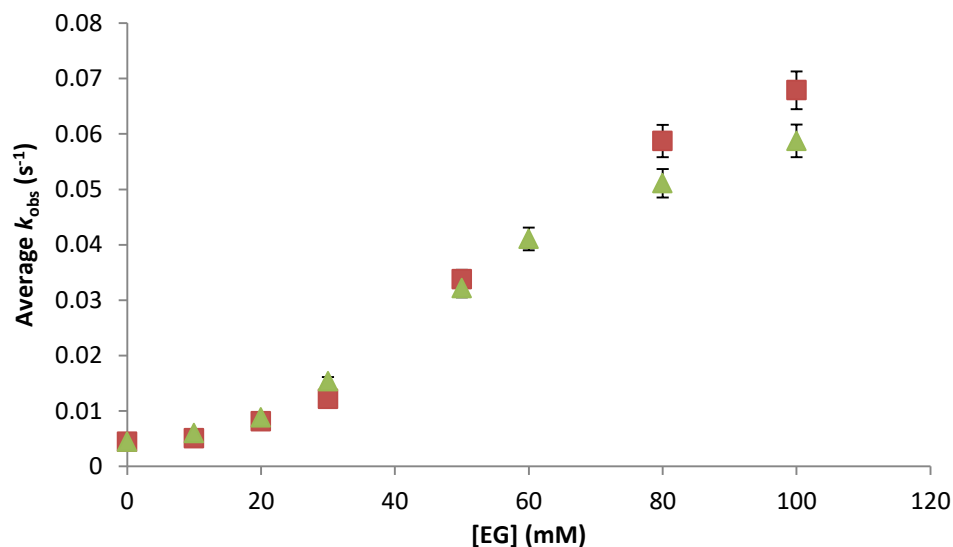
Figure 3.11 Rates of reduction of benzyl chloride with increasing concentrations of eg (■) and egD$_2$(▲).

The lack of a significant difference in kinetic isotope effect suggests that protonation is not rate-limiting in the case of either proton donor.

3.3.2.3 Mechanism for the Reduction of Benzyl Chloride

Since the rate orders indicate first order dependence on both samarium and benzyl chloride, a kinetic isotope effect is not observed, and the substrate undergoes reduction with a non-coordinating proton donor like TFE, the data supports the expected mechanism in Scheme 3.5, a rate-limiting dissociative electron transfer similar to previously reported SmI$_2$-based halide reductions.[2,11,17]
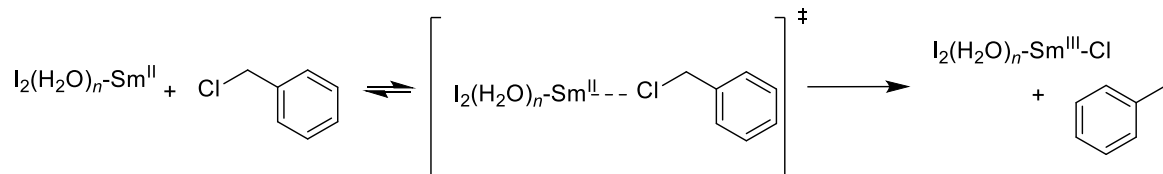
Scheme 3.5 Initial steps in the reduction of benzyl chloride by SmI_2.

3.3.3 Kinetic Analysis for the Reduction of Anthracene

3.3.3.1 Rate Orders

To determine the order of each component of the reaction, rates were measured under pseudo-first order conditions. The order for each component was determined independently. The rate order of SmI_2 was determined by the method of fractional times. The rate order of anthracene was determined with a fixed concentration of eg where the order of eg was 2 to remain at synthetically-relevant proton donor concentration. Similar to the observations detailed in Chapter 2 for water, eg produced a saturation curve with a concentration-dependent order, as in Figure 3.12.
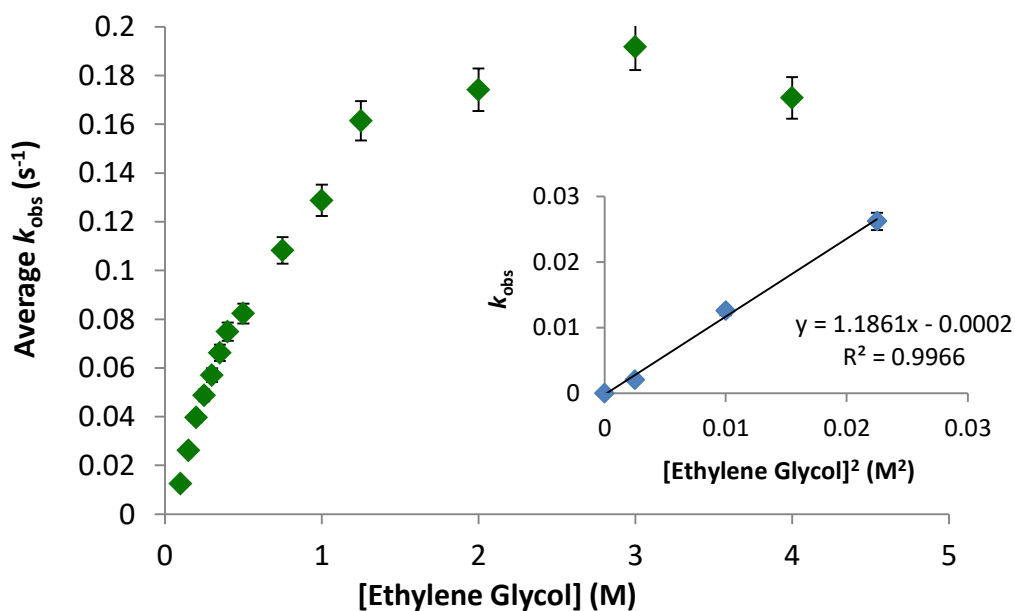
Figure 3.12. Influence of [eg] on the rate of reduction of 125 mM anthracene by 10 mM SmI_2. Inset: Second order eg dependence at low concentrations.

Table 3.2 Rate data for the reduction of anthracene by SmI_2-eg.

Reaction Component	Rate Order
SmI_2	1^a
Anthracene	1.1 ± 0.1^b
Ethylene glycol	2 ± 0.1 (0-1.2 M)^c

Conditions: [a]Fractional times method. [b]10 mM SmI_2, 100-120 mM anthracene, 1 M H_2O. [c] 10 mM SmI_2, 125 mM anthracene, 0-0.5M eg.   The rate orders are the average of 3 independent experiments.

The rate orders obtained mirror that of the reduction with SmI_2-H_2O, which indicates that eg performs a similar function to H_2O in this reaction. Figure 3.13 shows that although H_2O and eg plateau at a similar maximum, because eg has a higher affinity for Sm(II), it saturates at a lower concentration.
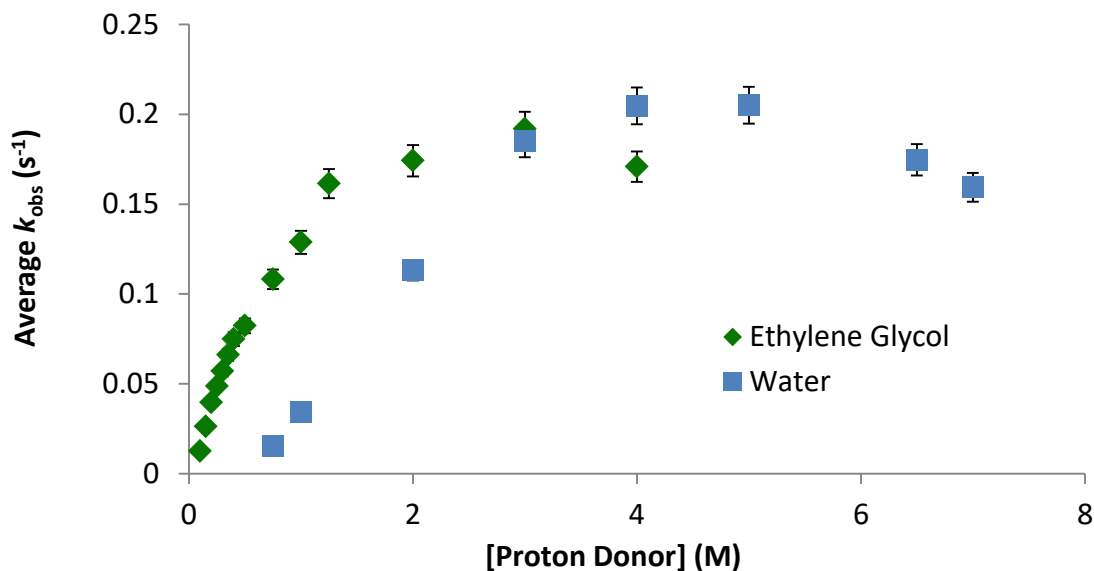
Figure 3.13 Comparison of the reduction of 100 mM anthracene by SmI_2-eg and SmI_2-H_2O.

3.3.3.2 Kinetic Isotope Effect

The rate of reduction of anthracene was measured with a range of concentrations of both eg and deuterated egD$_2$ to determine whether protonation was involved in the rate-limiting step. Figure 3 shows that the rate of reduction with egD$_2$ is consistently lower and the k_H/k_D averages 1.8, which is indicative of rate-limiting protonation. This resembles the data from Chapter 2 in which the k_H/k_D averaged 1.7 for the reduction of anthracene with SmI$_2$-H$_2$O.
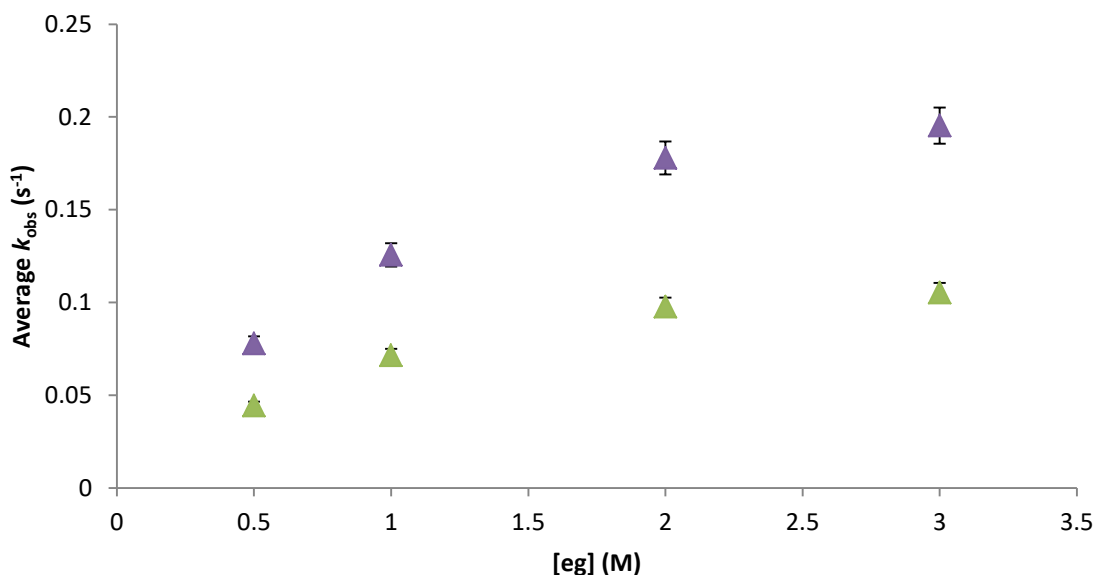
Figure 3.14 Rate difference for the reduction of anthracene with eg (▲) compared to egD$_2$ (▲).

3.3.3.3 Bulk Protonation Study

Similar to the bulk protonation experiment performed in Chapter 2 and first described by the Hoz group, an experiment where the rate of reduction was measured in the presence of TFE to distinguish between directly coordinated and bulk protonation events.[4] Using this approach, if protonation of anthracene in the reduction with ethylene glycol arose from the bulk solution, the addition of a more acidic non-coordinating proton

source would increase the rate of reduction. For this experiment, the rate of reduction was monitored at constant concentrations of ethylene glycol, anthracene, and SmI_2 while the concentration of TFE was increased and is shown in Figure 3.15.
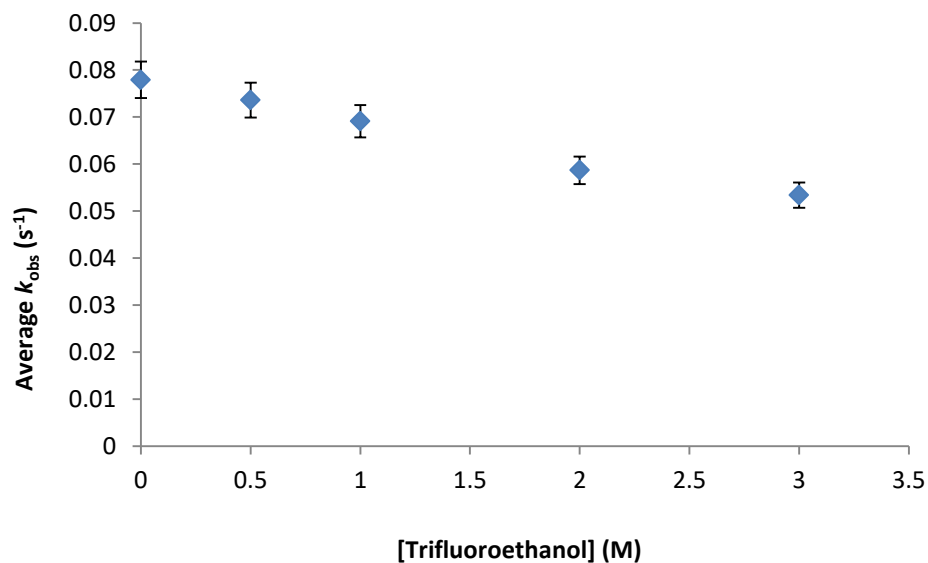
Figure 3.15 Effect of increasing concentrations of TFE on the reduction of a constant concentration of anthracene by SmI_2-eg.

The rate of reduction of anthracene in the presence of TFE is not enhanced, which suggests the presence of an acidic bulk proton source is not advantageous and further supports that protonation arises from coordinated proton donor.

3.3.3.4 Activation Parameters

Activation parameters for the reduction of anthracene were determined by measuring the rate of reduction with fixed concentrations of all components over a range of 20 degrees and preparing an Eyring plot to solve for each parameter.
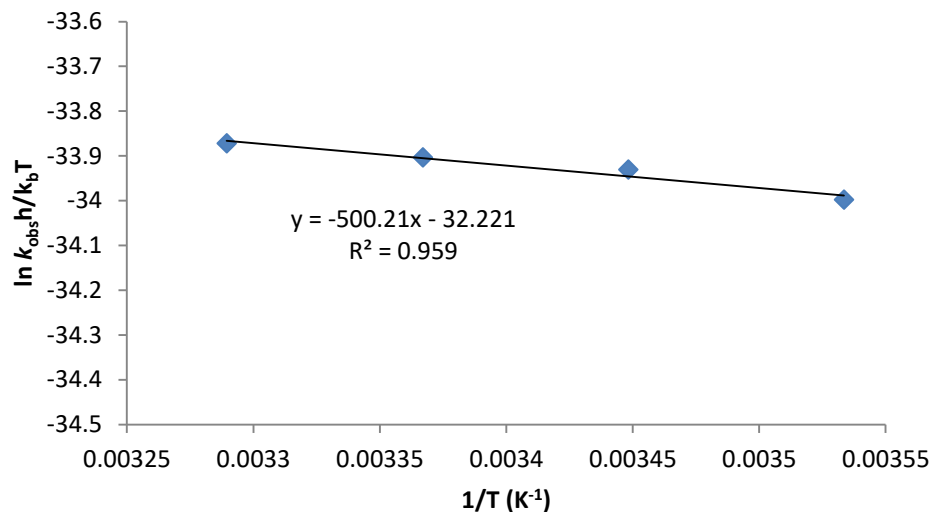
Figure 3.16 Erying plot for the rate of reduction of 120 mM anthracene by 10 mM SmI$_2$ and 100 mM eg from 10-30 $^{\circ}$C.

Table 3.3 Activation parameters for the reduction of anthracene by SmI$_2$-eg.

ΔH‡ (kcal/mol)^a	ΔS‡ (cal/mol*K)^a	ΔG‡ (kcal/mol)^b	E$_a$ (kcal/mol)
1.4 ± 0.3	-62 ± 2	20 ± 1	2.0 ± 0.3

Conditions: 10 mM SmI$_2$, 100 mM eg, and 120 mM anthracene in THF. The activation parameters are the average of 3 independent experiments from 10-30 $^{\circ}$C and are reported as ± σ. ^{a}Obtained from ln($k_{obs}h/k_bT$)- ΔH‡/RT + ΔS‡/R. ^{b}Calculated from ΔG‡= ΔH‡-TΔS‡.

The activation parameters are consistent with an early, highly-ordered transition state where the transition state closely resembles the reactants in their ground state.

3.3.4 Coordination-Induced Bond-Weakening and PCET

To further assess the relationship between proton donor structure and possible modes of reactivity, bond dissociation free energies (BDFE's) were determined through density functional calculations (UB3LYP/6-31G) CPCM(THF) using the approach

93

described by Knowles.[18] (See Appendix) The BDFE data contained in Table 3.4 shows little variation among the glycol derivatives; the only difference being the values are somewhat lower compared to TFE and water.   Examination of pK_a's shows little difference among the glycols with water having the highest pK_a and TFE the lowest. The interesting feature of the data contained in Table 3.4 is the lack of any relationship between the acidity of each proton donor in the rate of reduction of anthracene by SmI_2. This is in spite of the fact that water, dg, and eg addition to SmI_2 enables reduction of anthracene and no reduction occurs in their absence.

Table 3.4 pK_a and impact of Sm(II) coordination on the O-H bond strength of proton donors.

Entry	Proton Donor	BDFE (kcal, mol^{-1})	Bond-Weakening (kcal, mol^{-1})	pK_a
1	eg	86.4	49.8	14.1
2	egme	86.6	-	14.8
3	dg	86.7	50.1	14.0
4	dgme	86.7	-	14.4
5	TFE	94.7	-	12.4
6	H_2O	103.4	66.8	15.7

There are several plausible mechanistic scenarios for anthracene reduction by Sm(II)-proton donor complexes: (1) A rate-limiting electron transfer followed by a rapid proton transfer, (2) An electron transfer followed by a rate-limiting proton transfer, and

(3) PCET.   Previous initial work on the reduction of anthracene by SmI_2-water demonstrated that reduction likely occurs through a PCET process. Comparisons of the impact of water and glycols on SmI_2 are useful to determine the likely pathway of reduction and similarities between both types of proton donors.

R = H, CH_2CH_2OH, $CH_2CH_2OCH_2CH_2OH$
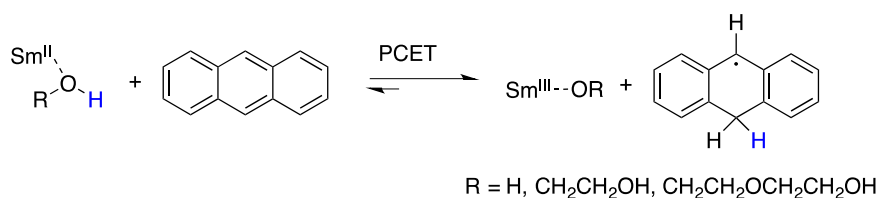
Scheme 3.6 Proposed mechanism for the reduction of anthracene by an alcohol.

3.4 Conclusions

The data presented *vide supra* demonstrates that in the systems studied here, proton donor coordination accelerates substrate reduction.[2,3] Another facet of coordination that may influence the mechanism of substrate reduction is the alteration of the reducing power (ease of oxidation) of Sm(II) upon ligation of proton donors.[19] Inclusion of cosolvents and additives are known to have an impact on the redox potential of SmI_2 through the production of a thermodynamically more powerful reductant or through stabilization of Sm(III).[20] When water is employed as an additive, large amounts (1000 equiv based on [SmI_2]) are required to significantly influence the redox potential.[19] Additionally, glycols have a limited impact on the redox potential of SmI_2 with dg providing a modest change of 0.13 V (3 kcal).[2]

In the reductions studied herein, the modest increase in the rate of reduction of benzyl chloride by SmI_2-proton donor reagent systems is likely a consequence of the

small change in the redox potential of Sm(II) containing ligated proton donor since the electron transfer is already exergonic. Conversely, it is unlikely that the reductions of anthracene proceed through an initial electron transfer since the process is significantly endergonic under the conditions of the experiment and as a consequence, an initial electron transfer is unlikely in the timescale measured by stopped-flow studies. If an initial electron transfer is unlikely, then how does reduction proceed? The seminal work of Mayer demonstrates that in most cases, PCET is favored over sequential electron-proton transfer since ΔG is always lower for PCET than it is for an initial ET or PT.[21–24] Additionally, the small k_H/k_D measured for the reduction of anthracene by SmI_2-eg is consistent with PCET.[25–29] In addition, there is a great deal of precedence for the coordination of water or alcohols to low-valent metals leading to significant weakening of the O-H bond.[30–34] Based on previous precedent[11], the impact of coordination on the ability of the Sm(II)-proton donor complex can be evaluated for eg, dg, and H_2O in THF using the BDFE's displayed in Table 3.4 and the calculated BDFE of the initial radical formed through hydrogen atom transfer to anthracene (36.6 kcal/mol). The degree of bond-weakening for each coordinating donor is also shown in Table 3.4.

A previous estimate for the decrease in the homolytic dissociation energy of the O-H bond of water upon coordination to SmI_2 was determined using experimental gas phase BDE's and found to be 72.7 kcal/mol. The present estimate of bond-weakening determined from calculated BDFE's in THF is nearly 6 kcal/mol smaller, but in reasonable agreement with previous data. The degree of bond-weakening for eg and dg upon coordination to SmI_2 is approximately 50 kcal/mol. The smaller values for eg and

dg are a consequence of the lower BDFE of the glycols compared to water and not their affinity for Sm(II). Although these values are substantial, it is our supposition that the decrease in BDFE's obtained using this approach are a measure of the minimum impact of coordination to Sm(II) on the ability to reduce anthracene through a formal hydrogen atom transfer. Further experiments will be required to determine the limits (ie maximum impact) of coordination.

Overall, the results of this study demonstrate that the combination of Sm(II)-water does not provide a unique reagent system for hydrogen atom transfer. The use of isothermal titration calorimetry and UV-Vis spectroscopy from this work and previous studies shows that only those proton donors that coordinate to SmI_2 promote substrate reduction through PCET. Therefore, with the requirements of a hydrogen atom transfer promoter in hand, novel SmI_2-based reagent combinations are accessible and are described subsequently. With a foundational grasp of the role of proton donors and their ability to promote formal hydrogen atom transfer in reductions featuring non-coordinating substrates, Chapter 4 describes the effects of substrate coordination on these systems.

3.5 References

(1)   Yacovan, A.; Hoz, S. *J. Am. Chem. Soc.* **1996**, *118*, 261–262.

(2)   Teprovich, J. A.; Balili, M. N.; Pintauer, T.; Flowers, II, R. A. *Angew. Chem. Int. Ed. Engl.* **2007**, *46*, 8160–8163.

(3)   Dahlen, A.; Hilmersson, G. *Tetrahedron Lett.* **2001**, *42*, 5565–5569.

(4)   Tarnopolsky, A.; Hoz, S. *Org. Biomol. Chem.* **2007**, *5*, 3801–3804.

(5)   Tarnopolsky, A.; Hoz, S. *J. Am. Chem. Soc.* **2007**, *129*, 3402–3407.

(6)   Szostak, M.; Spain, M.; Sautier, B.; Procter, D. *Org. Lett.* **2014**, *16*, 5694–5697.

(7)   Chopade, P. R.; Prasad, E.; Flowers, II, R. A. *J. Am. Chem. Soc.* **2004**, *126*, 44–45.

(8)   Szostak, M.; Spain, M.; Procter, D. *J. Org. Chem.* **2014**, *79*, 2522–2537.

(9)   Amiel-levy, M.; Hoz, S. *J. Am. Chem. Soc.* **2009**, *131*, 8280–8284.

(10)   Andrieux, C. P.; Gorande, A. L.; Savéant, J.-M. *J. Am. Chem. Soc.* **1992**, *114*, 6892–6904.

(11)   Chciuk, T. V.; Flowers, II, R. A. *J. Am. Chem. Soc.* **2015**, *137*, 11526–11531.

(12)   Knetsch, D.; Groeneveld, W. L. In *Proceedings*; 1974; pp. R52–R55.

(13)   Miyake, A. *J. Am. Chem. Soc.* **1960**, *82*, 3040–3043.

(14)   Miyake, A. *Bull. Chem. Soc. Jpn.* **1959**, *32*, 1381–1383.

(15)   Freyer, M. W.; Lewis, E. A. *Methods Cell Biol.* **2008**, *84*, 79–113.

(16)   Sadasivam, D. V; Teprovich, J. A.; Procter, D. J.; Flowers, II, R. A. *Org. Lett.* **2010**, *12*, 4140–4143.

(17)   Miller, R. S.; Sealy, J. M.; Shabangi, M.; Kuhlman, M. L.; Fuchs, J. R.; Flowers, II, R. A. *J. Am. Chem. Soc.* **2000**, *122*, 7718–7722.

(18)   Tarantino, K. T.; Miller, D. C.; Callon, T. A; Knowles, R. R. *J. Am. Chem. Soc.* **2015**, *137*, 6440–6443.

(19)   Prasad, E.; Flowers, II, R. A. *J. Am. Chem. Soc.* **2005**, *127*, 18093–18099.

(20)   Halder, S.; Hoz, S. *J. Org. Chem.* **2014**, *79*, 2682–2687.

(21)   Mayer, J. M. *Annu. Rev. Phys. Chem.* **2004**, *55*, 363–390.

(22)   Mayer, J. M.; Rhile, I. J. *Biochim. Biophys. Acta - Bioenerg.* **2004**, *1655*, 51–58.

(23) Warren, J. J.; Tronic, T. A.; Mayer, J. M. *Chem. Rev.* **2010**, *110*, 6961–7001.

(24) Mayer, J. M. *Acc. Chem. Res.* **2011**, *44*, 36–46.

(25) Warren, J. J.; Menzeleev, A. R.; Kretchmer, J. S.; Miller, T. F.; Gray, H. B.; Mayer, J. M. *J. Phys. Chem. Lett.* **2013**, *4*, 519–523.

(26) Megiatto Jr., J. D.; Mendez-Hernandez, D. D.; Tejeda-Ferrari, M. E.; Teillout, A. L.; Llansola-Portoles, M. J.; Kodis, G.; Poluektov, O. G.; Rajh, T.; Mujica, V.; Groy, T. L.; Gust, D.; Moore, T. A; Moore, A. L. *Nat Chem* **2014**, *6*, 423–428.

(27) Warren, J. J.; Mayer, J. M. *J. Am. Chem. Soc.* **2011**, *133*, 8544–8551.

(28) Schrauben, J. N.; Cattaneo, M.; Day, T. C.; Tenderholt, A. L.; Mayer, J. M. *J. Am. Chem. Soc.* **2012**, *134*, 16635–16645.

(29) Tarantino, K. T.; Liu, P.; Knowles, R. R. *J. Am. Chem. Soc.* **2013**, *135*, 10022–10025.

(30) Spiegel, D. A.; Wiberg, K. B.; Schacherer, L. N.; Medeiros, M. R.; Wood, J. L. *J. Am. Chem. Soc.* **2005**, *127*, 12513–12515.

(31) Pozzi, D.; Scanlan, E. M.; Renaud, P. *J. Am. Chem. Soc.* **2005**, *127*, 14204–14205.

(32) Jonas, R. T.; Stack, T. D. P. *J. Am. Chem. Soc.* **1997**, *119*, 8566–8567.

(33) Cuerva, J. M.; Campaña, A. G.; Justicia, J.; Rosales, A.; Oller-López, J. L.; Robles, R.; Cárdenas, D. J.; Buñuel, E.; Oltra, J. E. *Angew. Chemie - Int. Ed.* **2006**, *45*, 5522–5526.

(34) Paradas, M.; Campaña, A. G.; Jiménez, T.; Robles, R.; Oltra, J. E.; Buñuel, E.; Justicia, J.; Cárdenas, D. J.; Cuerva, J. M. *J. Am. Chem. Soc.* **2010**, *132*, 12748–12756.

Chapter 4. Proton-Coupled Electron-Transfer in the Reduction of Carbonyls by SmI$_2$-H$_2$O

4.1 Background and Significance of SmI$_2$-H$_2$O Reductions of Carbonyls

Not long after Kagan introduced samarium diiodide (SmI$_2$) to the synthetic community in the late 1970s[1], the versatility of this unique reagent has expanded considerably through the addition of additives.[2–6] Of these additives, proton donors have become the most widely-utilized and enable the reduction of a variety of functional groups[2,3,7,8] and mediate a range of carbon-carbon bond-forming reactions and reductive cyclizations important in synthesis.[9,10] The rate, selectivity, and product distribution of many reactions can be effectively tuned by altering both the concentration and identity of proton donor employed.[11–15] Understanding the underlying mechanisms behind the tunable reactivity of the combination of SmI$_2$ and different proton donors has presented a number of challenges, in part due to difficulties associated with direct observation of lanthanide-ligand interactions in solution. Because Sm(II) has a large coordination sphere and is highly reactive, it is difficult to directly characterize the interactions of additive, substrate, and solvent molecules coordinated to the metal.

Although the combination of SmI$_2$ and water provides highly useful synthetic reagent combination, the unique reactivity of the reagent system has been particularly challenging to study, especially with regard to substrates containing coordinating functional groups like carbonyls that are capable of coordinating to Sm(II), but are recalcitrant to reduction through single electron transfer.

Careful examination of the literature reveals significant clues that in part, provide insight into the unique behavior of SmI_2-water. Kagan was the first to show that 2-octanone could be effectively reduced to 2-octanol through the addition of water, which indicated a unique mechanistic role for water since the addition of the structurally similar methanol did not provide the corresponding alcohol.[16] Curran demonstrated that the addition of water could accelerate the reduction of multiple functional groups.[7] The versatility of functional group reductions by SmI_2-H_2O was further expanded by Kamochi to include aromatic carboxylic acids, esters, amides, nitriles, ketones, and nitro compounds.[8]
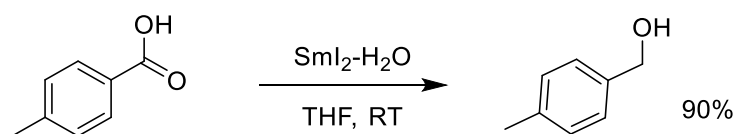
Scheme 4.1 Reduction of aromatic carboxylic acid by SmI_2-H_2O.

Since these seminal studies, the scope of SmI_2-H_2O reductions has been expanded significantly through the work of Procter to include lactones, Meldrum's acid derivatives and related systems.[17,18]
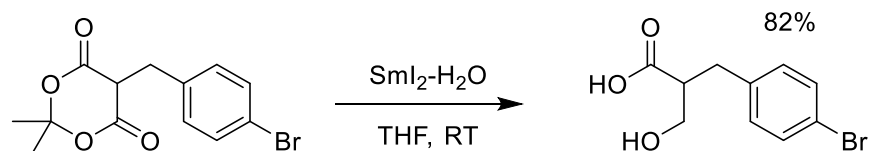
Scheme 4.2 Reduction of Meldrum's acid derivative by SmI_2-H_2O.

All of the systems described above were proposed to capitalize on Sm-carbonyl coordination to drive targeted reactivity through the stabilization of anion-radical intermediates[19] that provide significant rate enhancements[20,21].

An early kinetic study by our group focused on the reduction of acetophenone with varying proton donors and showed a substantial difference in rate enhancement from the addition of alcohols versus water at constant concentrations of proton donor. For alcohols, the difference in rate appeared to correlate to pK_a, but water strayed from this observed trend and combined with the observed shift in the visible absorption spectrum, was indicative of water having a high affinity for Sm(II).[22] It was later revealed that not only does water act as a proton source, but that coordination of water to Sm(II) provides a thermodynamically more powerful reductant.[23] Despite the production of a thermodynamically more powerful reductant that results from the addition of water, the reduction of ketones and lactones by SmI_2 is still an endergonic process as outlined in Scheme 4.3.
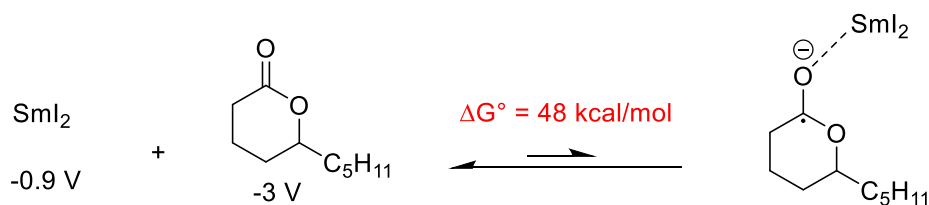
Scheme 4.3 Estimated endergoncity of the reduction of a lactone by SmI_2.

Although the oxophilicity of Sm(II) is well-established[24–27], further insight into the significance of the carbonyl-samarium interaction provides some rationale for the observed reactivity of samarium towards carbonyl-containing substrates. The electrostatic driving force for the reduction of an activated ketone through electron

transfer from SmI$_2$ in the absence of proton donor was quantified by Hoz. By measuring the rate of reduction of a series of *p*-substituted benzophenone derivatives, a linear Hammett correlation and electrochemical data were consistent with a strong Coulombic interaction between the ketyl radical anion and Sm(III) that facilitates an inner sphere electron transfer that decreases the overall endothermicity of the reaction by up to 25 kcal/mol.[28]

The work presented in Chapter 2 focused on elucidating the role of water by examining the reduction of non-coordinating substrates, 1-iodododecane and anthracene to isolate and compare the influence of proton donor on the reaction. The reduction of anthracene by SmI$_2$-H$_2$O revealed that this combination could effectively transfer a hydrogen atom in one kinetic step to bypass a high energy intermediate and demonstrated that SmI$_2$-H$_2$O likely reduces the substrate through a proton-coupled, electron transfer (PCET) as shown below in Scheme 4.4.[29]
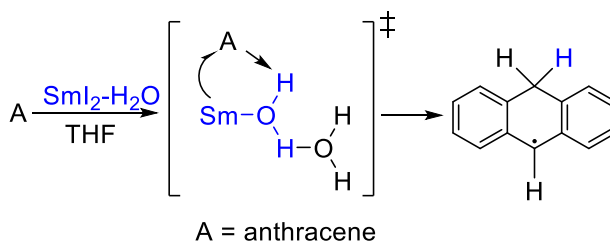
A = anthracene

Scheme 4.4 Mechanism of reduction of anthracene through PCET by SmI$_2$-H$_2$O.

In a subsequent study described in Chapter 3, the reductions of anthracene and benzyl bromide were surveyed with a range of sterically-hindered and unhindered glycols as well as water. These studies ultimately showed not only that proton donor coordination considerably enhanced the rate of reduction of both substrates, but was a crucial

prerequisite and driving force for reductions that occur through PCET from Sm(II)-water.[30]

Despite a number of mechanistic studies on these reactions, many fundamental questions still remain. In the following study, the reductions of a model aldehyde, ketone, and lactone were examined through kinetic and thermodynamic experiments to further ascertain whether the reduction of carbonyls by SmI_2-H_2O proceeds through PCET or an alternative mechanism.

4.2 Experimental Details

4.2.1 Materials

Samarium powder was purchased from Acros Organics. SmI_2 was generated by the standard method of samarium metal combined with iodine in THF and allowed to stir for at least 4 hours. Iodometric titrations were performed to verify concentration of SmI_2. Heptaldehyde and cyclohexanone were distilled and degassed with argon prior to use. 5-Decanolide was purified using a Kügelrohr distillation and then degassed with argon. Substrates were then stored over molecular sieves. Inhibitor-free tetrahydrofuran was purified by a Solvent Purification system (Innovative Technology Inc.; MA). H_2O and D_2O were deoxygenated by bubbling through with argon overnight. All solutions were prepared inside a drybox containing an argon atmosphere.

4.2.2 Instrumentation

UV-Vis spectra were obtained using a Shimadzu UV-1601 spectrophotometer controlled by UV Probe software (version 1.11). Solutions were prepared in a drybox and

placed inside an airtight cuvette. Kinetic experiments were performed using a computer-controlled SX.18 MV stopped-flow spectrophotometer (Applied Photophysics Ltd. Surrey, UK). Proton NMR spectra were recorded on a Bruker 500 MHz spectrometer in $CDCl_3$. Carbon NMR were performed at 125 MHz in $CDCl_3$. GC-MS analyses were done with an HP 5890 Series II Gas Chromatograph with an HP Mass Selector Detector.

4.2.3 Methods

4.2.3.1 General Procedure for Synthetic-Scale SmI₂-H₂O Reductions

4.2.3.1.1 Procedure for Reduction of Heptaldehyde

Inside an Ar glove box, 100 μL of heptaldehyde (0.715 mmols) was dissolved in 2.5 equiv (vs aldehyde) of 0.1 M SmI_2 in THF. Following dissolution, H_2O (100 equiv vs SmI_2) was added dropwise to the reaction. The reaction was left until the mixture became colorless and a white precipitate formed. The round bottom flask was removed from the box and quenched with air and saturated NH_4Cl. Heptanol was extracted using diethyl ether. The organic layer was then treated with saturated aqueous sodium thiosulfate, and then brine. The remaining solution was then dried with magnesium sulfate, filtered and then solvent was removed by rotary evaporation.

4.2.3.1.1 Procedure for Reduction of Cyclohexanone

Inside an Ar glove box, 100 μL of cyclohexanone (0.965 mmol) was dissolved in 2.5 equiv (vs cyclohexanone) of 0.1 M SmI_2 in THF in a stirring round bottom flask. Following dissolution, H_2O (100 equiv vs SmI_2) was added dropwise to the reaction. The reaction was left until the mixture became colorless and a white precipitate formed. The round bottom flask was removed from the box and quenched with air and saturated NH_4Cl. Cyclohexanol was extracted using diethyl ether. The organic layer was then

105

treated with saturated aqueous sodium thiosulfate, and then brine. The remaining solution was then dried with magnesium sulfate, filtered, and then solvent was removed by rotary evaporation to provide purified product.

4.2.3.1.1 Procedure for Reduction of 5-Decanolide

Inside an Ar glove box, 100 μL of 5-Decanolide (0.435 mmol) was dissolved in 5 equiv (vs 5-Decanolide) of 0.1 M SmI_2 in THF. Following dissolution, 100 equiv of water (vs SmI_2) was added dropwise to the reaction. The reaction was left until the mixture became colorless and a white precipitate formed. The round bottom flask was removed from the box and quenched with air and saturated NH_4Cl. 1,5-decanediol was extracted using ethyl acetate. The organic layer was then treated with saturated aqueous sodium thiosulfate, and then brine. The remaining solution was then dried with magnesium sulfate, filtered and then solvent was removed by rotary evaporation.

4.2.3.2 General Procedure for SmI_2-H_2O Stopped-Flow Kinetic Studies

The SmI_2, substrate, and proton donor solutions were injected independently into the stopped-flow system from airtight BD syringes prepared in a glove box. The cell block and the drive syringes of the stopped flow reaction analyzer were flushed a minimum of three times with dry, deoxygenated THF to make the system anaerobic and were subsequently primed by flushing through one set of syringes with solutions to be analyzed. Between each experiment, the cell block was washed with dilute HNO_3 (2x), DI H_2O (3x), and THF (3x) before additional anhydrous deoxygenated THF washes (3x). The reaction rates were determined by a single exponential fit of the decay of 10mM SmI_2 at 25 °C and 560 nm using Pro-Data SX software.

4.3 Results and Discussion

To evaluate the mechanism of carbonyl reduction by SmI_2-water, three model substrates were utilized: heptaldehyde **I**, cyclohexanone **II**, and 5-decanolide **III**. These substrates were chosen since they represent carbonyls spanning a range of redox potentials that are known to be reduced by SmI_2-H_2O. To ensure that all substrates yielded the expected reduction product, the reactions were performed on synthetic scale to verify the identity of the products. Rate studies on each substrate were carried out under pseudo first-order conditions with substrate in at least a ten-fold excess with respect to $[SmI_2]$. Water concentrations were examined over a range of 50 mM to 7 M. Each rate measurement was repeated a minimum of three times to examine reproducibility. A representative plot of each k_{obs} vs $[H_2O]$ for the reduction of **I-III** are shown below in Figure 4.1-3.
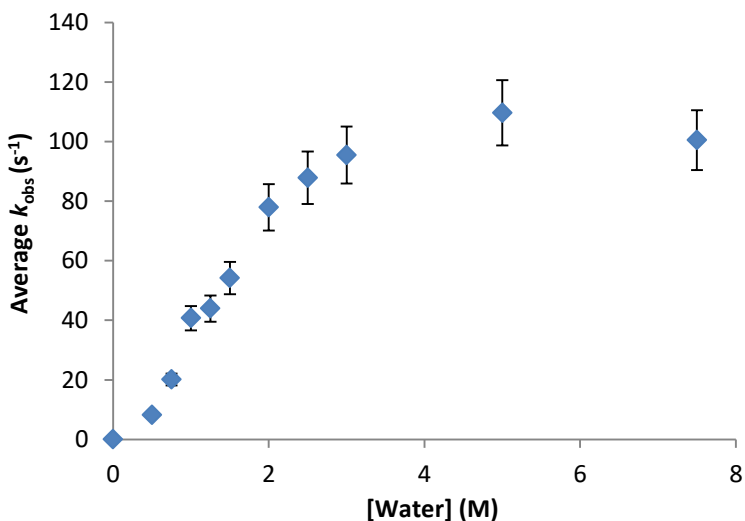
Figure 4.1. k_{obs} vs. $[H_2O]$ for reduction of **I** (100 mM) by SmI_2 (10 mM) at 25 ^{o}C.

107
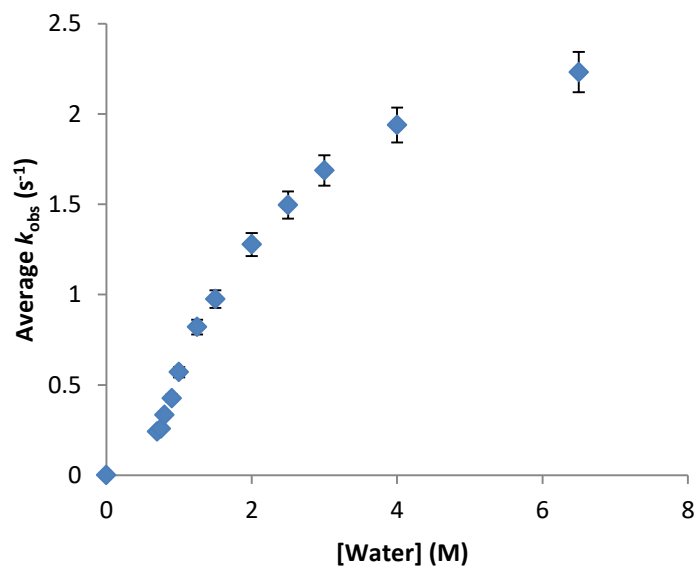
Figure 4.2. k_{obs} vs. [H_2O] for reduction of **II** (100 mM) by SmI_2 (10 mM) at 25 °C.
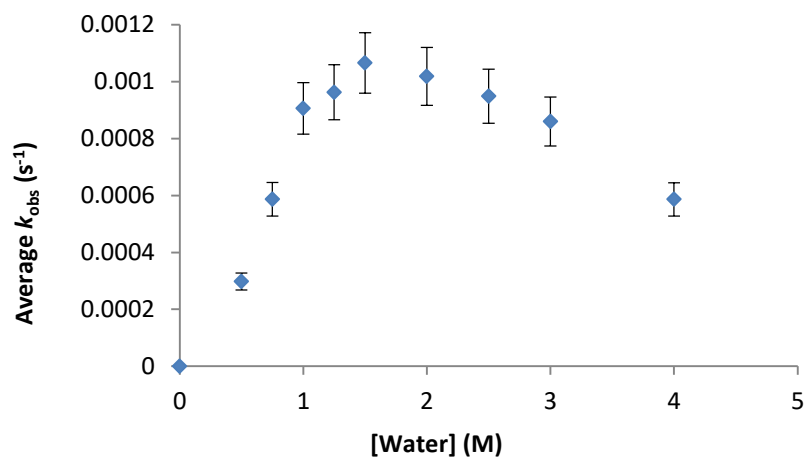
Figure 4.3. k_{obs} vs. [H_2O] for reduction of **III** (500 mM) by SmI_2 (10 mM) at 25 °C.

Inspection of the data shows that the rate of reduction increases until an apex at approximately 1.75 M and the rate then decreases at higher concentrations of water. Additionally, the rate plots showed curvature consistent with a rate order of water greater than unity as demonstrated in previous studies on the reduction of anthracene.[31,32] To

further examine the system, rate orders and constants were determined for each substrate. Studies were carried out up to 1 M water since this is the concentration range used in the majority of carbonyl reductions by SmI_2-water. The data are contained in Table 4.1.

Table 4.1. Rate orders for substrate reduction by SmI_2-water.

Substrate	Rate Constant $(M^{-3}s^{-1})$	Rate Orders		
		$H_2O^{a,d}$	Substrate[b]	$SmI_2^{c,d}$
I	$4.2 \pm 0.3 \times 10^4$	2	1.0 ± 0.1	1
II	570 ± 70	2	1.1 ± 0.1	1
III	0.18 ± 0.01	2	0.9 ± 0.1	1

Conditions: [a]Pseudo-1st order conditions with varying $[H_2O]$ (0 – 1 M) and constant $[SmI_2]$ (10 mM) and [substrate] (100 mM). [b]Pseudo-1st order conditions with varying [substrate] (**I**: 100-160 mM, **II**: 100-500 mM, **III**: 400-800 mM) and constant $[SmI_2]$ (10 mM) and $[H_2O]$ (1 M). [c]Determined via fractional times method averaged over multiple trials. [d] [**III**] = 500 mM.

For each substrate reduction examined, the rate order of SmI_2 and substrate were approximately one and water was second order. The fourth order rate constants spanned a range of 5 orders of magnitude with the rates of reduction **I** > **II** >> **III** correlating with substrate redox potential.[33]   In the absence of water, **I** and **II** were reduced several orders of magnitude more slowly affording pinacols instead of reduced products; whereas **III** was not reduced, providing only recovered starting material.

To further examine the mechanistic impact of substrate reduction by water, a series of rate experiments were carried out employing D_2O in place of water. Rate measurements were obtained from the reduction of substrates using either water or D_2O at 1 M under pseudo-first order conditions with $[SmI_2]$ = 10 mM and substrate in a minimum 10-fold

or greater excess. An example of the observed difference in rates is shown in Figure 4.4 for the reduction of **I**.
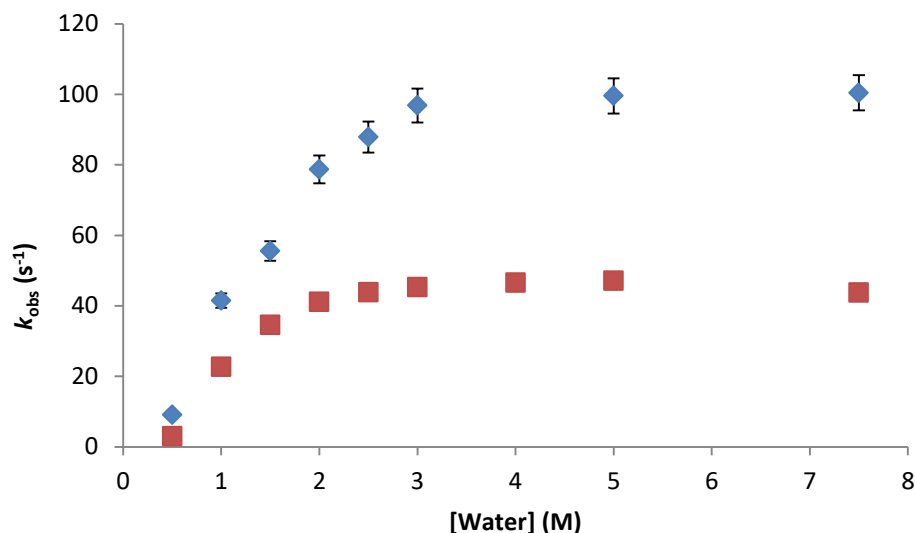
Figure 4.4. Rates of reduction of heptaldehyde (**I**) with increasing concentrations of H_2O(◆) and D_2O(■).

The k_H/k_D for substrates **I**, **II**, and **III** were determined to be 1.8 ± 0.1, 2.3 ± 0.1, and 1.7 ± 0.1, respectively. These values are somewhat different than those previously reported for similar reductions.[34] In previous reported studies, KIE's were obtained from deuterium incorporation in products and attributed to a secondary isotope effect.[34] In spite of the fact that isotope effects were studied by different methods, the question is whether the k_H/k_D represents a primary or secondary effect. In reactions that involve PCET, isotope effects vary and there are many examples where isotope effects are small.[35–39] In a classical ET-PT, a highly ordered early transition state would be expected to provide a low k_H/k_D since the zero-point vibrational energy differences for D and H are small between the reactant and activated complex.[40] As a consequence, it is probable that

the KIE obtained from independent rate experiments as described above are consistent with a primary isotope effect.

To acquire a more detailed understanding of the reduction of substrates **I-III** by SmI$_2$-water, and further examine the basis for deuterium isotope effects, rates of reduction were measured over a 30 degree temperature range to obtain activation parameters for the reaction. For these experiments, water was maintained at 1 M (100 equiv) based on [SmI$_2$] since this is the concentration where water exhibits a rate order of 2. During studies on the reduction of **I**, it was observed that the rate of reduction slowed with increasing temperature. The Eyring plot for the reduction of **I** is displayed in Figure 4.5. The activation parameters for the reduction of **I-III** are contained in Table 4.2. Without a rigorous analysis, transition state parameters can be susceptible to systematic errors.[41] Nonetheless, comparison of the data provides important insight into the activation process for a series of related reactions.
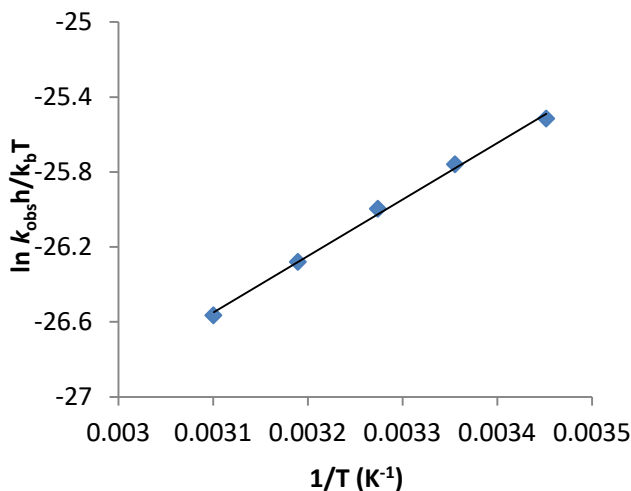
Figure 4.5. Sample Eyring plot for the reduction of **I** (100 mM) by SmI$_2$ (10 mM) and water (1 M) over a range of 30 °C.

111

Evaluation of the $\Delta H^{\ddagger}$ for the reduction of substrates displays the trend $\mathbf{I} < \mathbf{II} <$ $\mathbf{III}$ with $\mathbf{I}$ and $\mathbf{II}$ displaying negative enthalpies of activation and $\mathbf{III}$ providing a positive value for $\Delta H^{\ddagger}$. Negative enthalpies of activation are relatively rare, but several examples are known for systems involving PCET.[42–44] Negative values of $\Delta H^{\ddagger}$ are often ascribed to the presence of low concentrations of intermediates that are enthalpically favored.[42–44] All substrates display negative $\Delta S^{\ddagger}$ values with the trend being $\mathbf{I} < \mathbf{II} < \mathbf{III}$. Overall, these data show that the low activation barrier for $\mathbf{I}$ and $\mathbf{II}$ is compensated by a substantial entropic cost in the activated complex. The consequences of this finding are discussed *vide infra*.

Table 4.2. Activation parameters for the reduction of substrates by SmI_2-water.

Substrate	$\Delta H^{\ddagger}$ (kcal mol^{-1})^a	$\Delta S^{\ddagger}$ (cal mol^{-1} K^{-1})^a	$\Delta G^{\ddagger}$ (kcal mol^{-1})^b
I	-6.1 ± 0.2	-72 ± 1	15.3 ± 0.1
II	-1.7 ± 0.3	-65 ± 1	17.8 ± 0.1
III	9.6 ± 0.1	-41 ± 1	21.7 ± 0.1

Conditions: 10 mM SmI_2, 1 M H_2O, and 100 mM **I** and **II** or 500 mM **III** in THF. The activation parameters are the average of 3 independent experiments from 293-323 K and are reported as $\pm\sigma$. ^{a}Obtained from $\ln(k_{obs}h/k_bT)$- $\Delta H^{\ddagger}/RT + \Delta S^{\ddagger}/R$. ^{b}Calculated from $\Delta G^{\ddagger} = \Delta H^{\ddagger}$-$T\Delta S^{\ddagger}$.

The data presented above show that the ease of substrate reduction (as measured by redox potential) correlates with the enthalpy of activation. This raises the interesting question, does the formation of charge upon an initial ET from SmI_2-water stabilize the ketyl radical through the interaction between the ketyl oxygen and Sm(III) leading to a

strong coulombic attraction? If so, what are the differences between substrates **I**-**III** in the formal transfer of a hydrogen atom from SmI$_2$-water to each substrate?

To further assess the relationship between substrate structure and charge on the neutral carbonyl and radical anion, calculations were performed on **I**-**III** and their associated radical anions using Gaussian09(1) programs employing the APF-D(2) hybrid DFT method and the 6-311+g(2d,p) basis set. Solvation values were calculated using the polarizable continuum model with integral equation formalism, IEFPCM with tetrahydrofuran as the solvent. Charges were determined using natural population analysis (NPA) (see Appendix). Results for NPA are shown in Table 4.3.

Table 4.3. Natural population analysis for the carbonyl oxygens of substrates **I**-**III** and their associated radical anions.

Substrate	NPA for carbonyl	NPA for radical anion	ΔNPA
I	-0.580	-0.895	-0.315
II	-0.610	-0.899	-0.289
III[a]	-0.642	-0.871	-0.229

[a]Calculations were performed on δ-valerolactone.

The charges on the carbonyl oxygen of **I** -**III** follow the expected trend with **I** having the least electron density on the carbonyl oxygen and **III** having the most. The distribution of the electron density on the radical anions of these compounds demonstrates that the greatest increase in charge occurs for **I** and the least occurs for **III**. It was our supposition that the change in electron density from the neutral compound

113

upon reduction to the radical anion would correlate with the $\Delta H^{\ddagger}$ values if a coulombic interaction between the carbonyl oxygen and Sm was important during the reduction. A plot of $\Delta H^{\ddagger}$ vs. ΔNPA is shown in Figure 4.6 and provides a linear correlation.
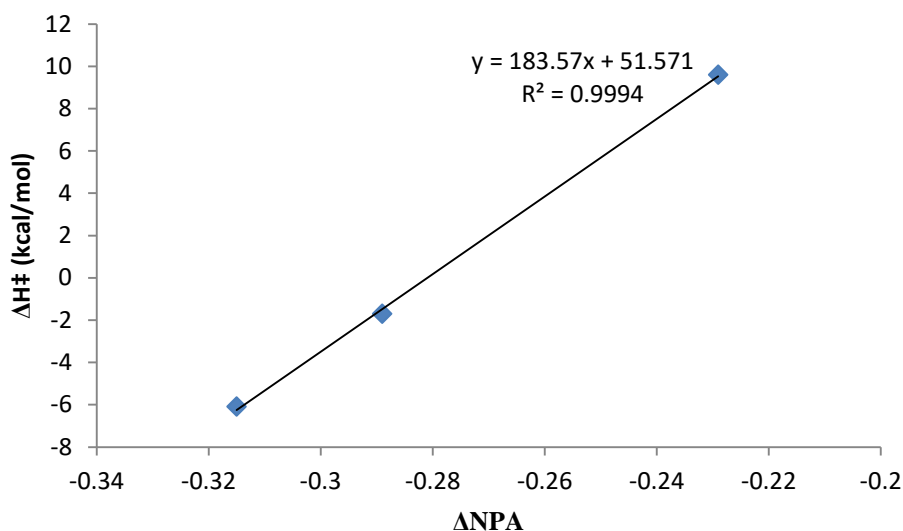
Figure 4.6 Plot of linear correlation between $\Delta H^{\ddagger}$ and ΔNPA.

While one should be cautious when evaluating a trend line based on 3 points, there is clearly a relationship between the change in charge on the carbonyl oxygen and the strength of the interaction between Sm and oxygen during the course of the reduction.

Overall, the studies presented above provide the following observations: 1) The rate of substrate reduction by SmI$_2$-water is **I** > **II** >>**III**. 2) In the absence of water, substrates **I** and **II** are reduced significantly more slowly by SmI$_2$ and **III** is not reduced even after extended periods of time. 3) All reductions are first-order in substrate and SmI$_2$ and second order in water (below 100 equivalents). 4) All reductions proceed through highly ordered transition states. Additionally, **I** and **II** display negative $\Delta H^{\ddagger}$

values and exhibit the trend **III** > **II** > **I**. 5) The $\Delta H^{\ddagger}$ values correlate well with the change in charge on the carbonyl oxygen of each substrate as measured by NPA.

In addition to the current findings, it is useful to consider the results in the context of previous studies. It is well-established that water and carbonyls have a high affinity for Sm(II). Water coordinates strongly to Sm(II) and spectroscopic studies have shown evidence for coordination between the metal and low concentrations of the proton donor in bulk THF.[22,23,45] In addition, carbonyls are known to have a high affinity for Sm(II).[21,46] To further test this finding, the UV-vis spectrum of a 2.5 mM solution of SmI_2 in THF containing increasing amounts of **III** was obtained and is shown in Figure 4.7.
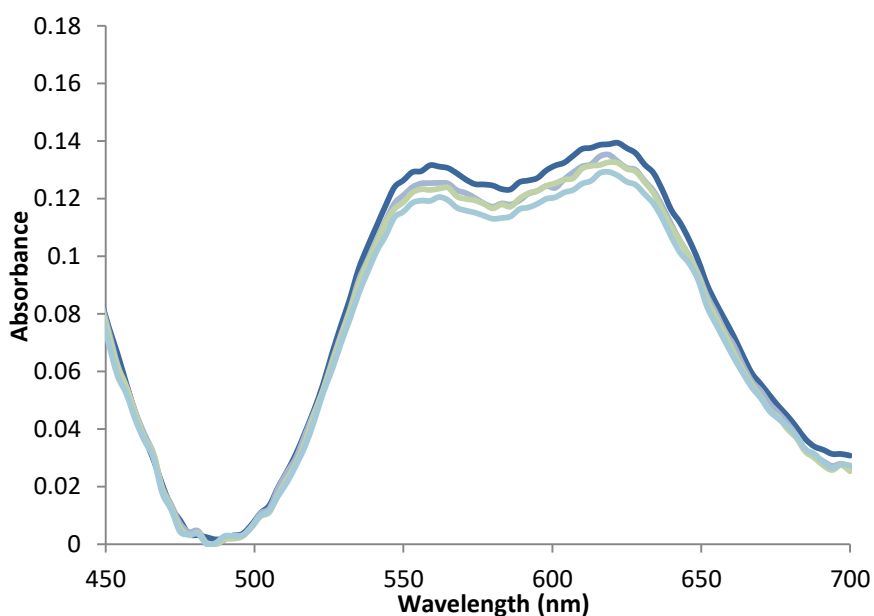
Figure 4.7 UV-vis spectra of SmI_2 (2.5 mM) in presence of increasing amount of **III** (5, 10, 15 equiv) in THF.

The spectra show evidence of coordination with as little as 5 equivalents of substrate, providing additional support for carbonyl coordination to Sm(II). Each increasing quantity of **III** causes a decrease in the observed absorbance. Overall, the collection of data demonstrates that it is probable that both water and carbonyl are coordinated to Sm during the course of the reduction. Previous studies have established that proton transfer from bulk water is unlikely,[31] so it is reasonable to assume that formal HAT occurs through a highly ordered activated complex with one or both waters bound to Sm(II) as shown in Scheme 4.5.
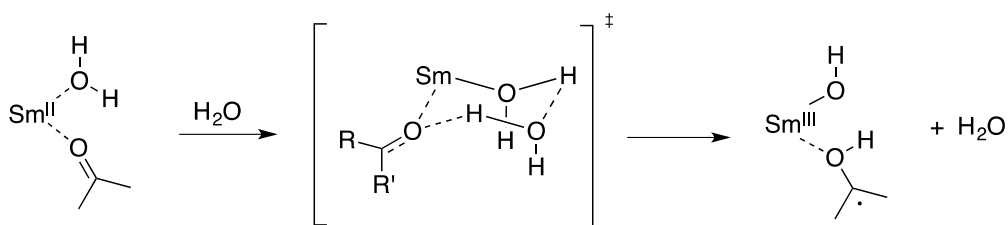
Scheme 4.5 Proposed mechanism for the reduction of carbonyl substrates by PCET from SmI$_2$-H$_2$O.

The question that remains is: Are these reactions a consequence of PCET? Reactions that proceed through PCET may be sequential or concerted.[47] In the former case, the transfer of an electron produces a stable intermediate that precedes proton transfer (or vice versa). In the latter instance, concerted PCET is favored when the stepwise pathways are significantly endergonic.[48–52] To further evaluate the process, it is instructive to consider the diagram displayed Scheme 4.6. If a carbonyl is coordinated to the Sm(II)-water complex **A**, a sequential process will produce intermediate **B**, followed

116

by internal proton transfer to produce intermediate **C**. In a concerted process where the stepwise ET-PT is significantly endergonic, direct conversion from **A** to **C** occurs.
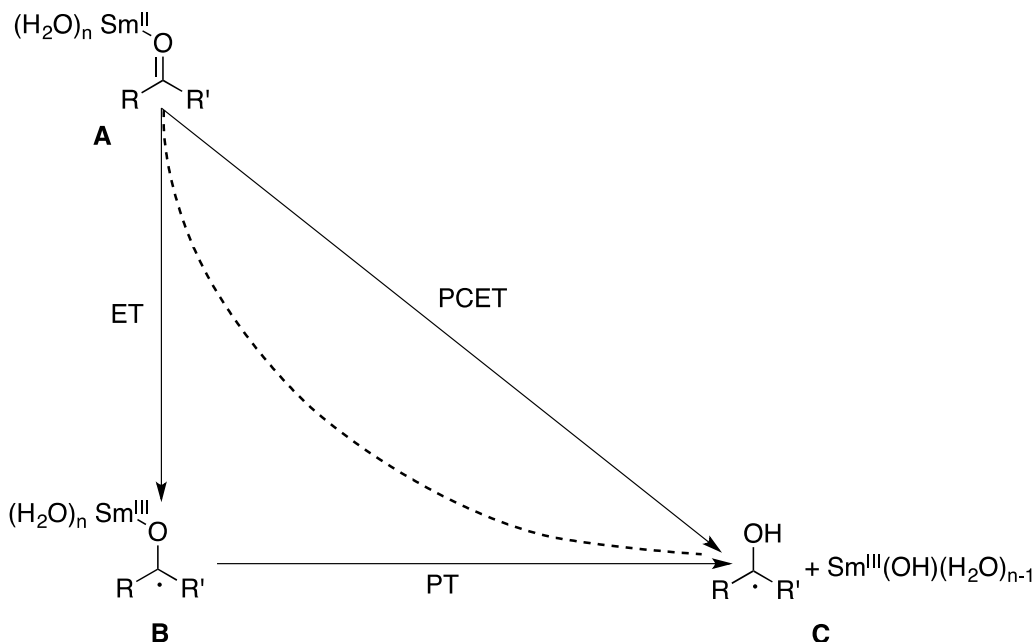
Scheme 4.6. Proposed continuum between concerted and stepwise reduction processes.

It is reasonable to assume that a hybrid process is also possible (dotted line in Scheme 4.6). For instance, as reduction commences, increasing positive charge on Sm enhances the interaction between the emerging ketyl while simultaneously increasing the acidity of bound water promoting proton transfer.

In light of the data presented above, and work described in previous studies, it is our supposition that in the case of substrates **I** and **II**, reduction occurs via asynchronous PCET that is driven by the stabilization of the developing charge through the coulombically favored interaction of the carbonyl oxygen and Sm during the reduction. In the case of **III**, the activation barrier for reduction through an initial ET is highly

117

endergonic. As a consequence, reduction of **III** proceeds through a concerted PCET from SmI$_2$-water.

4.4 Conclusions

Overall, the results and analysis presented in this chapter provide evidence that formal hydrogen atom transfer from SmI$_2$-water to carbonyl occurs through PCET. The degree of stabilization achieved through a favorable coulombic interaction between the carbonyl oxygen and Sm in the activated complex is a consequence of the degree of endergonicity of ET. While these studies clarify the mechanism of carbonyl reduction by SmI$_2$-water, the results may have implications for the activation and reduction or reductive coupling of other functional groups capable of coordinating to low valent metal-proton donor complexes.[53–66] Additionally, these results are consistent with formal hydrogen atom transfer to carbonyls, but not the reversibility of this process, which is addressed in the following chapter. Future work in this area will focus on the examination of a range of carbonyl functional groups to discern the impact of steric and electronic effects on reduction by SmI$_2$-water and other additives capable of promoting PCET from a complex with Sm(II).

4.5 References

(1)   Namy, J. L.; Girard, P.; Kagan, H. *Nouv. J. Chim.* **1977**, *1*, 5–7.

(2)   Dahlén, A.; Hilmersson, G. *Eur. J. Inorg. Chem.* **2004**, *2004* (17), 3393–3403.

(3)   Kagan, H. B.; Namy, J.-L. *Top. Organomet. Chem.* **1999**, *2* (Lanthanides), 155–

198.

(4)   Chciuk, T. V.; Flowers, II, R. A. In *Science of Synthesis*; Marek, I., Ed.; Georg Thieme Verlag KG: Stuttgart, 2016; pp 177–261.

(5)   Edmonds, D. J.; Johnston, D.; Procter, D. J. *Chem. Rev.* **2004**, *104* (7), 3371–3403.

(6)   Szostak, M.; Fazakerley, N. J.; Parmar, D.; Procter, D. J. *Chem. Rev.* **2014**, *114* (11), 5959–6039.

(7)   Hasegawa, E.; Curran, D. P. *J. Org. Chem.* **1993**, *58*, 5008–5010.

(8)   Kamochi, Y.; Kudo, T. *Chem. Lett.* **1993**, 1495–1498.

(9)   Nakata, T. *Chem. Rec.* **2010**, *10* (3), 159–172.

(10)   Nicolaou, K. C.; Ellery, S. P.; Chen, J. S. *Angew. Chemie Int. Ed.* **2009**, *48* (39), 7140–7165.

(11)   Szostak, M.; Spain, M.; Sautier, B.; Procter, D. *Org. Lett.* **2014**, *16*, 5694–5697.

(12)   Chopade, P. R.; Davis, T. A.; Prasad, E.; Flowers, II, R. A. *Org. Lett.* **2004**, *6* (16), 2685–2688.

(13)   Hutton, T. K.; Muir, K.; Procter, D. J. *Org. Lett.* **2002**, *4* (14), 2345–2347.

(14)   Kleiner, G.; Tarnopolsky, A.; Hoz, S. *Org. Lett.* **2005**, *7* (19), 4197–4200.

(15)   Upadhyay, S. K.; Hoz, S. *J. Org. Chem.* **2011**, *76* (5), 1355–1360.

(16)   Girard, P.; Namy, J. L.; Kagan, H. B. *J. Am. Chem. Soc.* **1980**, *102* (8), 2693–

2698.

(17) Szostak, M.; Spain, M.; Procter, D. J. *Nat. Protoc.* **2012**, *7* (5), 970–977.

(18) Szostak, M.; Collins, K. D.; Fazakerley, N. J.; Spain, M.; Procter, D. J. *Org. Biomol. Chem.* **2012**, *10* (30), 5820–5824.

(19) Taaning, R. H.; Lindsay, K. B.; Skrydstrup, T. *Tetrahedron* **2009**, *65* (52), 10908–10916.

(20) Szostak, M.; Spain, M.; Choquette, K. A.; Flowers, II, R. A.; Procter, D. J. *J. Am. Chem. Soc.* **2013**, *135* (42), 15702–15705.

(21) Prasad, E.; Flowers, R. A. *J. Am. Chem. Soc.* **2002**, *124* (22), 6357–6361.

(22) Chopade, P. R.; Prasad, E.; Flowers, II, R. A. *J. Am. Chem. Soc.* **2004**, *126* (1), 44–45.

(23) Prasad, E.; Flowers, II, R. A. *J. Am. Chem. Soc.* **2005**, *127* (51), 18093–18099.

(24) Inanaga, J.; Yamaguchi, M.; Kusuda, K. *Tetrahedron Lett.* **1989**, *30* (22), 2945–2948.

(25) Prasad, E.; Knettle, B. W.; Flowers, II, R. A. *J. Am. Chem. Soc.* **2002**, *124* (49), 14663–14667.

(26) Maity, S.; Choquette, K. A.; Flowers, R. A.; Prasad, E. *J. Phys. Chem. A* **2012**, *116* (9), 2154–2160.

(27)   Chciuk, T. V.; Hilmersson, G.; Flowers, R. A. *J. Org. Chem.* **2014**, *79* (20), 9441–9443.

(28)   Farran, H.; Hoz, S. *Org. Lett.* **2008**, *10* (21), 4875–4877.

(29)   Chciuk, T. V.; Flowers, II, R. A. *J. Am. Chem. Soc.* **2015**, *137*, 11526–11531.

(30)   Chciuk, T. V.; Anderson, W. R.; Flowers, II, R. A. *Angew. Chemie - Int. Ed.* **2016**, *55*, 6033–6036.

(31)   Chciuk, T. V.; Flowers, II, R. a. *J. Am. Chem. Soc.* **2015**, *137* (Ii), 11526–11531.

(32)   Chciuk, T. V.; Anderson, W. R.; Flowers, R. A. *Angew. Chemie - Int. Ed.* **2016**, *55* (20), 6033–6036.

(33)   Roth, H. G.; Romero, N. A.; Nicewicz, D. A. *Synlett* **2016**, *27* (5), 714–723.

(34)   Szostak, M.; Spain, M.; Procter, D. J. *J. Am. Chem. Soc.* **2014**, *136* (23), 8459–8466.

(35)   Megiatto Jr., J. D.; Mendez-Hernandez, D. D.; Tejeda-Ferrari, M. E.; Teillout, A. L.; Llansola-Portoles, M. J.; Kodis, G.; Poluektov, O. G.; Rajh, T.; Mujica, V.; Groy, T. L.; Gust, D.; Moore, T. A; Moore, A. L. *Nat Chem* **2014**, *6* (5), 423–428.

(36)   Warren, J. J.; Menzeleev, A. R.; Kretchmer, J. S.; Miller, T. F.; Gray, H. B.; Mayer, J. M. *J. Phys. Chem. Lett.* **2013**, *4* (3), 519–523.

(37)   Tarantino, K. T.; Liu, P.; Knowles, R. R. *J. Am. Chem. Soc.* **2013**, *135* (27), 10022–10025.

(38)   Schrauben, J. N.; Cattaneo, M.; Day, T. C.; Tenderholt, A. L.; Mayer, J. M. *J. Am. Chem. Soc.* **2012**, *134* (40), 16635–16645.

(39)   Warren, J. J.; Mayer, J. M. *J. Am. Chem. Soc.* **2011**, *133* (22), 8544–8551.

(40)   Anslyn, E. V; Dougherty, D. A. *Moder Physical Organic Chemistry*; University Science Books: Sausalito, CA, 2006.

(41)   Remenar, J. F.; Collum, D. B. *J. Am. Chem. Soc.* **1997**, *119* (24), 5573–5582.

(42)   Yoder, J. C.; Roth, J. P.; Gussenhoven, E. M.; Larsen, A. S.; Mayer, J. M. *J. Am. Chem. Soc.* **2003**, *125* (9), 2629–2640.

(43)   Mader, E. A.; Larsen, A. S.; Mayer, J. M. *J. Am. Chem. Soc.* **2004**, *126* (26), 8066–8067.

(44)   Maneiro, M.; Ruettinger, W. F.; Bourles, E.; Mclendon, G. L.; Dismukes, G. C. *Proc. Natl. Acad. Sci. USA* **2003**, *100* (7), 3707–3712.

(45)   Sadasivam, D. V; Teprovich, J. A.; Procter, D. J.; Flowers, II, R. A. *Org. Lett.* **2010**, *12* (18), 4140–4143.

(46)   Prasad, E.; Flowers, II, R. A. *J. Am. Chem. Soc.* **2002**, *124*, 6895–6899.

(47)   Hammes-Schiffer, S.; Soudackov, A. V. *J. Phys. Chem. B* **2008**, *112* (45), 14108–14123.

(48)   Mayer, J. M. *J. Phys. Chem. Lett.* **2011**, *2*, 1481–1489.

(49)   Mayer, J. M. *Acc. Chem. Res.* **2011**, *44* (1), 36–46.

(50)   Warren, J. J.; Tronic, T. A.; Mayer, J. M. *Chem. Rev.* **2010**, *110* (12), 6961–7001.

(51)   Mayer, J. M.; Rhile, I. J. *Biochim. Biophys. Acta - Bioenerg.* **2004**, *1655* (1–3), 51–58.

(52)   Mayer, J. M. *Annu. Rev. Phys. Chem.* **2004**, *55* (1), 363–390.

(53)   Zhang, Y. Q.; Jakoby, V.; Stainer, K.; Schmer, A.; Klare, S.; Bauer, M.; Grimme, S.; Cuerva, J. M.; Gans??uer, A. *Angew. Chemie - Int. Ed.* **2016**, *55* (4), 1523–1526.

(54)   Tarantino, K. T.; Miller, D. C.; Callon, T. a; Knowles, R. R. *J. Am. Chem. Soc.* **2015**, *137*, 6440–6443.

(55)   Semproni, S. P.; Milsmann, C.; Chirik, P. J. *J. Am. Chem. Soc.* **2014**, *136* (25), 9211–9224.

(56)   Estes, D. P.; Grills, D. C.; Norton, J. R. **2014**, *4*, 4–7.

(57)   Fang, H. Y.; Ling, Z.; Lang, K.; Brothers, P. J.; de Bruin, B.; Fu, X. F. *Chem. Sci.* **2014**, *5* (3), 916–921.

(58)   Paradas, M.; Campaña, A. G.; Jiménez, T.; Robles, R.; Oltra, J. E.; Buñuel, E.; Justicia, J.; Cárdenas, D. J.; Cuerva, J. M. *J. Am. Chem. Soc.* **2010**, *132* (36), 12748–12756.

(59)   Manner, V. W.; Mayer, J. M. *J. Am. Chem. Soc.* **2009**, *131* (29), 9874–9875.

(60) Wu, A.; Mayer, J. M. *J. Am. Chem. Soc.* **2008**, *130* (44), 14745–14754.

(61) Wu, A.; Masland, J.; Swartz, R. D.; Kaminsky, W.; Mayer, J. M. *Inorg. Chem.* **2007**, *46* (26), 11190–11201.

(62) Cuerva, J. M.; Campaña, A. G.; Justicia, J.; Rosales, A.; Oller-López, J. L.; Robles, R.; Cárdenas, D. J.; Buñuel, E.; Oltra, J. E. *Angew. Chemie - Int. Ed.* **2006**, *45* (33), 5522–5526.

(63) Spiegel, D. A.; Wiberg, K. B.; Schacherer, L. N.; Medeiros, M. R.; Wood, J. L. *J. Am. Chem. Soc.* **2005**, *127* (36), 12513–12515.

(64) Pozzi, D.; Scanlan, E. M.; Renaud, P. *J. Am. Chem. Soc.* **2005**, *127* (41), 14204–14205.

(65) Roth, J. P.; Mayer, J. M. *Inorg. Chem.* **1999**, *38* (12), 2760–2761.

(66) Jonas, R. T.; Stack, T. D. P. *J. Am. Chem. Soc.* **1997**, *119*, 8566–8567.

Chapter 5. The Reversibility of Ketone Reduction by SmI_2-H_2O

5.1 Background and Significance

The reduction of a carbonyl by samarium diiodide (SmI_2) is the first step in a range of reactions of synthetic importance.[1] Activated carbonyls are frequently reduced in the absence of additives, however alkyl aldehydes, dialkyl ketones and related substrates often require the inclusion of additives such as Lewis bases, inorganic salts, or proton donors (water, alcohols, glycols) to accelerate the reactions.[2–5] An early seminal review on the samarium Barbier reaction used the synthetic data available at the time to deduce the mechanism of ketone reduction. This limited data was consistent with the reduction of a ketone being a fast, reversible process with the reaction equilibrium lying to the side of unreacted ketone and SmI_2.[6]
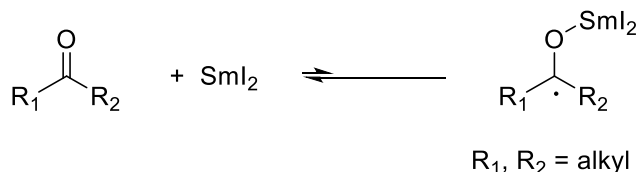
Scheme 5.1. Proposed initial electron transfer to ketone from SmI_2.

This hypothesis was based on the premise that the presence of a pendant alkene would drain the intermediate ketyl through rapid cyclization. Since this general hypothesis was presented, a range of cross-coupling reactions and cyclizations have been examined using HMPA and other additives in concert with SmI_2.[6] Reductive cyclizations featuring SmI_2 and a proton donor such as H_2O, methanol, or t-butanol have been developed, particularly by the Procter group.[7–15] In the example shown in Scheme 5.2, for

instance, a lactone is ring-opened and cyclization of the pendant alkene occurs to yield a five-membered ring.[16]
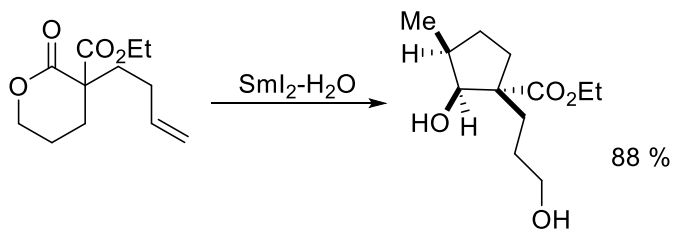
Scheme 5.2. Reductive of cyclization of lactone using SmI_2-H_2O with the aid of directing groups developed by Procter.

In these studies, reductions and cyclizations using SmI_2-H_2O were proposed to proceed through a rate-limiting second ET after cyclization.[15] Therefore, the overall mechanism for the reductive cyclization of a ketone containing a pendant olefin would be expected to proceed through an initial reversible electron transfer, fast cyclization, and then a second rate-limiting electron transfer to the primary carbon radical that would drive the reaction to cyclized product as in Scheme 5.3.
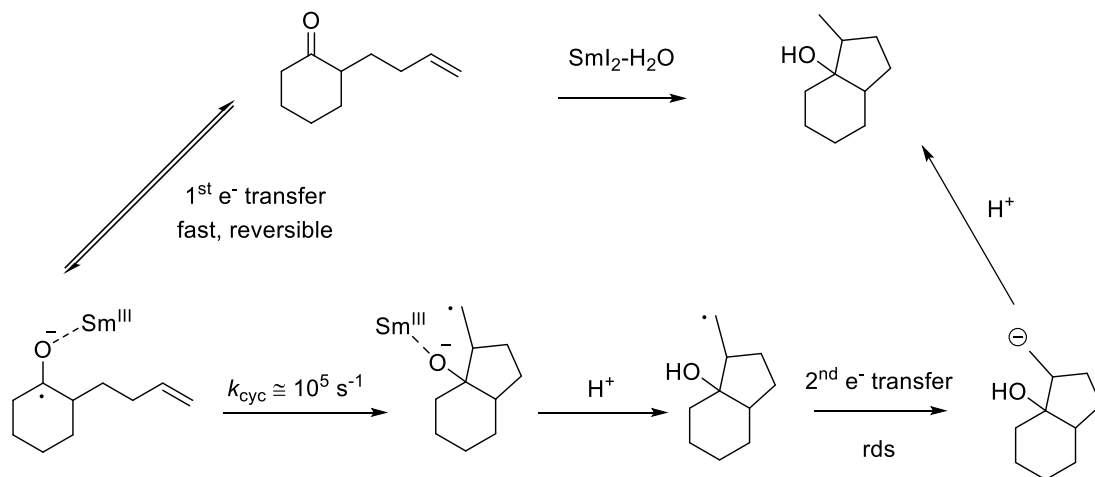
Scheme 5.3. Proposed mechanism for the cyclization promoted by SmI_2-H_2O.

126

The work described in chapters have established experimental evidence consistent with a rate-limiting PCET from SmI_2-H_2O in the reduction of arenes and carbonyls.[17,18] Although the supposition of a reversible ET in the reduction of a carbonyl by SmI_2- H_2O is reasonable, it has not been directly tested through kinetic study. This chapter addresses the reversibility of the initial electron transfer proposed in the literature and provides experimental data that is consistent with a rate-limiting PCET as the first step in the reduction of carbonyls.

When considering the reduction of a carbonyl by SmI_2-H_2O, it is useful to consider elementary processes for each step (Scheme 5.4). To simplify the rate expression, the transfer of an electron and proton are shown together in each step based on evidence the initial reduction takes place through a proton-coupled electron-transfer (PCET).[17–19] For the reduction of a ketone, the first step involves the transfer of an electron from Sm(II) and a proton from water to produce an intermediate ketyl (**I**). In the second step, **I** is reduced by SmI_2- H_2O affording the alcohol (**P**).
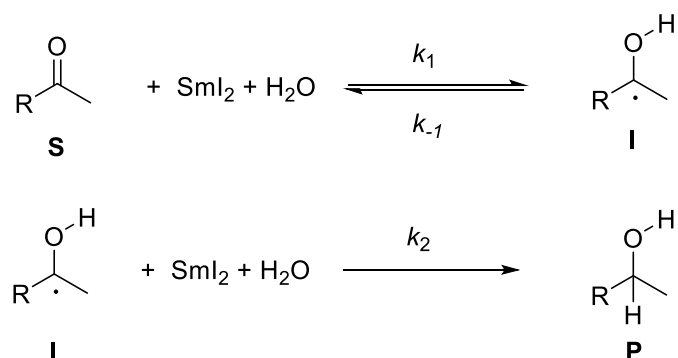
Scheme 5.4 Reduction of a ketone through PCET from SmI_2- H_2O.

For a ketone containing a pendant alkene the same approach can be used, although the process is somewhat more complex, as shown in Scheme 5.5. Initial

reduction of substrate **S-1** by SmI$_2$- H$_2$O leads to intermediate **I-1**. Cyclization of **I-1** leads to a primary radical (**I-2**). Reduction of **I-2** produces carbocycle **P-1**.
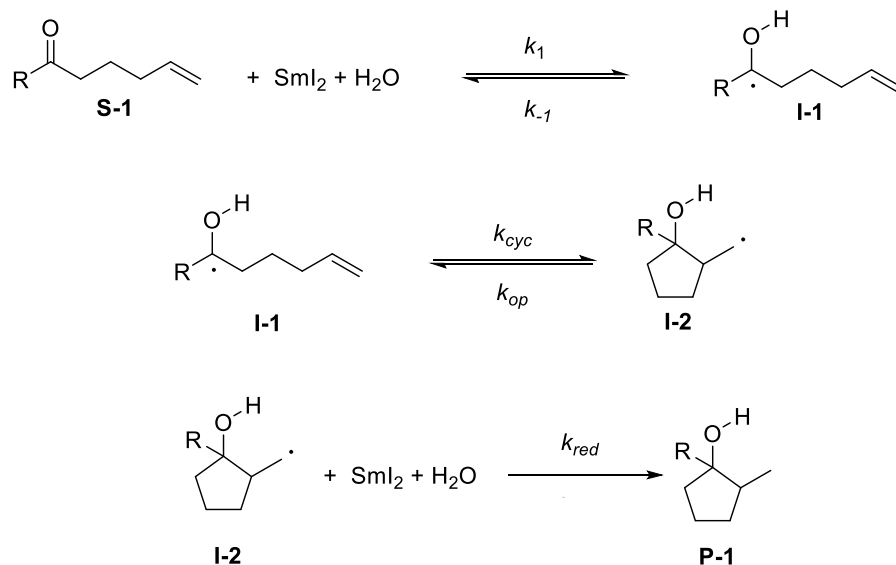
Scheme 5.5 Proposed steps of reduction of a ketone containing a pendant alkene by SmI$_2$-H$_2$O.

With this basic mechanistic framework in hand for each component, rate expressions can be derived for each step. The rate expression for the first step of the reduction of a ketone by SmI$_2$- H$_2$O (Scheme 5.4) can be derived as shown in Scheme 5.6 where superscripts x, y, and z are rate orders determined from kinetic experiments.

rate = $k_1[\mathbf{S}]^x [\text{SmI}_2]^y [\text{H}_2\text{O}]^z$
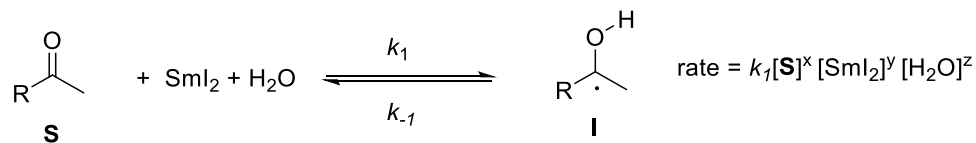
Scheme 5.6 Rate expression for initial reduction of a ketone.

Another expression was derived for the second step that altered the rate orders for SmI$_2$ and water and provide a different observed rate constant in kinetic studies as shown in Scheme 5.7.

$$\text{rate} = \frac{k_1 k_2 [\mathbf{S}]^x [\text{SmI}_2]^{2y} [\text{H}_2\text{O}]^{2z}}{(k_{-1} + k_2 [\text{SmI}_2]^y [\text{H}_2\text{O}]^z)}$$
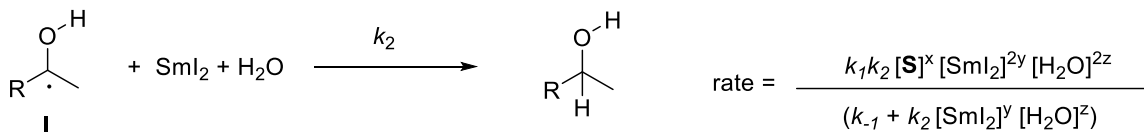
Scheme 5.7. Rate expression for second electron transfer to a ketone.

For the alkenyl substituted ketone shown in Scheme 5.5, the same approach can be used. In the first step of the reduction of **S-1** the rate expressed in Scheme 5.8 is derived. Since the pendant alkene is not directly involved in this step, the rate expression is similar to that of the one derived for the ketone in Scheme 5.6.

$$\text{rate} = k_1 [\mathbf{S}]^x [\text{SmI}_2]^y [\text{H}_2\text{O}]^z$$
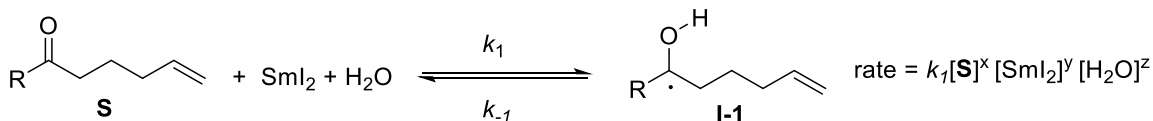
Scheme 5.8 Rate expression for initial electron transfer to alkenyl ketone.

Rate expressions for subsequent steps can be derived to include the rate of cyclization of **I-1** to **I-2** and the rate of reduction of **I-2** to **P-1** as in Scheme 5.9.

$$\text{rate} = \frac{k_{cyc} k_1 [\mathbf{S}]^x [\text{SmI}_2]^y [\text{H}_2\text{O}]^z}{k_{-1} + k_{cyc}}$$
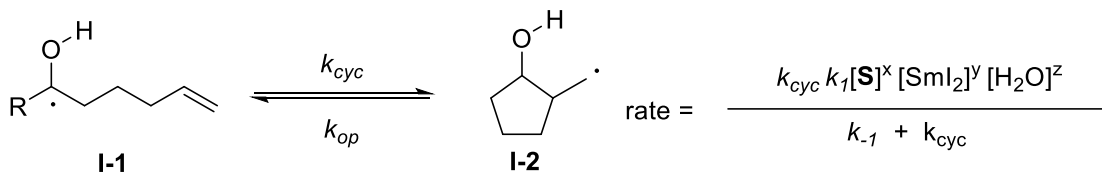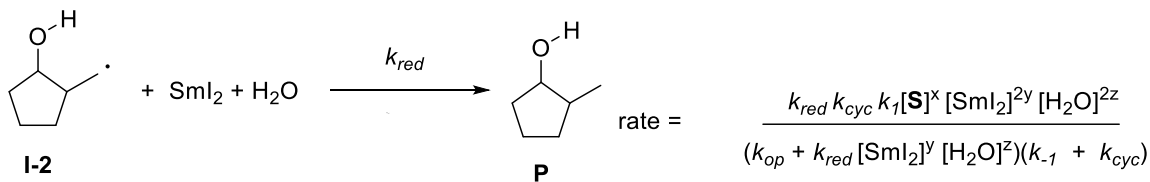
Scheme 5.9 Rate expressions for following steps of alkenyl ketone reductive cyclization.

A consequence of including subsequent steps is a more complex rate expression that would lead to different observed rate constants and/or rate orders for SmI_2 and water. What is clear from this analysis is that the first step of each process provides essentially the same rate expression. If the first step is rate-limiting, kinetic experiments on a ketone and a structurally similar ketone containing a pendant alkene should provide a system to test if the first step is rate-limiting. If the kinetics for the two systems are demonstrably different, the data would provide insight into whether a follow-up step is rate-limiting. Conversely, if the kinetics for the two types of substrates are similar within experimental error, a common rate-limiting initial step is expected.

5.2 Experimental Details

5.2.1 Materials

Samarium powder was purchased from Acros Organics. SmI_2 was generated by the standard method of samarium metal combined with iodine in THF and allowed to stir for at least 8 hours. Iodometric titrations were performed to verify the concentration of SmI_2. Substrates were synthesized as per below procedures and were distilled, degassed, and stored over sieves. 2-Methylcyclohexanone was purchased from VWR and distilled and degassed prior to use. Inhibitor-free tetrahydrofuran was purified by a Solvent

Purification system (Innovative Technology Inc.; MA). H_2O and D_2O were deoxygenated by bubbling through with argon overnight.

2.2.2 Instrumentation

Proton NMR spectra were recorded on a Bruker 500 MHz spectrometer in $CDCl_3$. Carbon NMR were performed at 125 MHz in $CDCl_3$. GC-MS analyses were done with an HP 5890 Series II Gas Chromatograph with an HP Mass Selector Detector. GC analyses were done using a Shimadzu Gas Chromatograph GC-14B with biphenyl standard. Kinetic experiments were performed with a computer-controlled SX.18 MV stopped-flow spectrophotometer (Applied Photophysics Ltd. Surrey, UK). The kinetic solutions were injected separately into the stopped-flow system from airtight Hamilton syringes prepared in a glove box. The cell block and the drive syringes of the stopped flow reaction analyzer were flushed a minimum of three times with dry, deoxygenated THF to make the system anaerobic. Between each experiment, the cell block was washed with dilute HNO_3 (2x), DI H_2O (3x), and THF (3x) before additional anhydrous deoxygenated THF washes (3x). The reaction rates were determined from the decay of SmI_2 at 560 nm.

5.2.3 Methods

5.2.3.1 Synthesis of Starting Materials

5.2.3.1.1 Synthesis of 2-But-3-enyl-cyclohexan-1-one

Synthesis of this substrate was performed as per the procedure in :

Sadasivam, D. V; Teprovich, J. A.; Procter, D. J.; Flowers, II, R. A. *Org. Lett.* **2010**, *12*, 4140–4143.

5.2.3.1.2 Synthesis of 1-phenyl-6-hepten-2-one

The Grignard reagent of 5-bromo-1-pentene was generated by stirring 5-bromo-1-pentene (7.74 mL, 65.3 mmol) and magnesium turnings (1.606 g, 65.3 mmol) in 80 mL THF in a round bottom flask equipped with a condenser and under a positive pressure of argon.

In another round bottom flask with a stir bar, phenylacetyl chloride (8.55 mL, 65.4 mmol) and 5 mol% copper(I) iodide were combined with 50 mL THF under argon and cooled in an ice/MeOH bath to -15 °C. To this solution, the Grignard reagent previously prepared was added dropwise with a syringe pump. Once the Grignard reagent was completely added, the solution was allowed to warm to room temperature. The solution was quenched with sat. NH_4Cl and extracted with diethyl ether. It was then washed with DI H_2O and then $NaHCO_3$. It was dried over Na_2SO_4 and concentrated by rotary evaporation to yield crude product. This was then purified by column chromatography (hexanes/EtOAc) followed by vacuum distillation to yield pure product.

5.2.3.1.3 Synthesis of 1-phenyl-2-butanone

In a round bottom flask with a stir bar, phenylacetyl chloride (5.83 mL, 44.5 mmol) and 5 mol% copper(I) iodide were combined with 40 mL THF under argon and cooled in an ice and MeOH bath to -15 °C. To this solution, purchased ethyl Grignard reagent (13.5 mL of 3M in ether) was added dropwise with a syringe pump. Once the Grignard reagent was completely added, the solution was allowed to warm to room temperature. The solution was then quenched with sat. NH_4Cl and extracted with ether. It was then washed with DI H_2O and then $NaHCO_3$. It was dried over Na_2SO_4 and

concentrated by rotary evaporation to yield crude product. This was then purified by vacuum distillation to yield pure product.

5.2.3.1.2 General Procedure for Reduction/Cyclization with SmI₂-H₂O

In a round bottom flask equipped with a stir bar, SmI$_2$ (2.5 mol equivalents vs. substrate of 0.1 M solution) was added in an argon glovebox. To this, degassed H$_2$O was added neat (150 equivalents vs. Sm) to produce a deep purple solution of SmI$_2$-H$_2$O. To this solution, the desired substrate was added (1 equivalent) neat. Once the purple color was lost and white precipitate formed, the solution was removed from the glovebox. The reaction was quenched with 10% vol HCl (50 mL) and extracted with ethyl acetate (3 x 50 mL). The organic layers were combined and washed with DI H$_2$O, followed by saturated Na$_2$S$_2$O$_3$. Once dried with MgSO$_4$ and filtered, the organic solution was concentrated by rotary evaporation. Reduced and cyclized products were separated from one another by column chromatography (EtOAc/hexanes). Structures were verified by ^{1}H and ^{13}C NMR and are included subsequently.

5.2.3.3 General Procedure for SmI₂-H₂O Stopped-Flow Kinetic Studies

Kinetic experiments were performed with a computer-controlled SX.18 MV stopped-flow spectrophotometer (Applied Photophysics Ltd. Surrey, UK). The SmI$_2$-H$_2$O and substrate solutions were injected independently into the stopped-flow system from airtight BD syringes prepared in a glove box. The cell block and the drive syringes of the stopped flow reaction analyzer were flushed a minimum of three times with dry, degassed THF to make the system anaerobic. The reaction rates were determined from the decay of SmI$_2$ at 25 °C and 560 nm. Precipitation or phase separation were not observed in any cases (even at

high concentrations of water) for any substrates. All concentrations of water provided clean

exponential decays over three half-lives.

5.3 Results and Discussion

5.3.1 Cyclization/Reduction Determination of 1-phenyl-6-hepten-2-one (IV)

Prior to kinetic study, the cyclization of 1-phenyl-6-hepten-2-one was performed

to ensure that the major product was the result of 5-*exo-trig* cyclization and not reduction.

Table 5.1 shows that increasing the concentration of water did not significantly impact

the ratio of cyclized product, but that under typical synthetic conditions the major product

was cyclized product (C).

Table 5.1. Cyclization of 1-phenyl-6-hepten-2-one by SmI_2-H_2O.
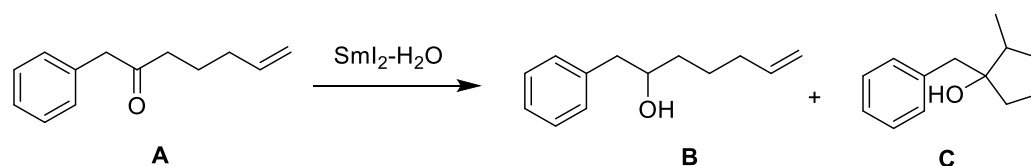
Eq H_2O	B ppm	B Integral	B Product	C ppm	C Integral	C Prod.	(%) Yield C
100	5.80	0.18	0.18	0.96	3.00	1.00	85
250	5.80	1.00	1.00	0.96	19.93	6.64	87

5.3.2 Kinetic Analysis for the Reduction and Reductive Cyclizations

To analyze the mechanism of ketone reduction by SmI_2- H_2O and to determine the

rate-limiting step, a series of kinetic studies were initiated to elucidate the role of SmI_2,

water, and ketone. Scheme 5.10 contains two parent ketones I and III and two related

substrates II and IV containing pendant alkenes that undergo 5-*exo-trig* cyclizations upon

reduction by SmI_2- H_2O.[20]
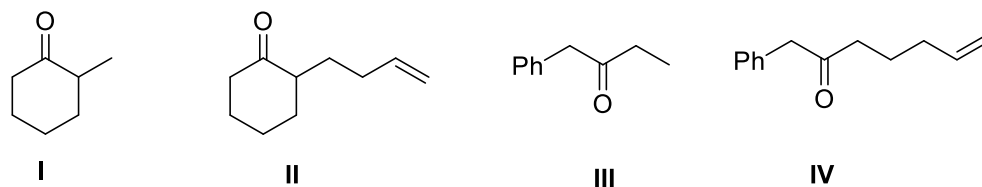
Scheme 5.10. Ketones and pendant alkenylketones for kinetic comparison.

These substrates were chosen to carefully compare the impact of a pendant alkene on the rate of carbonyl reduction using a system with similar steric demands. Rate studies were carried out under pseudo first-order conditions with substrate and water in at least a ten-fold excess by monitoring the decay of the Sm(II) absorption at 560 nm. All experiments were carried out at least 3 times on independently prepared samples to ensure reproducibility.

The rate orders and constants for the reduction of substrates **I-IV** are contained in Table 5.2. In all cases, the rate orders of substrate and SmI_2 were approximately 1, and the rate order of water up to 1.5 M was 2. The order of substrate is slightly greater than unity, but is consistent with other ketone rate orders slightly greater than one as is discussed in detail in Chapter 4.

Table 5.2. Rate constants and rate orders for substrate, SmI_2, and H_2O.

Ketone	k (M^{-3}, s^{-1})[a]	Substrate[b]	SmI_2[c]	H_2O[d]
I	67 ± 4	1.2 ± 0.1	1	2
II	73 ± 4	1.2 ± 0.1	1	2
III	150 ± 10	1.4 ± 0.3	1	2

IV	180 ± 10	1.3 ± 0.1	1	2

[a] 10 mM SmI_2, 1 M H_2O, and 100 mM substrate [b] 10 mM SmI_2, 1 M H_2O, 80-140 mM substrate [c] Obtained via fractional times method [d] 100 mM substrate, 10 mM SmI_2, 0-5 M H_2O.

To further explore the impact of water on the rate of ketone reduction, the rates of reduction of **I-IV** were monitored over a broad concentration range of water as displayed graphically in Figure 1. The results of this study demonstrate two important
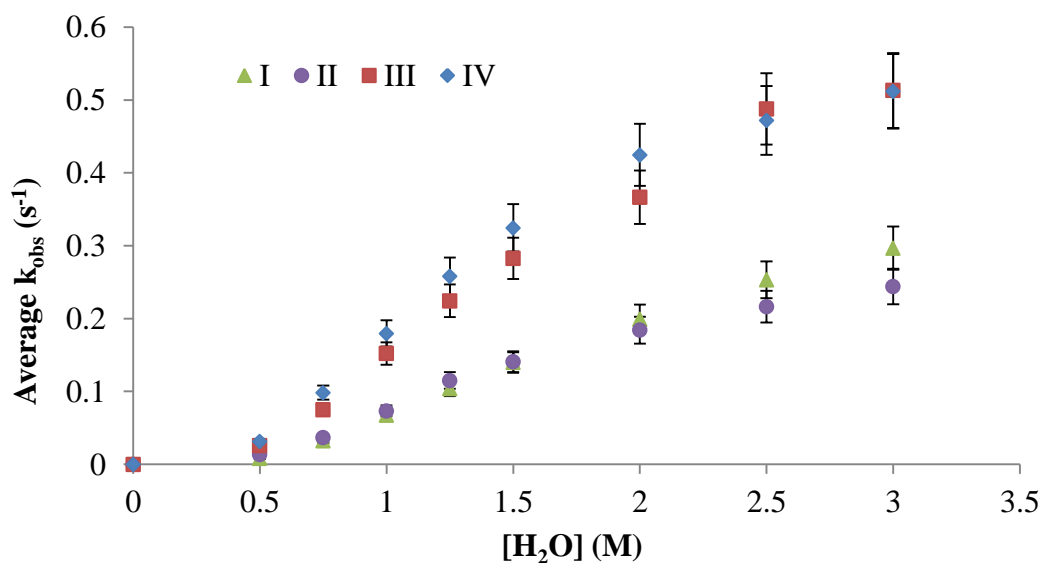
Figure 5.1. Impact of [H_2O] on the rate of reduction of substrates **I-IV** by SmI_2. Conditions: 10 mM SmI_2, 100 mM substrate, 0-3 M H_2O, 25 ^{o}C.

characteristics: 1) The impact of water on the rate of reduction of all substrates saturates only at high concentrations of the additive, and 2) the presence of a pendant alkene has no effect on the rate of ketone reduction within the error of the experiments.

To further examine the process, kinetic studies were carried out employing D_2O in place of water. As is evident in Figure 5.2, the isotope effect for both I and II are

136

remarkably similar. The k_H/k_D values for all substrates averaged between 1.7-1.8. These data are consistent with previous studies on the reduction of anthracene and ketones showing reduction proceeds through a PCET from SmI_2-H_2O and is indicative of a primary isotope effect.[17–19,21–25]
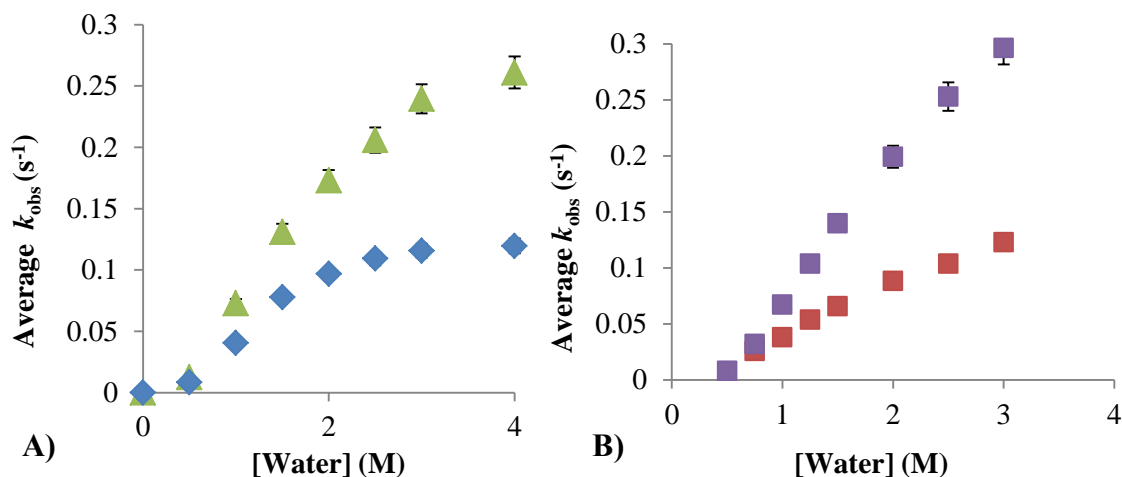
Figure 5.2. A) Rates of reduction of 2-But-3-enyl-cyclohexan-1-one with increasing concentrations of H_2O (▲) and D_2O (◆). **B**) Rates of reduction of 2-methylcyclohexanone with increasing concentrations of H_2O (■) and D_2O (■).

5.3.3 Activation Parameters

In addition to these studies, activation parameters were determined for the reduction of each substrate and the values for the ketone containing a pendant alkene and the parent ketone were the same within experimental error as shown in Table 5.3. All substrates displayed a very low enthalpy of activation consistent with very little bond

reorganization in the transition state. Additionally, a very large negative entropy of activation was observed and is consistent with a highly ordered transition state.

Table 5.3. Activation parameters for reduction/reductive cyclization by SmI_2-H_2O.

Substrate	$\Delta H^{\ddagger}$ (kcal/mol)[a]	$\Delta S^{\ddagger}$ (cal/mol*K)[a]	$\Delta G^{\ddagger}$ (kcal/mol)[b]
I	-1 ± 1	-67 ± 2	19 ± 0.1
II	0 ± 1	-65 ± 1	19 ± 0.1
III	2 ± 1	-56 ± 3	19 ± 0.1
IV	1 ± 1	-59 ± 4	19 ± 0.1

Conditions: 10 mM SmI_2, 1 M H_2O, and 100 mM substrate. The activation parameters are the average of 3 independent experiments from 293-323 °K and are reported as $\pm \sigma$. [a]Obtained from $\ln(k_{obs}h/k_bT)$- $\Delta H^{\ddagger}/RT$ + $\Delta S^{\ddagger}/R$. [b]Calculated from $\Delta G^{\ddagger} = \Delta H^{\ddagger}$-$T\Delta S^{\ddagger}$.

The kinetic experiments presented *vide supra* demonstrate that it is reasonable that the first step in the reduction of a ketone by SmI_2- H_2O is rate-limiting, but do not address the rates of follow-up processes. There are a large number of rate studies on the related 5 exo-trig cyclizations and the rate constants for these processes are fast and typically in the range of 10^6-10^7.[26,27] Rate constants are not available for the cyclization of substrates II and IV through intermediate ketyls. However, even if they are on the low end of the known range for 5-*exo-trig* cyclizations, they are still several orders of magnitude faster than the values shown in Table 5.2.

There are limited studies on the reduction of alkyl radicals by SmI_2, but studies on related systems are known and provide a great deal of insight into the rate of radical reduction by SmI_2. Fluorescence experiments by Scaiano and coworkers demonstrated that the bimolecular rate constant for the reduction of a benzyl radical by SmI_2 in THF at

room temperature is (5.3 ± 1.4) x 10^7 M^{-1} s^{-1}.[28] In addition to this work, Curran and Hasegawa employed a hexenyl radical clock to determine the rate constant for reduction of a primary radical by SmI_2 containing various amounts of HMPA.[29] Bimolecular rate constants for the reduction were on the order of 5 x 10^5 M^{-1} s^{-1} to 7 x 10^6 M^{-1} s^{-1} employing 2 to 6 equiv of HMPA respectively. Cyclic voltammetry studies on the impact of HMPA on redox potential of SmI_2 demonstrate that 2 equivalents of the additive have only a modest impact on the reducing power of SmI_2, similar to the impact of water at the concentrations employed in this study.[30] While direct kinetic measurements on the reduction of an alkyl radical by SmI_2 alone are unavailable, the kinetic studies of Curran in concert with previous voltammetric data are consistent with fast reduction of a primary radical that is several orders of magnitude faster than the rate constants observed for the reduction of substrates I-IV. This analysis demonstrates that ET from SmI_2 to the primary radical formed after formal HAT and cyclization of II and IV is highly unlikely to be rate-limiting.

5.3.4 Conclusions from Calculation of BDFE

It is constructive to examine the initial reduction of a substrate through PCET and the follow-up reduction of the intermediate radical through a formal HAT from SmI_2-water. The bond dissociation free energies (BDFE's) for the O-H bond of water bound to Sm(II), the O-H bond of a ketyl, and the C-H bond formed in the final reduction of a primary and ketyl radical can be estimated using DFT methods (see Appendix for computational data and methods). The work contained in previous chapters have demonstrated that considerable bond-weakening occurs when water coordinates to

139

samarium decreasing the BDFE substantially. The estimated BDFE for water was revised

with a new basis set and derived from the reduction of *trans*-stilbene since it is reduced

by about 50% under synthetic conditions with SmI_2-H_2O. The resulting bond-weakening

is derived in Scheme 5.11 and is about 74 kcal/mol.

O-H BDFE = 108.0 kcal/mol   C-H BDFE = 34.1 kcal/mol

Bond-weakening of at
least at least 73.9 kcal/mol
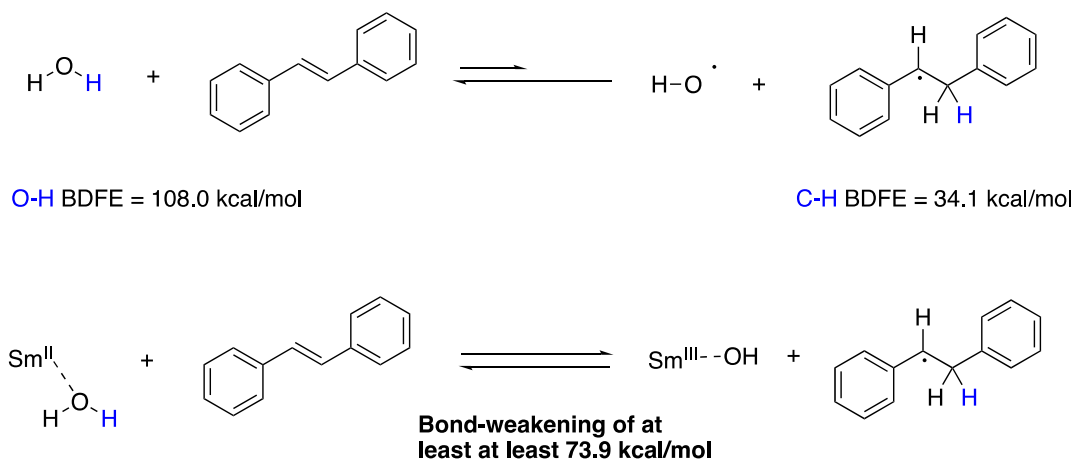
Scheme 5.11. Derived bond-weakening of bound H_2O in the reduction of *trans*-stilbene.

Using an estimate of the 34.1 kcal/mol for the BDFE of water bound to Sm and

values obtained from computational studies, the thermochemical driving force for each

step can be estimated (Scheme 5.12). The reduction of a ketone (A) is endergonic by

approximately 17 kcal/mol. Conversely, the reduction of the intermediate ketyl radical

(B) and after ketyl cyclization (C) are both significantly exergonic.
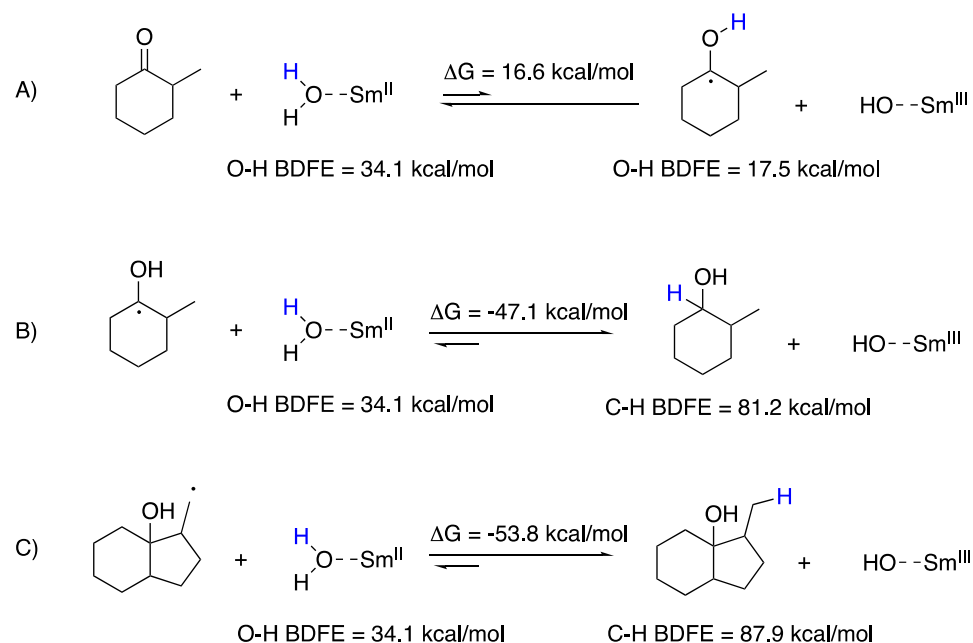
Scheme 5.12. Thermochemical driving force for reduction by SmI_2- H_2O.

5.4 Conclusions

Overall, this analysis demonstrates that there is a substantially greater thermodynamic driving force for radical reduction. While one must use caution when comparing thermodynamic and kinetic arguments, the Hammond postulate in concert with the Bell-Evans-Polanyi principle demonstrate that the rate of a reaction is affected by its driving force.[31,32] As a consequence, this analysis is consistent with the first step being rate-limiting.

The combination of kinetic and thermodynamic analyses provides a compelling argument that the reduction of ketones by SmI_2- H_2O does not proceed through a reversible ET, but likely occurs through an irreversible PCET. Furthermore, this first step is rate-limiting for the reduction of ketones and the intramolecular reductive

141

coupling of ketones with alkenes examined in this study. This study further demonstrates that care should be employed when using product distributions to draw conclusions about the mechanism of complex processes. Additionally, this study suggests that SmI_2- H_2O - induced reductive cyclizations of ketones proceed through PCET, but other reagent combinations that perform similar transformations, such as SmI_2-HMPA, likely do not. At this point, the present study is limited to ketone reduction by SmI_2- H_2O while future studies will examine how this information relates to other functional groups, particularly the reductive cyclization of lactones.

5.5 References

(1)   Just-Baringo, X.; Procter, D. J. *Acc. Chem. Res.* **2015**, *48*, 1263–1275.

(2)   Dahlén, A.; Hilmersson, G. *Eur. J. Inorg. Chem.* **2004**, *2004*, 3393–3403.

(3)   Szostak, M.; Spain, M.; Parmar, D.; Procter, D. J. *Chem. Commun.* **2012**, *48*, 330–346.

(4)   Chciuk, T. V.; Flowers, II, R. A. In *Science of Synthesis*; Marek, I., Ed.; Georg Thieme Verlag KG: Stuttgart, 2016; pp. 177–261.

(5)   Gopalaiah, K.; Kagan, H. B. *Chem. Rec.* **2013**, *13*, 187–208.

(6)   Curran, D. P.; Fevig, T. L.; Jasperse, C. P.; Totleben, M. J. *Synlett* **1992**, *1992*, 943–961.

(7)   Huang, H. M.; Procter, D. J. *J. Am. Chem. Soc.* **2016**, *138*, 7770–7775.

(8)   Just-Baringo, X.; Clark, J.; Gutmann, M. J.; Procter, D. J. *Angew. Chemie - Int. Ed.* **2016**, *55*, 12499–12502.

(9)   Huang, H.-M.; Procter, D. J. *J. Am. Chem. Soc.* **2016**, jacs.6b12077.

(10)   Yalavac, I.; Lyons, S. E.; Webb, M. R.; Procter, D. J. *Chem. Commun.* **2014**, *50*, 12863–12866.

(11)   Szostak, M.; Spain, M.; Procter, D. J. *Chem. Commun. (Camb).* **2011**, *47*, 10254–10256.

(12)   Guazzelli, G.; Grazia, S. De; Collins, K. D.; Matsubara, H.; Procter, D. J. *J. Am. Chem. Soc.* **2009**, *131*, 7214–7215.

(13)   Szostak, M.; Spain, M.; Choquette, K. A.; Flowers, II, R. A.; Procter, D. J. *J. Am. Chem. Soc.* **2013**, *135*, 15702–15705.

(14)   Duffy, L. A.; Matsubara, H.; Procter, D. J. *J. Am. Chem. Soc.* **2008**, *130*, 1136–1137.

(15)   Szostak, M.; Spain, M.; Procter, D. J. *J. Am. Chem. Soc.* **2014**, *136*, 8459–8466.

(16)   Parmar, D.; Price, K.; Spain, M.; Matsubara, H.; Bradley, P. A.; Procter, D. J. *J. Am. Chem. Soc.* **2011**, *133*, 2418–2420.

(17)   Chciuk, T. V.; Flowers, II, R. A. *J. Am. Chem. Soc.* **2015**, *137*, 11526–11531.

(18)   Chciuk, T. V.; Anderson, W. R.; Flowers, R. A. *J. Am. Chem. Soc.* **2016**, *138*.

(19)   Chciuk, T. V.; Anderson, W. R.; Flowers, R. A. *Angew. Chemie - Int. Ed.* **2016**, *55*, 6033–6036.

(20)   Sadasivam, D. V.; Teprovich, J. A.; Procter, D. J.; Flowers, R. A. *Org. Lett.* **2010**, *12*, 4140–4143.

(21) Warren, J. J.; Menzeleev, A. R.; Kretchmer, J. S.; Miller, T. F.; Gray, H. B.; Mayer, J. M. *J. Phys. Chem. Lett.* **2013**, *4*, 519–523.

(22) Megiatto Jr., J. D.; Mendez-Hernandez, D. D.; Tejeda-Ferrari, M. E.; Teillout, A. L.; Llansola-Portoles, M. J.; Kodis, G.; Poluektov, O. G.; Rajh, T.; Mujica, V.; Groy, T. L.; Gust, D.; Moore, T. A; Moore, A. L. *Nat Chem* **2014**, *6*, 423–428.

(23) Warren, J. J.; Mayer, J. M. *J. Am. Chem. Soc.* **2011**, *133*, 8544–8551.

(24) Schrauben, J. N.; Cattaneo, M.; Day, T. C.; Tenderholt, A. L.; Mayer, J. M. *J. Am. Chem. Soc.* **2012**, *134*, 16635–16645.

(25) Tarantino, K. T.; Liu, P.; Knowles, R. R. *J. Am. Chem. Soc.* **2013**, *135*, 10022–10025.

(26) Newcomb, M. Radical Kinetics and Clocks. *Encyclopedia of Radicals in Chemistry, Biology and Materials*, 2012, 1–18.

(27) Newcomb, M. *Tetrahedron* **1993**, *49*, 1151–1176.

(28) Skene, W. G.; Scaiano, J.; Cozens, F. L. *J Org Chem* **1996**, *61*, 7918–7921.

(29) Hasegawa, E.; Curran, D. P. *Tetrahedron Lett.* **1993**, *34*, 1717–1720.

(30) Shabangi, M.; Flowers, II, R. A. *Tetrahedron Lett.* **1997**, *38*, 1137–1140.

(31) Sun, X. *Organic Mechanisms: Reactions, Methodology, and Biological Applications*; John Wiley & Sons, Ltd.: Hoboken, 2013.

(32) Anslyn, E. V; Dougherty, D. A. *Moder Physical Organic Chemistry*; University Science Books: Sausalito, CA, 2006.

Chapter 6. Alternative Hydrogen Atom Transfer Promoters for Reductions of SmI$_2$

6.1 Background and Significance

6.1.1 Coordinating Additives in Synthetic Reactions of SmI$_2$

The use of additives in reactions of samarium diiodide (SmI$_2$) in THF and other solvents has a profound impact on the reactivity of the reagent.[1–4] In early synthetic work, alcohols and water were used with SmI$_2$ solely as proton donors. It was later discovered that some donors coordinate to Sm(II), while others do not and that coordination has a significant impact on the reactivity of the SmI$_2$-proton donor complex.[5–8]

Among proton donors, water is unique because its addition to SmI$_2$ in THF enables the reduction and reductive coupling of functional groups well outside of the reducing power of SmI$_2$ alone.[9] The elegant work of Procter has utilized this unusual increase in reactivity for the reduction of lactones, and other related functional groups to enable carbon-carbon bond-forming reactions that are of great synthetic importance.[10–14] Given the unusual reactivity of the Sm(II)-water complex, the origin of this unique reactivity was investigated and it was proposed that some substrate reductions proceed through proton-coupled electron-transfer (PCET), which was reported in Chapter 2.[15,16] Additionally, the work described in Chapter 3 established that proton donors that strongly interact with Sm(II) through chelation promote reduction through a PCET process, demonstrating the potential of other Sm(II)-proton donor combinations to reduce substrates typically recalcitrant to reduction through single electron transfer (SET).[17] Therefore, with an understanding of the requirements necessary for Sm(II)-induced

hydrogen atom transfer (HAT), alternative additives can be employed to provide similar or optimized reactivity.

6.1.2 DMAE as an Additive with SmI_2

Although water has been established as a proton donor for many functional group reductions, a high affinity ligand for Sm(II) containing a strong X-H bond that is weakened upon coordination to the low valent metal may produce an alternative approach for HAT reductions and reductive coupling reactions. Seminal work in this area was carried out by Hilmersson who discovered that the combination of SmI_2 with water and amines produced a powerful reductant capable of reducing a wide range of functional groups.[18–29] Procter and coworkers have recently expanded on Hilmersson's work by demonstrating its ability to reduce a wide range of carboxylic acid derivatives.[30]

The additive *N*,*N*-dimethyl-2-aminoethanol (DMAE), appeared promising as a HAT promotor since it contained a proton donor and amine functionality in the same molecule. In addition, due to the presence of the hydroxyl moiety, it should have a high affinity as a chelating ligand and as a consequence have the potential for high reactivity at relatively low concentrations. Inspection of the literature revealed that the additive has been employed in the selective opening of α,β-epoxy esters and 2-acylaziridines, aziridine-2-carboxylates, and aziridine-2-carboxamides to β-hydroxy esters and β-aminocarbonyls respectively as shown below in Scheme 6.1.[31–33]
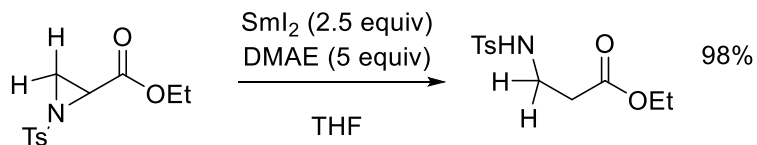
Scheme 6.1. Reduction of aziridine derivatives by SmI$_2$-DMAE.

6.1.3 Amides as Additives for SmI$_2$

In considering additional potential choices, notable work by Knowles and Gansauer has demonstrated significant weakening of the N-H bonds of secondary amides bound to low-valent titanocenes.[34–37] Knowles has shown that coordination of a secondary amide to Cp*$_2$Ti$^{(III)}$Cl led to a 33 kcal/mol weakening of the N-H bond to catalytically yield a series of heterocycles as exemplified in Scheme 6.2.[34]
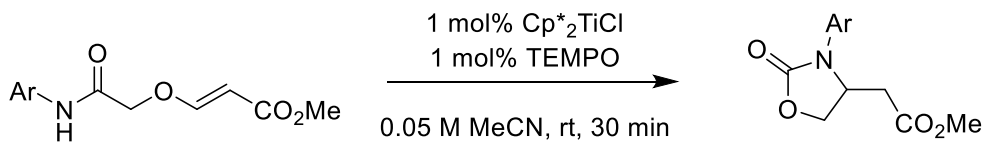
Scheme 6.2 Conjugate amination through N-H bond-weakening by Ti(III).

Gansauer and coworkers demonstrated that a low-valent titanocene containing a pendant amide on one of the Cp ligands led to a reversible coordination of the amide carbonyl that weakened the N-H bond by 39 cal/mol.[37] With this precedent established, coordination of a secondary amide to the highly reducing Sm(II) should lead to similar bond-weakening.

147

If bond-weakening occurs as proposed above, producing a reagent that reduces substrates through HAT, it may be possible to develop alternative approaches for substrates resistant to reduction through SET. Because amides are relatively hard ligands, they may further enhance the reactivity of Sm(II) by stabilizing the +3 oxidation state of Sm in a manner analogous to that proposed for HMPA.[38–40]

The suppositions described *vide supra* suggest that two criteria should be met for an additive to act as an effective HAT agent in concert with Sm(II): 1) The additive should have a high affinity for Sm(II), and 2) The reductant formed upon coordination to Sm(II) should oxidize more readily producing a stronger reductant upon coordination. To test the assertions above, the following coordinating additives were studied, dimethylaminoethanol (DMAE), N-methyl acetamide (NMA), and 2-pyrrolidinone (2-P) and their reactivity was compared to existing Sm-based systems. These additives were chosen since they are readily available from commercial sources and highly soluble in THF.

6.2 Experimental Details

6.2.1 Materials

Samarium powder was purchased from Acros Organics. SmI_2 was generated by the standard method of samarium metal combined with iodine in THF and allowed to stir for at least 4 hours. Iodometric titrations were performed to verify concentration of SmI_2. Substrates and additives were purchased from VWR. Substrates and additives were stored over sieves and deoxygenated prior to use. Inhibitor-free tetrahydrofuran was further purified by a Solvent Purification system (Innovative Technology Inc.; MA).

6.2.2 Instrumentation

Proton NMR spectra were recorded on a Bruker 500 MHz spectrometer in CDCl$_3$. Carbon NMR were performed at 125 MHz in CDCl$_3$. GC-MS analyses were done with an HP 5890 Series II Gas Chromatograph with an HP Mass Selector Detector with biphenyl standard. Cyclic voltammetry was performed with a Princeton Applied Research Parstat 3000 equipped with VersaStudio 2.46.2. Kinetic experiments were performed with a computer-controlled SX.18 MV stopped-flow spectrophotometer (Applied Photophysics Ltd. Surrey, UK).

6.2.3 Methods

6.2.3.1 General Procedure for Synthetic-Scale SmI$_2$-DMAE Reductions

6.2.3.1.1 Procedure for the Reduction of Anthracene/Alkyl Halides

To an oven dried round bottom flask containing a magnetic stir bar under argon, a desired amount of substrate along with 2.5 eq with respect to substrate of SmI$_2$ (0.1 M in THF) were added. To the stirred mixture, 12.5 eq of DMAE with respect to substrate was added. The reaction was stirred at ambient temperature until the reaction mixture became colorless and a white precipitate formed (~24 h). The round bottom flask was then removed from the box and quenched with air and excess 0.1M HCl. The result was partitioned between diethyl ether and water. The organic layer was separated and washed with saturated aqueous sodium thiosulfate, followed by saturated aqueous NaCl. The remaining solution was then dried with MgSO$_4$, filtered and then concentrated in vacuo. The resulting organic mixture was then placed under a high vacuum system to ensure

complete removal of solvent.

6.2.3.1.2 Procedure for the Reduction of 2-Heptanone

To an oven dried round bottom flask containing a magnetic stir bar under argon, a desired amount of substrate along with 2.5 eq with respect to substrate of SmI_2 (0.1 M in THF) were added. To the stirring flask, 15 eq of DMAE with respect to ketone was added. The reaction was stirred at ambient temperature until the reaction mixture became colorless and a white precipitate formed (24 h). The round bottom flask was then removed from the box and quenched with air and excess 0.1M HCl. The result was partitioned between ethyl acetate and water. The organic layer was separated and then treated with saturated aqueous $Na_2S_2O_3$, and then saturated aqueous NaCl washes. The remaining solution was then dried with $MgSO_4$, filtered and then solvent was removed in vacuo. The resulting substance was then placed under a high vacuum system to ensure complete removal of solvent.

6.2.3.1.3 Procedure for the Reduction of 5-Decanolide

To an oven dried round bottom flask containing a magnetic stir bar under argon, a desired amount of substrate along with 7 eq with respect to substrate of SmI_2 (0.1 M in THF) were added. To the stirring flask, 42 eq of DMAE with respect to decanolide was added. The reaction was stirred at ambient temperature until the reaction mixture became colorless and a white precipitate formed (24 h). The round bottom flask was then removed from the box and quenched with air and 0.1M HCl. Product was extracted using

ethyl acetate and water. The organic layer was then treated with saturated aqueous sodium thiosulfate. The remaining solution was then dried with magnesium sulfate, filtered and then solvent was removed by rotary evaporation. The resulting substance was then placed under a high vacuum system to ensure complete removal of solvent.

6.2.3.1.4 General GC Yield Procedure for SmI$_2$-DMAE

GC yields were obtained with the same equivalents as per synthetic yields but with substrate concentrations around 70 mM. Once the solution lost the blue/green color, 0.1M HCl (10mL) and a biphenyl-containing ether extract mixture was utilized (2-3mL).

6.2.3.2. Kinetic Conditions and Procedures for SmI$_2$-DMAE

The SmI$_2$, substrate, and water solutions were injected separately into the stopped-flow system from airtight Hamilton syringes prepared in a glove box. The cell block and the drive syringes of the stopped flow reaction analyzer were flushed a minimum of three times with dry, degassed THF to make the system anaerobic. The reaction rates were determined from the decay of SmI$_2$ at 560 nm. Unless specified otherwise, all kinetic measurements for the reduction of anthracene were carried out at 25 $^\circ$C.

6.2.3.3. General Procedure for Synthetic-Scale SmI$_2$-Amide Reductions
6.2.3.3.1 General Synthetic Procedure for the Reduction of Arenes

To an oven dried round bottom flask containing a magnetic stir bar under argon, arene substrate (100 mg) was added along with 2.5 eq of 0.1 M SmI$_2$ with respect to substrate. To the stirred solution, the desired amount of amide was added (see Table 6.5).

The reaction was allowed to stir overnight at ambient temperature. The reaction was then quenched with air and excess 10%vol HCl. Product was extracted using hexanes (20 mL x 3). The organic layers were combined and washed with DI H_2O (30 mL x 3) and then with saturated aqueous $Na_2S_2O_3$, and finally with saturated NaCl aqueous solution. The remaining solution was then dried with $MgSO_4$, filtered and then solvent was removed by rotary evaporation. The resulting substance was then placed under a high vacuum system to ensure complete removal of solvent. Conversion was confirmed or calculated relative to remaining starting material by ^{1}H NMR. For the reduction of anthracene, 99 mg of isolated 9,10-dihydroanthracene was obtained with 2-P as the amide promoter (Table 6.5, Entry 2). For the reduction of anthracene, 94 mg of isolated 9,10-dihydroanthracene was obtained with NMA as the amide promoter (Table 6.5, Entry 1). For the reduction of trans-stilbene, 90 mg of bibenzyl was obtained with both 2-P and NMA as the amide promoter (Table 6.5, Entries 3-4). For the reduction of phenanthrene, % conversion was obtained by ^{1}H NMR. Clean 9,10-dihydrophenanthrene was obtained by repeated column chromatography with EtOAc/hexanes.

6.2.3.3.2 General Synthetic Procedure for the Reductive Coupling of Aldehydes

To an oven dried round bottom flask containing a magnetic stir bar under argon, aldehyde (200 μL) along with 2.5 eq of 0.1 M SmI_2 with respect to substrate were added. To the stirred solution, 12.5 eq of amide was added with respect to substrate. The reaction was allowed to stir overnight at ambient temperature. The reaction was quenched with air and excess 10%vol HCl. Product was extracted using EtOAc (20 mL x 3). The organic

layers were combined and washed with DI H_2O (30 mL x 3), folllwed by saturated aqueous $Na_2S_2O_3$, and then NaCl aqueous solution. The remaining solution was then dried with $MgSO_4$, filtered and then solvent was removed in vacuo. The resulting substance was then placed under a high vacuum system to ensure complete removal of solvent. Conversion was confirmed or calculated relative to remaining starting material by ^1H NMR. For the coupling of benzaldehyde, 171 mg of isolated hydrobenzoin was obtained with 2-P as the amide promoter (Table 6.6, Entry 2). For the coupling of benzaldehyde, 188 mg of isolated hydrobenzoin was obtained with NMA as the amide promoter (Table 6.6, Entry 1). For the coupling of heptaldehyde, 127 mg of isolated 7,8-tetradecanediol was obtained with 2-P as the amide promoter. For the coupling of heptaldehyde, 120 mg of isolated 7,8-tetradecanediol was obtained with NMA as the amide promoter. Products were further purified by column chromatography EtOAc/hexanes to provide clean NMR spectra.

6.2.3.3.3 General Synthetic Procedure for the Reduction of 2-Octanone

To an oven dried round bottom flask containing a magnetic stir bar under argon, 2-octanone (200 µL) was added along with 2.5 eq of 0.1 M SmI_2 with respect to substrate. To the stirred solution, 25 eq of amide was added with respect to substrate. The reaction was allowed to stir overnight at ambient temperature. The round bottom flask was then removed from the box and quenched with air and excess 10%vol HCl. Product was extracted using EtOAc (20 mL x 3). The organic layer combined and washed with DI H_2O (30 mL x 3), followed by saturated aqueous $Na_2S_2O_3$, and then saturated NaCl

aqueous solution. The remaining solution was then dried with MgSO$_4$, filtered and then solvent was removed in vacuo. For the reduction of 2-octanone, 120 mg of isolated 2-octanol was obtained with 2-P as the amide promoter (Table 6.6, Entry 6). For NMA, a GC-yield of the resulting isolate was obtained with biphenyl standard to determine quantities of coupled verses reduced products. For the reduction of 2-octanone with NMA as the amide promoter, yield was obtained by GC-MS and showed 12% coupled product (7,8-dimethyl-7,8-tetradecanediol) and 82% reduced product (2-octanol) (Table 6.6, Entry 5).

6.2.3.3.4 General Synthetic Procedure for the Reduction of Esters

To an oven dried round bottom flask containing a magnetic stir bar under argon, ester (200 µL) was added along with 6 eq of 0.1 M SmI$_2$ with respect to substrate. To the stirred solution, 60 eq of amide was added with respect to substrate. The reaction was allowed to stir overnight at ambient temperature. The reaction was quenched with air and excess 10%vol HCl. Product was extracted using EtOAc (20 mL x 3). The organic layers were combined and washed with DI H$_2$O (30 mL x 1), followed by saturated aqueous Na$_2$S$_2$O$_3$. The remaining solution was then dried with MgSO$_4$, filtered and then solvent was removed in vacuo followed by high vacuum system to remove remaining solvent. ^{1}H NMR was employed to confirm conversion based on remaining starting material for NMA reactions (Table 6.6, Entries 7,9). For the reduction of 5-decanolide, 192 mg of 1,5-decanediol was isolated when 2-P was used as the amide promoter (Table 6.6, Entry 8). For the reduction of methyl anisate, 124 mg of 4-Methoxybenzylalcohol was isolated

with 2-P as the amide promoter.(Table 6.6, Entry 10).

6.2.3.3.5 General Synthetic Procedure for the Reduction of 2,4-dimethoxy-1-nitrobenzene

To an oven dried round bottom flask containing a magnetic stir bar under argon, 2,4-dimethoxy-1-nitrobenzene (100 mg) was added along with 6 eq of 0.1 M SmI_2 with respect to substrate. To the stirred solution, 60 eq of amide was added with respect to substrate. The reaction was allowed to stir overnight at ambient temperature. The reaction was then quenched with air and excess saturated NH_4Cl. Product was extracted using EtOAc (20 mL x 3). The organic layers were combined and washed with DI H_2O (30 mL x 1), followed by saturated aqueous $Na_2S_2O_3$. The remaining solution was then dried with $MgSO_4$, filtered and then solvent was removed by rotary evaporation followed by high vacuum system to remove remaining solvent. For the reduction of 2,4-dimethoxynitrobenzene, 76 mg of 2,4-dimethoxyaniline was obtained when NMA was used as the amide promoter (Table 6.6, Entry 11). For the reduction of 2,4-dimethoxynitrobenzene, 78 mg of 2,4-dimethoxyaniline was obtained when 2-P was used as the amide promoter (Table 6.6, Entry 12).

6.2.3.3.6 General Synthetic Procedure for the Reduction of 1-Bromododecane

To a vial equipped with a magnetic stir bar in a glove box, 1-bromododecane (50 µL, 0.208 mmol) was added along with 2.5 eq of 0.1 M SmI_2 with respect to substrate under argon. To the stirred solution, amide was added as per quantities provided in Table 6.5. The reaction was allowed to stir overnight at ambient temperature. The vial was then

quenched with air and excess 10%vol HCl. Product was extracted using 3 mL hexanes standardized with biphenyl. The extract was then washed with DI H_2O and $Na_2S_2O_3$ and finally dried with $MgSO_4$. The yield was then determined by GC-MS.

6.2.3.3.7 Procedure for Cyclization/Reduction with 2-but-3-enyl-cyclohexan-1-one

To an oven dried round bottom flask containing a magnetic stir bar under argon, 2-but-3-enyl-cyclohexan-1-one (100 µL) was added along with 2.5 eq of 0.1 M SmI_2 with respect to substrate. To the stirred solution, 20 eq of amide was added with respect to substrate. The reaction was allowed to stir overnight at ambient temperature. The round bottom flask was then quenched with air and excess 10%vol HCl. Product was extracted using EtOAc (20 mL x 3). The organic layers were combined and washed with DI H_2O (30 mL x 3), followed by saturated aqueous $Na_2S_2O_3$, and then saturated NaCl aqueous solution. The remaining solution was then dried with $MgSO_4$, filtered and then solvent was removed by rotary evaporation.

6.2.3.4 Procedure for Cyclic Voltammetry of SmI_2-Amides

Tetrabutylammonium hexafluorophosphate and tetrahexylammonium iodide were purchased and recrystallized from absolute ethanol. Inside a sealed cell, the working electrode was a glassy carbon disk, the counter electrode consisted of a platinum wire, and an Ag wire was used for the reference. The scan rate was 0.1 V/s. SmI_2 was used at a concentration of 15 mM in an electrolyte solution of 0.4 M tetrabutylammonium hexafluorophosphate and 0.02 M tetrahexylammonium iodide. Once the SmI_2

voltammagram was obtained, a new solution of SmI_2 in electrolyte was prepared and to it 10 eq 2-pyrrolidone was added. NMA addition was also attempted but resulted in immediate precipitation so a measurement could not be obtained.

6.3 Results and Discussion

6.3.1 Coordination of Additives by UV-vis

To confirm the coordination of additive to Sm(II), UV-vis experiments were performed to look for shifts in the well-characterized absorbance of SmI_2 in THF. The UV-vis spectrum of SmI_2 displays two distinct bands at 558 and 616 nm that broaden and shift upon complexation of ligands, including water. As is evident from Figure 6.1, DMA appears to cause a coalescence and shift of these peaks, which is consistent to DMAE coordination to Sm(II).
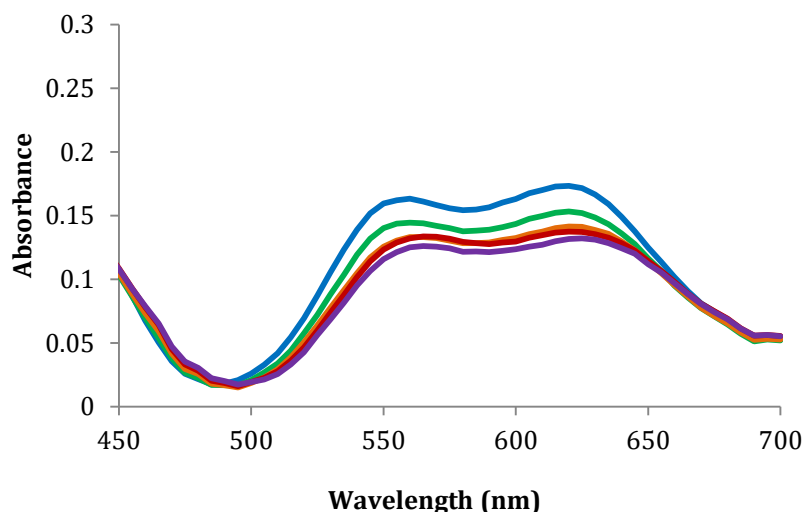
Figure 6.1 Representative UV-vis spectrum of 2 mM SmI_2 in THF with 5(green), 10(red), 15(orange), and 20 equiv(purple) of DMAE.
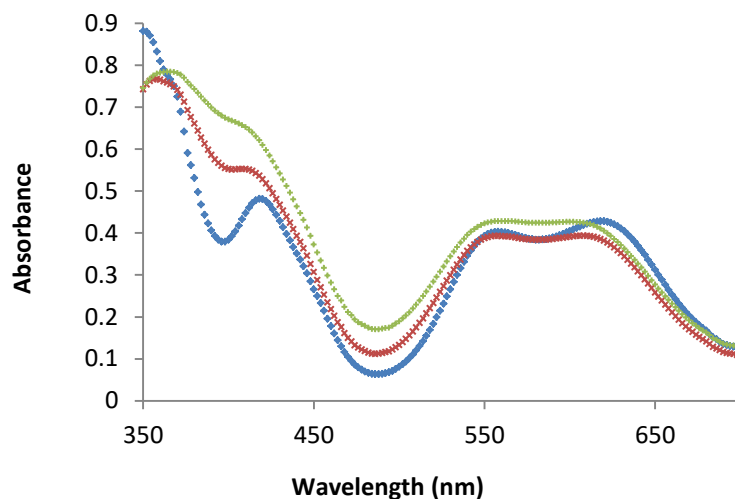
Figure 6.2 Representative UV-vis spectrum of 2.5 mM SmI_2 in THF(blue) with addition of 8(red) and 15(green) equiv 2-pyrrolidone.

The UV-vis spectrum of SmI_2 was examined with increasing amounts of NMA and 2-P as well. Unfortunately, the addition of NMA led to gradual precipitation, but addition of 2-P provided a soluble complex. Figure 6.2 contains UV-Vis spectra of SmI_2 and the impact of addition of 2-P. The data are fully consistent with coordination of the amide to Sm(II) in THF similar to previously reported data for the coordination of ligands to Sm(II).[6,7]

6.3.2 Scope of Reductions with DMAE

A range of functional groups were reduced using DMAE and the reactions proceeded quickly. As shown in Table 6.1, alkyl halides, a ketone, a model arene (anthracene), and lactone (5-decanolide) were readily reduced in good to excellent yields.

A white precipitate formed in all reactions as they progressed to completion. Characterization of the precipitate revealed that it was the ammonium iodide salt of DMAE (DMAE·HI$^+$). A range of DMAE concentrations were explored, but it was found that in the substrates examined, addition of 5-6 equivalents of DMAE (relative to [SmI$_2$]) was best. Lower concentrations of DMAE led to slow or inefficient reductions. Large concentrations of the additive (over 20 equiv) led to oxidation of SmI$_2$ and poor yield of product. For the reduction of 1-bromododecane, the addition of more DMAE led to a slight increase in the time required for conversion to product, but impact on yield was modest. This result is likely a result of coordinative saturation. In the case of anthracene, doubling the amount of DMAE led to a decrease in the time for conversion although the yield only increased slightly.

Table 6.1 Reactions of representative substrates with DMAE in THF at 25 °C.

Substrate	Product	equiv DMAE relative to [SmI$_2$]	Time[c] (min)	Yield (%)
1-iodododecane	dodecane	5	15	97 ± 1[d]
1-bromododecane	dodecane	5	20	83 ± 1[d]
1-bromododecane	dodecane	10	43	88 ± 1[d]
anthracene	9,10-dihydroanthracene	5	100	99 ± 1[d]
anthracene	9,10-dihydroanthracene	10	23	92 ± 1[d]
2-heptanone	2-heptanol	6	30	99± 1[d]
5-decanolide	1,5-decanediol	6	10	76[e]

[a]Conditions: 1 equiv substrate, 2.5 equiv SmI$_2$, 12.5 equiv DMAE. [b]Conditions: 1 equiv substrate, 7 equiv SmI$_2$, 35 equiv DMAE. [c]Time until solution decolorizes. [d]GC yields. [e]Isolated yield.

6.3.3 Kinetic Analysis for the Reduction of Anthracene by SmI$_2$-DMAE

To obtain more insight into the mechanism of the reduction of substrate by SmI$_2$-DMAE, the rate of reduction of anthracene and rate orders for the components were determined under pseudo first order conditions by monitoring the decay of SmI$_2$ in THF at 25 $^{\circ}$C. Anthracene was chosen as the substrate to simplify the analysis since it is unlikely to coordinate to Sm(II). The stability of SmI$_2$-DMAE under experimental conditions used in the rate studies was determined by measuring the decay of the reagent combination in the absence of anthracene. The natural decay was determined to be less than 1% of that obtained in the presence of anthracene. A representative decay for the reduction of anthracene by SmI$_2$-DMAE is shown in Figure 6.3. The decay of SmI$_2$ displayed first-order behavior over >4 half-lives for all SmI$_2$-DMAE-anthracene combinations.
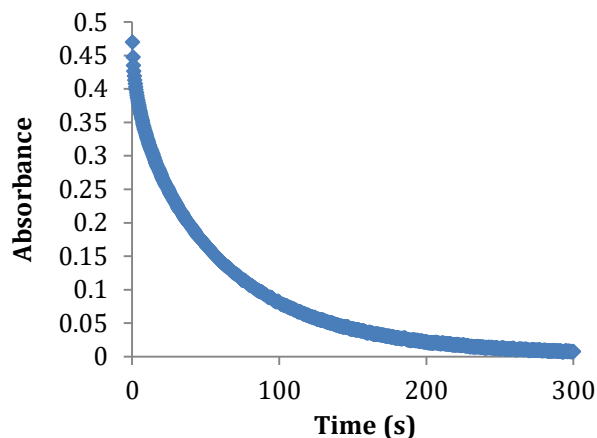
Figure 6.3 Example decay for the reduction of anthracene by SmI$_2$-DMAE at 560 nm.

6.3.3.1 Kinetic Order Experiments

160

In order to obtain a mechanistic understanding of the SmI_2-DMAE system, rate orders were acquired and are listed in Table 6.2. Similar to previous findings for coordinating HAT promoters in Chapters 2 and 3, DMAE was second order while SmI_2 and anthracene were unity. This dual coordination of two promoter molecules is consistent with providing a stronger reductant and coordination-induced bond-weakening of X-H bonds.

Table 6.2 Rate orders for the reduction of anthracene by SmI_2-DMAE[a]

Reaction Component	Rate Order
DMAE	1.9 ± 0.1 (0-1.75 M)[b]
Anthracene	1.0 ± 0.1[c]
SmI_2	1[d]

[a]All rate studies were performed at 25 °C. [b]Conditions: 10 mM SmI_2, 120 mM anthracene, 100-180 mM DMAE. [c]Conditions: 10 mM SmI_2, 50 mM DMAE, 100-120 mM anthracene. [d]Determined using fractional times method.

6.3.3.2 Activation Parameters for SmI_2-DMAE

To acquire a more detailed insight into the electron transfer process for the reduction of anthracene by SmI_2-DMAE, rates were measured over a temperature range to obtain activation enthalpy ($\Delta H^{\ddagger}$) and entropy ($\Delta S^{\ddagger}$) from the linear form of the Eyring equation. The data obtained from this set of experiments are displayed in Table 6.3. The data show a small degree of bond reorganization and a high degree of order in the activated complex and appear very similar to values reported in Chapter 2 for the reduction of anthracene by SmI_2-H_2O.

Table 6.3. Activation parameters for the reduction of anthracene by SmI$_2$-DMAE in THF.[a]

$\Delta H^{\ddagger}$ (kcal/mol)[b]	$\Delta S^{\ddagger}$ (cal/mol, K)[b]	$\Delta G^{\ddagger}$ (kcal/mol)[c]
1.2 ± 0.4	-68 ± 1	21.1 ± 0.1

[a]Activation parameters are the average of three independent experiments and are reported as $\pm\sigma$. Conditions: 10mM SmI$_2$, 50 mM DMAE, 120 mM anthracene in THF monitored from 12-32 °C at 560 nm. [b]Obtained from $\ln(k_{obs}h/kT) = -\Delta H^{\ddagger}/RT + \Delta S^{\ddagger}/R$. [c]Calculated from $\Delta G^{\ddagger} = \Delta H^{\ddagger} - T\Delta S^{\ddagger}$.

6.3.3.3 Comparison of SmI$_2$-DMAE with SmI$_2$-H$_2$O-Amine

One interesting comparison is whether this system behaves like a traditional proton donor or the SmI$_2$-water-amine system. To examine this, the rate of reduction of anthracene by SmI$_2$-water-triethylamine was determined for each system under an identical set of conditions to examine the rates of substrate reduction. The data are displayed in Table 6.4. The observed rate of reduction for the SmI$_2$-water-triethylamine reagent system is three times faster than the SmI$_2$-DMAE reduction, but within the same order of magnitude. Water was examined as well since it is recognized to have a high affinity for Sm(II) and reduce substrates through a Sm(II)-water complex.[8,41] Addition of 5-10 equiv of water led to very slow reduction of anthracene that was two orders of magnitude slower than SmI$_2$-DMAE or SmI$_2$-water-amine. Significantly higher concentrations of water (above 75 equivalents) provided similar rates of reduction, which indicates that the SmI$_2$-DMAE reagent combination is capable of reducing substrates typically recalcitrant to reduction through a single electron transfer process, even at low DMAE concentrations.

162

Table 6.4. Observed rate constants for the reduction of anthracene by SmI_2-water-triethylamine and SmI_2-DMAE.[a]

k_{obs} (s^{-1}) SmI_2-water-triethylamine[b]	k_{obs} (s^{-1}) SmI_2-DMAE[c]
$3.4 \pm 0.1 \times 10^{-2}$	$1.1 \pm 0.1 \times 10^{-2}$

[a]Rate experiments were performed at 25 °C. [b]Conditions: 10 mM SmI_2, 120 mM anthracene, 50 mM water, 50 mM triethylamine. [c]Conditions: 10 mM SmI_2, 120 mM anthracene, 50 mM DMAE.

6.3.3.4 Proposed Mechanism for Reduction of Anthracene with SmI_2-DMAE

Taken together, the experiments described herein show the following: (1) DMAE coordinates strongly to SmI_2, causing a blue shift in the UV-vis spectrum (2) The addition of DMAE to SmI_2 provides a reagent system capable of reducing a range of functional groups including alkyl halides, a model arene (anthracene), ketones, and a model lactone (5-decanolide). (3) Substrate reductions do not proceed, or proceed very slowly in the absence of DMAE. (4) The reaction of SmI_2-DMAE with anthracene is first order in substrate and SmI_2 and second order in DMAE. (5) Activation parameters for the reduction of anthracene shows that the reaction occurs through a highly ordered activated complex with an early transition state (*ie* little bond-cleavage has occurred at the transition state). (6) SmI_2-DMAE reduces anthracene faster than SmI_2-water and at a rate of the same order of magnitude as the SmI_2-water-triethylamine reagent system.

On the basis of these studies, the mechanism shown below in Scheme 6.3 is consistent with the mechanistic data obtained. In the first step, DMAE coordinates (or chelates) to SmI_2 in a manner similar to glycols.[6,7] Coordination of the DMAE to the Lewis acidic Sm increases the acidity of the O-H significantly.[42] In the second step, another molecule

163

of coordinated DMAE acts as a base to deprotonate the O-H of another DMAE bound to Sm(II). As the deprotonation occurs, the increasing electron density on the coordinated oxygen enhances the reducing power of the Sm(II) by producing a more powerful reductant[40,43] or through stabilization of Sm(III).[38,44] Thus, as the Sm(II) is activated by the deprotonation (PT) of coordinated ligand, it reduces anthracene through PCET to produce the protonated radical of anthracene in a coupled PT-PCET process. As this process occurs, insoluble Sm(III) salts precipitate from solution leading to an irreversible process. The high-energy anthracene radical anion is bypassed, which provides a lower energy pathway for the reduction.
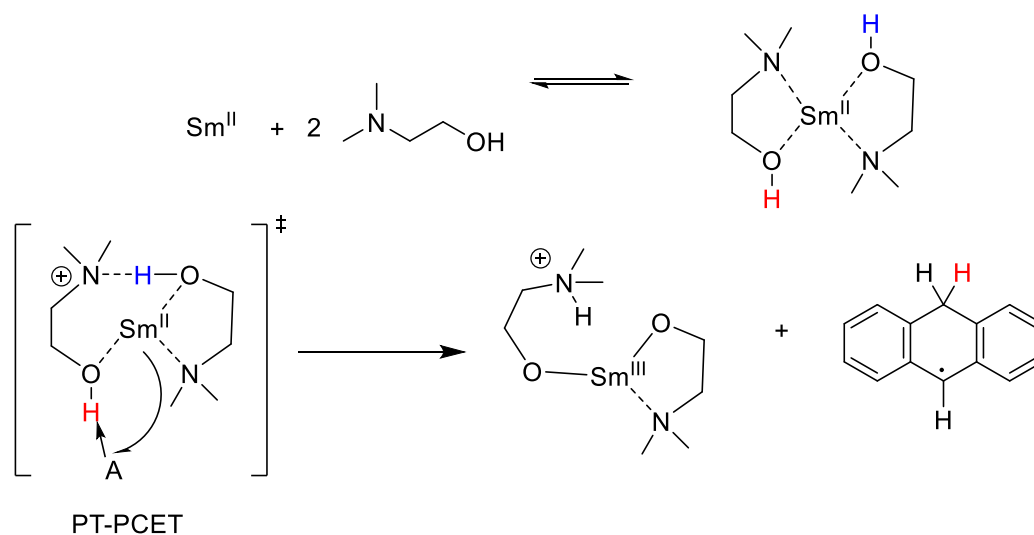
Scheme 6.3 Reduction of anthracene through SmI_2-DMAE-induced PT-PCET.

Overall, the process shown above is consistent with the first order in Sm and anthracene and the second order in DMAE as shown in the empirical rate law in equation (6.1):

164

$$\frac{-d[Sm^{II}]}{dt} = k_{obs}[Sm^{II}] \ [DMAE]^2[anthracene] \qquad (6.1)$$

6.3.4 Analysis of Amides as HAT Promoters with SmI_2

Since the addition of the tertiary amino alcohol, DMAE to SmI_2 provided a stronger reductant, secondary amides, with a coordinating carbonyl group and labile N-H bond, were the next potential HAT promoters investigated.

6.3.4.1 Impact on Reduction Potential

First, the influence of amide addition to the redox potential of SmI_2 was examined using cyclic voltammetry (CV). The CV data demonstrates that the addition of 10 equivalents of 2-P to SmI_2 shifts the redox potential by -0.3 V, providing a more powerful reductant as shown in Figure 6.4.
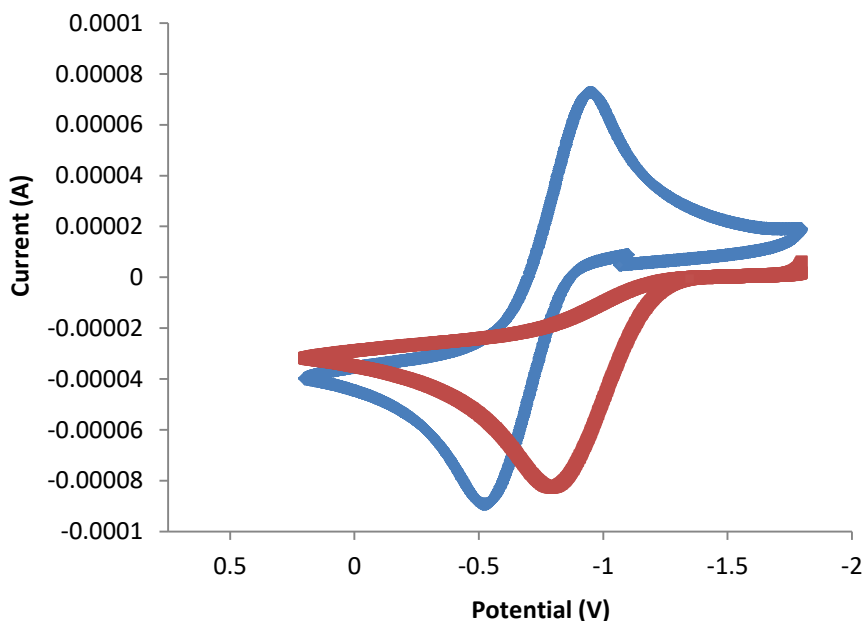
Figure 6.4. Cyclic voltammagram of SmI_2(blue) and SmI_2 with 10 equivalents 2-P (red).

6.3.4.2 Scope of Reductions with Amides

To further assess the impact of 2-P concentration on the reducing power of SmI_2, 1-bromododecane was employed as a substrate. This substrate was chosen since it is resistant to reduction by SmI_2 alone, does not coordinate to the metal, and is reduced through a rate-limiting dissociative electron transfer.[45–47] As a consequence, it provides a useful measure of the impact of additive concentration on the reactivity of Sm(II) in the absence of competing mechanistic pathways. Complete conversion to dodecane was obtained with at least 13 equivalents of the additive in relation to $[SmI_2]$. Lower concentration of the reductant led to incomplete conversion as shown in Table 6.5. Taken together, the UV-vis, CV, and substrate reduction experiments demonstrate that 2-P coordinates to Sm(II) while simultaneously providing a more powerful reductant.

Table 6.5. GC yields for the reduction of 1-bromododecane by SmI_2-amides.

Equivs Amide vs SmI_2	% Yield Dodecane
2[a]	42
5[a]	78
7[a]	73
10[a]	85
13[a]	87
2[b]	49
5[b]	68
7[b]	79
10[b]	83
13[b]	80

Conditions: [a] 2-pyrrolidone [b] N-methylacetamide. 2.5 equivalents of SmI_2 vs. [1-bromododecane].

Having ascertained that both NMA and 2-P coordinate to Sm(II) and also provide an increase in redox potential, the scope of functional group reductions accessible with this reagent combination was investigated. Both NMA and 2-P were employed as additives in the reduction of anthracene, *trans*-stilbene, and phenanthrene (Table 6.6). Previous work by Procter established that the addition of water to SmI_2 promoted the reduction of anthracene and partial reduction of stilbene, but phenanthrene was found to be unreactive.[48] In the present case, only 5 equivalents of NMA or 2-P (based on $[SmI_2]$) are required to reduce anthracene (Table 6.6, entries 1 and 2). Both amide promoters also fully reduce *trans*-stilbene in concert with SmI_2 (Table 6.6, entries 3 and 4). Interestingly, addition of up to 20 equivalents of NMA to SmI_2 lead to only recovered starting material, whereas the same amount of 2-P provides some reduction of phenanthrene (Table 6.6, entries 5 and 6). Increasing the concentration of SmI_2 leads to further conversion (Table 6.6, entry 7).

Table 6.6 Reduction of arenes by SmI_2-amide systems.

Entry	Substrate	Additive (equiv)	% product
1	anthracene	NMA (5)	99[a]
2	anthracene	2-P (5)	94[a]
3	*trans*-stilbene	NMA (15)	90[a]
4	*trans*-stilbene	2-P (10)	90[a]
5	phenanthrene	NMA (20),	NR
6	phenanthrene	2-P (20)	26[b]
7	phenanthrene	2-P (20)	39[c]

| 8 | phenanthrene | NMP (20) | NR |
| 9 | phenanthrene | NMP (20), TFE (20) | NR |

Conditions: 2.5 equivalents of SmI$_2$, RT, overnight. [a]isolated yield. [b] % conversion of starting material by ^{1}H NMR. [c]3 equivalents SmI$_2$.

The reactions described above demonstrate that 2-P facilitates the reduction of phenanthrene, but does not provide a basis for the effect of the promoter. Since CV and spectroscopic studies show that coordination of 2-P to SmI$_2$ enhances the ease of metal oxidation, it is possible that the effect of the additive is a consequence of the reagent combination providing a more powerful reductant. To investigate further the basis of the effect, *N*-methyl-2-pyrrolidinone (NMP) was employed as an additive. The addition of NMP to SmI$_2$ is known to produce a more powerful reductant[49], but the reagent lacks a labile proton. Addition of 20 equivalents of NMP to a solution of SmI$_2$ and phenanthrene led to the complete recovery of starting material (Table 6.6, entry 8) after 24 hours of reaction. Next NMP was employed in concert with 2,2,2-trifluoroethanol (TFE), a non-coordinating proton donor.[41,50] No reduction of phenanthrene was observed after an extended time (Table 6.6, entry 9). In addition, when *N*-deuterated 2-P was employed in the reduction of *trans*-stilbene, deuterium incorporation in the product was observed. The experiments described above are consistent with the hypothesis that secondary amides coordinated to Sm(II) can act as HAT promoters.

Next, the reduction of various carbonyl-containing compounds was attempted with both amides. The results are given below in Table 6.7.

Table 6.7. Reduction of substrates by SmI_2 and NMA or 2-P.

Substrate	Additive	Product	Yield %
Benzaldehyde	NMA[a]	Hydrobenzoin	90[d]
	2-P[a]		81[d]
Heptanal	NMA[a]	7,8-Tetradecanediol	73[d]
	2-P[a]		77[d]
2-Octanone	NMA[b]	2-Octanol	63[e]
	2-P[b]		72[d]
5-Decanolide	NMA[c]	1,5-Decanediol	52[f]
	2-P[c]		85[d]
Methyl anisate	NMA[c]	4-Methoxy benzylalcohol	73[f]
	2-P[c]		99[d]
2,4-dimethoxy-1-nitrobenzene	NMA[c]	2,4-Dimethoxy aniline	91[d]
	2-P[c]		93[d]

Conditions: [a]2.5 equivalents of SmI_2, 5 equivalents of additive (based on [SmI_2]). [b]2.5 equivalents of SmI_2, 10 equivalents of additive (based on [SmI_2]). [c]6 equivalents of SmI_2, 10 equivalents of additive (based on [SmI_2]). [d]isolated yield. [e]GC Yield. [f]% conversion of starting material by ^{1}H NMR

Both NMA and 2-P promote pinacol coupling of the two aldehydes examined. This could be a consequence of a sequential electron-proton transfer[15] or possibly reduced steric constraints that promote homocoupling after formal HAT. Reaction of 2-octanone with SmI_2 - 2-P led to reduced product exclusively whereas NMA provided the major reduced product with 12% of the minor pinacol coupled product. In the reduction of 5-decanolide, 2-P provided a very good yield of 1,5-decanediol whereas the use of

NMA provided only about 50% conversion. Conversely, both additives were equally effective for the reduction of methyl anisate and 2,4-dimethoxy-1-nitrobenzene.

In addition to the substrates contained in Table 6.6, we also examined a ketone alkene cyclization using 2-but-3-enyl-cyclohexan-1-one (**1**). The use of 20 equiv of 2-P provided complete conversion to the reduced product (**2**) and cyclized product (**3**) as shown in Scheme 3. The use of lower amounts of 2-P led to complete conversion, but provided a greater amount of reduced product. This finding demonstrates that a secondary amide can be used to successfully carry out a reductive coupling providing comparable yields to SmI_2-water.[5]
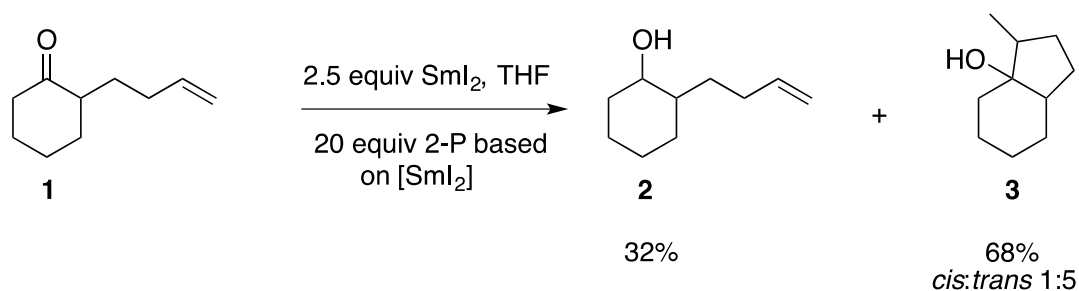
Scheme 6.4. Reaction of **1** with SmI_2 and 2-P.

6.3.4.3 Coordination-induced N-H Bond-weakening

To assess the degree of N-H bond-weakening upon amide coordination to SmI_2, the bond dissociation free energies (BDFE's) in THF for the N-H bond of 2-P, and the initial radical formed upon HAT to *trans*-stilbene and phenanthrene were calculated using density functional calculations employing standard methods (see Appendix VI).

170

Subtraction of the N-H BDFE from the arene radical provides an estimate of bond-weakening as demonstrated in Scheme 5 for the reduction of phenenathrene by the combination of SmI$_2$ and 2-P. Using this approach, the bond-weakening required for reduction of *trans*-stilbene is 63.1 kcal/mol while the limit of N-H bond-weakening for reduction of phenanthrene is 70.8 kcal/mol. The range of N-H bond-weakening of 63-71 kcal/mol is greater than that displayed for amide-Ti(III) complexes[34–37] but consistent with O-H bond-weakening in Sm(II)-water and glycol complexes.[15–17]
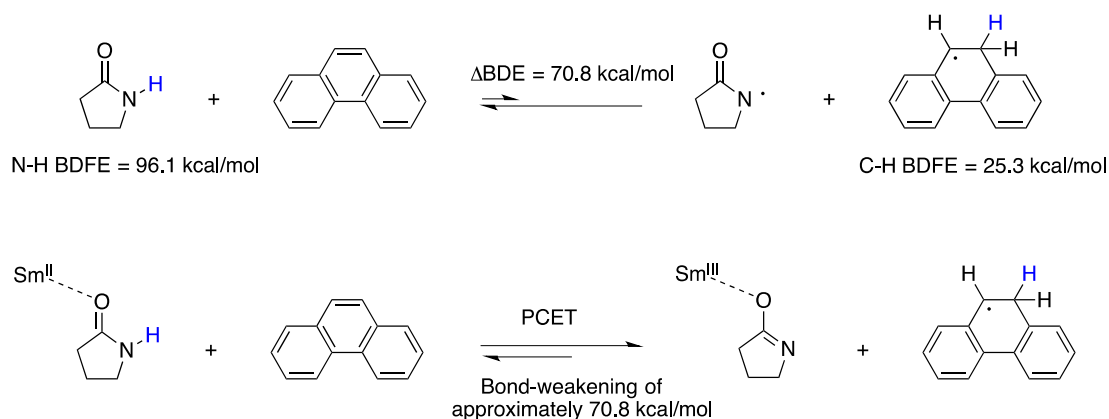
Scheme 6.5. Estimate of degree of N-H bond weakening upon coordination of 2-pyrrolidinone to Sm(II) in THF.

6.4 Conclusions

In conclusion, the results shown herein describe insight into the general utility of DMAE, 2-P, and NMA as additives in SmI$_2$-based reductions. This work demonstrates that water is not unique in its ability to increase the redox potential and activate SmI$_2$ for formal hydrogen atom transfer.

While these studies provide some mechanistic details in the reduction of arenes by SmI$_2$-DMAE, it is probable that the mechanism may be more complex for substrates capable of coordinating to Sm(II). In addition, it is likely that other amino alcohols may be useful as additives capable of accelerating reductions and reductive coupling reactions of SmI$_2$.

Overall, these studies demonstrate that secondary amides can be employed as additives to promote formal HAT to substrates when coordinated to SmI$_2$. The critical feature for successful implementation of this approach is the high affinity of the carbonyl oxygen for Sm(II) for bond-weakening of the N-H bond. While it is premature to state unequivocally that strong coordination leading to bond-weakening is a general phenomenon, water, glycols, amino alcohols, amides and other related additives capable of coordinating to Sm(II) can be considered HAT promoters in the cases described herein. Furthermore, there is substantial literature evidence demonstrating that interaction of ligands with low-valent metals can also lead significant weakening of N-H and C-H bonds proximal to the site of coordination[51–54], suggesting that this approach can be used for the activation of other strong bonds providing potential alternative avenues to reduction and bond-forming reactions.

In conclusion, this work shows that water and glycols are not unique in their ability to act as HAT promoters that can be utilized in SmI$_2$ reductions. Any molecule that can coordinate strongly to Sm(II) and has a labile X-H bond has potential for this

application, as long as it does not compete with substrate for reduction or sterically congest the metal center.

6.5 References

(1)   Chciuk, T. V.; Flowers, II, R. A. In *Science of Synthesis*; Marek, I., Ed.; Georg Thieme Verlag KG: Stuttgart, 2016; pp. 177–261.

(2)   Szostak, M.; Fazakerley, N. J.; Parmar, D.; Procter, D. J. *Chem. Rev.* **2014**, *114*, 5959–6039.

(3)   Dahlén, A.; Hilmersson, G. *Eur. J. Inorg. Chem.* **2004**, *2004*, 3393–3403.

(4)   Kagan, H. B.; Namy, J.-L. *Lanthanides Chem. Use Org. Synth.* **1999**, 155.

(5)   Sadasivam, D. V; Teprovich, J. A.; Procter, D. J.; Flowers, II, R. A. *Org. Lett.* **2010**, *12*, 4140–4143.

(6)   Teprovich, J. A.; Balili, M. N.; Pintauer, T.; Flowers, II, R. A. *Angew. Chem. Int. Ed. Engl.* **2007**, *46*, 8160–8163.

(7)   Prasad, E.; Flowers, II, R. A. *J. Am. Chem. Soc.* **2005**, *127*, 18093–18099.

(8)   Chopade, P. R.; Prasad, E.; Flowers, II, R. A. *J. Am. Chem. Soc.* **2004**, *126*, 44–45.

(9)   Just-Baringo, X.; Procter, D. J. *Acc. Chem. Res.* **2015**, *48*, 1263–1275.

(10)   Just-Baringo, X.; Clark, J.; Gutmann, M. J.; Procter, D. J. *Angew. Chemie - Int. Ed.* **2016**, *55*, 12499–12502.

(11)   Huang, H. M.; Procter, D. J. *J. Am. Chem. Soc.* **2016**, *138*, 7770–7775.

(12)   Szostak, M.; Spain, M.; Choquette, K. A.; Flowers, II, R. A.; Procter, D. J. *J. Am. Chem. Soc.* **2013**, *135*, 15702–15705.

(13) Guazzelli, G.; Grazia, S. De; Collins, K. D.; Matsubara, H.; Procter, D. J. *J. Am. Chem. Soc.* **2009**, *131*, 7214–7215.

(14) Duffy, L. A.; Matsubara, H.; Procter, D. J. *J. Am. Chem. Soc.* **2008**, *130*, 1136–1137.

(15) Chciuk, T. V.; Anderson, W. R.; Flowers, R. A. *J. Am. Chem. Soc.* **2016**, *138*, 8738–8741.

(16) Chciuk, T. V.; Flowers, II, R. A. *J. Am. Chem. Soc.* **2015**, *137*, 11526–11531.

(17) Chciuk, T. V.; Anderson, W. R.; Flowers, R. A. *Angew. Chemie - Int. Ed.* **2016**, *55*, 6033–6036.

(18) Dahlen, A.; Hilmersson, G. *Tetrahedron Lett.* **2002**, *43*, 7197–7200.

(19) Dahlén, A.; Petersson, A.; Hilmersson, G. *Org. Biomol. Chem.* **2003**, *1*, 2423–2426.

(20) Dahlén, A.; Hilmersson, G. *Chem. - A Eur. J.* **2003**, *9*, 1123–1128.

(21) Dahlen, A.; Hilmersson, G. *Tetrahedron Lett.* **2003**, *44*, 2661–2664.

(22) Dahlen, A.; Hilmersson, G.; Knettle, B. W.; Flowers, II, R. A. *J. Org. Chem.* **2003**, *68*, 4870–4875.

(23) Dahlén, A.; Sundgren, A.; Lahmann, M.; Oscarson, S.; Hilmersson, G. *Org. Lett.* **2003**, *5*, 4085–4088.

(24) Davis, T. A.; Chopade, P. R.; Hilmersson, G.; Flowers, II, R. A. *Org. Lett.* **2005**, *7*, 119–122.

(25) Dahlén, A.; Hilmersson, G. *J. Am. Chem. Soc.* **2005**, *127*, 8340–8347.

(26) Ankner, T.; Hilmersson, G. *Tetrahedron Lett.* **2007**, *48*, 5707–5710.

(27) Ankner, T.; Hilmersson, G. *Org. Lett.* **2009**, *11*, 503–506.

(28) Ankner, T.; Hilmersson, G. *Tetrahedron* **2009**, *65*, 10856–10862.

(29) Ankner, T.; Stålsmeden, A. S.; Hilmersson, G. *Chem. Commun. (Camb).* **2013**, *49*, 6867–6869.

(30) Szostak, M.; Spain, M.; Parmar, D.; Procter, D. J. *Chem. Commun.* **2012**, *48*, 330–346.

(31) Otsubo, K.; Inanaga, J.; Yamaguchi, M. *Tetrahedron Lett.* **1987**, *28*, 4437–4440.

(32) Molander, G. A.; Stengel, P. J. *Tetrahedron* **1997**, *53*, 8887–8912.

(33) Zhao, W.; Lu, Z.; Wulff, W. D. *J. Org. Chem.* **2014**, *79*, 10068–10080.

(34) Nguyen, L. Q.; Knowles, R. R. *ACS Catal.* **2016**, *6*, 2894–2903.

(35) Gentry, E. C.; Knowles, R. R. *Acc. Chem. Res.* **2016**, *49*, 1546–1556.

(36) Tarantino, K. T.; Miller, D. C.; Callon, T. A.; Knowles, R. R. *J. Am. Chem. Soc.* **2015**, *137*, 6440–6443.

(37) Zhang, Y. Q.; Jakoby, V.; Stainer, K.; Schmer, A.; Klare, S.; Bauer, M.; Grimme, S.; Cuerva, J. M.; Gansauer, A. *Angew. Chemie - Int. Ed.* **2016**, *55*, 1523–1526.

(38) Halder, S.; Hoz, S. *J. Org. Chem.* **2014**, *79*, 2682–2687.

(39) Pedersen, H. L.; Christensen, T. B.; Enemaerke, R. J.; Daasbjerg, K.; Skrydsrtup, T. *Eur. J. Org. Chem.* **1999**, *1999*, 565–572.

(40) Shabangi, M.; Flowers, II, R. A. *Tetrahedron Lett.* **1997**, *38*, 1137–1140.

(41) Tarnopolsky, A.; Hoz, S. *Org. Biomol. Chem.* **2007**, *5*, 3801–3804.

(42) Neverov, A. A.; Gibson, G.; Brown, R. S. *Inorg. Chem.* **2003**, *42*, 228–234.

(43) Enemærke, R. J.; Daasbjerg, K.; Skrydstrup, T. *Chem. Commun.* **1999**, 343–344.

(44)   Farran, H.; Hoz, S. *Org. Lett.* **2008**, *10*, 4875–4877.

(45)   Prasad, E.; Flowers, II, R. A. *J. Am. Chem. Soc.* **2002**, *124*, 6895–6899.

(46)   Andrieux, C. P.; Gorande, A. L.; Savéant, J.-M. *J. Am. Chem. Soc.* **1992**, *114*, 6892–6904.

(47)   Andrieux, C. P.; Gallardo, I.; Saveant, J. M. *J. Am. Chem. Soc.* **1989**, *111*, 1620–1626.

(48)   Szostak, M.; Spain, M.; Procter, D. J. *J. Org. Chem.* **2014**, *79*, 2522–2537.

(49)   Shabangi, M.; Sealy, J. M.; Fuchs, J. R.; Flowers, R. A. *Tetrahedron Lett.* **1998**, *39*, 4429–4432.

(50)   Amiel-levy, M.; Hoz, S. *J. Am. Chem. Soc.* **2009**, *131*, 8280–8284.

(51)   Guo, S.; Chirik, P. J. *Science.* **2016**, *354*, 730–733.

(52)   Pappas, I.; Chirik, P. J. *J. Am. Chem. Soc.* **2015**, *137*, 3498–3501.

(53)   Milsmann, C.; Semproni, S. P.; Chirik, P. J. *J. Am. Chem. Soc.* **2014**, *136*, 12099–12107.

(54)   King, A. E.; Huffman, L. M.; Casitas, A.; Costas, M.; Ribas, X.; Stahl, S. S. *J. Am. Chem. Soc.* **2010**, *132*, 12068–12073.

Chapter 7. Solvent-Dependent Substrate Reduction by {Sm[N(SiMe₃)₂]₂(THF)₂}: Elucidating the Role of Solvent Coordination in Sm(II) Chemistry

7.1 Background and Significance

7.1.1 Previous Work on the Role of Solvent in Sm(II) Chemistry

Although SmI₂ was first prepared in tetrahydrofuran (THF)[1], additional solvent choices have been examined. This has led to the observation of striking changes in reactivity and selectivity. Over the last 20 years, synthetic reactions utilizing SmI₂ have been performed in THF, tetrahydropyran (THP), dimethoxyethane (DME), acetonitrile (MeCN), and benzene/ hexamethylphoshoramide (HMPA) mixtures[2,3].

The solvation of SmI₂ in THF was first studied in detail by Evans, identifying five THF molecules solvated to SmI₂ in the crystal structure as shown in Figure 7.1.[4] It is evident from the crystal structure, the coordination of THF to Sm(II) is significant in the case of oxygen-containing solvents.
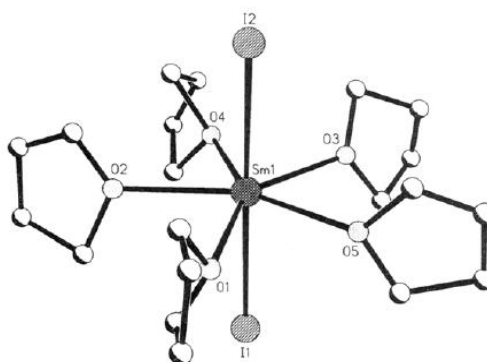
Figure 7.1. Crystal structure of THF solvated SmI₂. [4]

The influence of solvent coordination on reactions of SmI₂ was probed by the

Flowers group in 2004 with the reduction of β-hydroxyketones to the corresponding 1,3 diols in THF, DME, and MeCN. This early work provided evidence of substantial differences in diastereoselectivity based on solvent choice. [5] It was suggested that the distribution of products was affected by the coordination of the solvent and the subsequent ability of the substrate to displace coordinated solvent, which in turn affected the transition state energies. DME coordinates to samarium in a bidentate fashion, provided the highest selectivity and is indicative of the advantage in diastereoselectivity gained by generation of a sterically-congested reductant.[5]
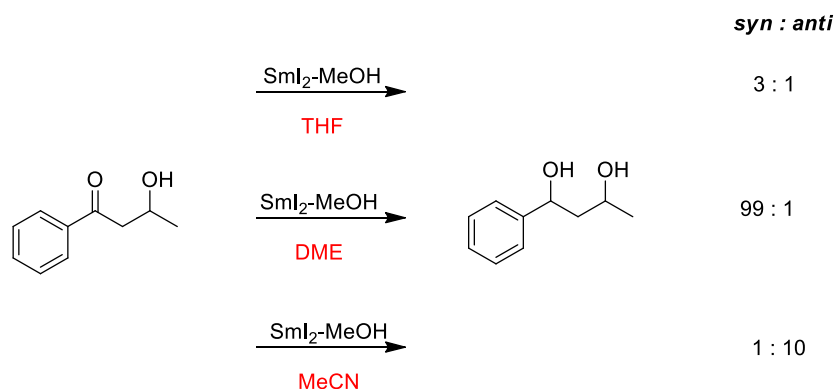
Figure 7.2. Observed solvent-based diastereoselectivities in the reduction of β-hydroxyketones. [5]

In addition to solvent, the coordination of oxygen-containing Lewis bases such as HMPA have been shown to compete with bound solvent, which leads to a more-accessible metal center, thereby increasing rate and selectivity.[6] The influence of solvent coordination is therefore of interest, especially if it could be an inhibiting factor for certain reactions. Use of a non-coordinating solvent could ease congestion around the reaction center and increase rate

and product yield similar to the effect of HMPA.

7.1.2 Sm(HMDS)$_2$THF$_2$ as a Soluble Sm(II) Reductant

Because SmI$_2$ is relatively soluble in a few organic solvents and its solubility in THF is limited to 0.1 M and is decreased in acetonitrile and DME[5], large volumes of the reagent are often required to achieve synthetic utility. When iodide is displaced from SmI$_2$ and replaced with an organic ligand, the resulting complex's solubility in organic solvents is increased. Though Sm(HMDS)$_2$THF$_2$ requires a multistep synthesis, it is readily soluble in hexanes, THF, toluene, cyclohexane, and DME. Therefore, this system allows examination of reactivity in non-coordinating solvents previously inaccessible with SmI$_2$.

Evans performed the first synthesis of Sm(HMDS)$_2$THF$_2$ as outlined in Scheme 7.1 and obtained a crystal structure confirming the coordination of two THF molecules in addition to the silylamide ligands.[7] With the ability to perform reactions in an array of solvents, the impact of differences in coordinating and non-coordinating solvents on reaction rate can be readily compared.

$$\text{Sm} + \text{I}_2 \xrightarrow{\text{THF}} \text{SmI}_2 + 2\text{NaN(Si(CH}_3)_2) \xrightarrow{\text{THF}} \text{Sm(HMDS)}_2\text{THF}_2 + 2\text{NaI}$$
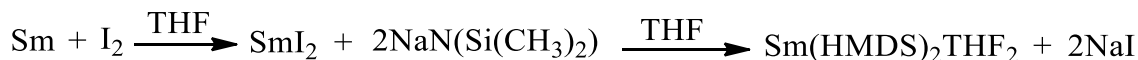
Scheme 7.1. Evans' synthesis of Sm(HMDS)$_2$THF$_2$.

Initial kinetic studies by the Flowers group explored the reductions of 1-iodobutane, 2-butanone and methylacetoacetate with this system in contrast to that of SmI$_2$-THF and [Sm(HMPA)$_6$]I$_2$ -THF. It was found that the Sm(HMDS)$_2$THF$_2$ system provided significant

enhancement to reaction rates, particularly with respect to ketone reduction. Although the redox potential of Sm(HMDS)$_2$THF$_2$ suggests it is not as powerful a reductant as [Sm(HMPA)$_6$]I$_2$, the rates of reduction revealed it is able to reduce alkyl iodides and ketones at a faster rate than SmI$_2$ alone. This observation was attributed to the proposed structure of Sm(HMDS)$_2$THF$_2$ in solution, which provides a complex with a bent shape that increases the probability of interaction between the metal center and substrate despite the bulky ligands, providing more inner-sphere character to the reductions. This distorted shape was similar to that of Sm-HMPA and Sm(C$_5$Me$_5$)$_2$ complexes.[7–9] This indicated the possibility of preferential reduction of ketones in the presence of halides in THF due to increased access to the metal center due to steric effects.[10]

Table 7.1. Rate data for the reduction of carbonyl-containing substrates by Sm(II).[10]

Reaction	Rate ($M^{-1}s^{-1}$)
SmI$_2$-2-butanone	$(7 \pm 3) \times 10^{-4}$
[Sm(HMPA)$_6$]I$_2$-2-butanone	$(8 \pm 1) \times 10^{-3}$
[Sm(HMDS)$_2$](THF)$_2$]-2-butanone	$(1.7 \pm 0.3) \times 10^{2}$
SmI$_2$-methylacetoacetate	$(2.0 \pm 0.4) \times 10^{-1}$
[Sm(HMPA)$_6$]I$_2$-methylacetoacetate	9 ± 2
[Sm(HMDS)$_2$](THF)$_2$]-methylacetoacetate	$(2.0 \pm 0.2) \times 10^{3}$

Further mechanistic study in this area showed that although addition of HMPA to Sm(HMDS)$_2$THF$_2$ provided a more powerful reductant according to redox potentials, it also led to steric hinderance around Sm(II) and as a consequence, decreased reactivity was observed in the reduction of 1-iodobutane.[6]

The impact of solvent coordination on reactivity of the $Sm(HMDS)_2THF_2$ system was recently investigated by Hilmersson and coworkers. The impact of solvent had a large effect on the ability of Sm(II) to reduce 1-fluorodecane, as illustrated in Table 7.2. Following this, the yields of reductive defluorinations of primary, secondary, and tertiary alkyl fluorides were also significantly improved in n-hexane compared to THF. A THF addition study revealed a diminished yield as concentration of THF increased.[11] This work concluded that the competition between substrate and THF for metal coordination significantly inhibits the reactivity of $Sm(HMDS)_2THF_2$ and suggested that the reactivity of Sm(II) can be significantly enhanced in noncoordinating solvents.

Table 7.2. Yields in the Reduction of 1-fluorodecane by Sm(II).[11]

Sm(II) Source	Solvent	Yield
SmI_2-Et_3N-H_2O	THF	0
$Sm(HMDS)_2THF_2$	THF	26
$Sm(HMDS)_2THF_2$	n-hexane	55
$NaSm(HMDS)_3THF_2$	THF	0
$NaSm(HMDS)_3THF_2$	n-hexane	30

Although additives can impact the reactivity of the reagent through the production of a thermodynamically more powerful reductant[12–14] or through the stabilization of Sm(III),[15] the key feature in many of these processes is the displacement of THF or iodide ligands creating open sites for substrate coordination.[6] Given the oxophilicity of the reagent, and the importance of oxygen donor molecules in facilitating reactions of SmI_2, several questions

come to mind: 1) Do oxygen coordinating solvents inhibit substrate access to the metal? 2) Does dissolution of a Sm(II)-based reagent in a non-donor solvent facilitate electron transfer? 3) If so, can this be used as a means to accelerate substrate reduction without the use of additives? This chapter summarizes studies designed to answer these questions using the highly soluble $Sm(HMDS)_2THF_2$ reagent system in THF, hexanes, DME, toluene, and cyclohexane to examine the role of donor solvents and alternative means of accelerating the rate of substrate reduction by Sm(II)-based reagents.

7.2 Experimental Details

7.2.1 Materials

Samarium powder was purchased from Acros Organics. SmI_2 was generated by the standard method of samarium metal combined with iodine in THF and allowed to stir for at least 4 hours. Iodometric titrations were performed to verify concentration of SmI_2. Following this, the synthesis of $Sm(HMDS)_2THF_2$ was performed according to the method described by Evans.[7] 1-Bromododecane was obtained from VWR and purified via column chromatography. Solvents were purified via distillation and deoxygenated prior to use. Substrates were stored over 4Å sieves and deoxygenated prior to use by bubbling through with argon overnight. Inhibitor-free tetrahydrofuran was purified by a Solvent Purification system (Innovative Technology Inc.; MA).

7.2.2 Instrumentation

Proton NMR spectra were recorded on a Bruker 500 MHz spectrometer in $CDCl_3$. Carbon NMR were performed at 125 MHz in $CDCl_3$. GC-MS analyses were done with an HP 5890 Series II Gas Chromatograph with an HP Mass Selector Detector. GC analyses were

done using a Shimadzu Gas Chromatograph GC-14B with biphenyl standard. Kinetic experiments were performed with a computer-controlled SX.18 MV stopped-flow spectrophotometer (Applied Photophysics Ltd. Surrey, UK). The kinetic solutions were injected separately into the stopped-flow system from airtight Hamilton syringes prepared in a glove box. The cell block and the drive syringes of the stopped flow reaction analyzer were flushed a minimum of three times with dry, deoxygenated solvent to make the system anaerobic and one drive syringe was primed with $Sm(HMDS)_2THF_2$. Between each experiment, the cell block was washed with dilute HNO_3 (2x), DI H_2O (3x), and THF (3x) before additional anhydrous deoxygenated solvent washes (3x). The reaction rates were determined from the decay of Sm(II) corresponding to the λ_{max} in each solvent.

7.2.3 Methods

7.2.3.1 Procedure for GC-Yield of Reaction Products

To a flame-dried round bottom flask containing a magnetic stir bar in a glove box, 2.2 equivalents with respect to substrate of $Sm(HMDS)_2THF_2$ was dissolved in a sufficient quantity of solvent to yield an approximately 0.1M solution. The substrate was mixed with 2 mL of the same solvent and added dropwise to the flask and stirred. The reaction was allowed to proceed until a color change from dark purple to black (4-24 hours) was observed. The flask was removed from the glove box. Solvent was removed via rotovap. The resulting mixture was then partitioned with 1M HCl and solvent containing a biphenyl standard. The pinacol product was extracted with ethyl acetate and the dodecane products were extracted with ether. Yields and corresponding spectra are provided in Appendix VII.

7.2.3.2 General Procedure for Sm(HMDS)$_2$THF$_2$ Stopped-Flow Kinetic Studies

Kinetic experiments were performed with a computer-controlled SX.18 MV stopped-flow spectrophotometer (Applied Photophysics Ltd. Surrey, UK). The Sm(HMDS)$_2$THF$_2$ and substrate solutions were injected separately into the stopped-flow system from airtight Hamilton syringes prepared in a glove box. The cell block and the drive syringes of the stopped flow reaction analyzer were flushed a minimum of three times with dry, degassed solvent to make the system anaerobic followed by priming with Sm(HMDS)$_2$THF$_2$ and solvent. The reaction rates were determined from a fit of the exponential decay of Sm(II). Unless specified otherwise, all kinetic measurements for the reduction of 1-chlorododecane and 1-bromododecane were performed at 15 °C while the coupling of 3-pentanone was observed at 5 °C.

7.2.3.3 General Procedure for Sm(HMDS)$_2$THF$_2$ UV-vis Studies

Spectra were obtained using the Spectra setting on the stopped-flow spectrophotometer. One solution of Sm(HMDS)$_2$THF$_2$ in the chosen solvent was generated for one syringe to remain at a constant concentration while the pure solvent was placed in the other syringe. All spectra were measured at 25 °C.

7.3 Results and Discussion

7.3.1 UV-vis Spectra of Sm(HMDS)$_2$THF$_2$
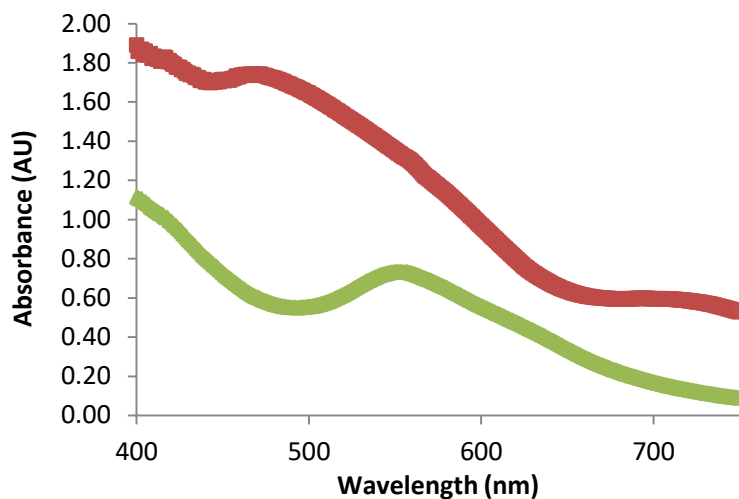
Figure 7.3 Sample UV-vis spectra of Sm(HMDS)$_2$THF$_2$ in THF(red) and hexanes (green).

The UV-vis spectra of 5 mM solutions of Sm(HMDS)$_2$THF$_2$ in each solvent revealed strong visible absorbance ranges that could be monitored by stopped-flow spectrophotometry. Table 7.3 indicates the λ_{max} determined for each solvent.

Table 7.3. λ_{max} values for monitoring Sm(HMDS)$_2$THF$_2$ in various solvents.

Solvent	λ_{max}
THF	400
Hexanes	470
Toluene	515
DME	470
Cyclohexane	470

7.3.2 Kinetic Experiments

185

To better understand the role of solvent in electron transfer, the rate of reduction of alkyl halides and ketones were obtained experimentally. The chosen substrates were representative of functionalities commonly utilized in samarium reactions that fell within a measureable window for stopped-flow rate measurements. The rate of reduction of 1-iodododecane was too fast for the timescale, requiring the use of 1-bromododecane and 1-chlorododecane. The ketone chosen for study was 3-pentanone. The average rate constants for the reduction of 1-bromododecane and 1-chlorododecane in each solvent are provided in Table 7.4.

Table 7.4 Rate Constants for the Reduction of Primary Alkyl Halides by Sm(HMDS)$_2$THF$_2$.

Solvent	Rate Constant 1-Bromododecane (M^{-1}s^{-1})	Rate Constant 1-Chlorododecane (M^{-1}s^{-1})
THF	0.35 ± 0.03 [a]	2×10^{-3} [b]
Hexanes	540 ± 37 [a]	9.4 ± 0.2 [b]
Toluene	217 ± 13 [e]	2.1 ± 0.3 [c]
DME	0.36 ± 0.01 [e]	5×10^{-3} [d]
Cyclohexane	218 ± 13 [f]	4.0 ± 0.3 [e]

Conditions: 5 mM Sm(HMDS)$_2$THF$_2$, 100 mM substrate, and 15 °C. [substrate] = [a] 0.05-0.2 M, [b] 0.075-0.2 M, [c] 0.15-0.35 M [d] 0.5-1 M [e] 0.1-0.5 M,[f] 0.1-0.3 M.

The rate constants provided in Table 7.4 show a large difference in reactivity between the two types of solvents: coordinating and noncoordinating. The reduction of alkyl halides in hexanes appears three orders of magnitude faster than that in THF with Sm(HMDS)$_2$THF$_2$. It is instructive to examine the rate enhancements for electron transfer

from $Sm(HMDS)_2THF_2$ to substrates by changing from an electron donor solvent to a noncoordinating solvent and compare the impact of HMPA addition to SmI_2 in THF for similar substrates. Reductions of alkyl bromides and chlorides by SmI_2 and SmI_2-HMPA are too slow to measure by stopped-flow, but the impact of HMPA addition to SmI_2 on the rates of reduction of alkyl iodides are known.[10] Addition of HMPA to SmI_2 increases the rate of reduction of alkyl iodides by 3 orders of magnitude.[10] This rate increase is similar to that obtained for alkyl bromide or chloride reduction by $Sm(HMDS)_2THF_2$ upon changing solvent from THF to hexanes, demonstrating that dissolution of the Sm(II) reductant in a non-donor solvent impacts the rate of electron transfer.

Because the rate of reduction of 3-pentanone was too fast to measure in the noncoordinating solvents, further studies in additional solvents were not attempted. The rate constants in hexanes and THF for the reductive coupling of 3-pentanone are listed in Table 7.5. With the data that was obtained, however, it is evident that the reduction of highly-coordinating oxygen-containing solvents is extremely facile. As seen in previous studies, the rate of reduction of ketone was significantly faster than that of alkyl halides and in this case was too large to measure in hexanes even at lowered temperatures. This is attributed to the oxophilic nature of the samarium, which encourages coordination of the carbonyl moiety of the substrate to the reaction site and provides inner-sphere reactivity.

Table 7.5 Rate Constants for the Coupling of 3-pentanone by $Sm(HMDS)_2THF_2$ in THF and hexanes.

187

	Rate Constant (THF)[a] (s^{-1})	Rate Constant (hexanes)[b] (s^{-1})
3-pentanone	26.0 ± 0.1	$> 10^4$

Conditions: 5 mM Sm(HMDS)$_2$THF$_2$, 100 mM substrate, and 5 °C. [a] Measured from the decay of Sm(II) at 400 nm [b] Measured from the decay of Sm(II) at 470.

Table 7.6 Rate Orders for the Reductions of 1-Bromododecane, 1-Chlorododecane, and 3-Pentanone.

Reaction Component	Approximate Rate Order
1-chlorododecane	1
1-bromododecane	1
3-pentanone	2
Sm(HMDS)$_2$THF$_2$	1

The approximate rate orders given in Table 7.6 were similar for all solvents and showed the alkyl halides were typically first order, which indicates the rate-limiting step in these reductions was the cleavage of the carbon-halide bond, which is consistent with other studies of Sm-mediated halide reductions.[10,16] The rate order of two for 3-pentanone indicates the ketyl coupling of the radical was the rate-limiting step in the reduction of 3-pentanone.

The faster reduction rates in hexanes are attributed to a more accessible metal center due to the lack of coordinating solvent molecules. To probe the influence of THF on the reduction of an alkyl halide, a study was initiated to examine the role of THF concentration on the rate of reduction in hexanes. Figure 7.4 contains a plot of $\ln k_{obs}$ vs. ln[THF] in hexanes for the reduction of 1-bromododecane. By keeping a constant concentration of reactants and increasing the ratio of THF to hexanes, an inverse rate

order is observed consistent with the observations of Hilmersson.[11] The rate decrease with increasing THF concentration is consistent with the involvement of THF in the rate-limiting step of reduction of 1-bromododecane and thus illustrates the deleterious effect of solvent coordination. The rate order of -1.0 ± 0.1 obtained from the plot is consistent with one molecule of THF being displaced during substrate reduction.
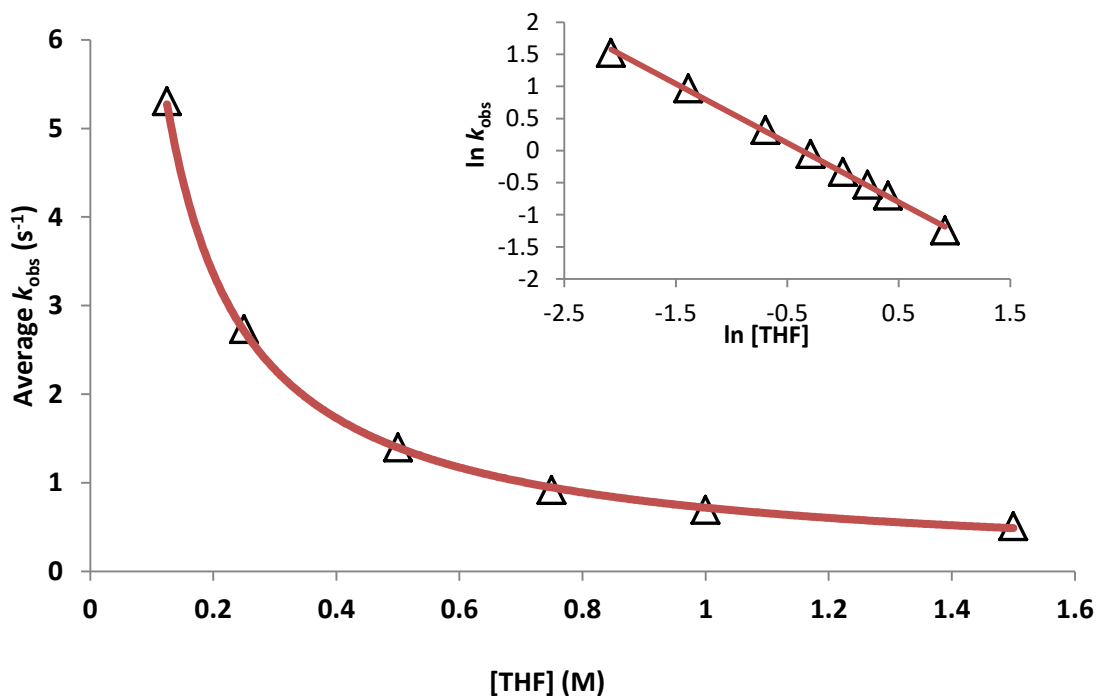
Figure 7.4 Influence of THF concentration on rate of reduction of 50 mM 1-bromododecane by 5 mM Sm(HMDS)$_2$THF$_2$ at 25 °C with [THF] 100 mM-1.5 M.

7.3.3 Activation Parameters

To obtain further insight into the reduction in both solvents activation parameters were obtained in THF and hexanes for the reduction of 1-chlorododecane and are shown in Table 7.7. This reactant was chosen because data were readily attained over a range of

temperatures in both solvents. Interestingly, there is a lower degree of bond reorganization ($\Delta H^{\ddagger}$) and a higher degree of order ($\Delta S^{\ddagger}$) in the transition state for the reduction in THF compared to hexanes. Solvent polarity and accessibility of substrate to the inner sphere of Sm(II) likely play a role in the reduction. In addition, solvent exchange in THF is likely to be rapid, whereas in hexanes, coordinated THF is likely to be more tightly bound to the oxophilic Sm.

Table 7.7. Activation Parameters for the Reduction of 1-Chlorododecane in Hexanes and THF.

Solvent	$\Delta H^{\ddagger}$ (kcal/mol)	$\Delta S^{\ddagger}$ (cal/mol*K)[a]	$\Delta G^{\ddagger}$ (kcal/mol)[b]
Hexanes	12.7 ±0.5	-15 ±2	17.3 ±0.1
THF	6.7 ±0.7	-51± 2	22.11 ±0.01

Activation parameters obtained with 5 mM Sm(HMDS)$_2$THF$_2$ and 75 mM 1-chlorododecane and are the average of 3 independent experiments (5-25 °C). Values reported as ±σ. [a] Obtained from $\ln(k_{obs}h/kT) = -\Delta H^{\ddagger}/RT + \Delta S^{\ddagger}/R$. [b] Calculated from $\Delta G^{\ddagger} = \Delta H^{\ddagger} - T\Delta S^{\ddagger}$.

7.3.4 Proposed Mechanism for the Reduction of Alkyl Halides

Information about the mechanism of reduction of primary alkyl halides with Sm(HMDS)$_2$THF$_2$ was determined by varying the type and concentrations of solvent, reductant and substrate and considering the activation parameters. It was found to be consistent with the rate law shown below in equation 7.1.

$$-d\{ Sm(HMDS)_2THF_2\}/dt = k[\{Sm(HMDS)_2THF_2\}][\text{alkyl halide}][THF]^{-1} \quad (\textbf{7.1})$$

Since Sm is oxophilic, it is reasonable to expect THF to have a higher affinity for the metal than the alkyl halide, thus impeding substrate access. These experiments show

that THF inhibits the reduction and is consistent with the mechanism shown in Scheme 7.2 for the reduction of 1-bromododecane, which is consistent with a dissociative electron transfer that requires displacement of one molecule of THF from the coordination sphere.
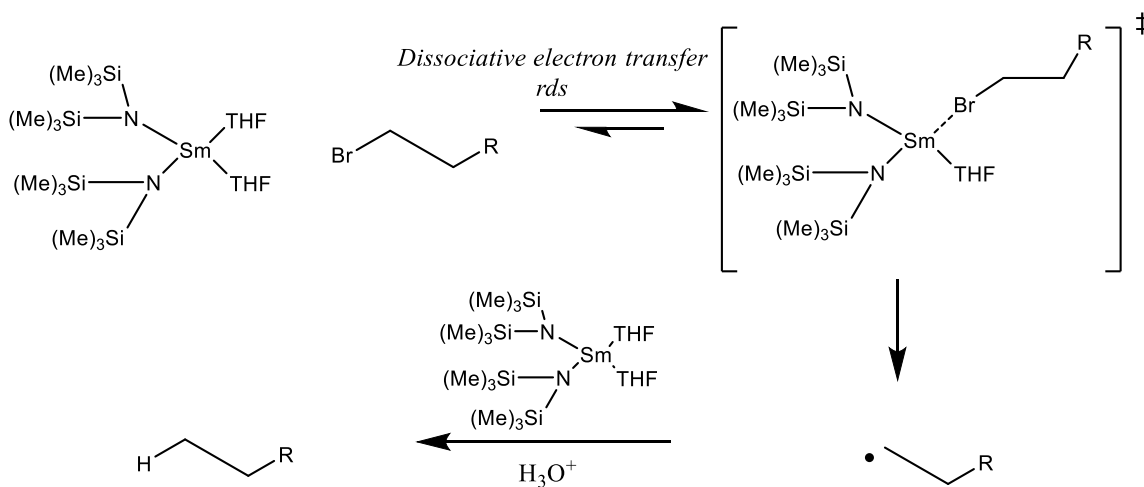

Scheme 7.2. Proposed mechanism for the reduction of 1-bromododecane.

This study echoes previous work examining the reduction of 1-iodobutane with Sm(II) by dissociative electron transfer[10,17], with the exception that this study was able to incorporate direct empirical evidence of THF displacement into the mechanism.

7.3.5 Influence of Solvent Coordination

An interesting literature study by Alvarez analyzed existing crystal structures reported in the literature for lanthanide complexes and quantified the coordinating character of a variety of solvents and anions to construct a table of their relative affinity for lanthanides. Thus, the lower the value of the coordination ability index, a^{Ln}, the less likely the solvent is to be directly coordinated to a lanthanide complex.[18] As shown in Figure 7.5, a linear relationship between the coordination index of the solvent and the

logarithm of the rate of reduction of 1-chlorododecane is observed. A similar relationship is also observed for 1-bromododecane (see Appendix). This is indicative of the detrimental effect of solvent coordination on the observed rate of reduction.
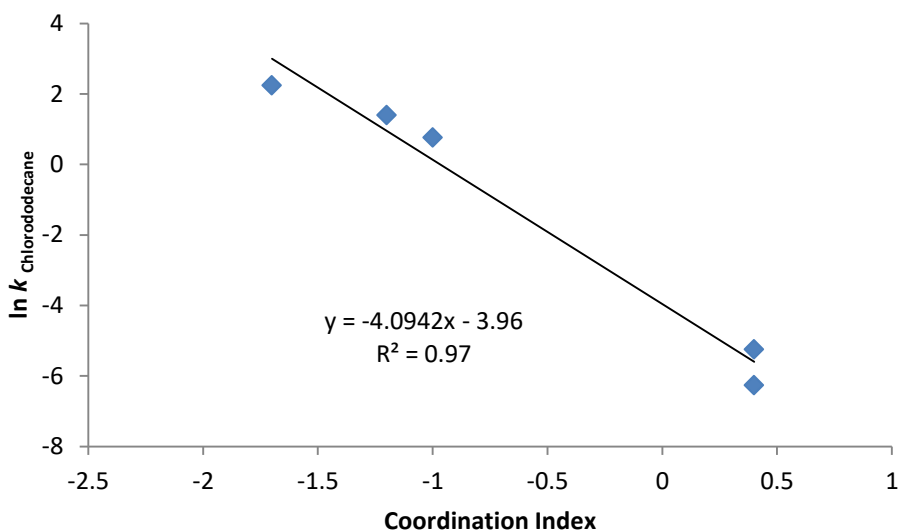
Figure 7.5. Linear correlation between coordination index and the rate of reduction of 1-chlorododecane.

The coordination ability of a solvent to influence the rate of reduction is therefore an important aspect to consider in Sm(II) chemistry. Unfortunately, because SmI_2 has such limited solubility in organic solvents, particularly noncoordinating ones, the development of easily accessible soluble Sm(II) complexes holds great promise based on this data.

7.3.6 Influence of Solvent Polarity

Another important correlation is observed between the rate of reduction and the dielectric constant, which is one of multiple measures of solvent polarity. This

relationship is provided for 1-bromododecane in Figure 7.6 and is consistent in the reduction of 1-chlorododecane as well (see Appendix).
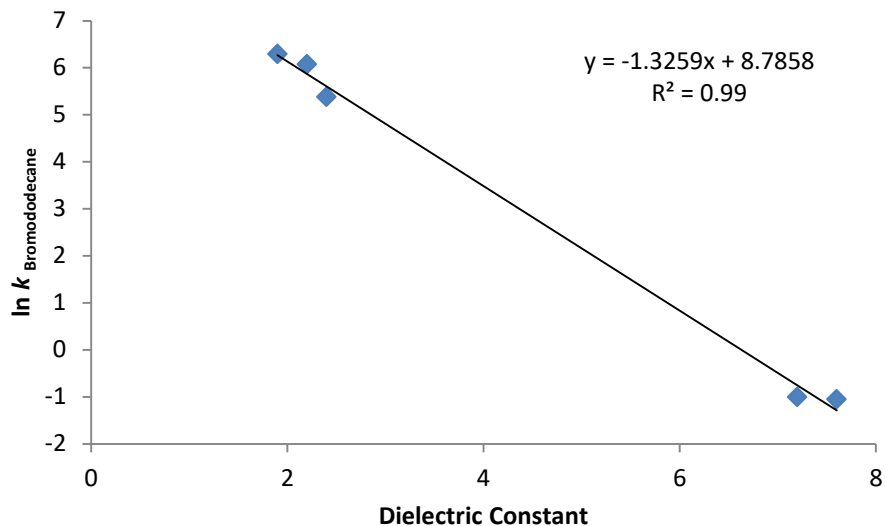
Figure 7.6. Linear correlation between dielectric constant and the rate of reduction of 1-bromododecane.

The observed relationship can be interpreted according to the Hughes-Ingold rules. According to these rules, an increase in solvent polarity results in a decrease in the rate of those reactions in which the charge density is lower in the activated complex than in the initial reactant molecules.[19] This is consistent with the above proposed mechanism for the reduction of alkyl halides by $Sm(HMDS)_2THF_2$ wherein the activated complex is without charge and a THF molecule is displaced. Therefore, these results show that a polar solvent is not required to aid in the reaction by solvating the charges that build up in the transition state, since the transition state is more neutral than the ground state reactants. The activation parameters are consistent with a very early transition state where

very little bond-reorganization has occurred, thus bonds have not yet broken to generate charge in the activated complex.

7.4 Conclusions

This work described in this chapter reports the first direct study of the mechanistic role of solvent coordination in reductions utilizing the soluble Sm(II) reductant, $Sm(HMDS)_2THF_2$. Overall, these studies show that changes in solvent can have a profound effect on Sm(II)-mediated reductions with changes of up to 3 orders of magnitude. The observed change in rates upon carrying out reductions in THF and hexanes are on the same order of magnitude for those obtained by the addition of HMPA in reductions of alkyl halides by SmI_2 in THF.[10] Furthermore, these results confirm the logarithmic effect of solvent polarity on the reduction of alkyl halides by dissociative electron transfer. Additionally, the inhibitory effect of solvent coordination on reduction rate is consistent with the coordination index calculated by Alvarez.[18] This work suggests that future synthetic applications of Sm(II) may be revealed through careful choice of solvent and additive combinations to optimize the accessibility of substrate to Sm(II), particularly to achieve highly diastereoselective pathways.

7.5 References

(1)   Namy, J. L.; Girard, P.; Kagan, H. *Nouv. J. Chim.* **1977**, *1*, 5–7.

(2)   Kagan, H. B.; Namy, J.-L. *Lanthanides Chem. Use Org. Synth.* **1999**, 155.

(3)   Chciuk, T. V.; Flowers, II, R. A. *Sci. Synth.* **2016**, 177–261.

(4)   Evans, W. J.; Gummersheimer, T. S.; Ziller, J. W. *J. Am. Chem. Soc.* **1995**, *117*,

8999–9002.

(5)   Chopade, P. R.; Davis, T. A.; Prasad, E.; Flowers, II, R. A. *Org. Lett.* **2004**, *6*, 2685–2688.

(6)   Prasad, E.; Knettle, B. W.; Flowers, II, R. A. *J. Am. Chem. Soc.* **2004**, *126*, 6891–6894.

(7)   Evans, W. J.; Drummond, D. K.; Zhang, H.; Atwood, J. L. *J. Inorg. Chem.* **1988**, *27*, 575–579.

(8)   Evans, W. J.; Grate, J. W.; Choi, H. W.; Bloom, I.; Hunter, W. E.; Atwood, J. L. *J. Am. Chem. Soc.* **1985**, *107*, 941–946.

(9)   Hou, Z.; Wakatsuki, Y. *J. Chem. Soc. Chem. Commun.* **1994**, *1*, 1205.

(10)   Prasad, E.; Knettle, B. W.; Flowers, II, R. A. *J. Am. Chem. Soc.* **2002**, *124*, 14663–14667.

(11)   Janjetovic, M.; Träff, A. M.; Ankner, T.; Wettergren, J.; Hilmersson, G. *Chem. Commun. (Camb).* **2013**, *49*, 1826–1828.

(12)   Pedersen, H. L.; Christensen, T. B.; Enemaerke, R. J.; Daasbjerg, K.; Skrydsrtup, T. *Eur. J. Org. Chem.* **1999**, *1999*, 565–572.

(13)   Shabangi, M.; Sealy, J. M.; Fuchs, J. R.; Flowers, R. A. *Tetrahedron Lett.* **1998**, *39*, 4429–4432.

(14)   Shabangi, M.; Flowers, II, R. A. *Tetrahedron Lett.* **1997**, *38*, 1137–1140.

(15)   Halder, S.; Hoz, S. *J. Org. Chem.* **2014**, *79*, 2682–2687.

(16)   Miller, R. S.; Sealy, J. M.; Shabangi, M.; Kuhlman, M. L.; Fuchs, J. R.; Flowers, II, R. A. *J. Am. Chem. Soc.* **2000**, *122*, 7718–7722.

(17)   Prasad, E.; Flowers, II, R. A. *J. Am. Chem. Soc.* **2002**, *124*, 6895–6899.

(18)   Diaz-Torres, R.; Alvarez, S. *Dalt. Trans.* **2011**, *40*, 10742–10750.

(19)   Reichardt, C. *Solvents and Solvent Effects in Organic Chemistry*; 3rd ed.; Wiley-VCH: Weinheim, Germany, 2003.

Chapter 8. Accessing Samarium(II) Halides Through Tetrabutylammonium Salts

8.1 Background and Significance

8.1.1 Introduction to Samarium Dibromide and Samarium Dichloride

Although SmI_2 is the most utilized Sm(II) halide in organic synthesis, samarium dibromide ($SmBr_2$) and samarium dichloride ($SmCl_2$) also have applications in organic synthesis. The principle shortcoming of $SmBr_2$ and $SmCl_2$ is their limited solubility in organic solvents. Nonetheless, there are several examples of targeted reactivity in total synthesis pathways and instances where there are advantages to using these reagents over SmI_2.
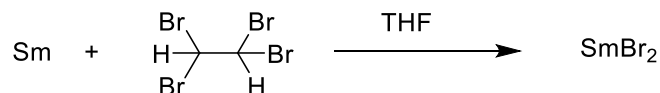
8.1.1.1 Synthesis of Samarium Dibromide

Kagan developed a synthesis of $SmBr_2$ that proceeds through the conversion of Sm_2O_3 to a Sm(III)bromide hydrate that is dried and subsequently reduced with lithium metal in THF to produce a suspension of $SmBr_2$ as shown in Scheme 8.1. This early report was the first to show that the rate of pinacol couplings of ketones and aldehydes occurred on the order of minutes for $SmBr_2$. It was also shown that water could be added as a proton source in these reactions .[1]

$$Sm_2O_3 \; + \; HBr \quad \xrightarrow{\;\; H_2O \;\;} \quad SmBr_3 \, 6H_2O \quad \xrightarrow{\;\; Li \; dispersion \;\;} \quad SmBr_2$$

Scheme 8.1 Synthesis of $SmBr_2$ reported by Kagan.

Two more recent methods for the synthesis of $SmBr_2$ from the reduction of 1,1,2,2-tetrabromoethane have been developed by Namy[2] and Brückner,[3] respectively.

The preparations are nearly identical and provide good yields of $SmBr_2$ as a suspension in THF.

$$Sm \quad + \quad \underset{\substack{Br \\ }}{\overset{\substack{Br \quad Br}}{H-\!\!\!\diagdown\!\!\!\diagup\!\!\!-Br}} \quad \xrightarrow{\text{THF}} \quad SmBr_2$$

Scheme 8.2 Synthesis of $SmBr_2$ by Namy and Brückner.

Using a similar approach, Hilmersson developed a rapid approach for the synthesis of $SmBr_2$ using excess Sm metal and 1,1,2,2-tetrabromoethane using microwave irradiation. The main advantage of this approach is that the synthesis of the reductant is reduced from several hours to five minutes.[4]
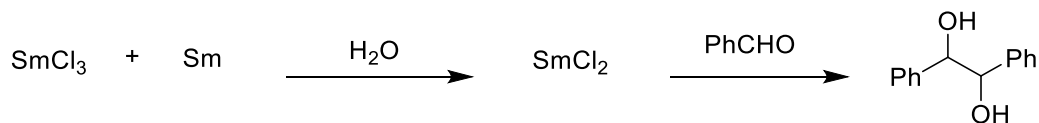
8.1.1.2 Synthesis of Samarium Dichloride

The first synthesis of $SmCl_2$ by reduction of commercially-available $SmCl_3$ by Li-naphthalide in THF was reported by Rossmanith in 1979. The procedure provides a high yield of insoluble $SmCl_2$. Therefore, although the complex can be generated, the utility of this approach is severely limited.[5]

$$SmCl_3 \quad + \quad Li \quad \xrightarrow[\text{THF}]{\text{naphthalene}} \quad SmCl_2 \quad + \quad LiCl$$
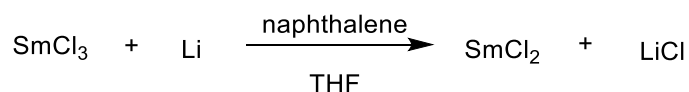
Scheme 8.3 Generation of $SmCl_2$ by reduction of $SmCl_3$.

Matsukawa developed an interesting synthesis of $SmCl_2$ in water using $SmCl_3$ and Sm. The reagent is capable of carrying out pinacol couplings and Barbier reactions in

water, but otherwise, the reagent produced by this method has had limited use in synthesis and is generated *in situ* with substrate present.[6]

$$SmCl_3 \quad + \quad Sm \quad \xrightarrow{\;H_2O\;} \quad SmCl_2 \quad \xrightarrow{\;PhCHO\;} \quad \underset{\substack{\\ OH}}{\overset{\substack{OH \\}}{Ph\diagup\diagdown Ph}}$$

Scheme 8.4 Synthesis of SmCl$_2$ by Matsukawa.

8.1.2 Addition of Lithium Halides for *in situ* Access to SmBr$_2$ and SmCl$_2$

The use of lithium halides (LiBr and LiCl) as additives in reactions of SmI$_2$ was first reported by Flowers. Drawing on recent reports of the addition of transition metal catalysts (FeCl$_3$) and bases (LiOCH$_3$), the addition of lithium halides was of interest. Lithium halides are highly soluble in THF and provided a visible color change of blue to purple, producing the respective samarium halide upon addition of SmI$_2$ and stirring. The addition of 4 to 10 equivalents of these salts provided the pinacol coupled product shown in Scheme 8.5 in over 90% after a few minutes. In the absence of any additive, the SmI$_2$-promoted coupling of cyclohexanone is very slow with a reaction time of 1-2 days.[7]

$$2 \quad \underset{}{\overset{O}{\bigcirc}} \quad \xrightarrow[\text{LiBr/LiCl}]{SmI_2} \quad \underset{\substack{OH \\ OH}}{\bigcirc\!\!\bigcirc}$$
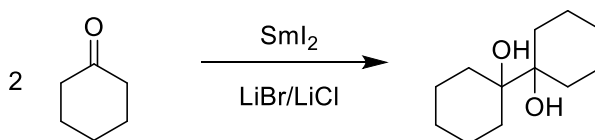
Scheme 8.5 Pinacol coupling of cyclohexanone using SmI$_2$-LiX.

This early finding was expanded upon in a subsequent study that compared the reactivity of lithium halide additives to HMPA in the reductive coupling of alkyl halides and ketones. Using the model coupling reaction of 1-iodododecane and 2-octanone, it was shown that rather than the expected samarium Barbier product, the pinacol coupled

product was the major product when lithium bromide was employed, which is shown in

Table 8.1.[8]

Table 8.1. Coupling Reaction of 1-Iodododecane and 2-Octanone by SmI_2 with Additives. [8]
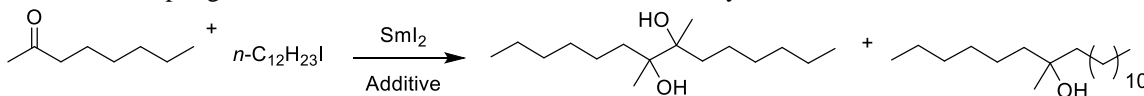
Additive	Pinacol Product (%)	Barbier Product (%)	Starting Material (%)
None	23	59	18
HMPA	< 1	91	8
LiCl	64	21	15
LiBr	98	< 1	< 1

Additional experiments revealed even more information about the generation of samarium dihalides resulting from the presence of lithium halides. When LiBr and LiCl are added to SmI_2, a color change is observed. The UV-vis spectra corresponding to these combinations are included in Figure 8.1[8] and matched those of the samarium complexes generated from previously reported methods.[1,5] It was posited that the charge-transfer bands of SmI_2 at 552 and 616 nm were shifted to lower wavelengths, suggesting an increase in the redox potential. This was confirmed by cyclic voltammetry (CV) studies showed that $SmBr_2$ and $SmCl_2$ are stronger reductants than SmI_2, having redox potentials of -1.55 and -1.78 V vs SCE respectively.[8]
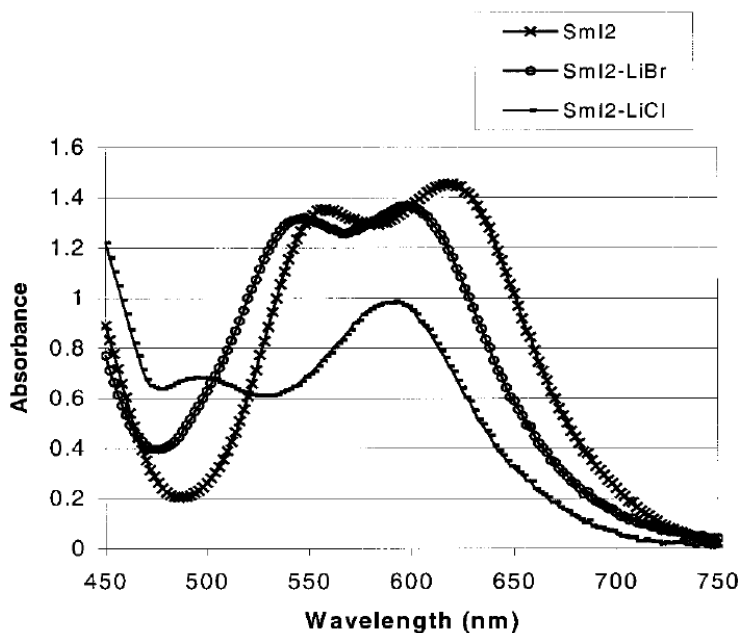
Figure 8.1 UV-vis spectra of SmI_2 with lithium halide additives. [8]

The importance of the presence of the lithium cation was examined through the addition of tetra-*n*-hexylammonium bromide (THAB) in place of lithium bromide. The UV-vis spectrum obtained for this combination matched that of the SmI_2-LiBr spectrum, confirming generation of $SmBr_2$. When the same coupling reaction was attempted, the major product was again the pinacol product. This indicated that soluble alkyl ammonium halides could provide similar reactivity to the lithium halide salts. [8]

The Mellah group employed tetrabutylammonium salts to synthesize samarium complexes $(Sm(OTf)_2, SmI_2, SmBr_2,$ and $SmCl_2)$ using an electrochemical method relying on a samarium anode. With this method of generation, they were able to produce each complex and confirm its identity by both UV-vis and CV. Additionally, they reported that 1-chlorododecane could be reduced effectively using this method of samarium dihalide synthesis. The addition of tetrabutylammonium hexafluorophosphate, which is typically employed as an electrolyte for electrochemical studies, also increased the reactivity of the samarium complexes, suggesting the ammonium cation is another source of enhanced chemistry for samarium complexes. [9] The reason for this, however, has not yet been explained.

More recently, the Procter group explored the combination of SmX_2 with the addition of large volumes of H_2O (50 equiv vs Sm) to test for enhanced reactivity. Since the addition of 50 equiv of H_2O is known to generate a stronger reductant with SmI_2, it was expected that a similar effect could be achieved with $SmBr_2$ and $SmCl_2$. Unfortunately, little change was noted in the yields of the reduction of a series of polycyclic aromatic compounds and alkyl halides with this combination. [10]

8.1.3 Recent Synthetic Applications of Sm(II) Dihalides

Since the introduction of LiBr and LiCl as additives for SmI_2 in 1997[7], the original report has been cited numerous times and this simple yet powerful reagent combination has been applied to many synthetic pathways.

General methods for the synthesis of β-methylenyl-γ-amino acid derivatives are relatively rare, but these derivatives are useful for generating β-methylenyl-γ-lactams. In most cases, the preparation of such compounds are limited to the synthesis of glutamic acid derivatives. As a consequence, a general method to prepare such intermediates would be useful. To address this problem, Py and coworkers designed the reductive coupling of nitrones with allenoates using a combination of SmI_2, LiBr, and *t*-butanol.[11]

Table 8.2 Cross-Coupling of Nitrones and Allenoates with LiBr. [11]

Entry	R^1	R^2	R^3	Yield (%)	Recovered nitrone (%)
1	*i*-Pr	H	Bn	80	16
2	Me	H	Bn	68	31
3	Et	H	Bn	74	23

Recently, the Reisman group made use of SmI_2 and LiBr for the reductive cyclization shown in Scheme 8.6, affording the desired alcohol intermediate as a single diastereomer in their total synthesis of *ent*-kauranoid natural products. Similar to previous examples, *t*-butanol was employed as a proton source.[12]
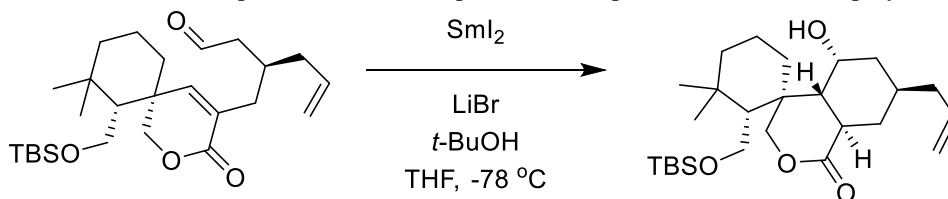
Scheme 8.6 Reductive cyclization of intermediate by SmI_2-LiBr-*t*-butanol.

8.1.4 Project Goals

The studies described above have demonstrated that the use of halide-containing additives to generate samarium dihalides is a promising area. Using the information gleaned from those studies leads to the following conclusions: 1) $SmBr_2$ and $SmCl_2$ can be generated from SmI_2 and lithium halide salts, 2) the inclusion of the lithium cation is not a crucial aspect of the enhanced reactivity observed with the addition of lithium bromide or chloride[8], 3) the tetrabutylammonium cation was shown to enhance the reactivity of Sm(II)[9] and 4) A proton source like *t*-butanol or water is generally utilized in reductions of $SmBr_2$ and $SmCl_2$ to further increase yield.[1,11–13] With these results in mind, the use of soluble tetrabutylammonium halide salts (TBAX), potentially in conjunction with a proton source was further examined. Finally, the most ambitious goal of this project was to test whether SmF_2 is an accessible reductant using this method, and if so, determine the upper limit of its reactivity.

8.2 Experimental Details

8.2.1 Materials

Samarium powder was purchased from Acros Organics. SmI_2 was generated by the standard method of samarium metal combined with iodine in THF and allowed to stir for at least 4 hours. Iodometric titrations were performed to verify concentration of SmI_2. TBAF, TBACl, and TBABr were purchased from VWR and used without further purification. TBAF was purchased as a 1 M solution in THF packaged under argon, and was stored in the glovebox. Arene substrates were purchased from VWR and used without further purification. Carbonyl substrates were purified by distillation or recrystallization. All liquid substrates were stored over 4Å molecular sieves. Cyclizable substrates were synthesized as outlined in Chapter 5. The purity and identity of substrates was verified by GC-MS and NMR. Water was degassed with argon overnight. All solutions were prepared inside a drybox containing an argon atmosphere. Inhibitor-free

tetrahydrofuran was purified by a Solvent Purification system (Innovative Technology Inc.; MA).

8.2.2 Instrumentation

Proton NMR spectra were recorded on a Bruker 500 MHz spectrometer in $CDCl_3$. Carbon NMR were performed at 125 MHz in $CDCl_3$. GC-MS analyses were done with an HP 5890 Series II Gas Chromatograph with an HP Mass Selector Detector and biphenyl standard.

8.2.3 Methods

8.2.3.1 Generation of SmBr$_2$ and SmCl$_2$

A solution of 0.1 M SmI_2 was generated from the commonly used method of samarium powder stirred with iodine in THF.[14] The SmI_2 was allowed to sit undisturbed to allow excess metal to settle and then the desired quantity of SmI_2 was removed and placed in a new flask equipped with a stir bar. To this solution, 3 equivalents with respect to SmI_2 of TBACl or TBABr was added and the solution was stirred until all the white TBAX salts were dissolved and the corresponding color change occurred.

8.2.3.2 General Procedure for Synthetic-Scale SmBr$_2$ and SmCl$_2$ Reactions

In a round bottom flask, the desired quantity of SmX_2 was prepared as described above, and to it the desired ketone substrate was added neat. The reaction was stirred overnight and then quenched with air followed by the addition of 10%-vol HCl solution. The product was then extracted with ethyl acetate. The organic layer was then treated with saturated aqueous sodium thiosulfate, and then brine. The remaining solution was then dried with magnesium sulfate, filtered and then solvent was removed by rotary evaporation. The identity of the product was verified by GC-MS, ^{1}H and ^{13}C NMR.

### 8.2.3.3 General Procedure for Synthetic-Scale SmI$_2$-TBAF-H$_2$O Reductions

In a round bottom flask, the desired quantity of SmI_2 was added followed by the desired substrate substrate was added neat. Next, a solution of H_2O and TBAF were premixed in a vial. Once mixed, the H_2O-TBAF solution was added quickly to the SmI_2-substrate solution. The reaction was stirred until completion and then quenched with air followed by the addition of 10%-vol HCl solution. The product was then extracted with the specified solvent. The organic layer was then treated with saturated aqueous sodium thiosulfate, and then brine. The remaining solution was then dried with magnesium sulfate, filtered and then solvent was removed by rotary evaporation. The identity of the product was verified by GC-MS, ^{1}H and ^{13}C NMR.

8.3 Results and Discussion

The addition of TBAX salts to SmI_2 was characterized by a combination of UV-vis spectroscopy and by examining the resulting reactivity toward organic varying functional groups. The initial results of this study are described below, although further evaluation of TBAX salt addition is forthcoming.

8.3.1 Characterization of Samarium Halides from TBAX Salts

The generation of $SmBr_2$ and $SmCl_2$ upon addition of the TBAX salts was verified by UV-vis spectroscopy. As shown in Figure 8.2, the spectra clearly mirror those obtained through the addition of LiX salts as shown in Figure 8.1. The UV-vis spectra and observed color of SmI_2 when combined with TBAF is red. This color change is indicative of a hypsochromic shift and, if consistent with the observations reported previously for correlation to a shift in redox potential[8], SmI_2-TBAF is an even stronger reductant.
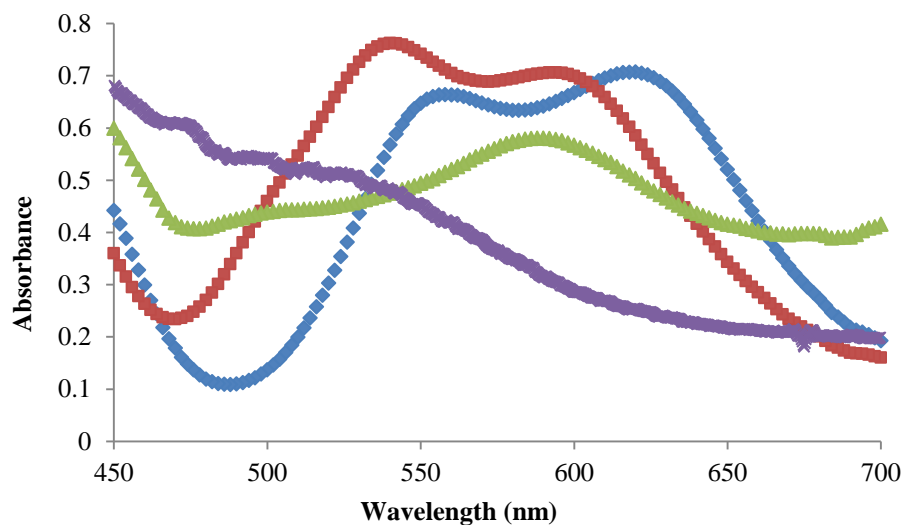
Figure 8.2 Representative UV-vis spectrum of 2 mM SmI_2 in THF alone (blue), with 2 equiv TBABr (red), TBACl (green), and TBAF (purple).

Although attempts were made to crystallize the TBAF-based samarium complex to further characterization, a crystalline solid was not successfully isolated. Because the resulting complex is so reactive and contains some H_2O, it is likely that it does not exist in the divalent state for very long under the conditions it is generated in this study.

An examination of the literature revealed that Templeton *et al* successfully generated and characterized a series of lanthanide trifluoride complexes using the addition of hydrofluoric acid. Once synthesized, they were able to show that pure SmF_3 is isostructural with YF_3 and LaF_3, because both orthorhombic and hexagonal structures were observed.[15] The YF_3 isostructure reported in the literature shows that despite the direct coordination of three anionic fluorides to form a neutral YF_3 complex, there are nine total fluorines arranged around the metal center, as shown in Figure 8.3. Thus, although we can assume fluorides are coordinated to the metal following a reduction, it is difficult to draw conclusions about the exact nature of the trivalent complex. What is

known about the identity of the complex is that the Sm(III) cation has a coordination number of nine and there is competing coordination of H_2O, OH^-, and THF.
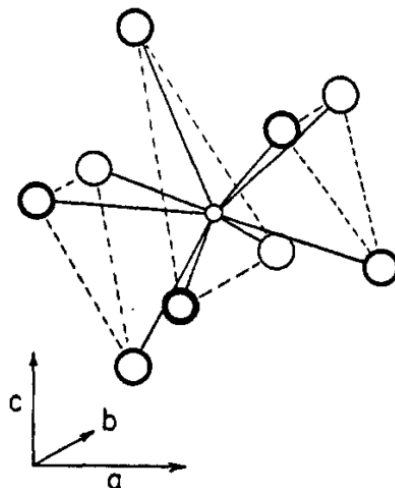
Figure 8.3 Structure of YF_3 proposed by Templeton. [15]

8.3.2 Synthetic Reactions of SmI_2-TBABr and TBACl

The generation of $SmBr_2$ and $SmCl_2$ from the addition of the corresponding TBAX salts was further confirmed by the reduction of cyclohexanone. Using TBABr, the corresponding $SmBr_2$ was generated followed by the addition of cyclohexanone. In the original report, the pinacol coupling with LiBr was found to be nearly quantitative in ca. 10 minutes.[7] Similarly, after 10 minutes, the only product observed by GC-MS for the reaction performed with TBABr as the bromide source was the expected pinacol.
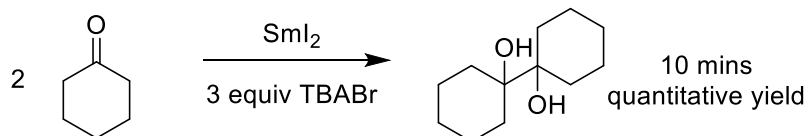
Scheme 8.7 Pinacol coupling of cyclohexanone using SmI_2-TBABr.

206

8.3.3 Synthetic Reactions of SmI$_2$-TBAF-H$_2$O

To probe whether SmF$_2$ was an accessible reductant, a series of reactions were performed with the alkyl ester, methyl 3-phenylpropionate and is included in Table 8.3. This substrate was chosen because it has a high redox potential, making it nonreducible by reaction with SmI$_2$-H$_2$O alone. The initial reduction utilized NH$_4$F, which although fairly insoluble in THF, produced a red solution after stirring overnight and approximately 50% yield of the corresponding alcohol. To ensure that the reactivity towards the ester was a result of fluoride and did not arise from the presence of ammonium, the same reduction was attempted with NH$_4$I. This reaction produced no product and suggested the enhanced reactivity of Sm(II) in the previous reaction was a consequence of the fluoride. Next, an even more insoluble fluoride salt was employed, KF, which produced only a trace amount of product. This suggested that increasing the solubility of the fluoride source was important for the reaction and that the reduction did not occur heterogeneously. Finally, the highly soluble tetrabutylammonium fluoride salt was used and a quantitative yield of the alcohol was obtained.

Table 8.3 Control reactions for SmF$_2$ with the reduction of methyl 3-phenylpropionate.

Additive	Equivalents vs SmI$_2$	Yield of 3-phenylpropanol
NH$_4$F	3	50 %
NH$_4$I	3	NR
KF	3	trace
TBAF	3	quantitative

None	-	NR

Conditions: 25 μL of substrate, 2 equiv H_2O, stirred overnight. Approximate yields and product identity obtained by GC-MS.

For all of the above reactions, H_2O was added as a coordinating proton source because 2 equivalents of H_2O is not high enough of a concentration to significantly enhance the redox potential of the Sm(II) complex.[16] It should be noted that the H_2O equivalents mentioned in this study correspond to *added* H_2O and that commercially-available TBAF is stabilized with small concentrations of H_2O (~5%).

Next, the reduction limit of the system was tested by reduction of a series of primary alkyl halides. The results of this study are listed in Table 8.4 and clearly show that this reagent combination is able to promote electron transfer to alkyl halides including alkyl chlorides. 1-Chlorododecane appears to be the upper limit for electron transfer from SmI_2-TBAF-H_2O, suggesting that the reduction potential of this combination is close to the reduction potential of a primary alkyl chloride, measured to be approximately -1.2 V vs. SCE.[17] Thus, from these results it can be concluded that this system rivals the powerful reagent combination of SmI_2-Et_3N-H_2O.[18]

Table 8.4 Yields in the reduction of various alkyl halides by SmI_2-TBAF-H_2O.

Alkyl Halide	% Reduced Product
1-Iododoecane	91
1-Bromododecane	71
1-Chlorododecane	44
1-Fluorodecane	0

Conditions: 25 µL of substrate, 2.5 equiv SmI₂, 2 equiv H₂O vs Sm, 3 equiv TBAF vs Sm, stirred overnight. Approximate yields and product identity obtained by GC-MS.

Because 1-chlorododecane provided a modest yield under the conditions of the previous experiment, it was utilized for the optimization study. The concentrations of TBAF and H_2O were varied to ascertain the optimum conditions for alkyl chloride reduction. The yields in Table 8.5 reveal that small changes in the equivalents of TBAF and H_2O used do not have a large influence on the yield of *n*-dodecane. It appears that for optimum results, the combination of 2 or 3 equivalents of TBAF with 2 equivalents of H_2O provides the highest yield of product.

Table 8.5 Optimization of SmI_2-TBAF-H_2O by reduction of 1-chlorododecane.

Equiv. TBAF	Equiv. H₂O	Yield Dodecane (%)
2	2	44
3	3	37
4	4	39
2	3	39
3	2	44

Conditions: 25 µL of substrate, 2.5 equiv SmI₂, stirred 4 hours. Yields obtained by GC-MS with biphenyl internal standard.

The next class of substrates investigated with this system was a selection of arenes of varying redox potential. Using a standard set of reaction conditions, the yields or percent conversions were determined and are listed in Table 8.6. When the quantity of SmI_2 employed for the reduction was increased to up to 10 equivalents vs. substrate, multiple products were observed consistent with over-reduction. For example, in the reduction of biphenyl, multiple products were obtained with varying degrees of

209

saturation. The existence of these over-reduction products suggests that this system is capable of reducing benzene derivatives.

Table 8.6 Reduction of selected arene substrates by SmI_2-TBAF-H_2O.

Arene	% Product	Redox Potential[19]
Anthracene	99[a]	-1.98
Trans-Stilbene	94[a]	-2.21
Phenanthrene	98[a]	-2.46
Naphthalene	86[b]	-2.51
Biphenyl	19[b]	-2.60

[a] Indicates isolated yield of expected $2e^-$, $2H^+$ reduction product. [b] Indicates % conversion to $2e^-$, $2H^+$ reduction product vs. starting material by ^1H NMR Conditions: 3 equiv SmI_2, 3 equiv TBAF vs SmI_2, 2 equiv H_2O vs SmI_2.

With these promising results in hand, the reduction of a benzene derivative was attempted using an *n*-hexyl-substituted benzene derivative that could be easily isolated and characterized. The chromatogram presented in Figure 8.4 shows that this recalcitrant substrate did undergo some degree of reduction.
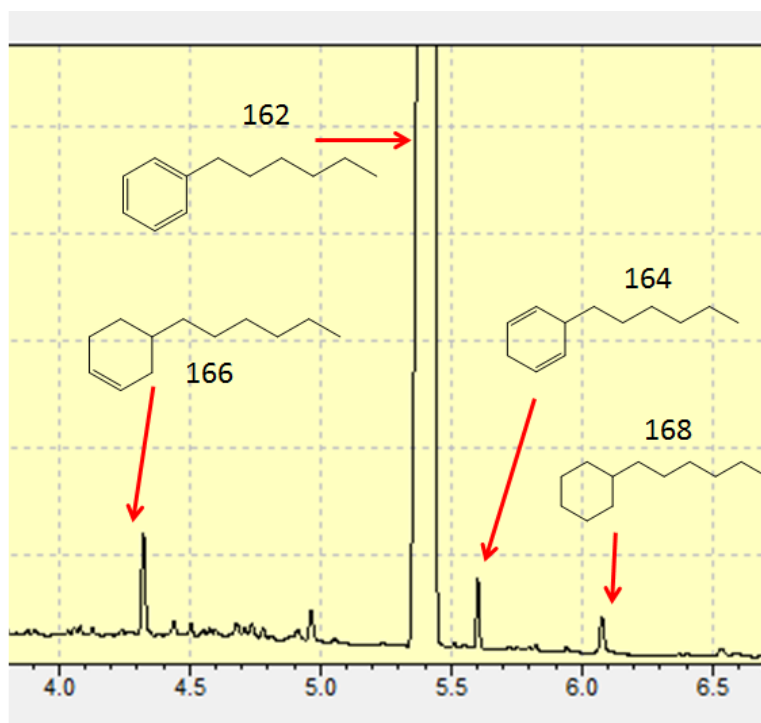
Figure 8.4. GC-MS of the reduction of *n*-hexylbenzene by SmI$_2$-TBAF-H$_2$O. Conditions: 100 µL of substrate, 15 equivalents of SmI$_2$, 3 equiv TBAF vs Sm, 2 equiv H$_2$O vs Sm.

Multiple products, generated from varying degrees of reduction, were obtained from this reaction. Although this is not a synthetically useful means of achieving benzene reduction, this experiment does provide important information about the nature of the reagent. The literature value for the reduction potential of benzene is -3.42 V vs. SCE.[19] Because the reduction limit estimated from Table 8.6 suggests the redox potential of SmI$_2$-TBAF-H$_2$O is not high enough to reduce an alkyl fluoride but it does promote a small amount of reduction of benzene, the mechanism of reduction for these two classes of substrate are ostensibly different. Similar to the results presented in previous chapters, this observation suggests that the combination of SmI$_2$-TBAF-H$_2$O likely promotes HAT

211

since the redox potential of the arenes reduced are all significantly high. Although this system has not been studied in the same detail, the results imply a bond-weakening of the O-H bond of water coordinated to Sm(II) of at least 80 kcal/mol.

The next class of reductions examined with this reagent was the reduction of carbonyl-containing substrates. With the other TBAX salts, ketones provided pinacol products in excellent yield. Due to the presence of H_2O in the TBAF solution, the reduction of 2-methylcyclohexanone quantitatively yielded the alcohol product even when additional equivalents of H_2O were not added. Table 8.3 established that a primary alkyl ester could be reduced to the corresponding alcohol, but it was also shown that a primary alkyl amide could also be reduced. The reduction of an alkyl nitrile was unsuccessful, however.

Table 8.7 Reduction of selected carbonyl substrates by SmI_2-TBAF-H_2O.
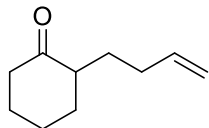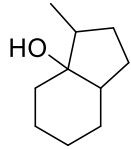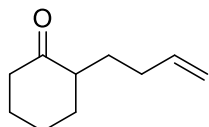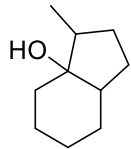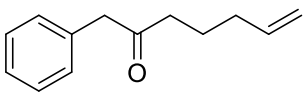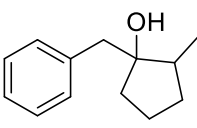
Substrate	Product	Conversion
2-methylcyclohexanone	2-methylcyclohexanol	quantitative
2-octanone	2-octanol	quantitative
3-phenylpropionate	3-phenylpropanol	quantitative
3-phenylpropionamide	3-phenylpropanol	quantitative
3-Phenylpropionitrile	-	0

Conditions: 6 equiv SmI_2, 3 equiv TBAF vs SmI_2, 2 equiv H_2O vs SmI_2. Conversion indicated by loss of starting material and growth of product by GC-MS.

Two model ketyl-olefin cyclizations were also attempted to determine whether this reagent provided a selectivity for either reduced or cyclized product. The results of this experiment are summarized in Table 8.8. These preliminary results suggest that while

cyclization does occur, it appears that a smaller quantity of added water better promotes cyclization over reduction.

Table 8.8 Ketyl-olefin cyclizations by SmI_2-TBAF-H_2O.

Substrate	Equiv TBAF	Equiv H_2O	Major Product	Yield (%)
	3	0		70
	3	2		55
	4	2		58

Conditions: 100 µL of substrate, 2.5 equiv SmI_2, stirred overnight. Yield of major product computed from ^{1}H NMR as per method in Chapter 6.

8.4 Conclusions and Significance

The significance of this work is two-fold. The results of this study, although incomplete, suggest that a divalent samarium fluoride complex of some kind can be efficiently generated using a soluble fluoride source. As expected, this resulting complex has been shown to have a higher reduction potential than the parent compound, SmI_2, and therefore is able to reduce a wide array of substrates.

The more remarkable feature of this work is that it has demonstrated that although inefficient, a new level of Sm(II) reactivity can be unlocked through the promotion of HAT to benzene that enables soluble Birch-type chemistry. This provides new insight into the upper limit of the reactivity of Sm(II) and the bond-weakening that occurs as a consequence of coordination.

8.5 Proposed Future Studies

Future work on this system will focus on enhancing the efficiency through which the observed reactivity toward organic substrates is achieved. This can be accomplished by introducing an agent to aid the solubility of the complex. Additionally, the scope of the reaction can be supplemented to determine if any unique reactivity can be obtained from this reagent combination. Finally, kinetic analysis of the system can be employed to further characterize the reagent and determine if this system is indeed capable of HAT as hypothesized. Ideally, the information contained in this study can be applied to the design of future systems capitalizing on this extended Sm(II) reactivity.

8.6 References

(1)   Lebrun, A.; Namy, J.-L.; Kagan, H. B. *Tetrahedron Lett.* **1993**, *34*, 2311–2314.

(2)   Hélion, F.; Lannou, M.-I.; Namy, J.-L. *Tetrahedron Lett.* **2003**, *44*, 5507–5510.

(3)   Zörb, A.; Brückner, R. *European J. Org. Chem.* **2010**, *2010*, 4785–4801.

(4)   Dahlén, A.; Hilmersson, G. *Eur. J. Inorg. Chem.* **2004**, *2004*, 3020–3024.

(5)   Rossmanith, K. *Monatshefte fur Chemie* **1979**, *110*, 109–114.

(6) Matsukawa, S.; Hinakubo, Y. *Org. Lett.* **2003**, *5*, 1221–1223.

(7) Fuchs, J. R.; Mitchell, M. L.; Shabangi, M.; Flowers, II, R. A. *Tetrahedron Lett.* **1997**, *38*, 8157–8158.

(8) Miller, R. S.; Sealy, J. M.; Shabangi, M.; Kuhlman, M. L.; Fuchs, J. R.; Flowers, II, R. A. *J. Am. Chem. Soc.* **2000**, *122*, 7718–7722.

(9) Sun, L.; Mellah, M. *Organometallics* **2014**, *33*, 4625–4628.

(10) Szostak, M.; Spain, M.; Procter, D. J. *J. Org. Chem.* **2014**, *79*, 2522–2537.

(11) Xu, C.-P.; Huang, P.-Q.; Py, S. *Org. Lett.* **2012**, *14*, 2034–2037.

(12) Yeoman, J. T. S.; Mak, V. W.; Reisman, S. E. *J. Am. Chem. Soc.* **2013**, *135*, 11764–11767.

(13) Szostak, M.; Spain, M.; Procter, D. *J. Org. Chem.* **2014**, *79*, 2522–2537.

(14) Imamoto, T.; Ono, M. *Chem. Lett.* **1987**, 501–502.

(15) Zalkin, A.; Templeton, D. H. *J. Amer. Chem. Soc.* **1953**, *75*, 2453–2458.

(16) Prasad, E.; Flowers, II, R. A. *J. Am. Chem. Soc.* **2005**, *127*, 18093–18099.

(17) Isse, A. A.; Lin, C. Y.; Coote, M. L.; Gennaro, A. *J. Phys. Chem. B* **2011**, *115*, 678–684.

(18) Dahlen, A.; Hilmersson, G.; Knettle, B. W.; Flowers, II, R. A. *J. Org. Chem.* **2003**, *68*, 4870–4875.

(19)   Dahlén, A.; Nilsson, A.; Hilmersson, G. *J. Org. Chem.* **2006**, *71*, 1576–1580.

Chapter 9. Conclusion

This work described in this dissertation explored a few of the many ways in which coordination of reaction components affects the reactivity of Sm(II). The most significant finding was that Sm(II) is capable of performing proton coupled electron transfer (PCET) to organic substrates to bypass high energy intermediates. Using this information, new additives were investigated and the scope of their reactivity was surveyed.

The first study, outlined in Chapter 2, isolated the role of H_2O in the reduction of anthracene and 1-iodododecane by SmI_2-H_2O. Using these non-coordinating substrates, it was revealed that anthracene reduced at a much faster rate than the alkyl iodide. This suggested that the mechanism for the reduction of anthracene differed from the expected electron transfer. Through additional experiments, it was determined that upon coordination to Sm(II), the O-H bond of H_2O undergoes a large degree of bond-weakening, which allows the SmI_2-H_2O complex to transfer a formal hydrogen atom to reduce anthracene.

This work was extended in Chapter 3 by examining whether H_2O was unique in the bond-weakening experienced upon coordination to Sm(II). Through the use of glycols and their monomethyl ethers and by kinetic analysis of the reduction of anthracene and benzyl chloride, it was discovered that proton donors that coordinate strongly to Sm(II) can also promote PCET. Further comparison of glycol coordination to Sm(II) was achieved using isothermal titration calorimetry. These studies suggested that H_2O is not

unique and that alternative coordinating proton sources could be employed in reductions that proceed through PCET.

In Chapter 4, the impact of substrate coordination to SmI_2-H_2O was isolated through kinetic and thermodynamic studies on an array of carbonyl-containing substrates. Using these substrates, the continuum between PCET and ET for Sm(II)-based reductions was probed. The work revealed that easier to reduce carbonyl-containing substrates are reduced through a more asynchronous coupled process while those with more negative redox potentials are reduced through a more concerted process.

The irreversibility of PCET in the reduction of carbonyl-containing substrates was examined through the kinetic study of two representative ketones and their pendant-olefin derivatives, and is outlined in Chapter 5. The similar rates obtained for the reduction of the ketones and the reductive cyclization of the ketyl-olefin substrates revealed that both proceed through a rate-limiting PCET. This suggested that the two classes of substrate proceeded through a similar irreversible process.

Using the information gleaned from the studies outlined in Chapters 2-5, alternative additives were proposed, their reactivities explored, and the mechanism through which they reduce substrates was investigated. Two types of additives were investigated: N,N-dimethylaminoethanol and amides (2-pyrrolidone and N-methylacetamide). It was found that these additives coordinate strongly to Sm(II) and can promote PCET from their resulting Sm(II) complex.

The impact of the coordination of solvent to Sm(II) was examined by comparing the reactivity in coordinating and noncoordinating solvents by using the highly-soluble

reductant, Sm[N(SiMe$_3$)$_2$]$_2$. The work in Chapter 7 revealed that noncoordinating solvents greatly accelerate the rate of alkyl halide reduction, which is a consequence of the displacement of THF from the coordination sphere of the metal.

Finally, in Chapter 8, the use of tetrabutylammonium halide salts was explored in combination with SmI$_2$ as a means of accessing the other samarium dihalides. Through UV-vis and reactivity studies, it was confirmed that direct addition of these salts provides the desired Sm(II) halide. Additionally, the use of tetrabutylammonium fluoride affords access to an even more powerful reductant capable of reducing a benzene derivative.

These studies have culminated in a new understanding of the reactivity of Sm(II) toward organic substrates. This work has expanded the understanding of bond-weakening induced upon coordination to low valent metals. These results provide information that will be applied to design more efficient applications of Sm(II) as well as the generation of a synthetically-useful catalytic Sm(II)-based reagent system. Most importantly, the studies provided herein serve as a reminder that even the fundamental principles governing simple reactions can be elusive and complex.

Chapter 10. Appendix

10.1 Proton-Coupled Electron-Transfer in the Reduction of Arenes by SmI_2-H_2O

Table 10.1. GC Yields of substrates reduced with proton donors.

Substrate	Quantity Substrate	Equivalents SmI_2	Proton Donor	Equivalents Proton Donor	Time	Yield (%)
Anthracene	0.009 g	2.5	H_2O	450	< 2 min	97
1-Iodododecane	75 uL	3	H_2O	100	<2 hrs	77
1-Iodododecane	75 uL	3	MeOH	100	12 hrs	53

Table 10.2. Table of the rate of decay of SmI_2-H_2O complexes in the absence of substrate.

Proton Donor	Concentration of Proton Donor (Equivalents vs. SmI_2)	Rate of Natural Decay (s^{-1})
H_2O	500	0.010
H_2O	1000	0.012

Model	Exponential		
Equation	y = y0 + A*exp (R0*x)		
Reduced Chi-Sqr	2.91862E-6		
Adj. R-Square	0.99978		
		Value	Standard Error
B	y0	-0.0033	7.67754E-5
B	A	0.46508	1.53205E-4
B	R0	-0.00198	1.49844E-6
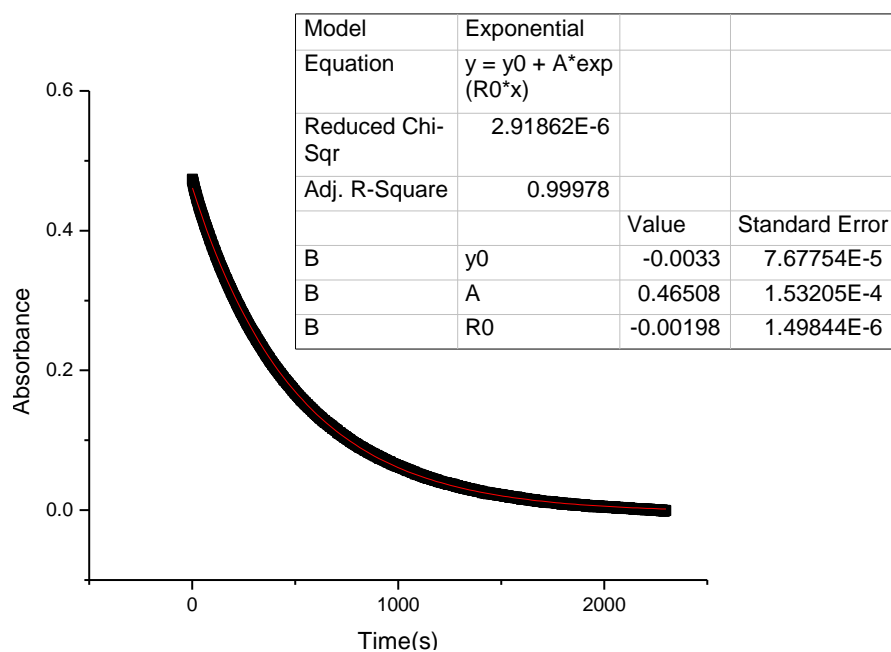
Figure 10.1. Representative plot of the decay of 10 mM Sm(II) at 560 nm in the presence of excess 1-Iodododecane and water fit to a single exponential equation where $y = y0 + A^{(R0*x)}$ and k_{obs} is represented by $|R0|$.

Model	Exponential		
Equation	y = y0 + A*exp(R0*x)		
Reduced Chi-Sqr	2.60509E-6		
Adj. R-Square	0.99961		
		Value	Standard Error
Absorbance	y0	-6.02415E-4	7.48146E-5
Absorbance	A	0.40298	3.53694E-4
Absorbance	R0	-0.01173	1.69069E-5
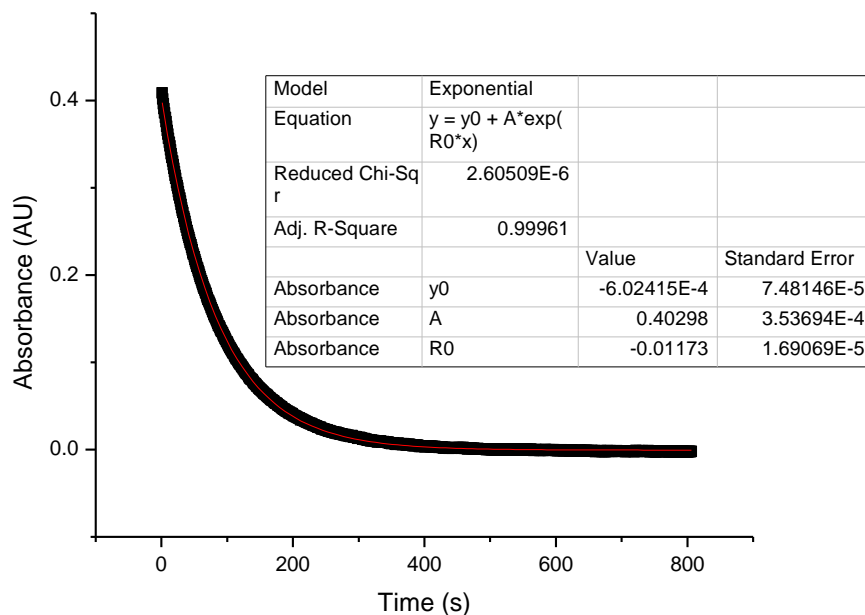
Figure 10.2. Sample decay for 0.75 M H_2O, 100 mM Anthracene, 10 mM SmI_2, measured at 25 ^{o}C, 560 nm fit to a single exponential equation to provide k_{obs}.
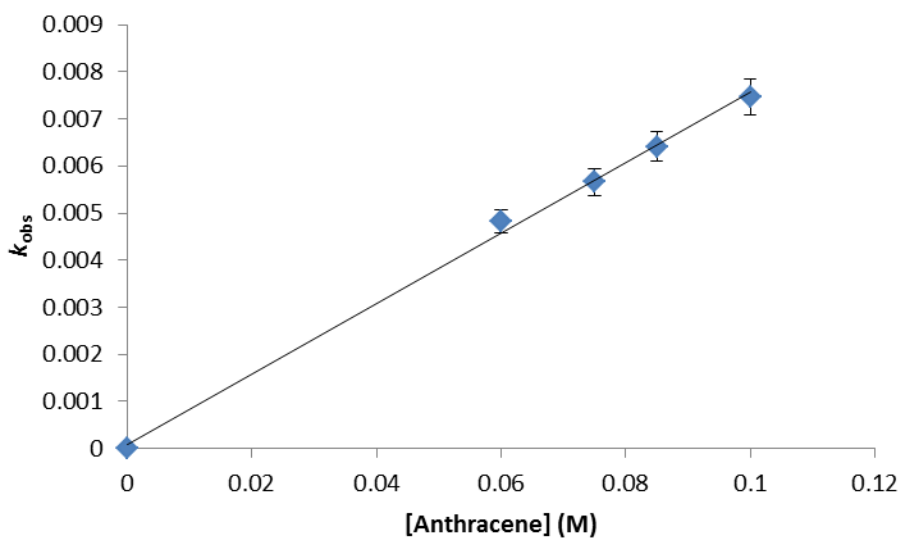
Figure 10.3. Plot of k_{obs} vs. concentration of anthracene with 5 mM SmI_2 and 125 equiv H_2O where [Anthracene] is varied from 0.06 M to 0.1 M and a linear regression provides $y = 0.075x + 9e\text{-}5$ with $R^2 = 0.998$.

Table 10.3 Explanation of Fractional times method for anthracene.

Fractional times method was applied to determine the order of SmI_2 over a range of concentrations of anthracene with a constant concentration of 1.25 M H_2O. The value for $(t_{3/4}\text{-}t_{1/2})/t_{1/2}$ was computed for each decay to provide an order as described below.[S2]

[Anthracene] (mM)	Trial	A_0	$A_{1/2}$	$A_{3/4}$	$t_{1/2}$	$t_{3/4}$	$(t_{3/4}\text{-}t_{1/2})/t_{1/2}$
90	A	0.357	0.1785	0.08925	20	45	1.25
90	B	0.306	0.153	0.0765	17	34	1.00
100	A	0.306	0.153	0.0765	14	28	1.00
100	B	0.314	0.157	0.0785	14	29	1.07
110	A	0.329	0.1645	0.08225	14	29	1.07
110	B	0.312	0.156	0.078	13	25	0.92
120	A	0.313	0.1565	0.07825	12	22	0.83
120	B	0.311	0.1555	0.07775	12	23	0.92
						Average:	1.01
						Order:	**1**

Figure 10.4 Plot and data points for the reduction of anthracene where k was measured under constant concentrations of SmI_2 (10 mM), anthracene (100 mM), and water (125 equiv vs Sm) with the temperature varied from 19.5-40.1 ^{o}C.

Temp ^{o}C	Temp ^{o}K	1/T (K^{-1})	1000/T (K^{-1})	k ($s^{-1}M^{-3}$)	$\ln(k/T)$
19.5	292.5	0.003418803	3.42	0.041642	-8.85712
25	298	0.003355705	3.36	0.041708	-8.87415
32.3	305.3	0.003275467	3.28	0.041999	-8.89141
40.1	313.1	0.003193868	3.19	0.042121	-8.91374
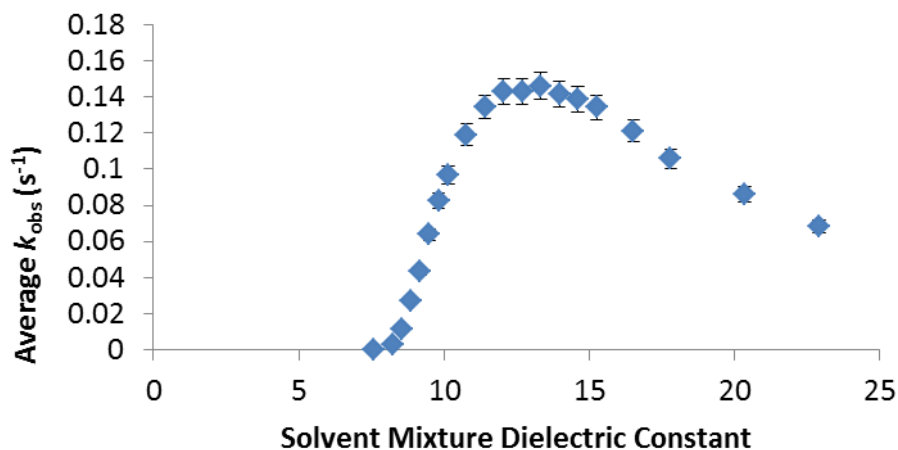
Figure 10.5. Plot of k_{obs} as a function of computed solvent dielectric constant (computed from the summation of each solvents volume fraction multiplied by its volume fraction)as

225

[water] is increased with 100 mM anthracene, 10 mM SmI_2 and with [H_2O] varied from 0-12 M in THF.
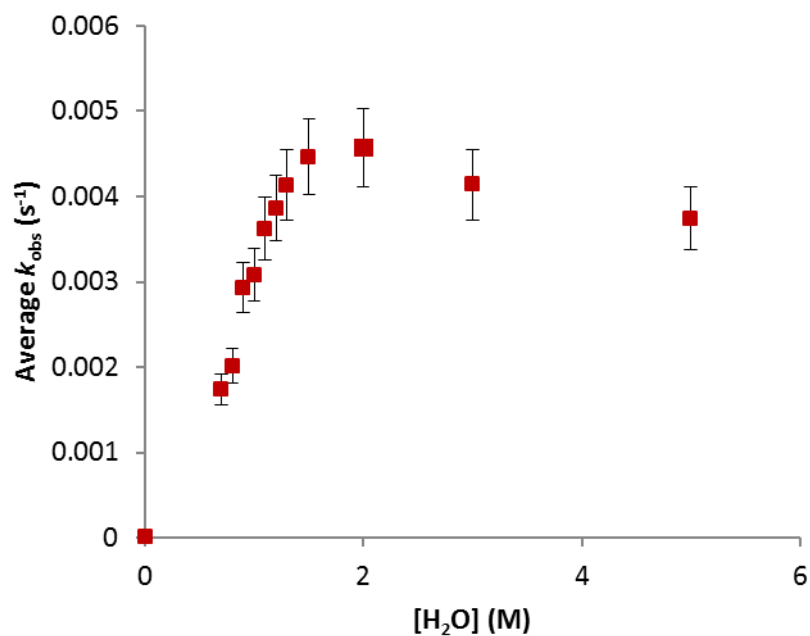
Figure 10.6. Plot of k_{obs} vs. [water] for the reduction of 1-Iodododecane with 10 mM SmI_2 in the presence of 0.70 - 5 M H_2O, and 100 mM 1-Iodododecane measured at 35 ^{o}C and 560 nm.
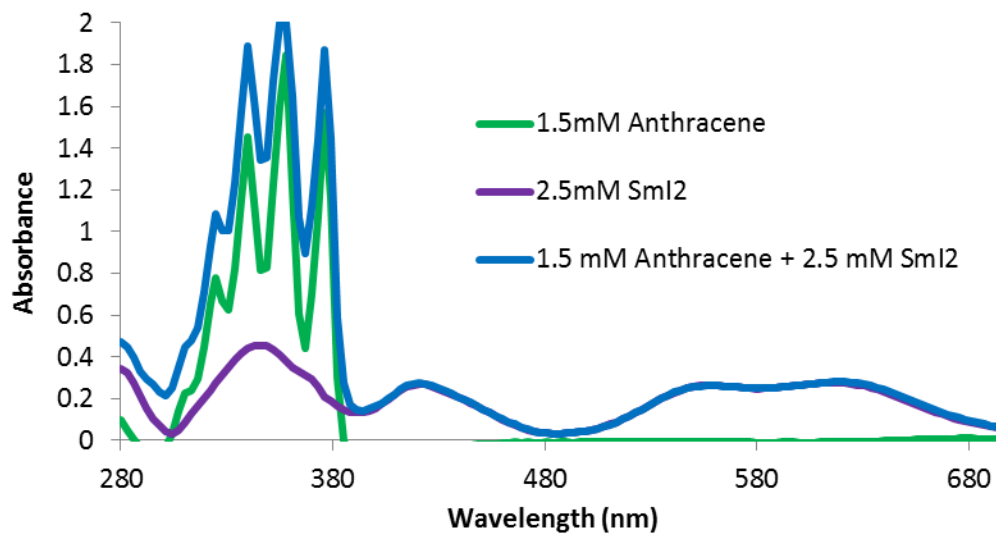
Figure S12. UV-vis spectra of anthracene, SmI_2, and anthracene-SmI_2 mixture to show lack of coordination to SmI_2 by anthracene.
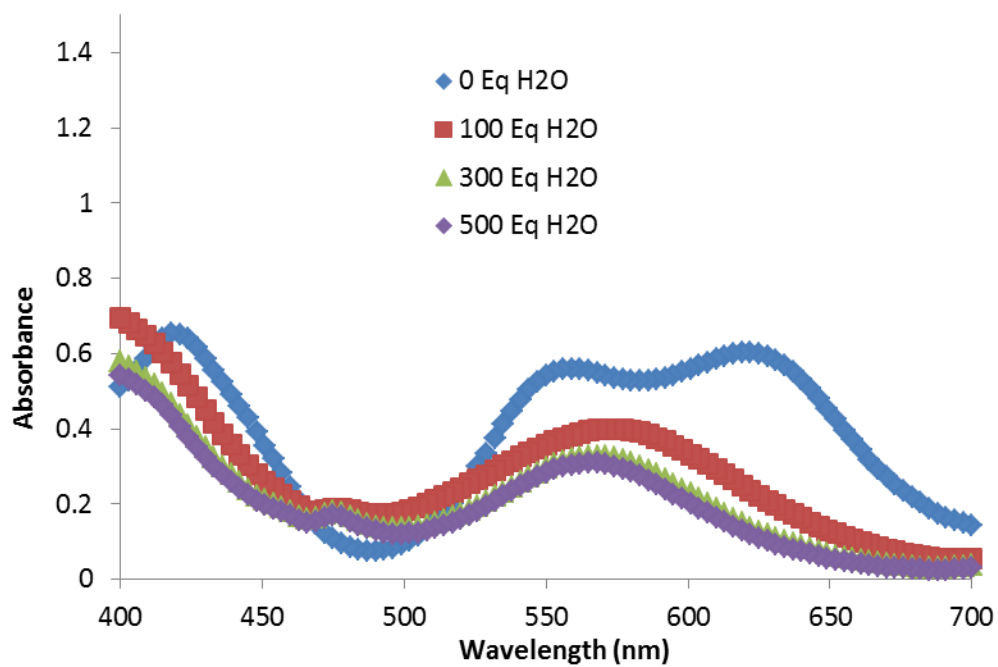
Figure 10.7. UV-vis spectra of SmI_2 with increasing $[H_2O]$ showing the coordination of H_2O as concentration increases.

227
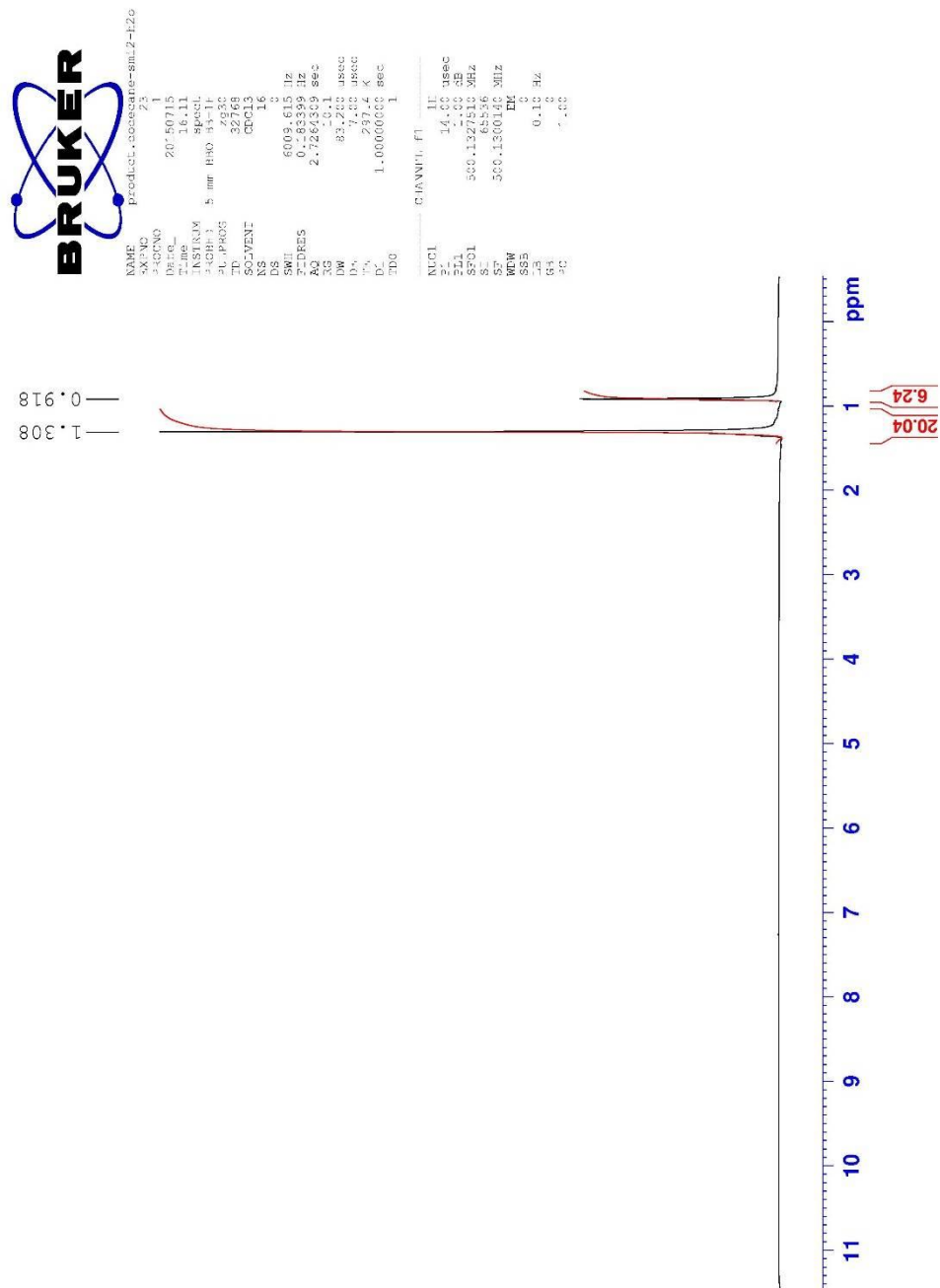
Figure 10.8 [1]H Spectrum of n-dodecane

Current Data Parameters
NAME   13C.pure.dodecane
EXPNO   2
PROCNO   1

F2 - Acquisition Parameters
Date_   20150714
Time   14.03
INSTRUM   spect
PROBHD   5 mm BBO BB-1H
PULPROG   zgdc30
TD   65536
SOLVENT   CDCl3
NS   41
DS   0
SWH   30030.029 Hz
FIDRES   0.458222 Hz
AQ   1.0912410 sec
RG   2048
DW   16.650 usec
DE   7.00 usec
TE   296.1 K
D1   1.00000000 sec
d11   0.03000000 sec
TD0   1

======== CHANNEL f1 ========
NUC1   13C
P1   8.60 usec
PL1   1.00 dB
SFO1   125.7703640 MHz

======== CHANNEL f2 ========
CPDPRG2   waltz16
NUC2   1H
PCPD2   100.00 usec
PL2   1.00 dB
PL12   17.50 dB
SFO2   500.1322150 MHz

F2 - Processing parameters
SI   32768
SF   125.7577789 MHz
WDW   EM
SSB   0
LB   1.00 Hz
GB   0
PC   1.40
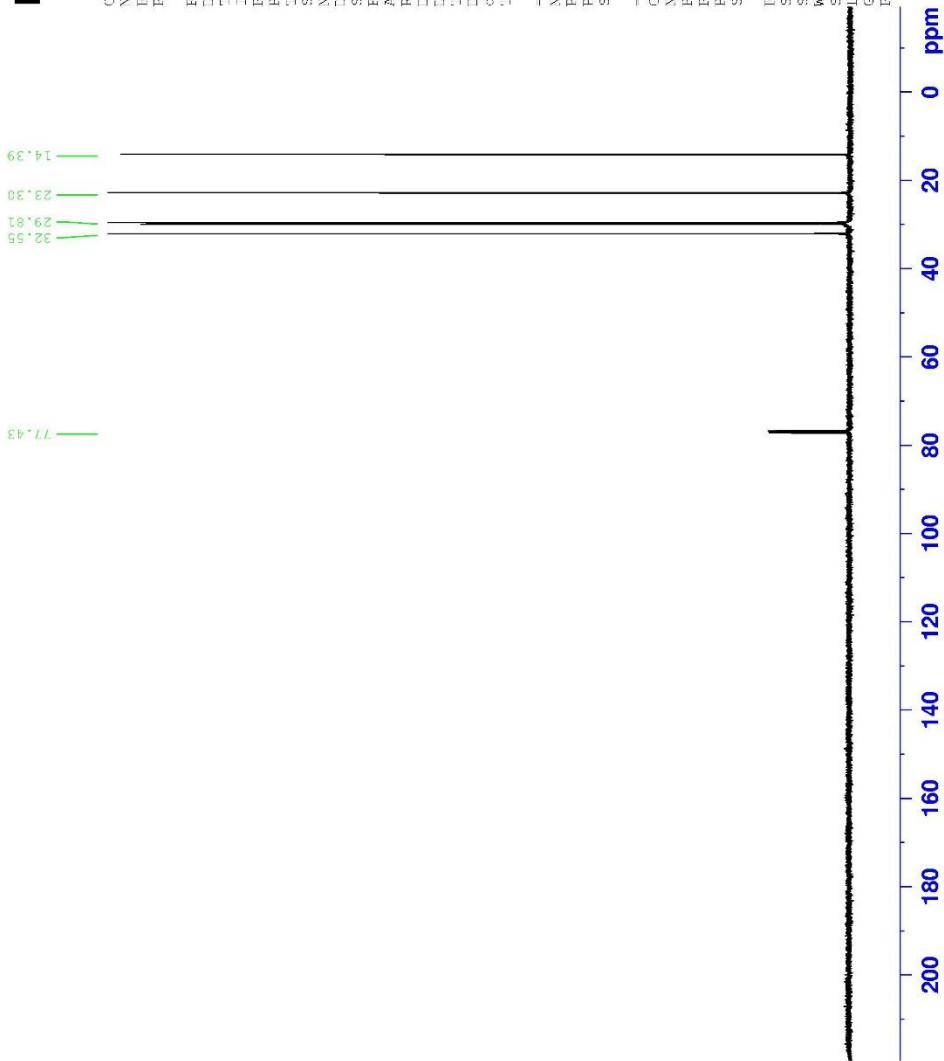
Figure 10.9 ^{13}C Spectrum of n-dododecane

229

Current Data Parameters
NAME   product.dihydroanthracene
EXPNO   3
PROCNO   1

F2 - Acquisition Parameters
Date_   20140813
Time   10.43
INSTRUM   spect
PROBHD   5 mm BBO BB-1H
PULPROG   zg30
TD   32768
SOLVENT   CDCl3
NS   16
DS   0
SWH   6009.615 Hz
FIDRES   0.183399 Hz
AQ   2.7264309 sec
RG   406.4
DW   83.200 usec
DE   7.00 usec
TE   295.2 K
D1   1.00000000 sec
TD0   1

======== CHANNEL f1 ========
NUC1   1H
P1   14.00 usec
PL1   1.00 dB
SFO1   500.1327510 MHz

F2 - Processing parameters
SI   65536
SF   500.1300078 MHz
WDW   EM
SSB   0
LB   0.10 Hz
GB   0
PC   1.00

0.103 ─────

1.586 ─────

3.982 ─────

7.206 ─────
7.327 ─────

2.00

4.09

ppm 11 10 9 8 7 6 5 4 3 2 1

Figure 10.10 [1]H Spectrum of 9,10-dihydroanthracene

230

Figure 10.11 ^{13}C Spectrum of 9,10-dihydroanthracene

Chapter 10.2. Glycols as Hydrogen Atom Transfer Promoters in Reactions by SmI$_2$
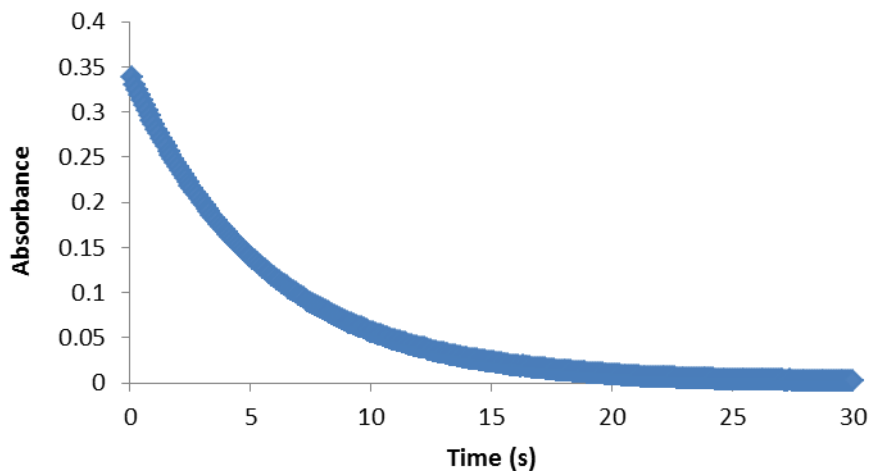
Figure 10.11. Sample decay of Sm(II) at 560 nm, 25 $^{\circ}$C, with 125 mM Anthracene, 1.25M H$_2$O and 10 mM SmI$_2$.

y = 0.0016x − 0.0245
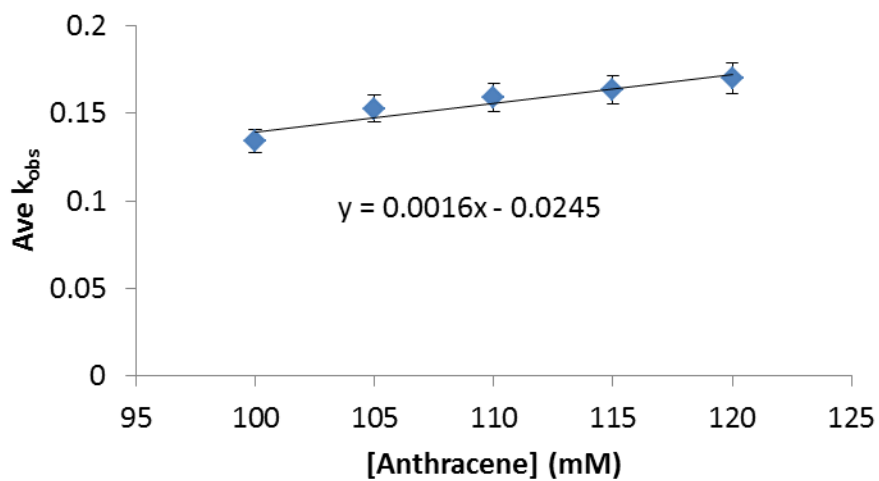
Figure 10.12. Rates for the reduction of anthracene with increasing concentration of anthracene.
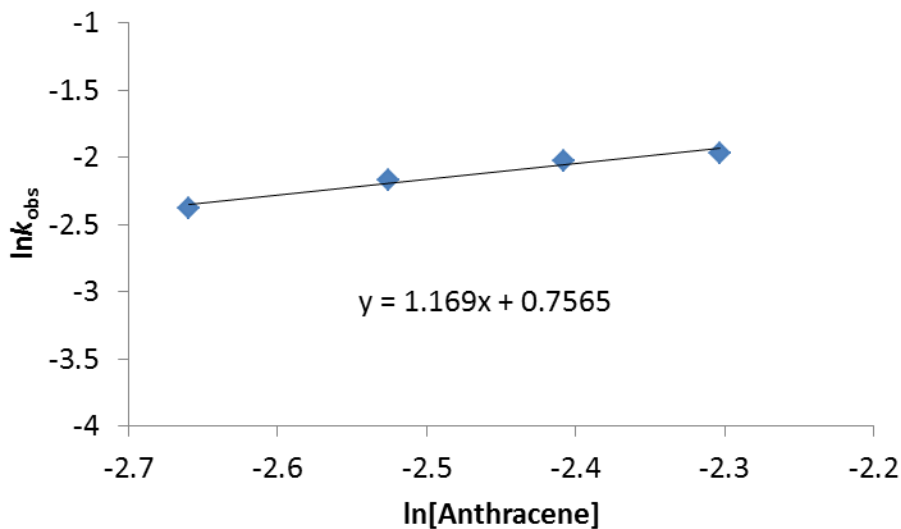
Figure 10.13. Linear rate dependence for the reduction of anthracene with increasing concentration of anthracene.

Table 10.4. Order of SmI_2 using Fractional Times Method for reduction of anthracene.

Fractional times method was applied to determine the order of SmI_2 over a range of concentrations of anthracene with a constant concentration of 1.25 M H_2O and 10 mM SmI_2. The value for $(t_{3/4}-t_{1/2})/t_{1/2}$ was computed for each decay to provide an order as described by House below.

[Anthracene]	Trial	A_0	$A_{1/2}$	$A_{3/4}$	$t_{1/2}$	$t_{3/4}$	$(t_{3/4}-t_{1/2})/t_{1/2}$
90	A	0.357	0.1785	0.08925	20	45	1.25
90	B	0.306	0.153	0.0765	17	34	1.00
100	A	0.306	0.153	0.0765	14	28	1.00
100	B	0.314	0.157	0.0785	14	29	1.07
110	A	0.329	0.1645	0.08225	14	29	1.07
110	B	0.312	0.156	0.078	13	25	0.92
120	A	0.313	0.1565	0.07825	12	22	0.83
120	B	0.311	0.1555	0.07775	12	23	0.92
						Average:	1.01
						Order:	**1**

Figure 10.14. Linear rate dependence on benzyl chloride with increasing concentrations of benzyl chloride. For the order of benzyl chloride, substrate concentration was varied from 100 mM to 300 mM. Substrate was combined with 10 mM SmI_2 and 100 eq H_2O in the stopped-flow and the decay of Sm(II) was observed at 560nm and $25 \pm 0.5\ {}^{\circ}C$. The experiment was repeated three times.

Table 10.5 Order of SmI_2 using Fractional Times Method for benzyl chloride

Fractional times method was applied to determine the order of SmI_2 over a range of concentrations of water with a constant concentration of 100 mM Benzyl chloride. The value for $(t_{3/4}-t_{1/2})/t_{1/2}$ was computed for multiple decays to provide an order as described by House below.

[H_2O]	A_0	$A_{1/2}$	$A_{3/4}$	$t_{1/2}$	$t_{3/4}$	$(t_{3/4}-t_{1/2})/t_{1/2}$
100 Eq A	0.371972	0.185986	0.092993	13	26	1
150 Eq A	0.345545	0.1727725	0.0863863	11.5	22	0.92
200 Eq A	0.335059	0.1675295	0.08376475	12	23	0.92
					Average:	0.95
					Order:	**1**

234
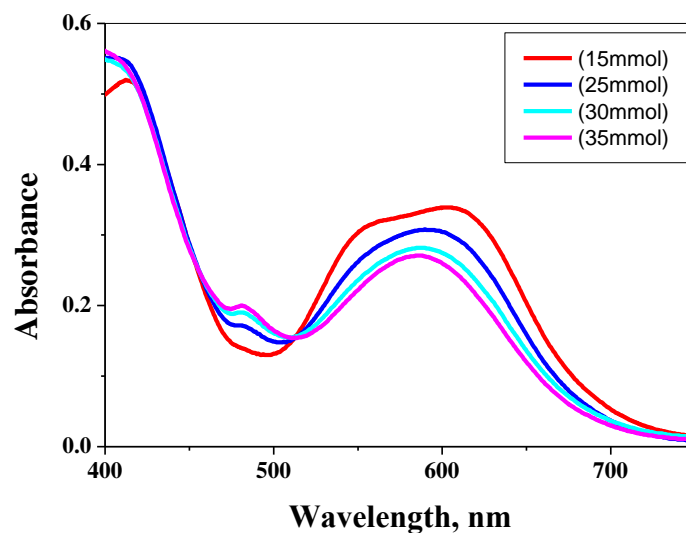
Figure 10.15: UV-Vis spectra of SmI$_2$ (1 mmol) in presence of increasing amount of ethylene glycol (15, 25, 30, 35 mmol) in THF.
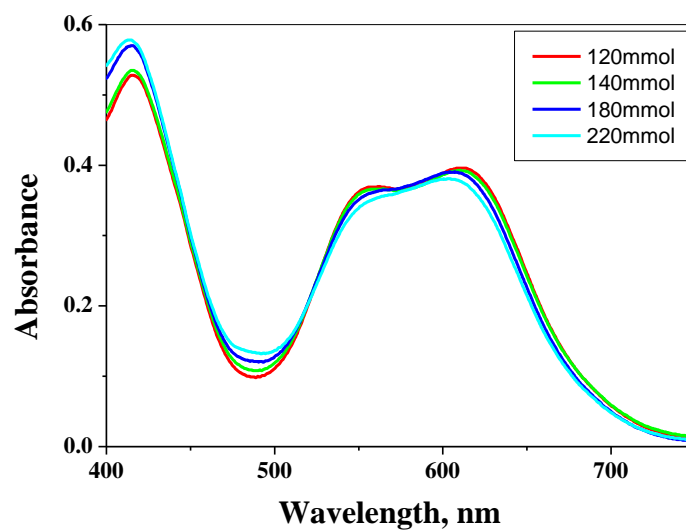
Figure 10.16: UV-Vis spectra of SmI$_2$ (1 mmol) in presence of increasing amount of ethylene glycol monomethyl ether (120, 140, 180, 220 mmol) in THF.
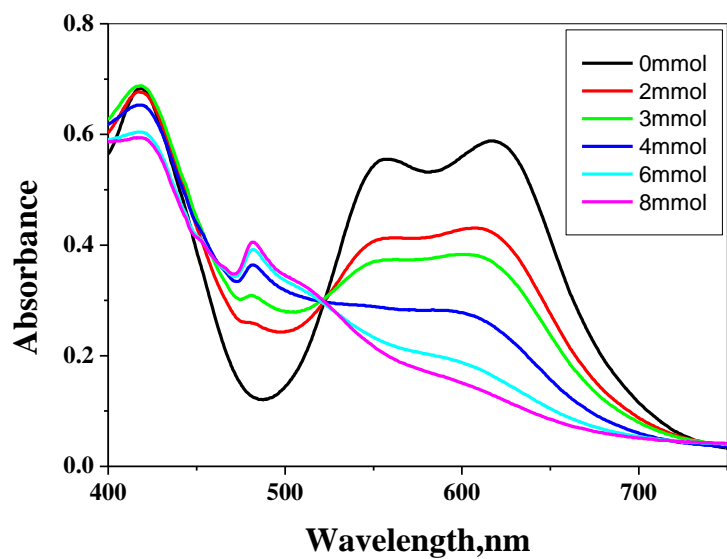
Figure 10.17: UV-Vis spectra of SmI_2 (1 mmol) in presence of increasing amount of diethylene glycol (2, 3, 4, 6, 8 mmol) in THF.
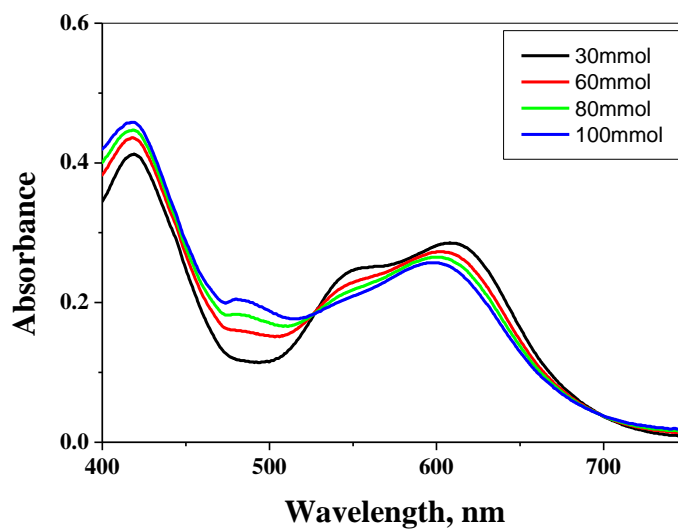
Figure 10.18: UV-Vis spectra of SmI_2 (1 mmol) in presence of increasing amount of diethylene glycol monomethyl ether (30, 60, 80, 100 mmol) in THF.

ITC Data for SmI$_2$-H$_2$O:
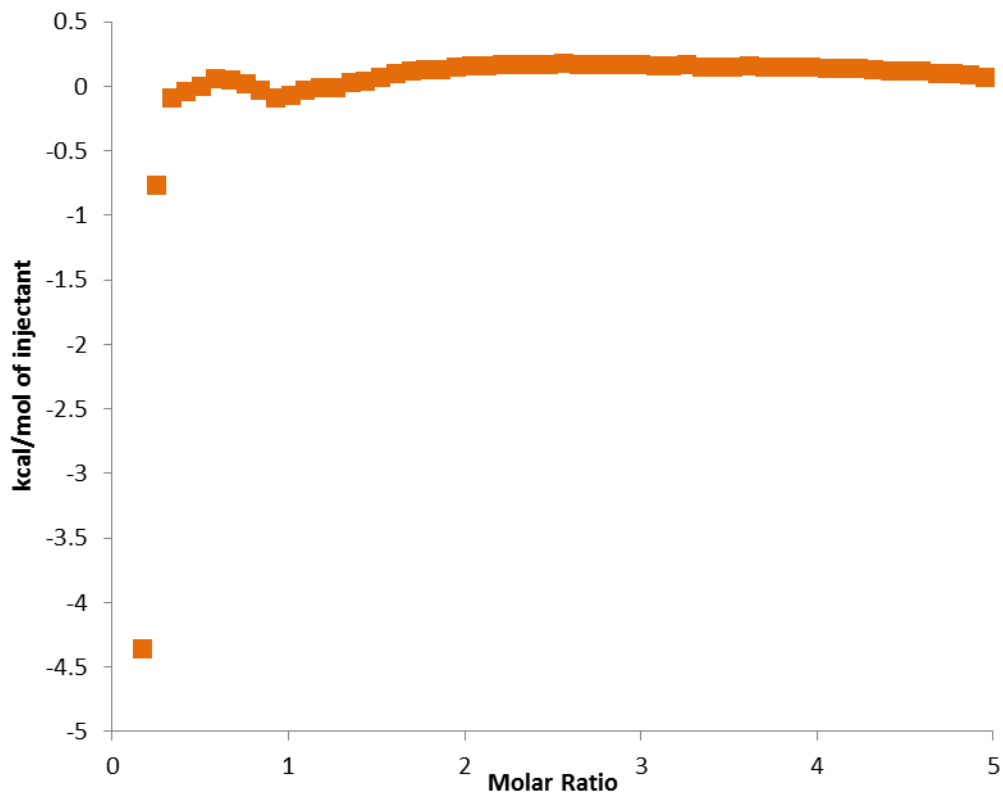
Figure 10.19: Isotherm for titration of 180 mM H$_2$O into 3 mM SmI$_2$ performed under the same parameters as glycol ITC experiments.

Chapter 2 Computational Information:

Gaussian09(1) programs were used for the calculations at DFT(2) level with the unrestricted B3LYP functional(3)and 6-31Gd basis set. Solvation values were calculated using the polarizable conductor calculation model CPCM(4), with tetrahydrofuran as the solvent. The geometries and frequencies were calculated with UB3LYP/6-31G(d) opt=tight.

References

1) Gaussian 09, Revision D.01,

M. J. Frisch, G. W. Trucks, H. B. Schlegel, G. E. Scuseria,

M. A. Robb, J. R. Cheeseman, G. Scalmani, V. Barone, B. Mennucci,

G. A. Petersson, H. Nakatsuji, M. Caricato, X. Li, H. P. Hratchian,

A. F. Izmaylov, J. Bloino, G. Zheng, J. L. Sonnenberg, M. Hada,

M. Ehara, K. Toyota, R. Fukuda, J. Hasegawa, M. Ishida, T. Nakajima,

Y. Honda, O. Kitao, H. Nakai, T. Vreven, J. A. Montgomery, Jr.,

J. E. Peralta, F. Ogliaro, M. Bearpark, J. J. Heyd, E. Brothers,

K. N. Kudin, V. N. Staroverov, T. Keith, R. Kobayashi, J. Normand,

K. Raghavachari, A. Rendell, J. C. Burant, S. S. Iyengar, J. Tomasi,

M. Cossi, N. Rega, J. M. Millam, M. Klene, J. E. Knox, J. B. Cross,

V. Bakken, C. Adamo, J. Jaramillo, R. Gomperts, R. E. Stratmann,

O. Yazyev, A. J. Austin, R. Cammi, C. Pomelli, J. W. Ochterski,

R. L. Martin, K. Morokuma, V. G. Zakrzewski, G. A. Voth,

P. Salvador, J. J. Dannenberg, S. Dapprich, A. D. Daniels,

O. Farkas, J. B. Foresman, J. V. Ortiz, J. Cioslowski,

and D. J. Fox, Gaussian, Inc., Wallingford CT, 2013.

2) R. G. Parr and W. Yang, *Density-functional theory of atoms and molecules* (Oxford Univ. Press, Oxford, 1989).

3) (a)Becke, A. D. *Phys. Rev. A* **1988**, *38*, 3098-3100. (b) Lee, C.; Yang, W.; Parr, R. G. *Phys. Rev. B* **1988**,*37*, 785-789.

4) (a)V. Barone and M. Cossi *J. Phys. Chem. A*, **102** (1998) 1995-2001. (b)M. Cossi, N. Rega, G. Scalmani, and V. Barone
  J. Comp. Chem., **24** (2003) 669-81.

In the table below, E+ZPE, G, & H, energies are in hartree particle. S is in Cal/Mol.

	E+ZPE	G	H	S
Gas Phase Calculations:				
H20	-76.387790	-76.405457	-76.384011	45.137
OH radical	-75.715151	-75.732093	-75.711846	42.613
H atom	-0.500273	-0.510927	-0.497912	27.392
ETHANEDIOL	-230.150601	-230.178265	-230.144265	71.560
ETHANEDIOL radical	-229.502767	-229.530893	-229.496604	72.167
MeOEtOH	-269.432095	-269.462114	-269.424483	79.201
MeOEtO radical	-268.784225	-268.814683	-268.776791	79.751
HOEtOEtOH	-383.919426	-383.953976	-383.909303	94.022
HOEtOEtO radical	-383.271508	-383.306495	-383.261569	94.554
MeOEtOEtOH	-423.201019	-423.237928	-423.189569	101.780
MeOEtOEtO radical	-422.553054	-422.590373	-422.541798	102.234
Anthracene	-539.335972	-539.370053	-539.325605	93.548
Anthracene radical	-539.901391	-539.938920	-539.890346	102.233
Trifluoroethanol	-452.693664	-452.723678	-452.686643	77.947
Trifluoroethanol radical	-452.034730	-452.064740	-452.028332	76.627
CPCM Calculations(solvent=THF):				
H2O	-76.394229	-76.411901	-76.390450	45.147
OH radical	-75.719289	-75.736231	-75.715985	42.613
H atom	-0.500280	-0.510935	-0.497920	27.392
ETHANEDIOL	-230.157976	-230.185708	-230.151601	71.784
ETHANEDIOL radical	-229.508776	-229.537053	-229.502509	72.705
MeOEtOH	-269.437685	-269.467794	-269.430029	79.483
MeOEtO radical	-268.788361	-268.818894	-268.780874	80.021
HOEtOEtOH	-383.928119	-383.962835	-383.917925	94.521
HOEtOEtO radical	-383.278700	-383.313805	-383.268697	94.939
MeOEtOEtOH	-423.207850	-423.244924	-423.196337	102.260
MeOEtOEtO radical	-422.558421	-422.595901	-422.547102	102.706
Anthracene	-539.340097	-539.373538	-539.329726	92.211
Anthracene radical	-539.905431	-539.942791	-539.894392	101.865
Trifluoroethanol	-452.700073	-452.730028	-452.693071	77.784
Trifluoroethanol radical	-452.038238	-452.068252	-452.031826	76.664

	E+ZPE	G	H	S
H20	-76.387790	-76.405457	-76.384011	45.137
OH radical	-75.715151	-75.732093	-75.711846	42.613
H atom	-0.500273	-0.510927	-0.497912	27.392
ETHANEDIOL	-230.150601	-230.178265	-230.144265	71.560
ETHANEDIOL radical	-229.502767	-229.530893	-229.496604	72.167
MeOEtOH	-269.432095	-269.462114	-269.424483	79.201
MeOEtO radical	-268.784225	-268.814683	-268.776791	79.751
HOEtOEtOH	-383.919426	-383.953976	-383.909303	94.022
HOEtOEtO radical	-383.271508	-383.306495	-383.261569	94.554
MeOEtOEtOH	-423.201019	-423.237928	-423.189569	101.780
MeOEtOEtO radical	-422.553054	-422.590373	-422.541798	102.234
Anthracene	-539.335972	-539.370053	-539.325605	93.548
Anthracene radical	-539.901391	-539.938920	-539.890346	102.233
Trifluoroethanol	-452.693664	-452.723678	-452.686643	77.947
Trifluoroethanol radical	-452.034730	-452.064740	-452.028332	76.627

==

CPCM Jobs(solvent=THF)

H2O	-76.394229	-76.411901	-76.390450	45.147
OH radical	-75.719289	-75.736231	-75.715985	42.613
H atom	-0.500280	-0.510935	-0.497920	27.392
ETHANEDIOL	-230.157976	-230.185708	-230.151601	71.784

ETHANEDIOL radical   -229.508776   -229.537053   -229.502509   72.705

MeOEtOH   -269.437685   -269.467794   -269.430029   79.483

MeOEtO radical   -268.788361   -268.818894   -268.780874   80.021

HOEtOEtOH   -383.928119   -383.962835   -383.917925   94.521

HOEtOEtO radical   -383.278700   -383.313805   -383.268697   94.939

MeOEtOEtOH   -423.207850   -423.244924   -423.196337   102.260

MeOEtOEtO radical   -422.558421   -422.595901   -422.547102   102.706

Anthracene   -539.340097   -539.373538   -539.329726   92.211

Anthracene radical   -539.905431   -539.942791   -539.894392   101.865

Trifluoroethanol   -452.700073   -452.730028   -452.693071   77.784

Trifluoroethanol radical   -452.038238   -452.068252   -452.031826   76.664

==

OH_radical + H_atom --->   H2O

ΔH = -75.711846 -0.497912   -(-76.384011)= 0.174253   627.50 x 0.174253 = 109.3 kcal/mol

ΔG = -75.732093 -0.510927   -(-76.405457) = 0.162437   627.50 x 0.162437= 101.9 kcal/mol

OH_radical + H_atom --->   H2O   (cpcm,solvent=thf)
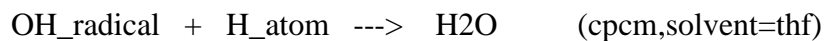
ΔH = -75.715985 -0.497920   -(-76.390450)   = 0.176545   627.50 x 0.176545
= 110.8 kcal/mol

ΔG = -75.736231 -0.510935   -(-76.411901)   = 0.164735   627.50 x 0.164735
= 103.4 kcal/mol

==

10.3 Proton-Coupled Electron-Transfer in the Reduction of Carbonyls by SmI$_2$-H$_2$O
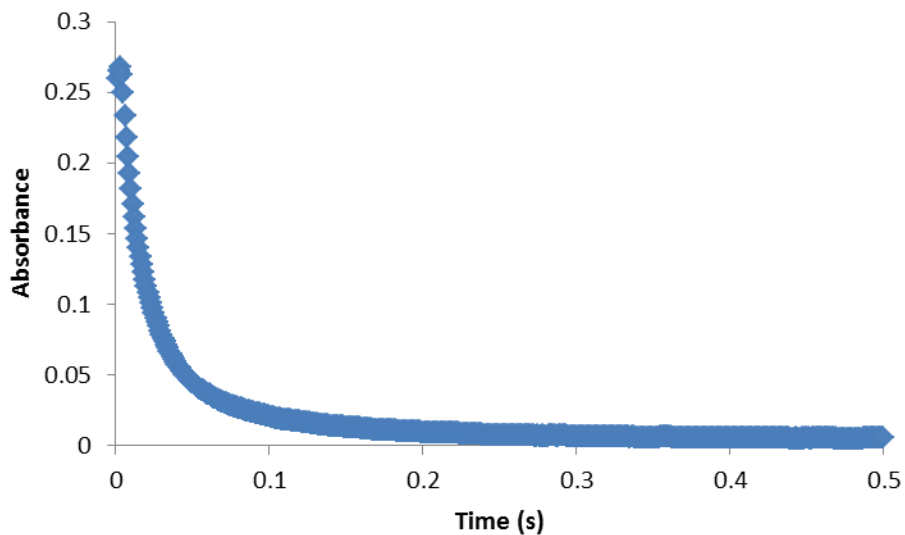
Figure 10.20. Sample decay of Sm(II) at 560 nm, 25 $^{\circ}$C, with 100 mM Heptaldehyde, 1 M H$_2$O and 10 mM SmI$_2$.
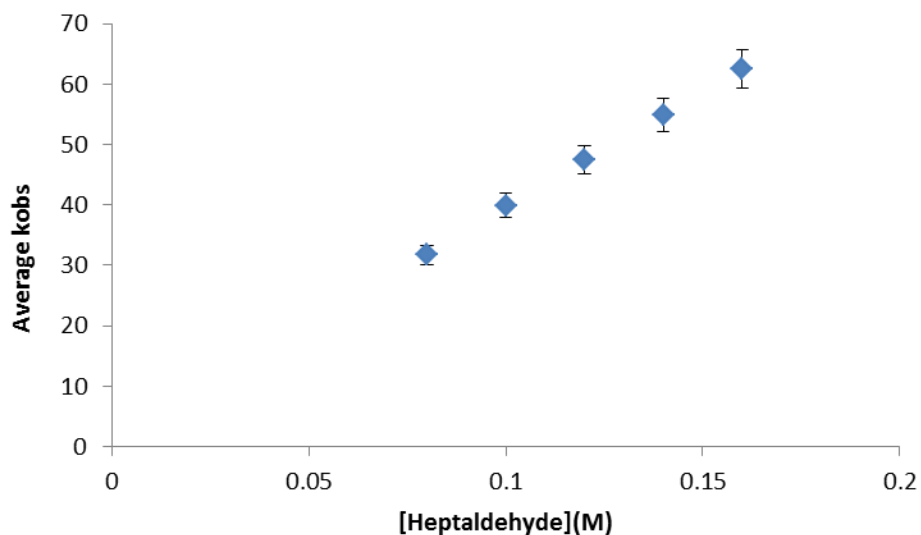
Figure 10.21. Rates for the reduction of heptaldehyde with increasing concentration of heptaldehyde. For the order of heptaldehyde, substrate concentration was varied from 80 mM to 160 mM. Substrate was combined with 10 mM SmI_2 and 100 eq H_2O in the stopped-flow and the decay of Sm(II) was observed. The experiment was repeated three times on different dates.
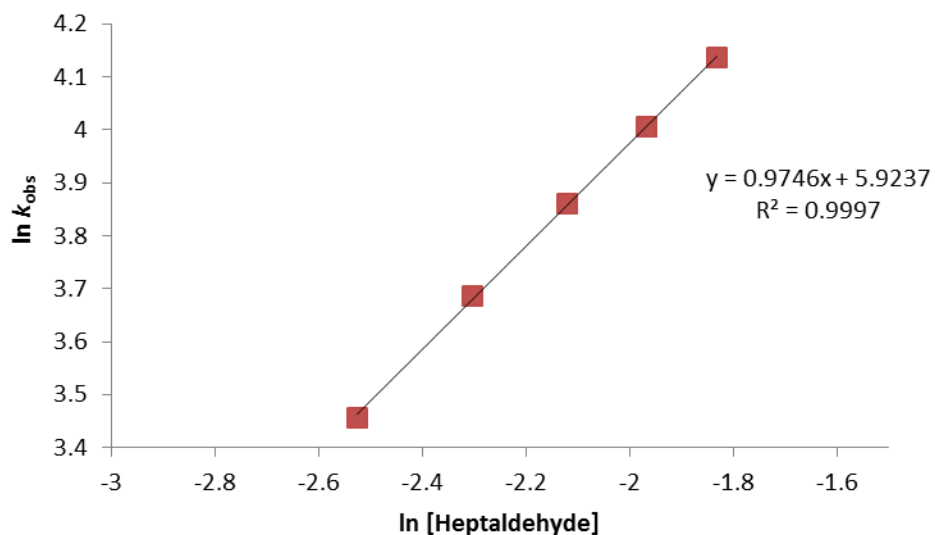
Figure 10.22. Linear rate dependence for the reduction of heptaldehyde with increasing concentration of heptaldehyde.
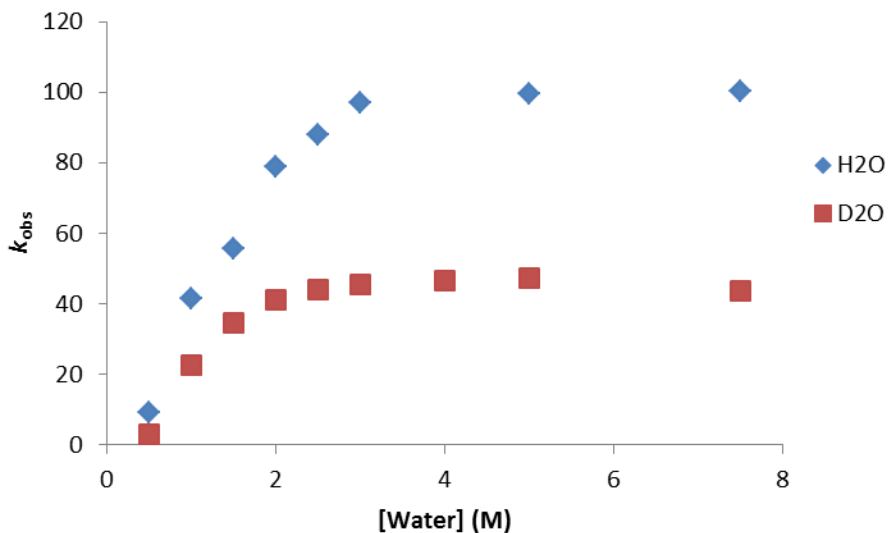
Figure 10.23. Rates of reduction of heptaldehyde with increasing concentrations of H_2O and D_2O. For KIE studies, the concentration of heptaldehyde was kept constant at 100 mM and was combined with 10 mM SmI_2. The concentration of D_2O was varied from 50 equivalents to 750 equivalents (0.5-7.5 M).

Table 10.5 Order of SmI_2 using Fractional Times Method for heptaldehyde.

Date	Trial	A_0	$A_{1/2}$	$A_{3/4}$	$t_{1/2}$	$t_{3/4}$	$(t_{3/4}-t_{1/2})/t_{1/2}$
01-14-16	100A	0.28322	0.14161	0.071	0.022	0.043	0.95
01-19-16	100A	0.291892	0.145946	0.072973	0.016	0.038	1.38
01-19-16	125A	0.250474	0.125237	0.0626185	0.014	0.032	1.29
						Average:	1.2
						Order:	**1**
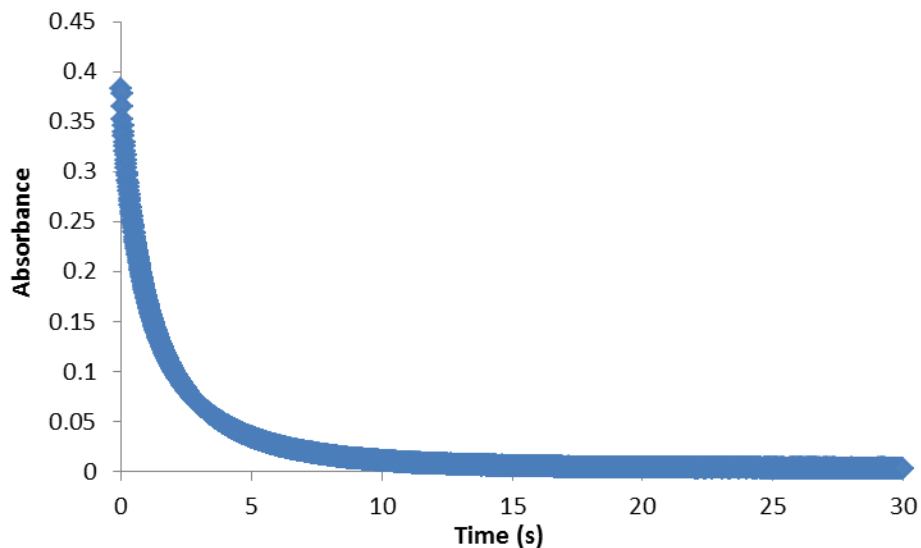
Figure 10.24. Sample decay for 1 M H_2O, 100 mM Cyclohexanone, 10 mM SmI_2, measured at 25 ^{o}C, 560 nm.

Figure 10.25. Linear rate dependence on cyclohexanone with increasing concentrations of cyclohexanone. For the order of cyclohexanone, substrate concentration was varied from 100 mM to 500 mM. Substrate was combined with 10 mM SmI_2 and 100 eq H_2O in the stopped-flow and the decay of Sm(II) was observed at 560nm and 25 ± 0.5 ^{o}C. The experiment was repeated three times.

245
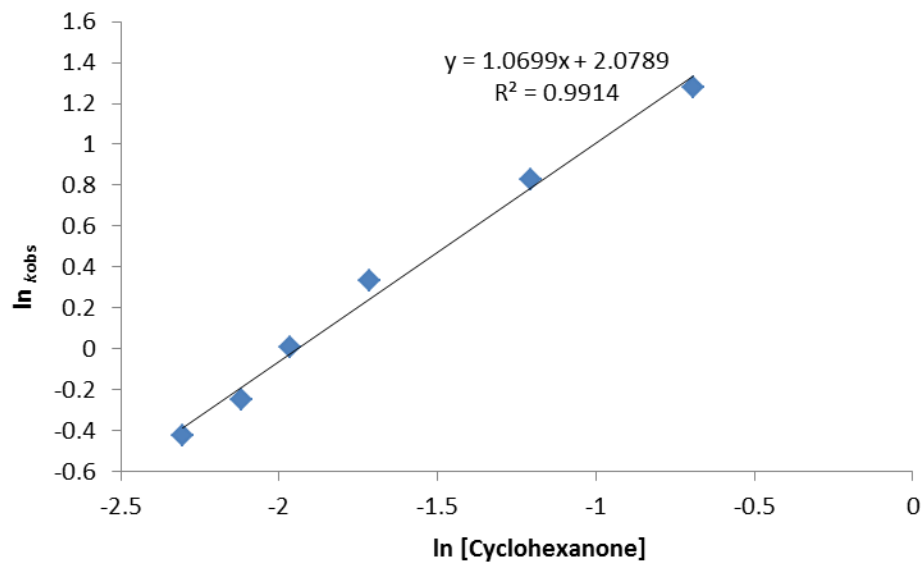
Figure 10.26. Linear rate dependence on cyclohexanone with increasing concentrations of cyclohexanone.

Table 10.6. Order of SmI_2 in the reduction of cyclohexanone by fractional times method.

Date	File	A_0	$A_{1/2}$	$A_{3/4}$	$t_{1/2}$	$t_{3/4}$	$(t_{3/4}-t_{1/2})/t_{1/2}$
10-26-15	100A	0.32791	0.1639	0.081978	1.75	3.75	1.14
11-06-15	150A	0.32142	0.160	0.0804	0.7	1.4	1
11-06-15	250A	0.28882	0.1444	0.072205	0.5	1	1
						Average:	1.05
						Order:	**1**

246
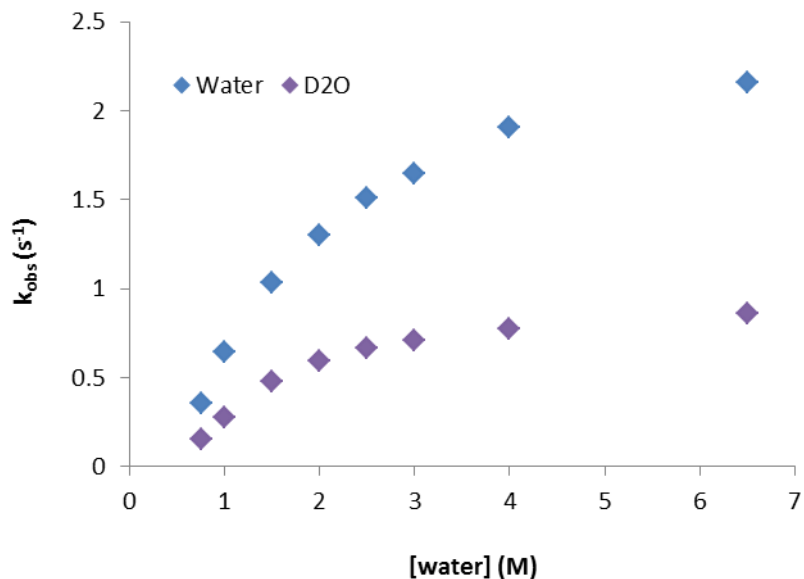
Figure 10.27. Rates of reduction of cyclohexanone with increasing concentrations of H_2O and D_2O.
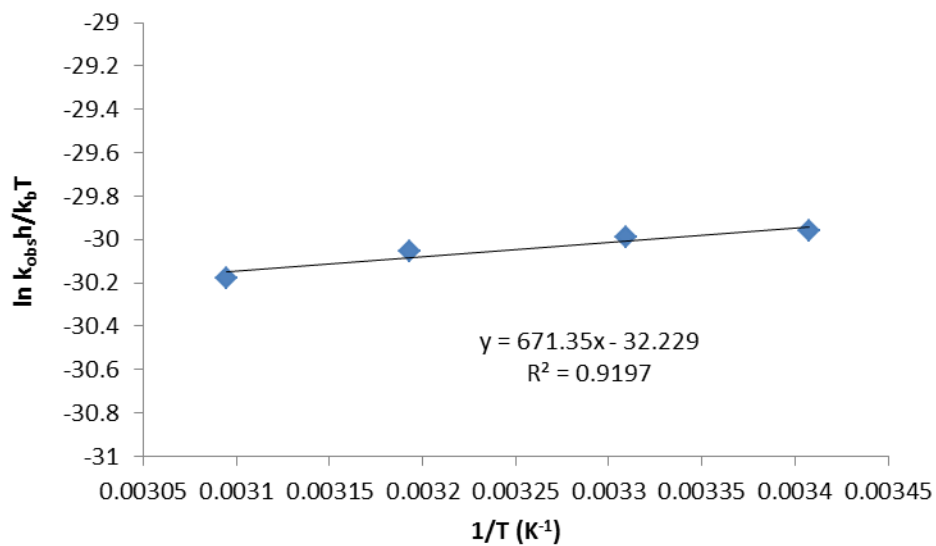
Figure 10.28. Sample eyring plot for the reduction of 100 mM cyclohexanone with 1 M H_2O and 10 mM SmI_2 from 20-50 ^{o}C. This experiment was performed three times and the reported activation parameters are an average of the values obtained.
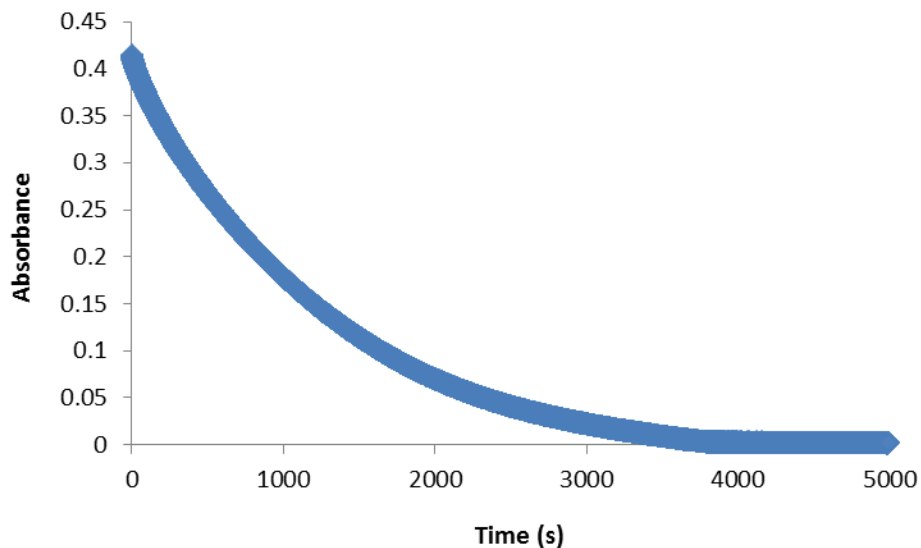
Figure 10.29. Sample decay for 1 M H_2O, 500 mM 5-decanolide, 10 mM SmI_2, measured at 25 C, 560 nm.
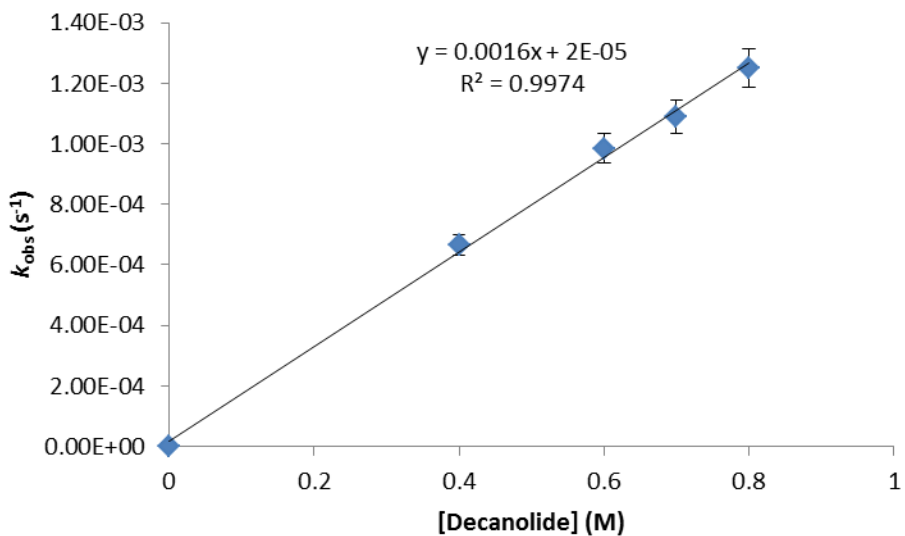
Figure 10.30. Linear rate dependence on 5-decanolide with increasing concentrations of 5-decanolide. For the order of 5-decanolide, substrate concentration was varied from 100 mM to 300 mM. Substrate was combined with 10 mM SmI_2 and 100 eq H_2O in the stopped-flow and the decay of Sm(II) was observed at 560nm and 25 ± 0.5 $^{\circ}$C. The experiment was repeated three times.

248
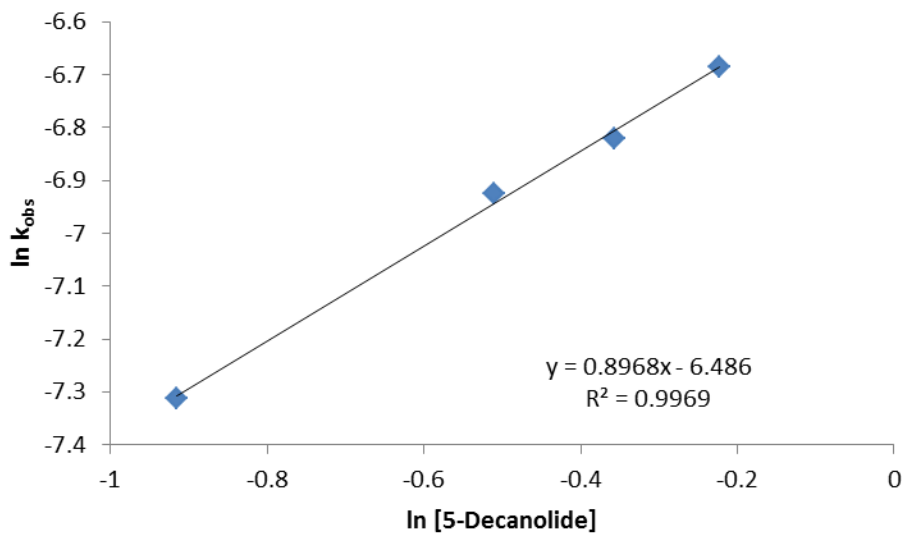
Figure 10.31 Linear rate dependence on 5-decanolide with increasing concentrations of 5-decanolide.

Table 10.7. Order of SmI_2 in the reduction of 5-decanolide by fractional times method.

Date	File	A_0	$A_{1/2}$	$A_{3/4}$	$t_{1/2}$	$t_{3/4}$	$(t_{3/4}-t_{1/2})/t_{1/2}$
09-08-15	100A	0.444386	0.22219	0.11109	665	1343	1.02
09-09-15	150A	0.410207	0.20510	0.10255	492	1006	1.05
09-15-15	200A	0.335609	0.16780	0.083902	528	1063	1.01
						Average:	1.03
						Order:	1
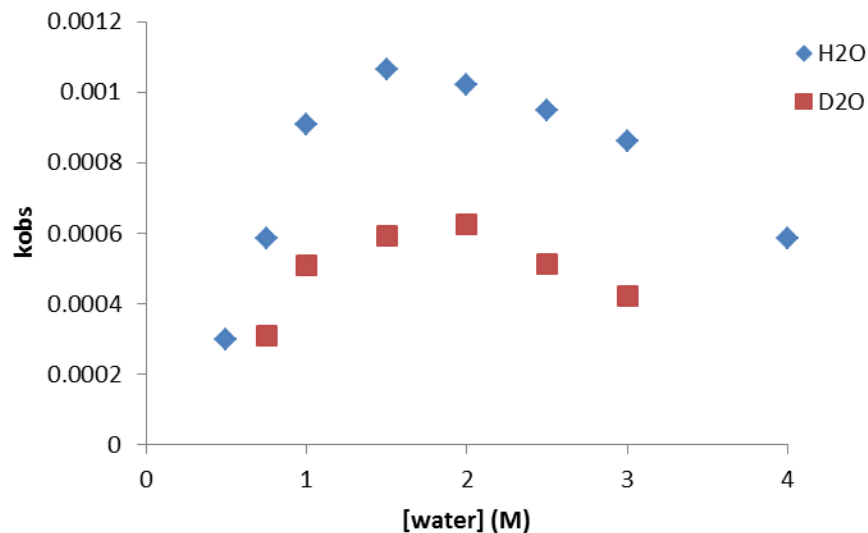
Figure 10.32. Rates of reduction of 5-decanolide with increasing concentrations of H_2O and D_2O. The kinetic isotope study was performed using equimolar quantities of degassed H_2O and D_2O where the water concentration was varied from $0.75 - 3$ M and the concentration of 5-decanolide was maintained at 500 mM and SmI_2 was maintained at 10 mM.
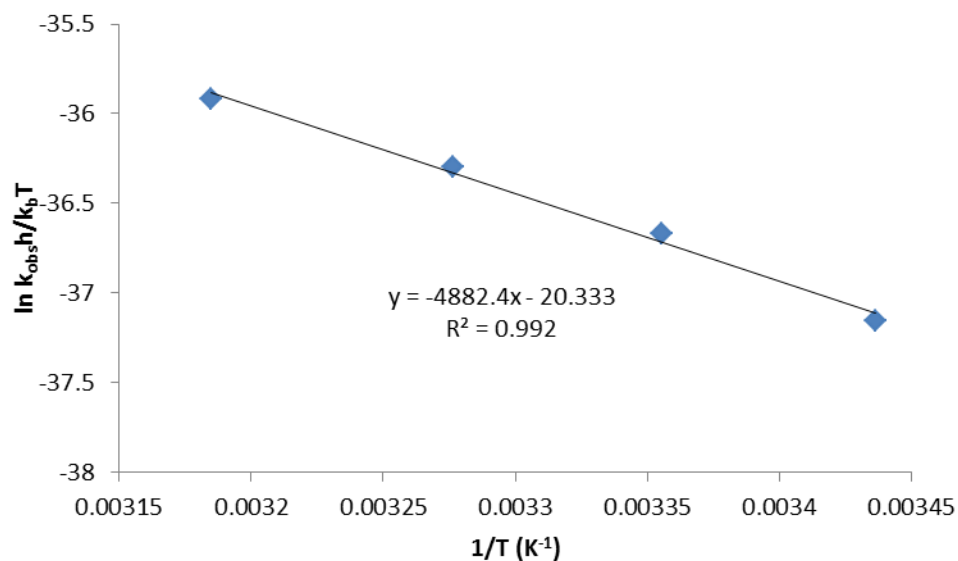
Figure 10.33. Sample eyring plot for the reduction of 500 mM 5-decanolide with 1 M H_2O and 10 mM SmI_2 from 20-50 ^oC. This experiment was performed three times and the reported activation parameters are an average of the values obtained.

0.878

1.291
1.549

3.631

ppm
0.5
1.0
1.5
2.0
2.5
3.0
3.5
4.0
4.5
5.0
5.5
6.0
6.5
7.0
7.5
8.0
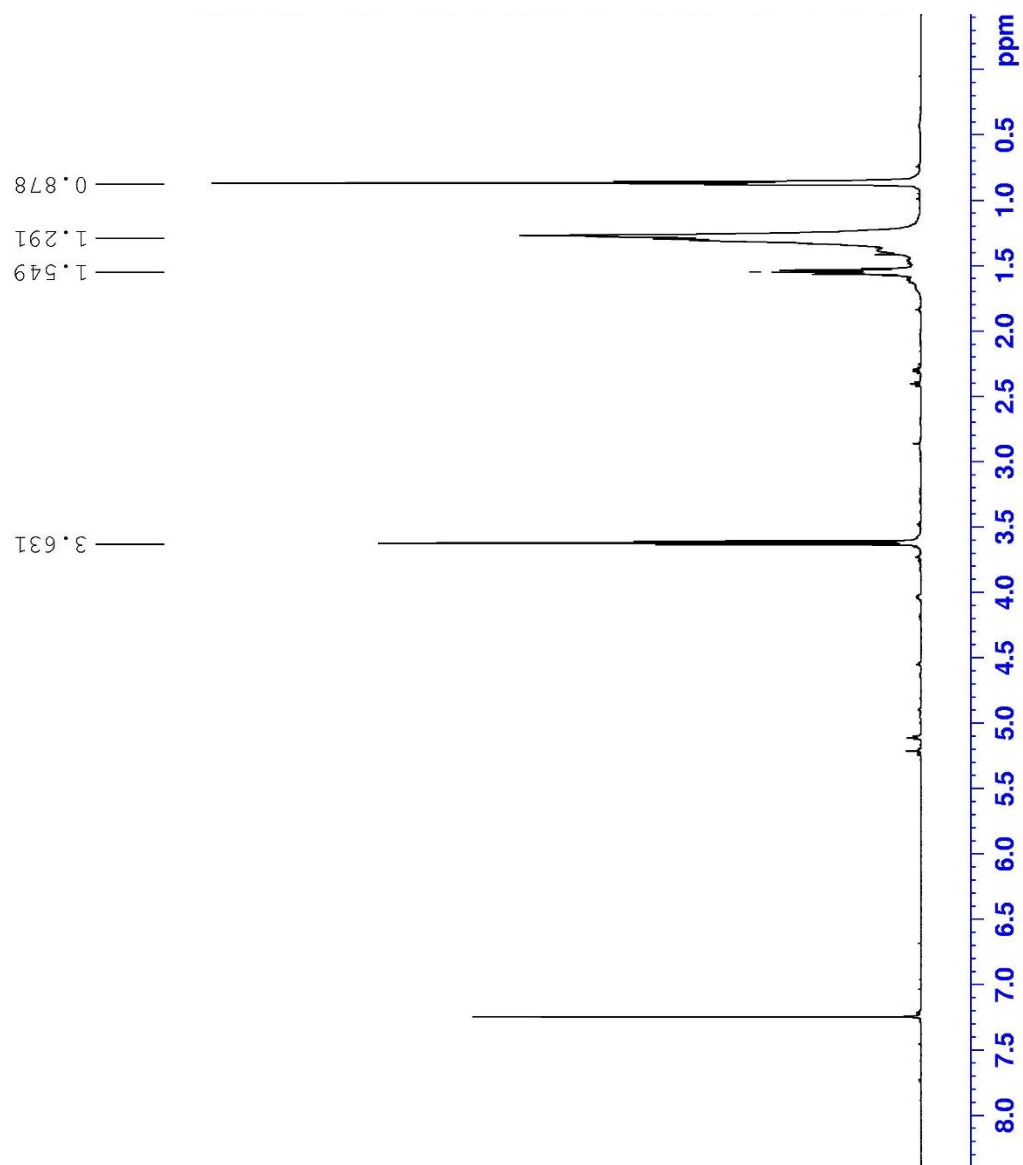
Figure 10.34 ^{1}H Spectrum of 1-heptanol.
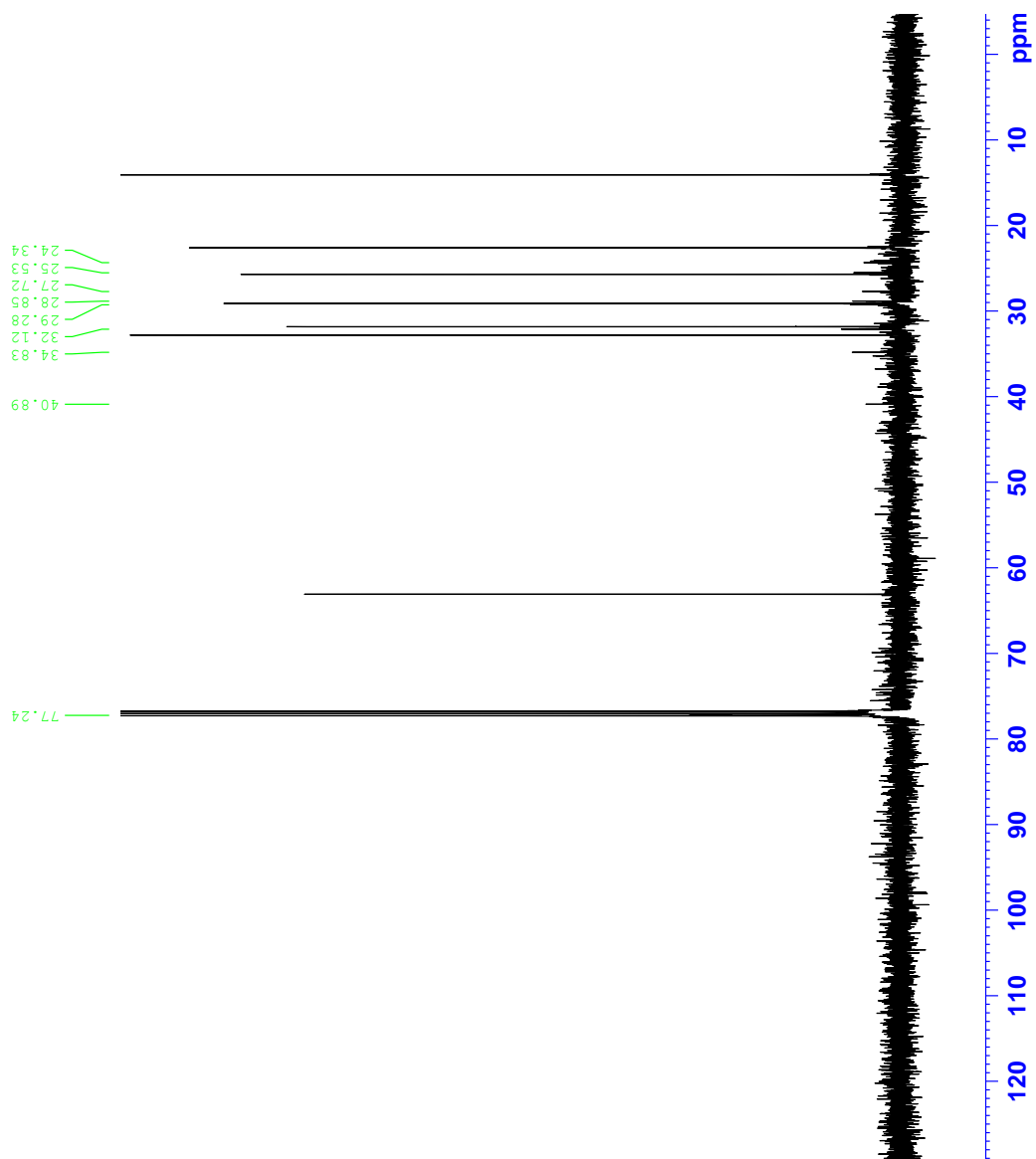
Figure 10.35 ^{13}C Spectrum of 1-heptanol.

24.34
25.53
27.72
28.85
29.28
32.12
34.83
40.89
77.24

1.121
1.241
1.517
1.690
1.879

3.586
3.724
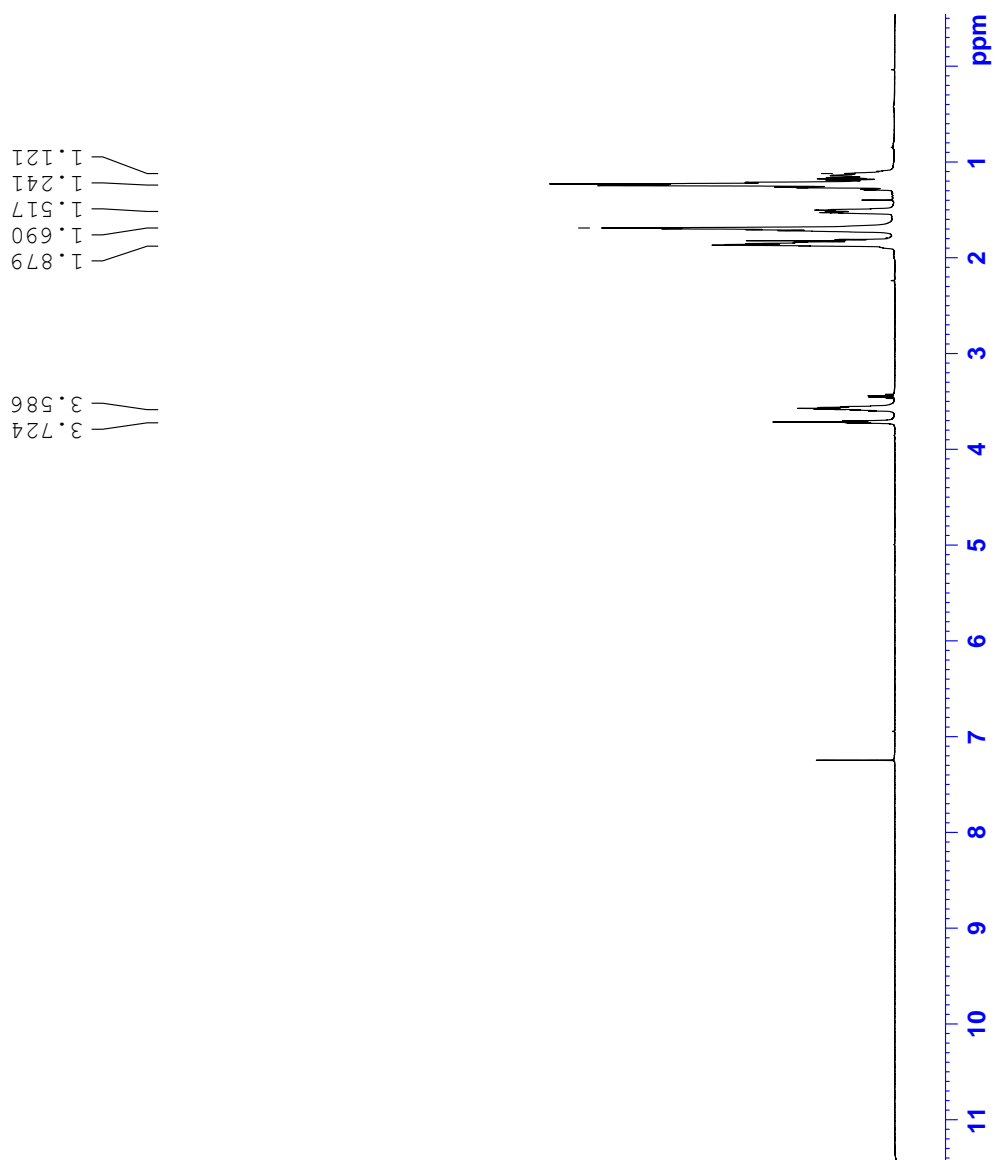
Figure 10.36 [1]H Spectrum of cyclohexanol.
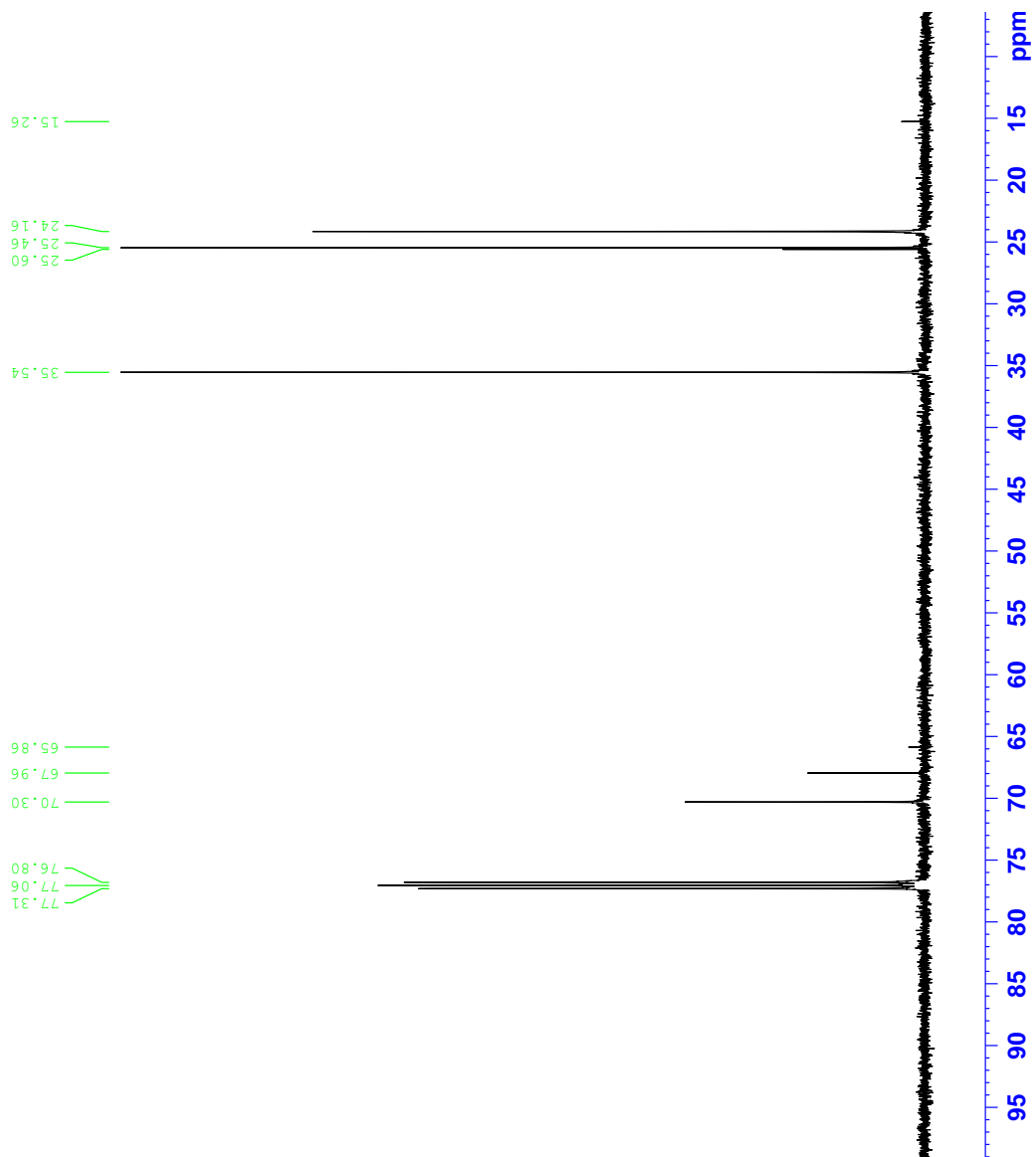
Figure 10.37 ^{13}C Spectrum of cyclohexanol.

254

0.896

1.310
1.448
1.552

2.310

3.655

100equiv H2O

ppm

3.00

13.66

1.85

2.86
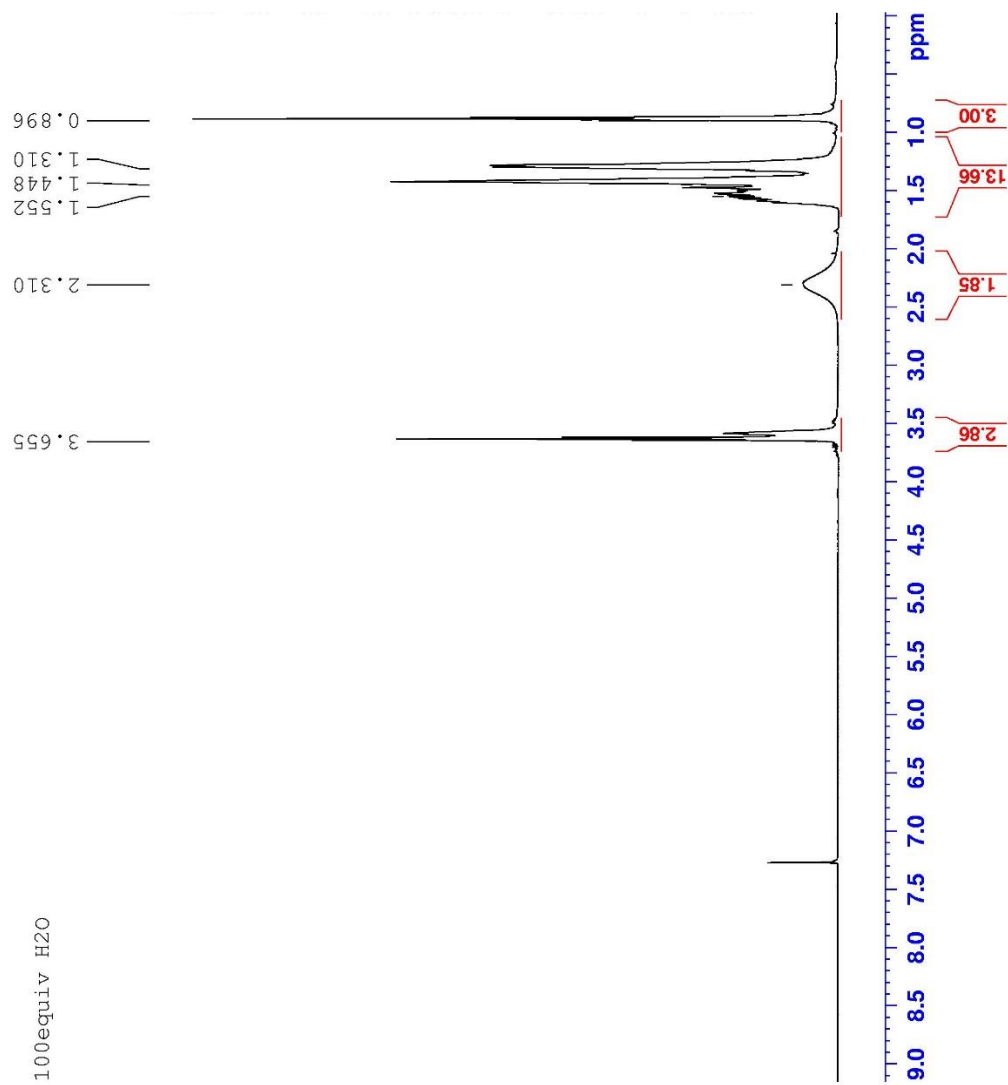
Figure 10.38 [1]H Spectrum of 1,5-decanediol.
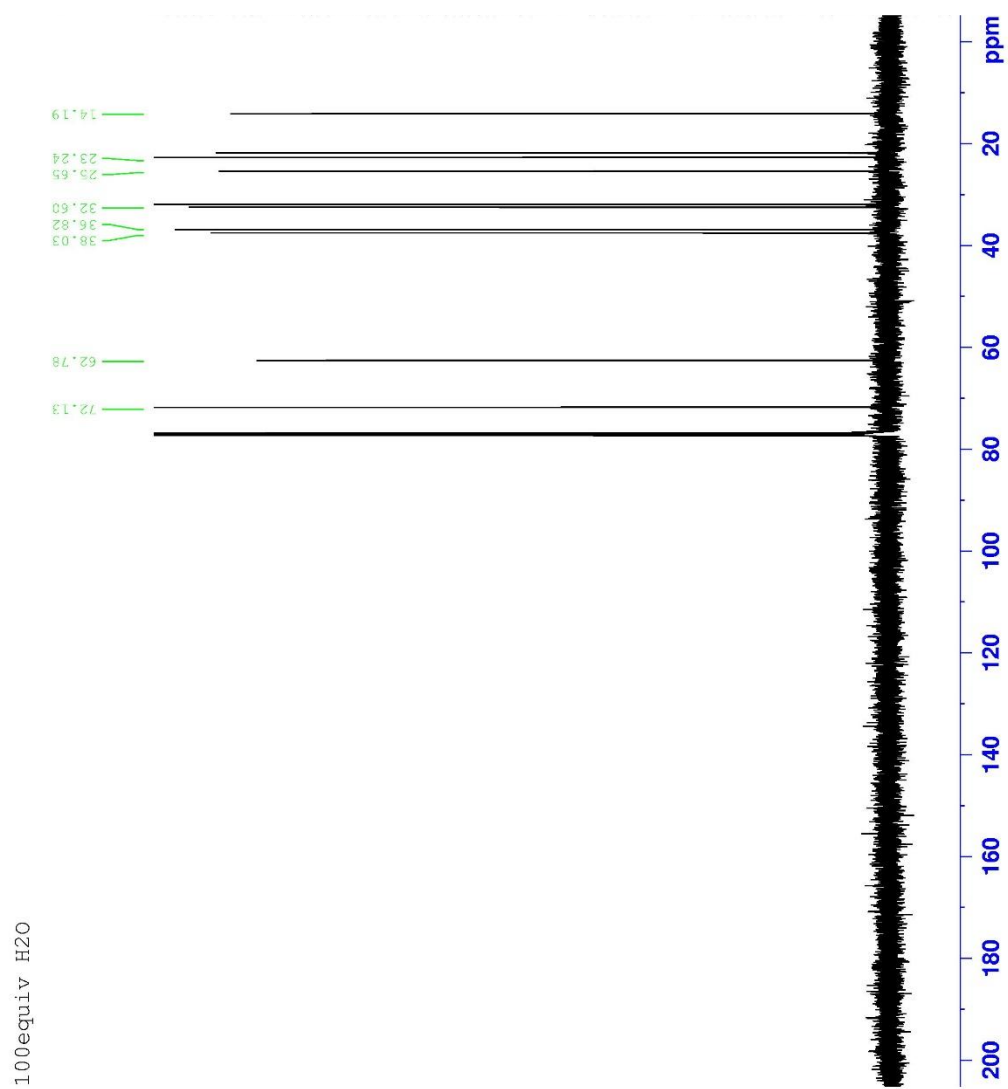
Figure 10.39 ^{13}C Spectrum of 1,5-decanediol.

1.119
1.359
1.617
1.704
1.790

SmI2-cyclohexanone-4 days

2.02
4.07
16.00

ppm
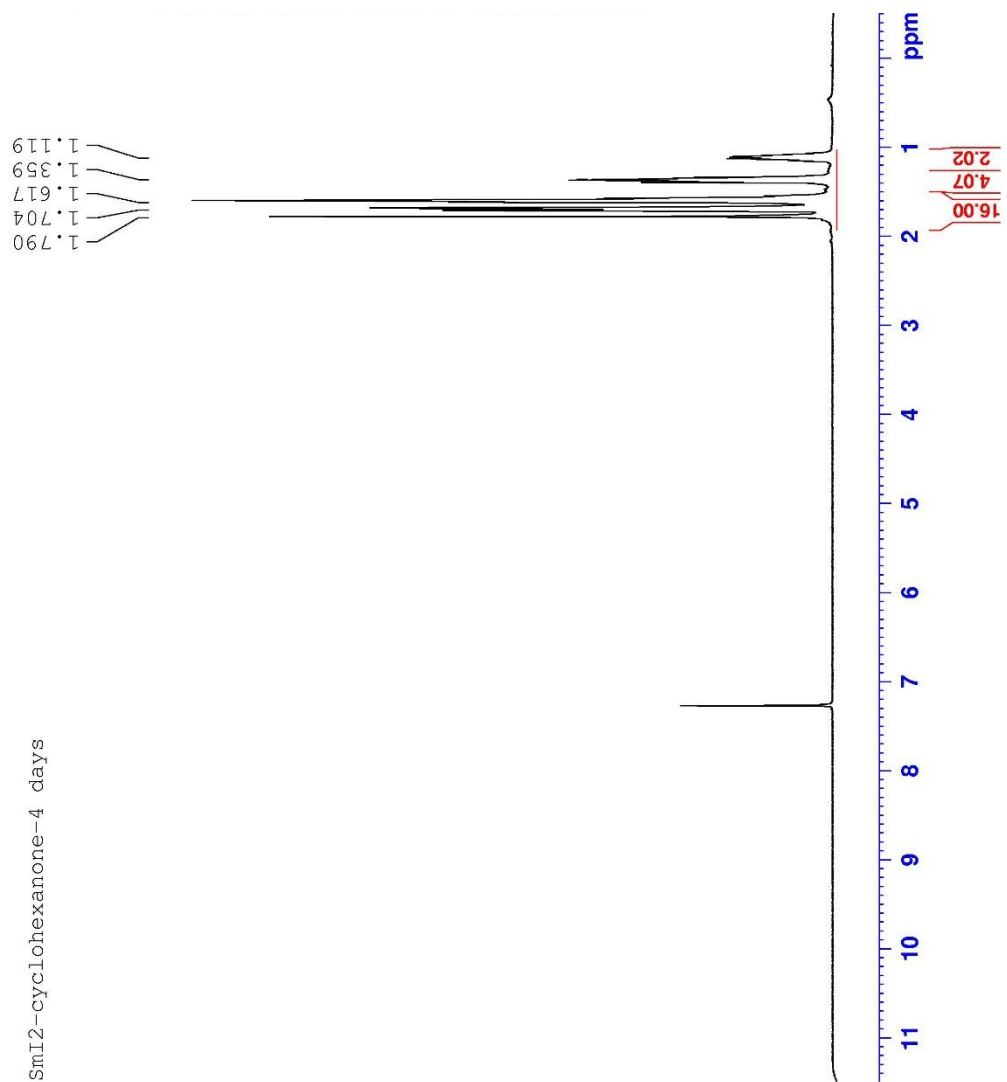
Figure 10.40 [1]H Spectrum of 1,1'-Dicyclohexanol.

257
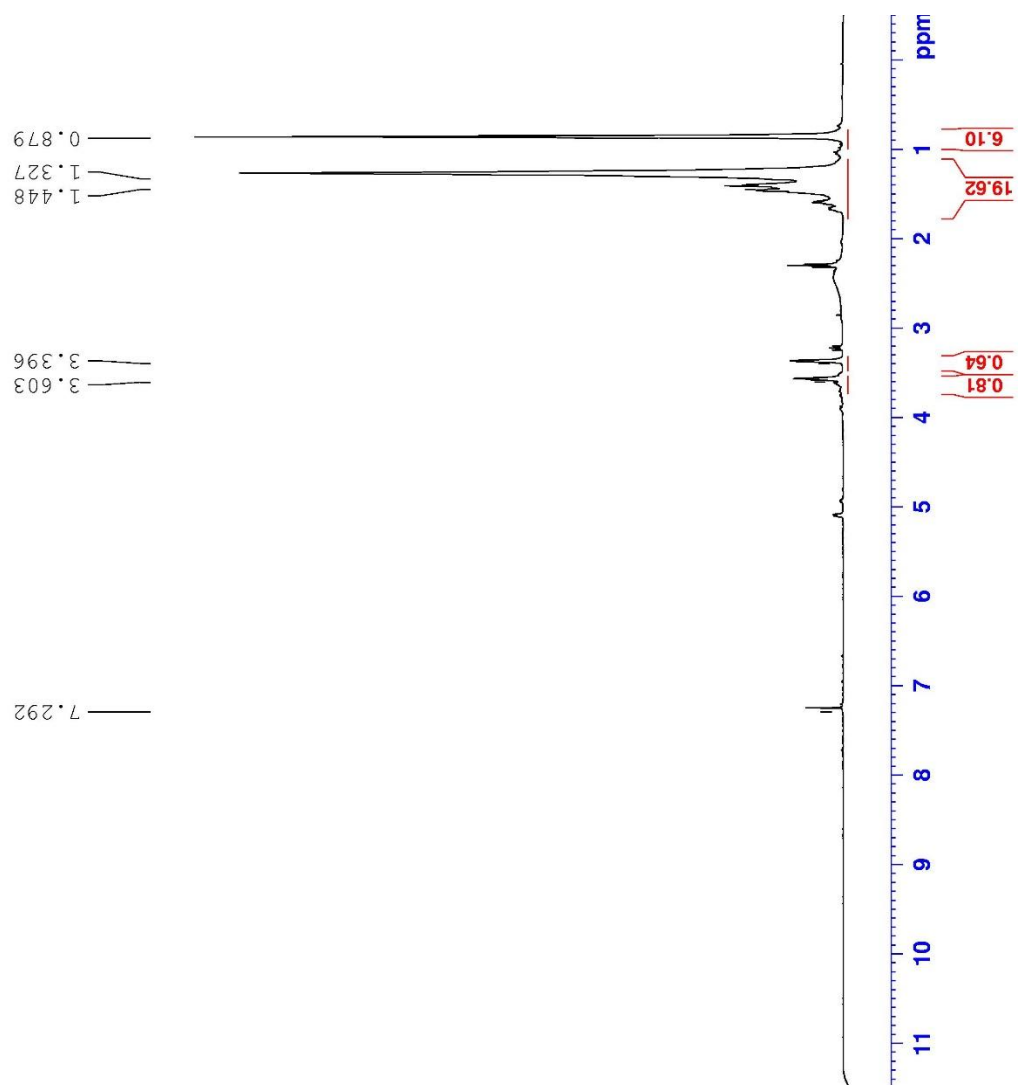
Figure 10.41 ^{1}H Spectrum of 7,8-Tetradecanediol.

258

Computational Methods

Gaussian09(1) programs were used for the calculations with the APF-D(2) hybrid DFT(3) method and the 6-311+g(2d,p) basis set(4,5). Solvation values were calculated using the polarizable continuum model with integral equation formalism. IEFPCM(6,7), with tetrahydrofuran as the solvent. The geometries and frequencies were calculated with uapfd/6-311+g(2d,p) opt=(calcfc,tight) int=(ultrafine,acc2e=12)pop=npa. scrf=(iefpcm,solvent=thf) was added to the route section for solvation. Natural-population analysis(8) was obtained by including pop=npa.

1) Gaussian 09, Revision D.01,
 M. J. Frisch, G. W. Trucks, H. B. Schlegel, G. E. Scuseria,
 M. A. Robb, J. R. Cheeseman, G. Scalmani, V. Barone, B. Mennucci,
 G. A. Petersson, H. Nakatsuji, M. Caricato, X. Li, H. P. Hratchian,
 A. F. Izmaylov, J. Bloino, G. Zheng, J. L. Sonnenberg, M. Hada,
 M. Ehara, K. Toyota, R. Fukuda, J. Hasegawa, M. Ishida, T. Nakajima,
 Y. Honda, O. Kitao, H. Nakai, T. Vreven, J. A. Montgomery, Jr.,
 J. E. Peralta, F. Ogliaro, M. Bearpark, J. J. Heyd, E. Brothers,
 K. N. Kudin, V. N. Staroverov, T. Keith, R. Kobayashi, J. Normand,
 K. Raghavachari, A. Rendell, J. C. Burant, S. S. Iyengar, J. Tomasi,
 M. Cossi, N. Rega, J. M. Millam, M. Klene, J. E. Knox, J. B. Cross,
 V. Bakken, C. Adamo, J. Jaramillo, R. Gomperts, R. E. Stratmann,
 O. Yazyev, A. J. Austin, R. Cammi, C. Pomelli, J. W. Ochterski,
 R. L. Martin, K. Morokuma, V. G. Zakrzewski, G. A. Voth,
 P. Salvador, J. J. Dannenberg, S. Dapprich, A. D. Daniels,
 O. Farkas, J. B. Foresman, J. V. Ortiz, J. Cioslowski,
 and D. J. Fox, Gaussian, Inc., Wallingford CT, 2013

2)A. Austin, G. Petersson, M. J. Frisch, F. J. Dobek, G. Scalmani, and K. Throssell, "A density functional with spherical atom dispersion terms", *J. Chem. Theory and Comput*. **8** (2012) 4989.

3) R. G. Parr and W. Yang, *Density-functional theory of atoms and molecules* (Oxford Univ. Press, Oxford, 1989).

4)A. D. McLean and G. S. Chandler, "Contracted Gaussian-basis sets for molecular calculations. 1. 2nd row atoms, Z=11-18," *J. Chem. Phys.*, **72** (1980) 5639-48

5)K. Raghavachari, J. S. Binkley, R. Seeger, and J. A. Pople, "Self-Consistent Molecular Orbital Methods. 20. Basis set for correlated wave-functions," J. Chem. Phys., 72 (1980) 650-54.

6)E. Cancès, B. Mennucci, and J. Tomasi, "A new integral equation formalism for the polarizable continuum model: Theoretical background and applications to isotropic and anistropic dielectrics," *J. Chem. Phys.*, **107** (1997) 3032-41.

7)J. Tomasi, B. Mennucci, and R. Cammi, "Quantum mechanical continuum solvation models," *Chem. Rev.*, **105** (2005) 2999-3093.

8)A. E. Reed, R. B. Weinstock, and F. Weinhold, "Natural-population analysis," *J. Chem. Phys.*, **83** (1985) 735-46.

Table 10.8 Natural Population Analysis (NPA) Summary

Heptaldehyde			Cyclohexanone			d-Valerolactone		
Gas			**Gas**			**Gas**		
	C=O	-0.533		C=O	-0.560		C=O	-0.582
							C-O-	-0.563
	C-O⁻	-0.740		C-O⁻	-0.711		C-O⁻	-0.658
							C-O-	-0.590
	Δ C=O→ C-O⁻	-0.207		Δ C=O→ C-O⁻	-0.151		Δ C=O→ C-O⁻	-0.076
							Δ C-O-→ C-O⁻	-0.027
iefpcm			**iefpcm**			**iefpcm**		
	C=O	-0.580		C=O	-0.610		C=O	-0.642
							C-O-	-0.567
	C-O⁻	-0.895		C-O⁻	-0.899		C-O⁻	-0.871
							C-O-	-0.675
	Δ C=O→ C-O⁻	-0.315		Δ C=O→ C-O⁻	-0.289		Δ C=O→ C-O⁻	-0.229
							Δ C-O-→ C-O⁻	-0.108

10.4. The Reversibility of Ketone Reduction by SmI$_2$-H$_2$O
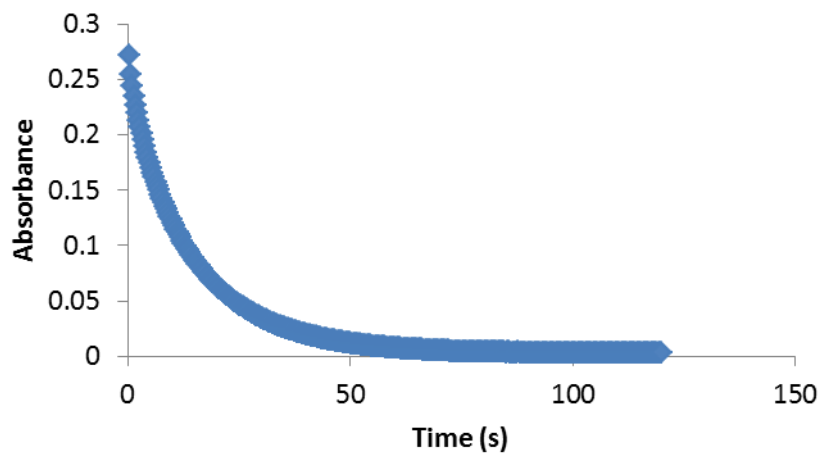
Figure 10.42. Sample decay for the loss of 10 mM Sm(II) with 100 mM 2-but-3-enyl-cyclohexan-1-one and 1 M H$_2$O.
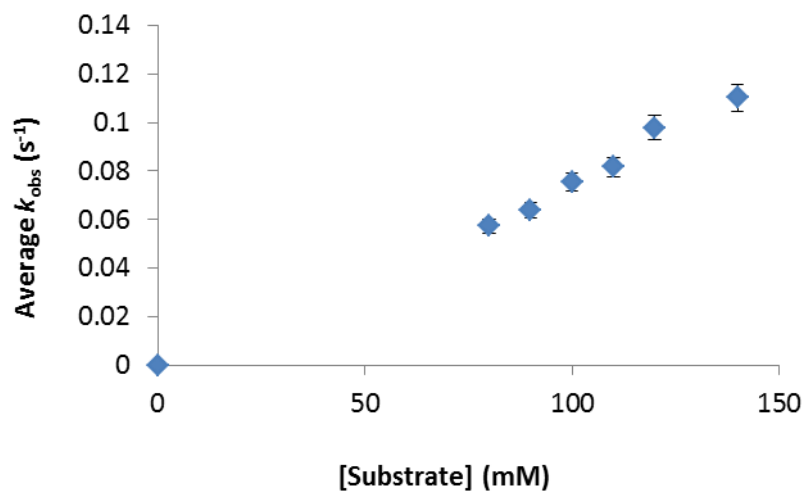
Figure 10.43. Rates for the reduction/cyclization of 2-But-3-enyl-cyclohexan-1-one with increasing concentration of substrate.
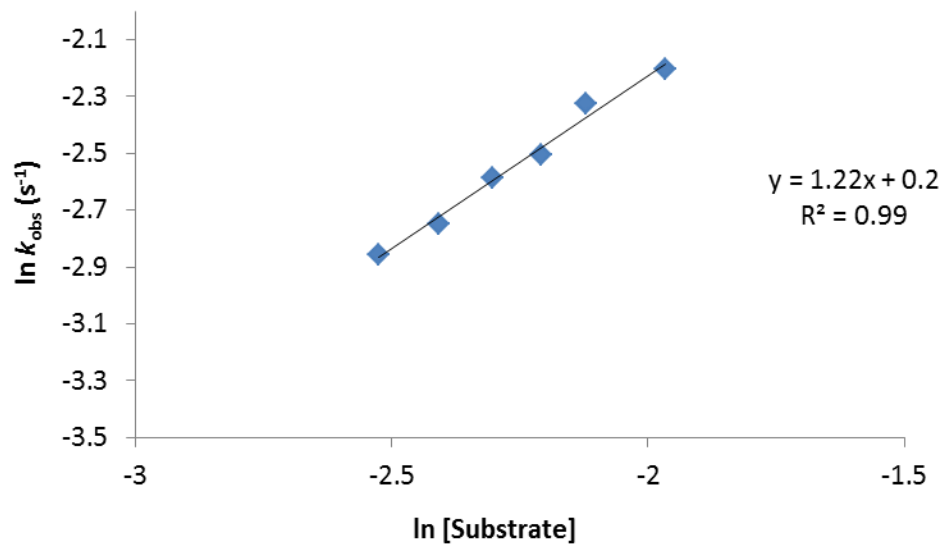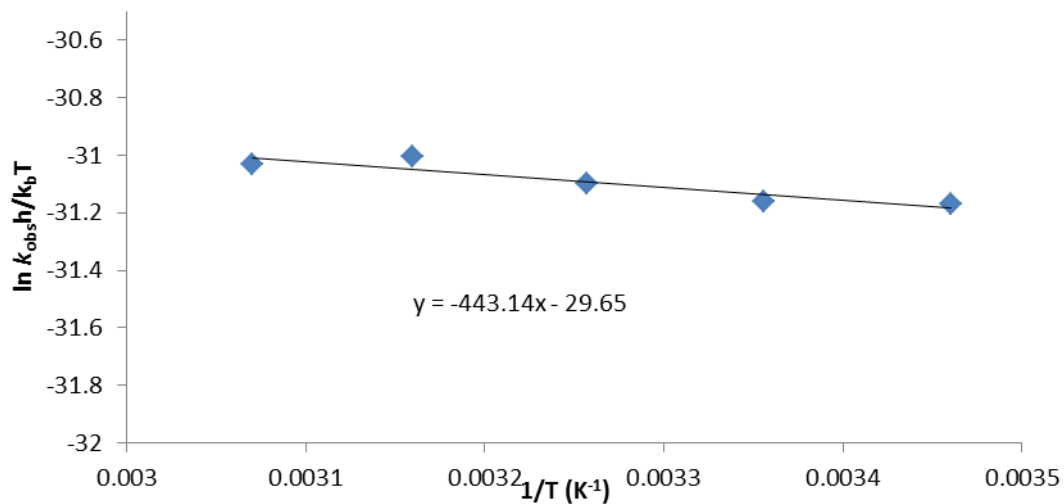
Figure 10.44. First-order rate dependence for the reduction/cyclization of 2-But-3-enyl-cyclohexan-1-one with increasing concentrations of substrate.

Table 10.9. Order of SmI_2 in the reduction of 2-But-3-enyl-cyclohexan-1-one by fractional times method applied to determine the order of SmI_2 over more than one day and at different water concentrations with a constant concentration of 100 mM 2-But-3-enyl-cyclohexan-1-one and 10 mM SmI_2.

Date	Trial	A_0	$A_{1/2}$	$A_{3/4}$	$t_{1/2}$	$t_{3/4}$	$(t_{3/4}-t_{1/2})/t_{1/2}$
04-01-16	300A-W	0.219789	0.109894	0.0549472	2.4	5.3	1.21
04-04-16	300A-W	0.237738	0.118869	0.0594345	2.58	5.22	1.02
04-05-16	300A-W	0.233441	0.11672	0.0583602	2.6	5.4	1.08
						Average:	1.10
						Order:	1
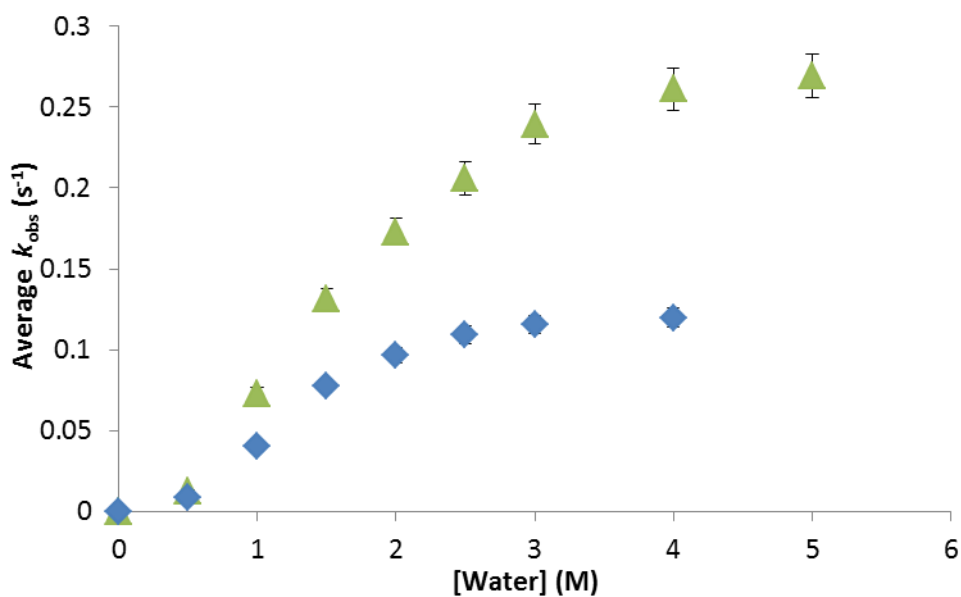
Figure 10.45. Rates of reduction of 2-But-3-enyl-cyclohexan-1-one with increasing concentrations of H_2O (▲) and D_2O (◆).

For KIE studies, the concentration of 2-But-3-enyl-cyclohexan-1-one was kept constant at 100 mM and was combined with 10 mM SmI_2 in the reaction cell. The concentration of D_2O was varied from 50 equivalents to 400 equivalents (0.5-4 M). The kinetic isotope at the concentrations of interest (1M H_2O, 100 mM substrate, 10 mM SmI_2) is 1.7 ± 0.1.
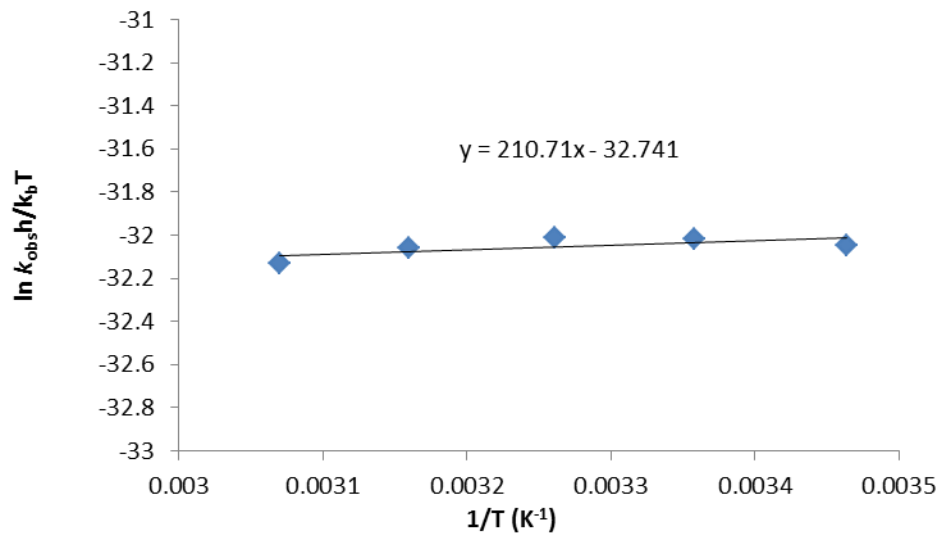
Figure 10.46. Sample Eyring plot for the reduction of 100 mM 2-But-3-enyl-cyclohexan-1-one with 1 M H_2O and 10 mM SmI_2 from 20-50 $^{\circ}$C. This experiment was performed three times and the reported activation parameters are an average of the values obtained.
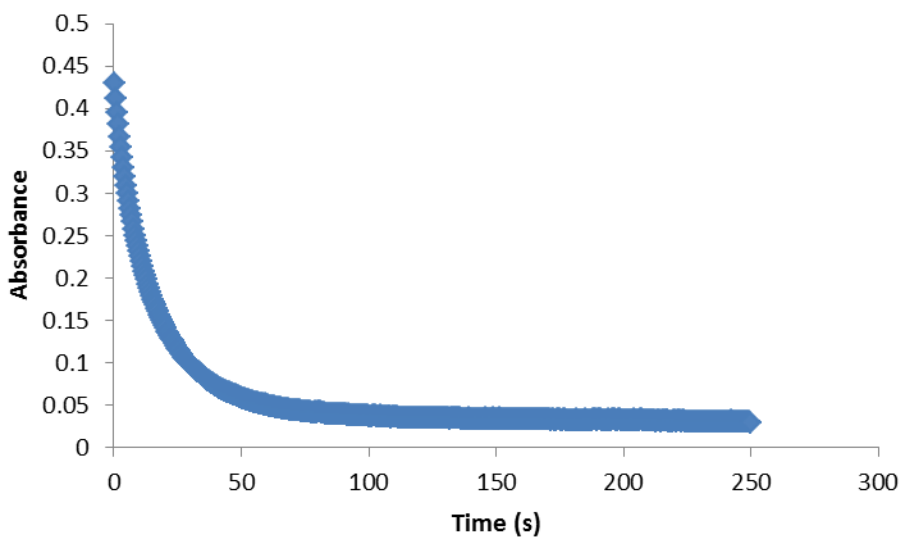
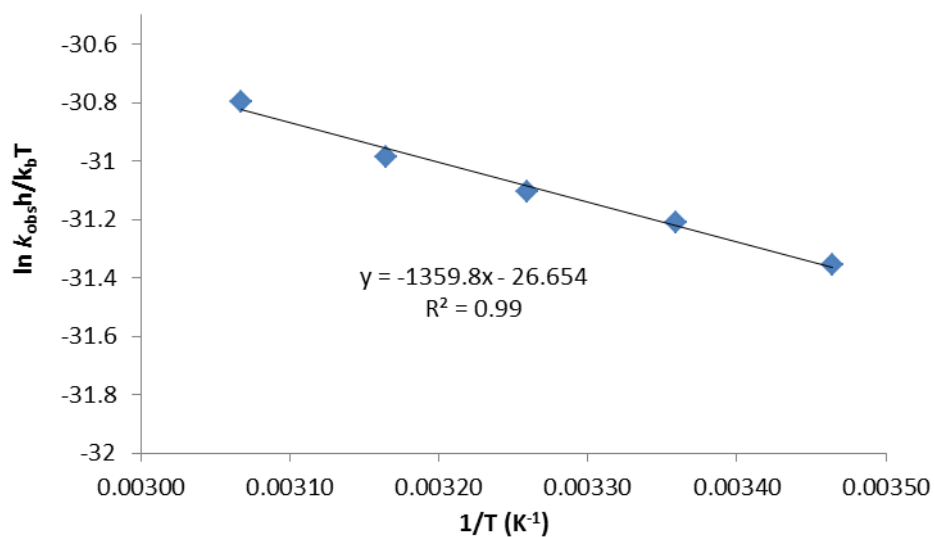**Figure 10.47.** Sample decay for the loss of 10 mM Sm(II) with 100 mM 2-methylcyclohexanone and 1 M H_2O.

264
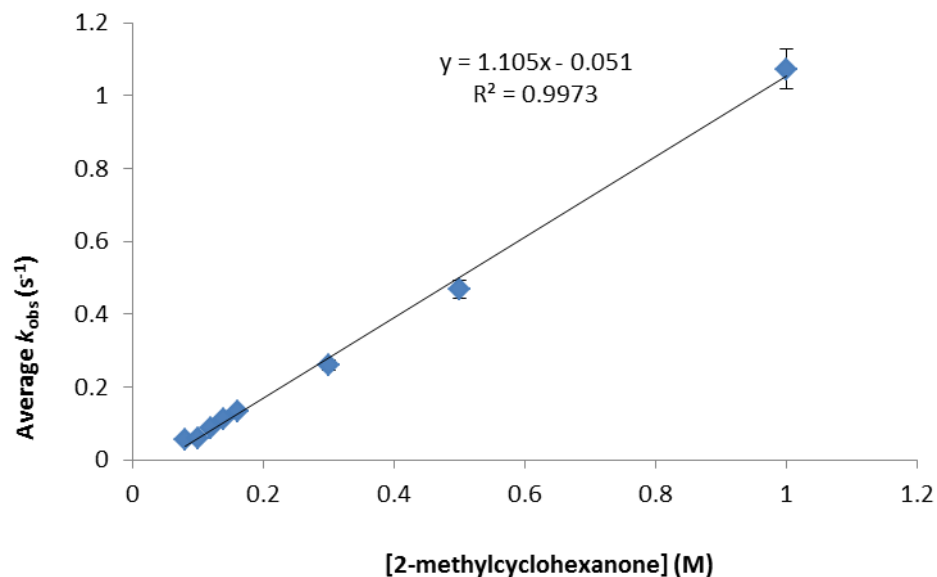
Figure 10.48. Rates for the reduction of 2-methylcyclohexanone with increasing concentration of substrate. For the order of 2-methylcyclohexanone, substrate concentration was varied from 80 mM to 1 M. Substrate was combined with 10 mM SmI_2 and 100 eq H_2O in the stopped-flow and the decay of Sm(II) was observed. The experiment was repeated three times on different dates.
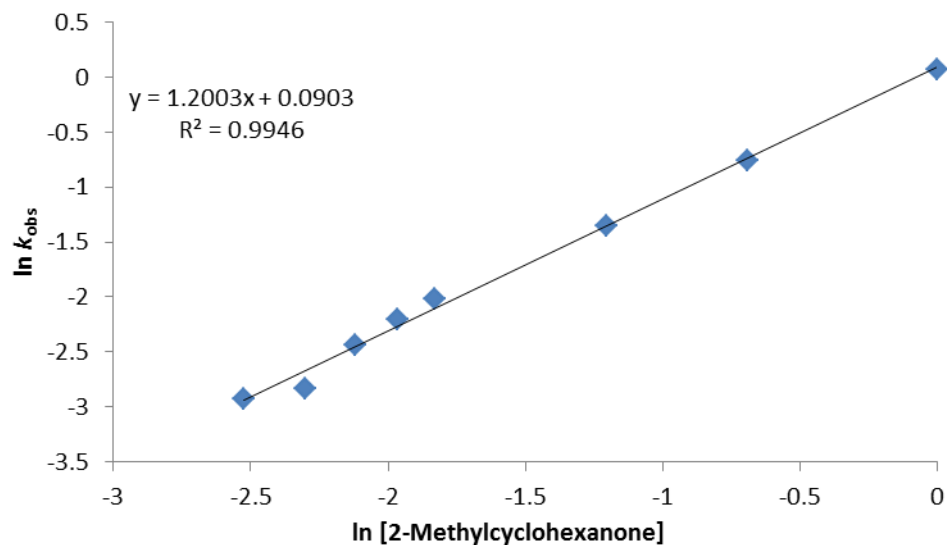
Figure 10.49. First-order rate dependence for the reduction/cyclization of 2-methylcyclohexanone with increasing concentrations of substrate.

265

Table 10.10. Order of SmI_2 in the reduction of 2-Methylcyclohexanone by fractional times method. Fractional times method was applied to determine the order of SmI_2 over more than one day and with a constant concentration of 100 mM 2-Methylcyclohexanone and 10 mM SmI_2. The value for $(t_{3/4}-t_{1/2})/t_{1/2}$ was computed for each decay.

A_0	$A_{1/2}$	$A_{3/4}$	$t_{1/2}$	$t_{3/4}$	$(t_{3/4}-t_{1/2})/t_{1/2}$
0.317207	0.158603	0.0793017	2.5	4.7	0.88
0.339564	0.169782	0.084891	2.35	5.15	1.19
0.321675	0.160837	0.0804187	3.00	6.00	1.00
				Average:	1.02
				Order:	1
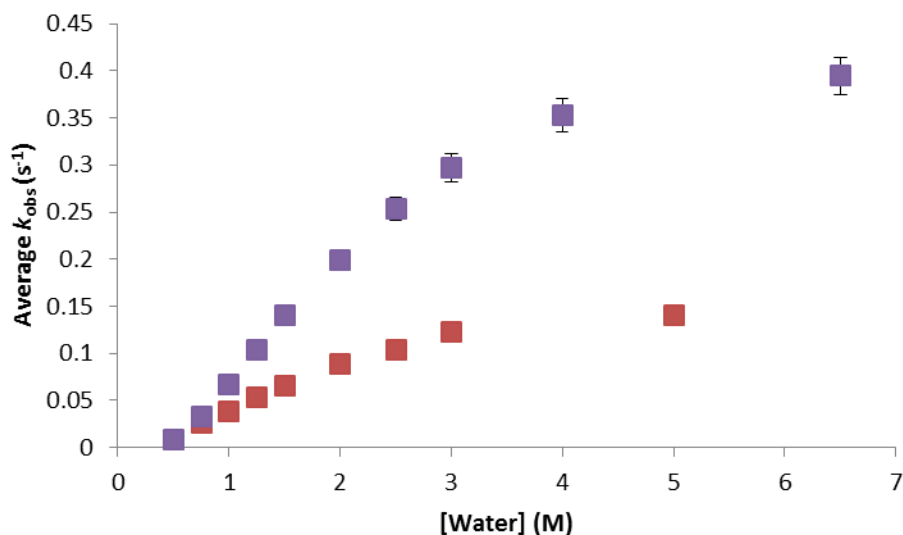
Figure 10.50. Rates of reduction of 2-methylcyclohexanone with increasing concentrations of H_2O (■) and D_2O (■). For KIE studies, the concentration of 2-methylcyclohexanone was kept constant at 100 mM and was combined with 10 mM SmI_2 in the reaction cell. The concentration of D_2O was varied from 50 equivalents to 500 equivalents (0.5-5 M). The kinetic isotope at the concentrations of interest (1M H_2O, 100 mM substrate, 10 mM SmI_2) is 2 ± 0.2.
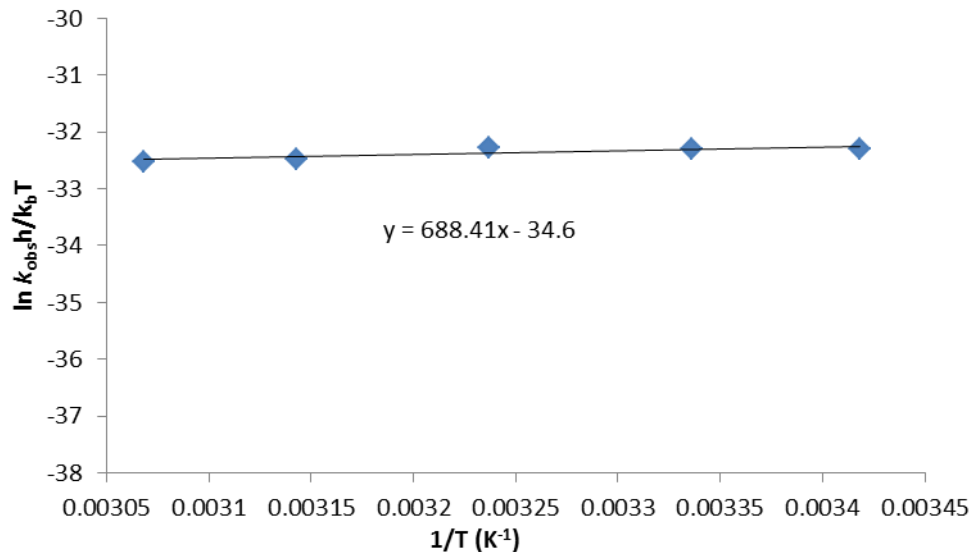
Figure 10.51. Sample Eyring plot for the reduction of 100 mM 2-methylcyclohexanone with 1 M H_2O and 10 mM SmI_2 from 20-50 $^{\circ}$C. This experiment was performed three times and the reported activation parameters are an average of the values obtained.
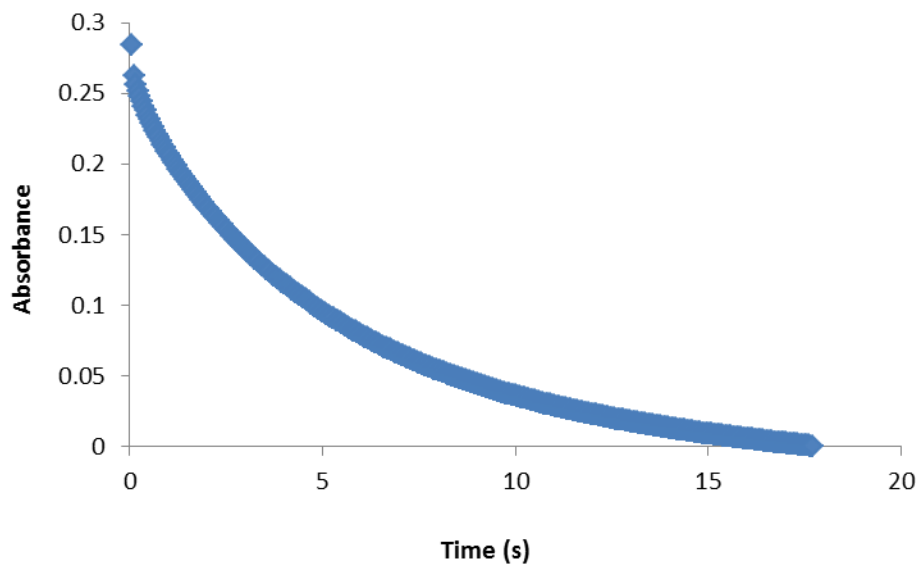
Figure 10.52. Sample decay for the loss of 10 mM Sm(II) with 100 mM 1-phenyl-6-hepten-2-one and 1 M H_2O.
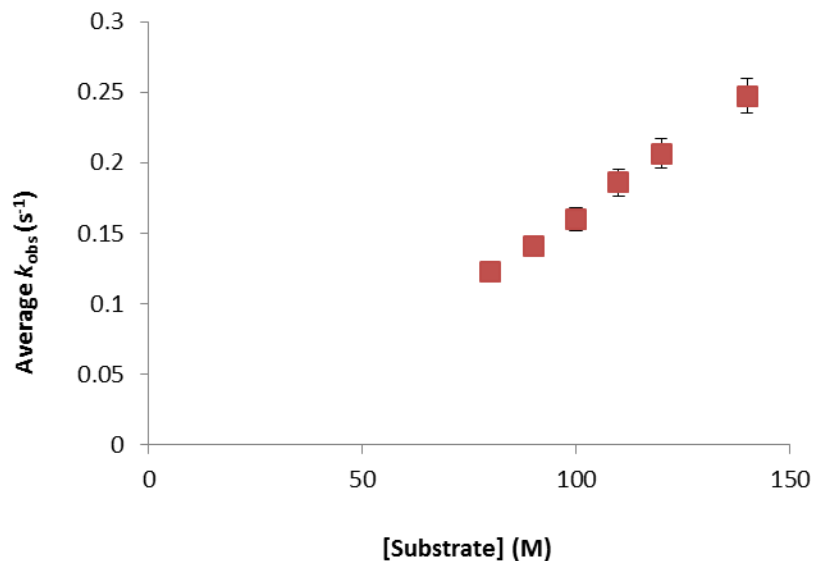
Figure 10.53. Rates for the reduction of 1-phenyl-6-hepten-2-one with increasing concentration of substrate. For the order of 1-phenyl-6-hepten-2-one, substrate concentration was varied from 80 mM to 140 mM. Substrate was combined with 10 mM SmI_2 and 100 eq H_2O in the stopped-flow and the decay of Sm(II) was observed. The experiment was repeated three times on different dates.
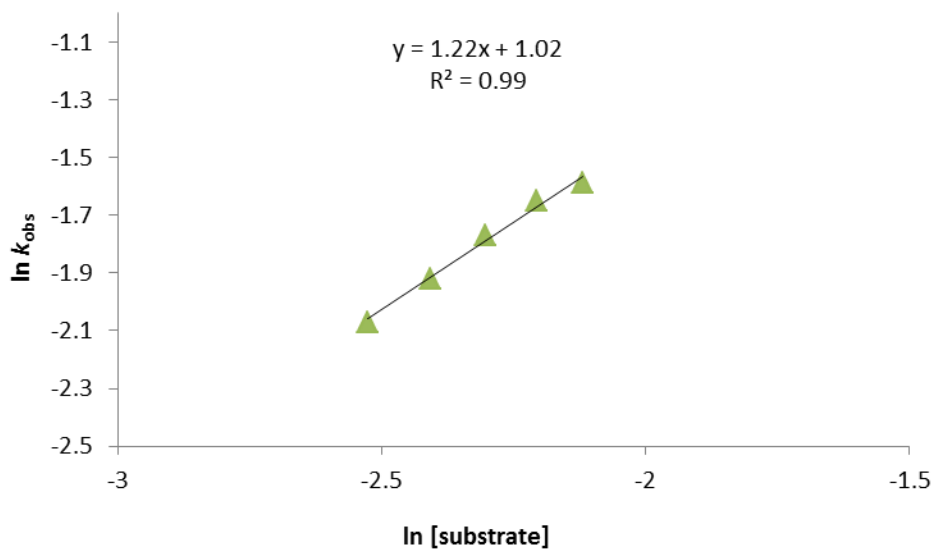
Figure 10.54. First-order rate dependence for the reduction/cyclization of 1-phenyl-6-hepten-2-one with increasing concentrations of substrate.

Table 10.11. Order of SmI_2 in the reduction of 1-phenyl-6-hepten-2-one by fractional times method. Fractional times method was applied to determine the order of SmI_2 over more than one day and with a constant concentration of 100 mM 1-phenyl-6-hepten-2-one and 10 mM SmI_2. The value for $(t_{3/4}-t_{1/2})/t_{1/2}$ was computed for each decay.

A_0	$A_{1/2}$	$A_{3/4}$	$t_{1/2}$	$t_{3/4}$	$(t_{3/4}-t_{1/2})/t_{1/2}$
0.248089	0.124044	0.062022	1.11	2.34	1.11
0.286803	0.143401	0.0717007	1.05	2.46	1.34
0.329580	0.16479	0.082395	1.04	2.42	1.32
				Average:	1.26
				Order:	**1**

Table 10.12. k_{obs} values for the kinetic isotope effect determination for 1-phenyl-6-hepten-2-one. For KIE studies, the concentration of 1-phenyl-6-hepten-2-one was kept constant at 100 mM and was combined with 10 mM SmI_2 in the reaction cell. The concentration of D_2O was constant at 1 M. The kinetic isotope at the concentrations of interest (1M H_2O, 100 mM substrate, 10 mM SmI_2) is 1.7 ± 0.2.

D_2O kobs	Trial 1	Trial 2	Trial 3		
A	0.12	0.12	0.08		
b	0.11	0.11	0.08		
ave	0.12	0.12	0.08		
Total ave value for 1 M D_2O					0.10
Ave k_{obs} for 1 M H_2O					0.18
				k_H/k_D	1.72
				Std dev.	0.17
				KIE=	1.72 ± 0.2

Figure 10.54. Sample Eyring plot for the reduction of 100 mM 1-phenyl-6-hepten-2-one with 1 M H_2O and 10 mM SmI_2 from 20-50 °C. This experiment was performed three times and the reported activation parameters are an average of the values obtained.
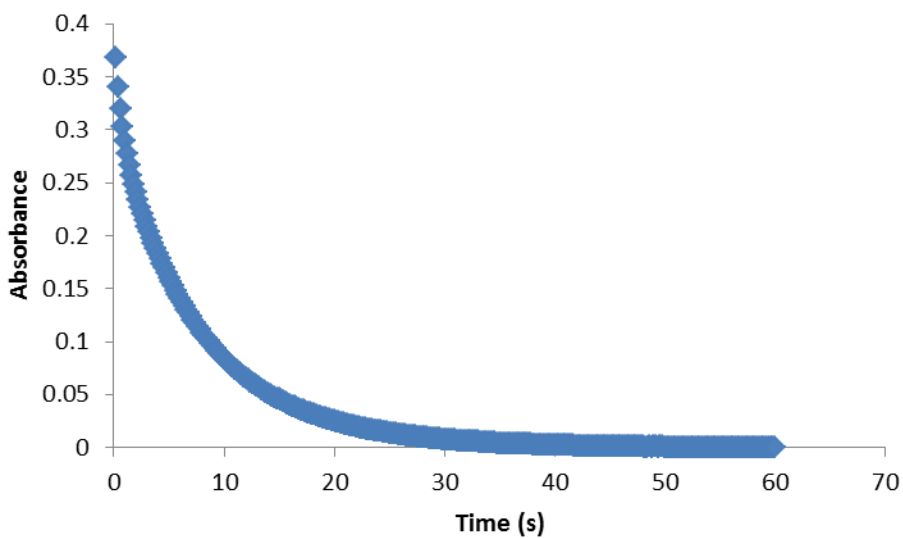
Figure 10.55. Sample decay for the loss of 10 mM Sm(II) with 100 mM 1-phenyl-2-butanone and 1 M H_2O.
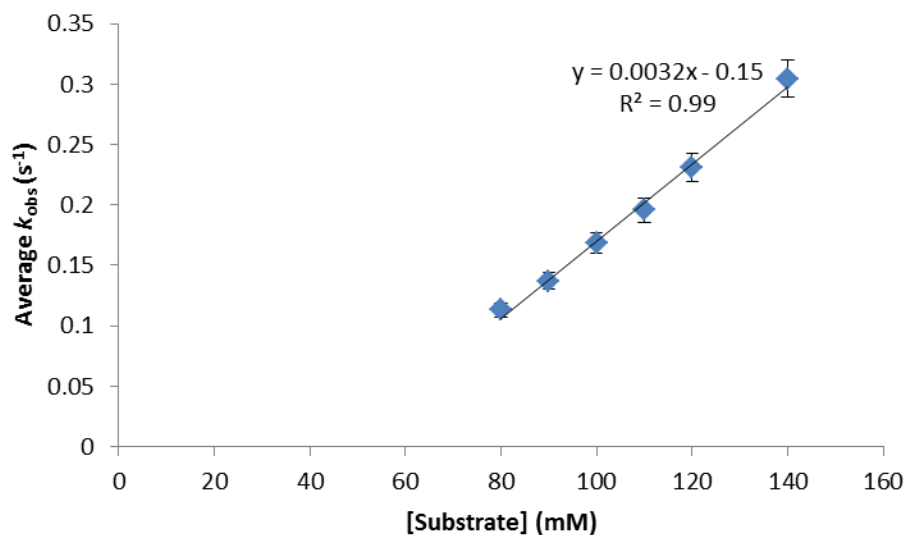
Figure 10.55. Rates for the reduction of 1-phenyl-2-butanone with increasing concentration of substrate. For the order of 1-phenyl-2-butanone, substrate concentration was varied from 80 mM to 140 mM. Substrate was combined with 10 mM SmI_2 and 100 eq H_2O in the stopped-flow and the decay of Sm(II) was observed. The experiment was repeated three times on different dates.

Table 10.13. Order of SmI_2 in the reduction of 1-phenyl-2-butanone by fractional times method.

A_0	$A_{1/2}$	$A_{3/4}$	$t_{1/2}$	$t_{3/4}$	$(t_{3/4}\text{-}t_{1/2})/t_{1/2}$
0.316442	0.158221	0.0791105	1.22	2.94	1.41
0.232405	0.116202	0.0581012	1.5	3.24	1.16
0.357261	0.178630	0.0893152	1.44	3.12	1.17
				Average:	1.25
				Order:	1

Table 10.14. k_{obs} values for the kinetic isotope effect determination for 1-phenyl-2-butanone.

D_2O kobs	Trial 1	Trial 2	Trial 3	
A	0.070	0.092	0.079	
b	0.072	0.094	0.082	
ave	0.071	0.093	0.0805	
Total ave value for 1 M D_2O				0.0815
Ave k_{obs} for 1 M H_2O				0.1520
			k_H/k_D	1.86
			Std dev.	0.19
			KIE=	1.86 ± 0.2

Figure 10.56. Sample Eyring plot for the reduction of 100 mM 1-phenyl-2-butanone with 1 M H_2O and 10 mM SmI_2 from 20-50 $^{\circ}C$. This experiment was performed three times and the reported activation parameters are an average of the values obtained.

Table 10.15. Cyclization/Reduction Determination for 1-phenyl-6-hepten-2-one

Eq H₂O	Red. ppm	Red. Integral	Red. Protons	Red. Product	Cycliz. ppm	Cycliz. Integral	Cycliz. Protons	Cycliz. Prod.	% Cyclized
100	5.80	0.18	1.00	0.18	0.96	3.00	3.00	1.00	84.75
250	5.80	1.00	1.00	1.00	0.96	19.93	3.00	6.64	86.92
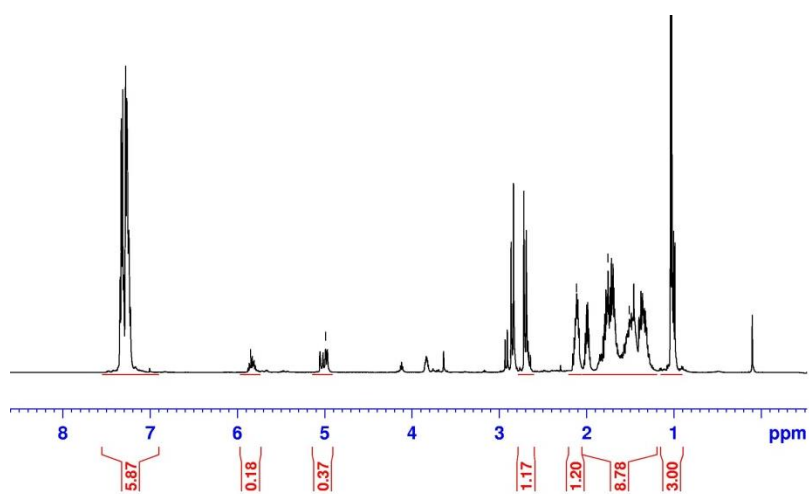
Figure 10.57 1-phenyl-6-hepten-2-one cyclization with 100 equivalents of H₂O

273
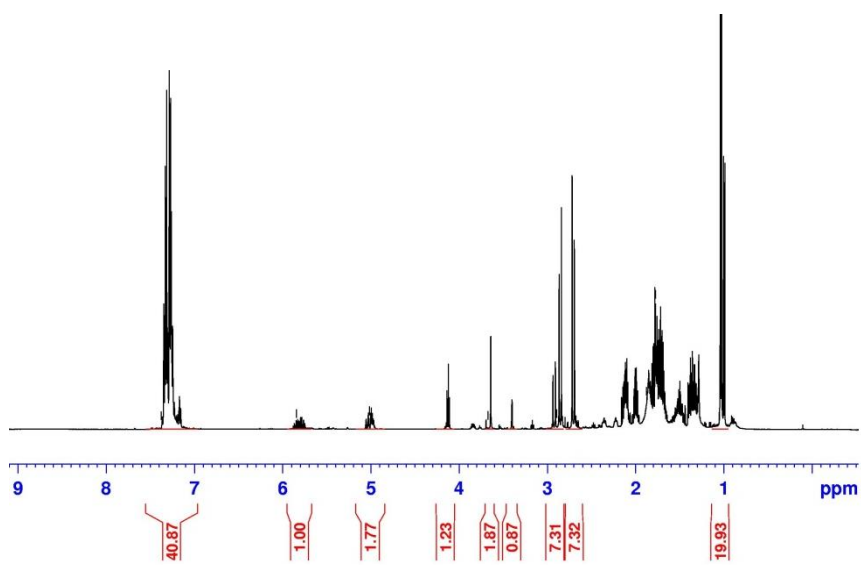
Figure 10.57 1-phenyl-6-hepten-2-one cyclization with 250 equivalents of H_2O.
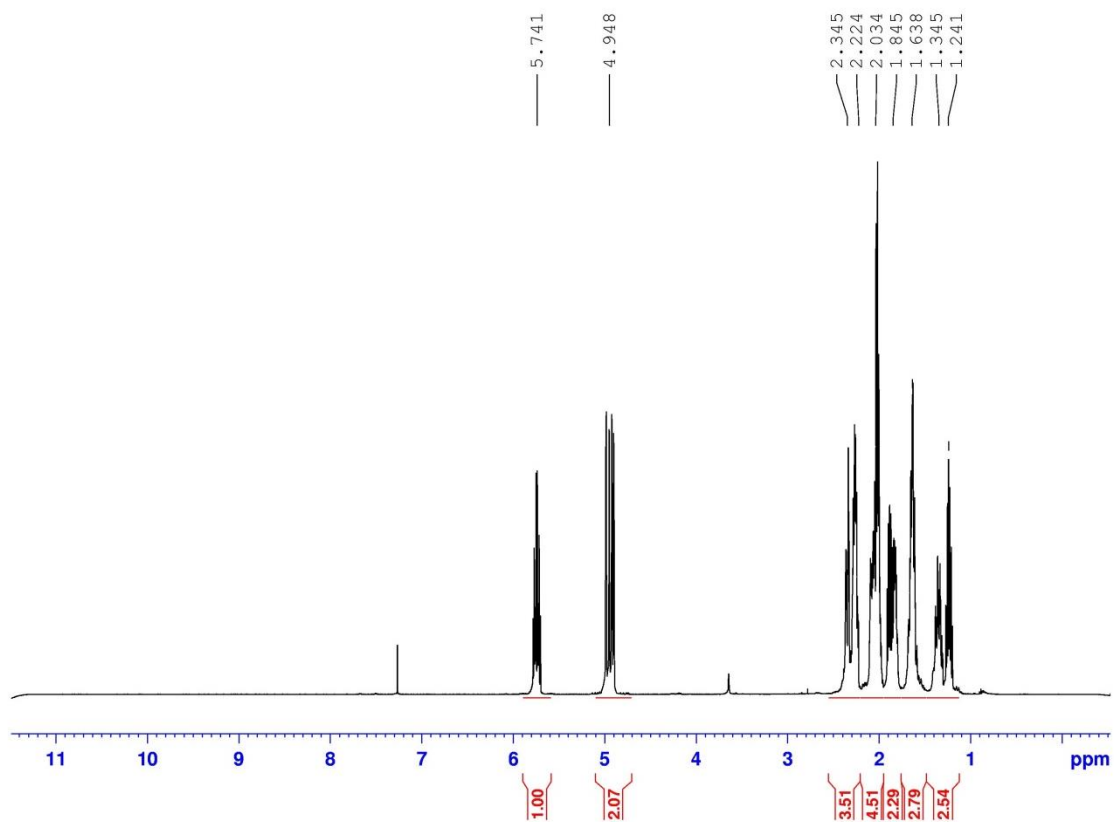
Figure 10.58 [1]H Spectrum of 2-But-3-enyl-cyclohexan-1-one
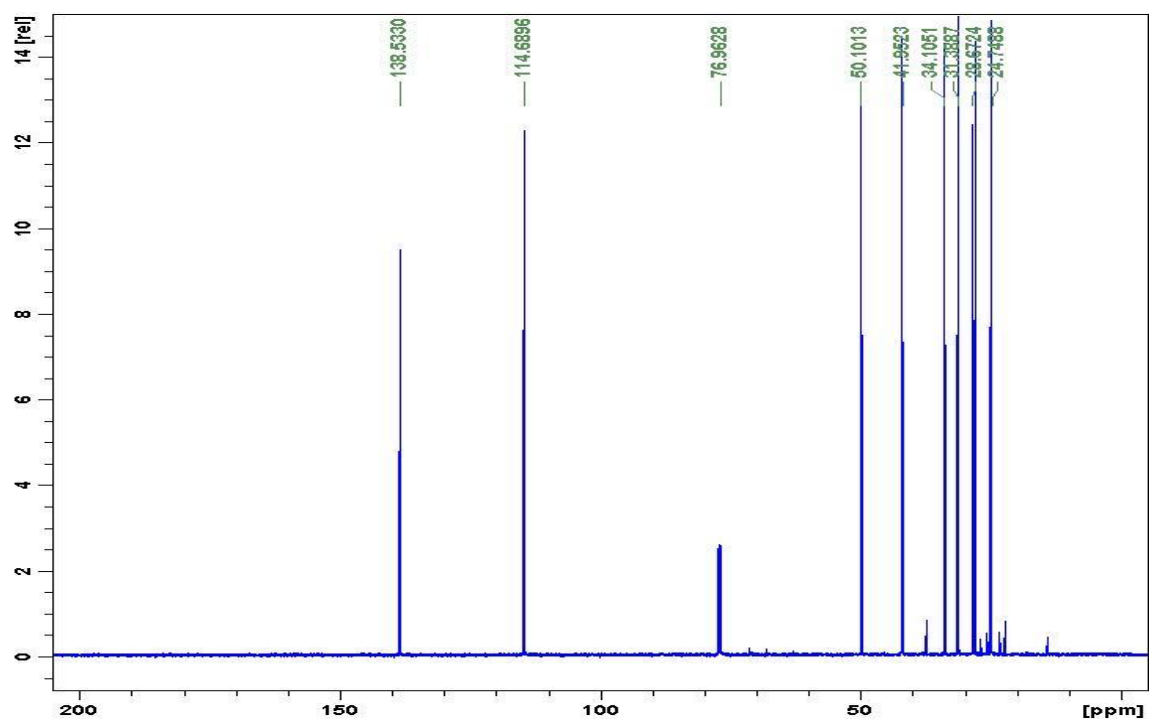
Figure 10.59 [13]C Spectrum of 2-But-3-enyl-cyclohexan-1-one
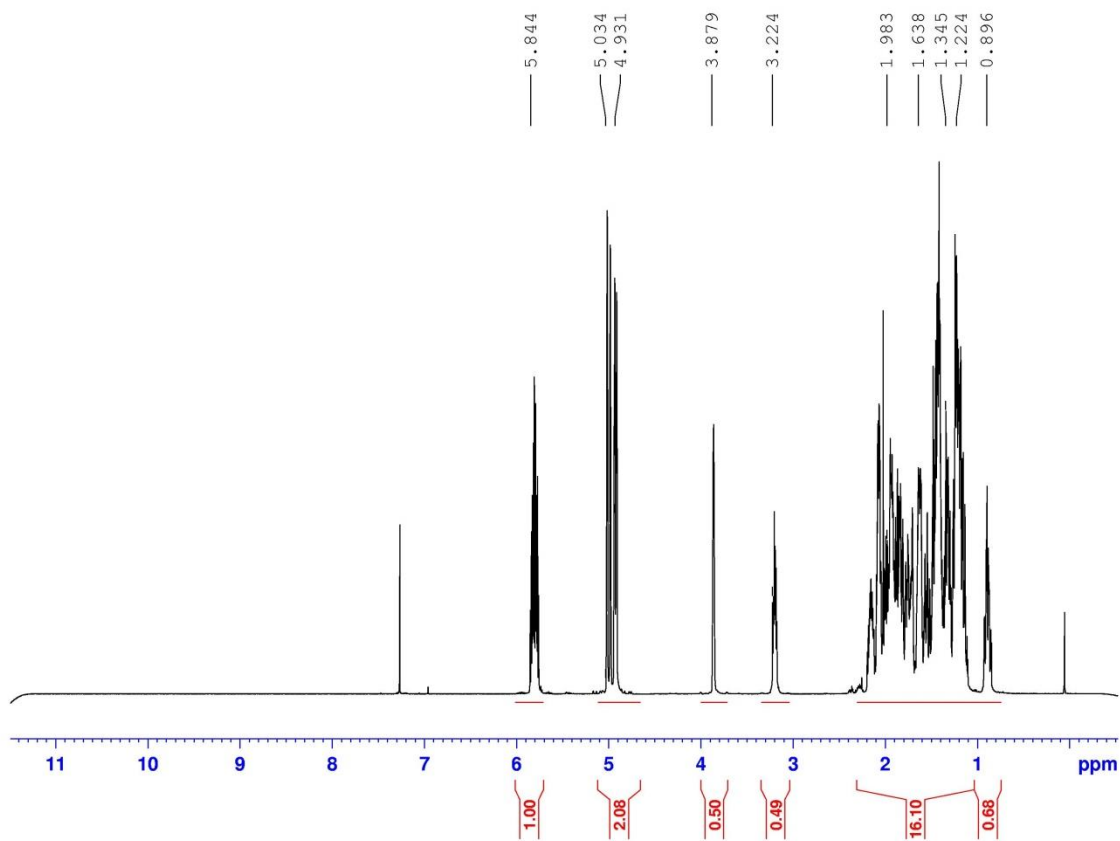
Figure 10.59 ^{1}H Spectrum of 2-But-3-enyl-cyclohexan-1-ol.
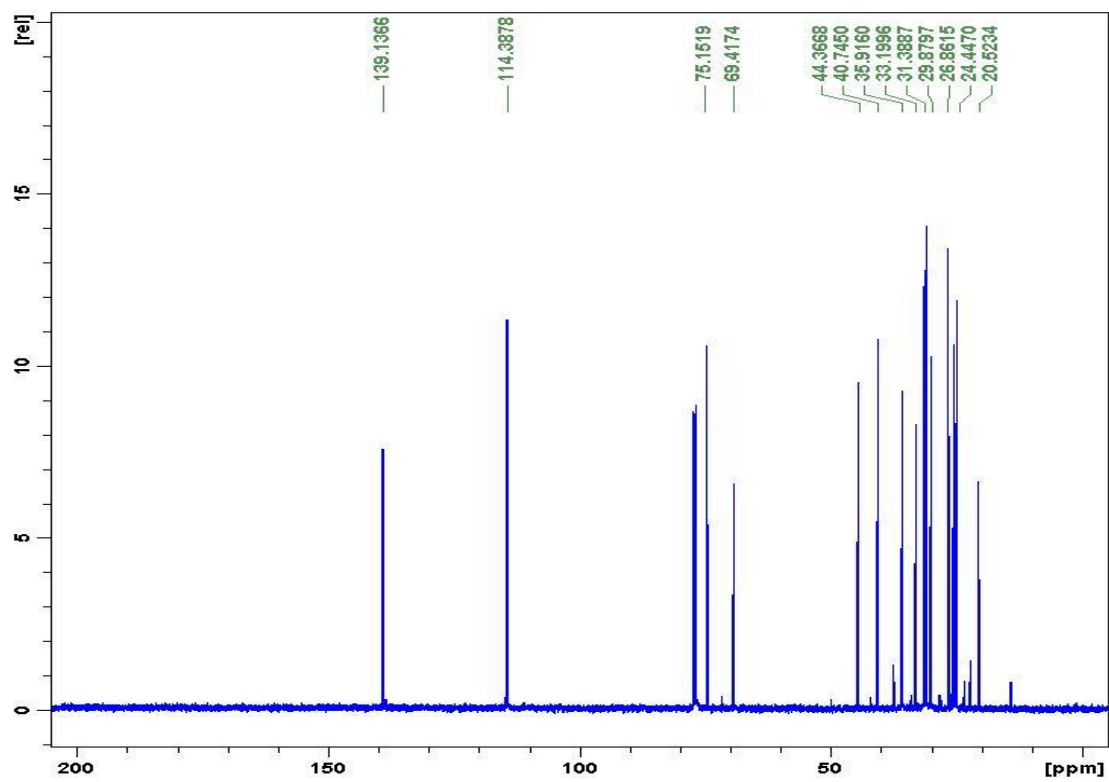
Figure 10.60 ^{13}C Spectrum of 2-But-3-enyl-cyclohexan-1-ol.
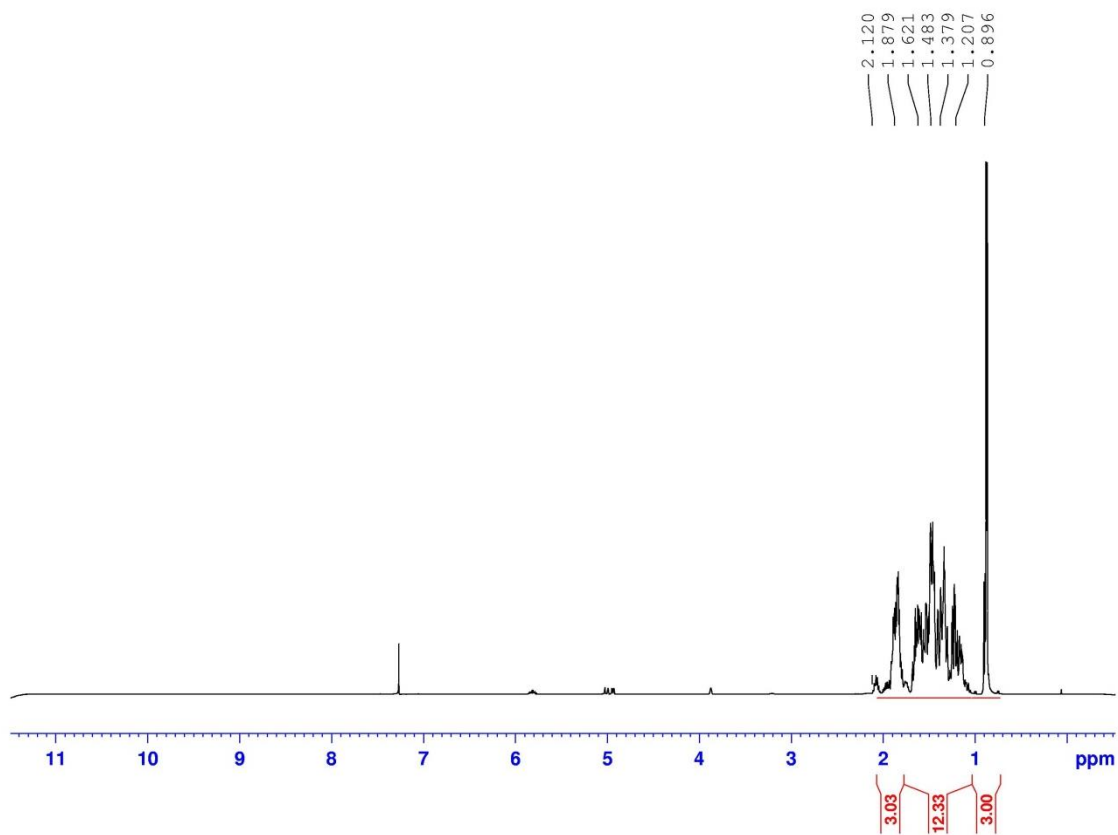
Figure 10.61 ^{1}H Spectrum of 3a*H*-Inden-3a-ol, octahydro-3-methyl-

279
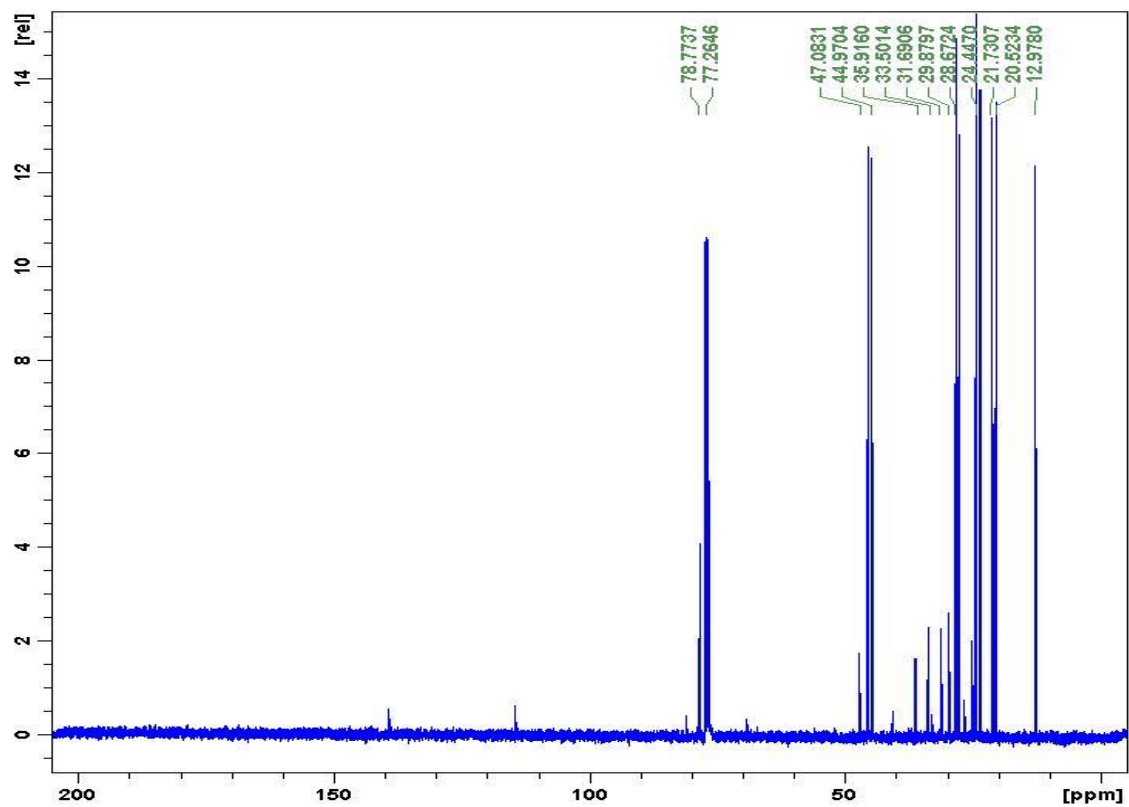
Figure 10.62 ^{13}C Spectrum of 3a*H*-Inden-3a-ol, octahydro-3-methyl-
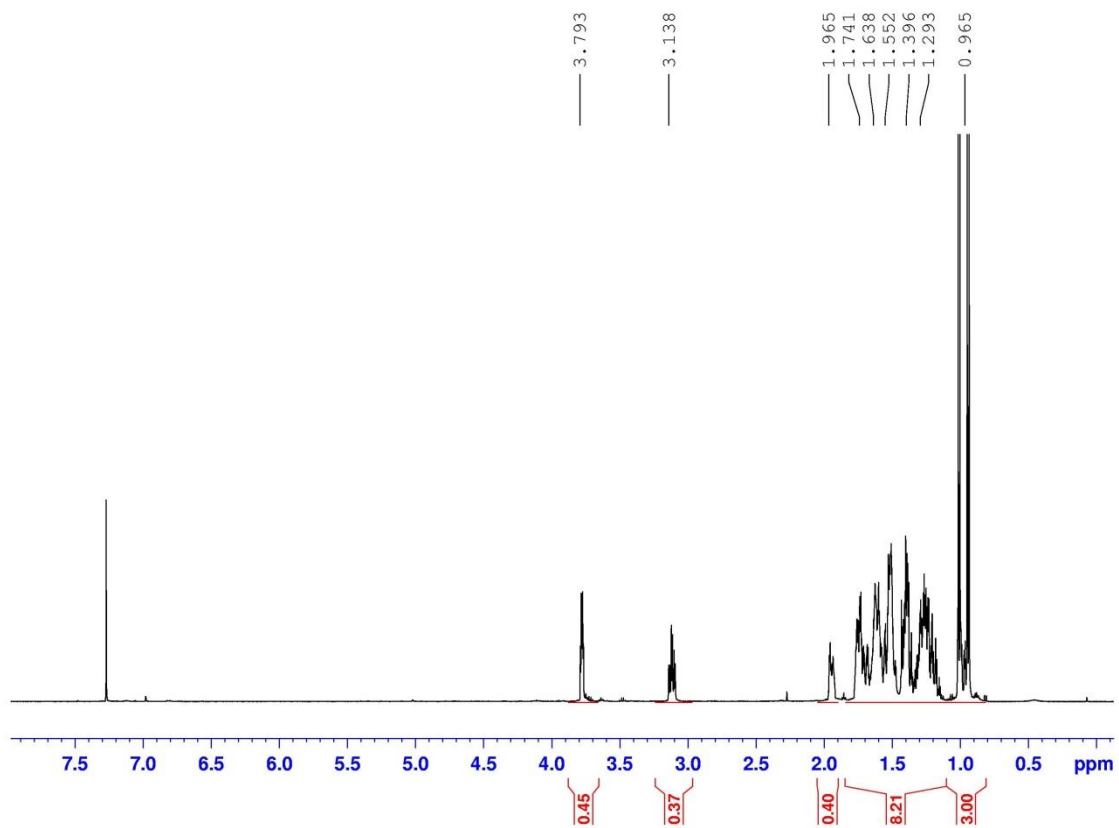
Figure 10.63 [1]H Spectrum of 2-methylcyclohexanol.
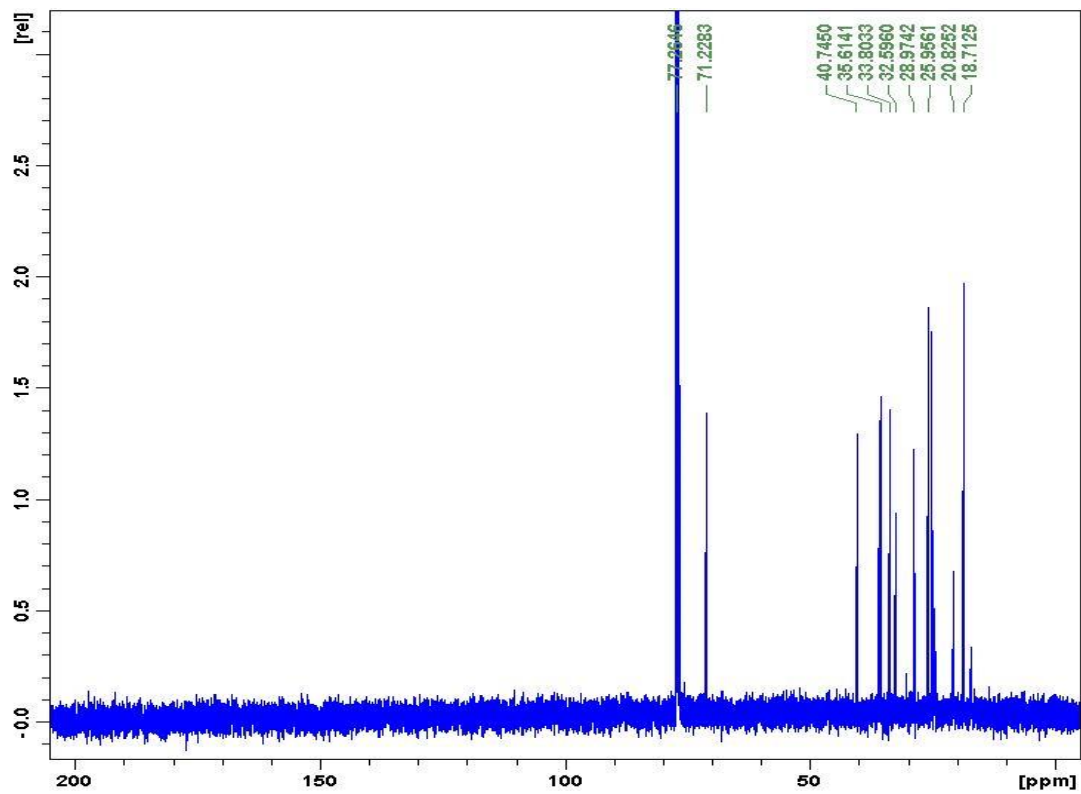
Figure 10.64 ¹³C Spectrum of 2-Methylcyclohexanol
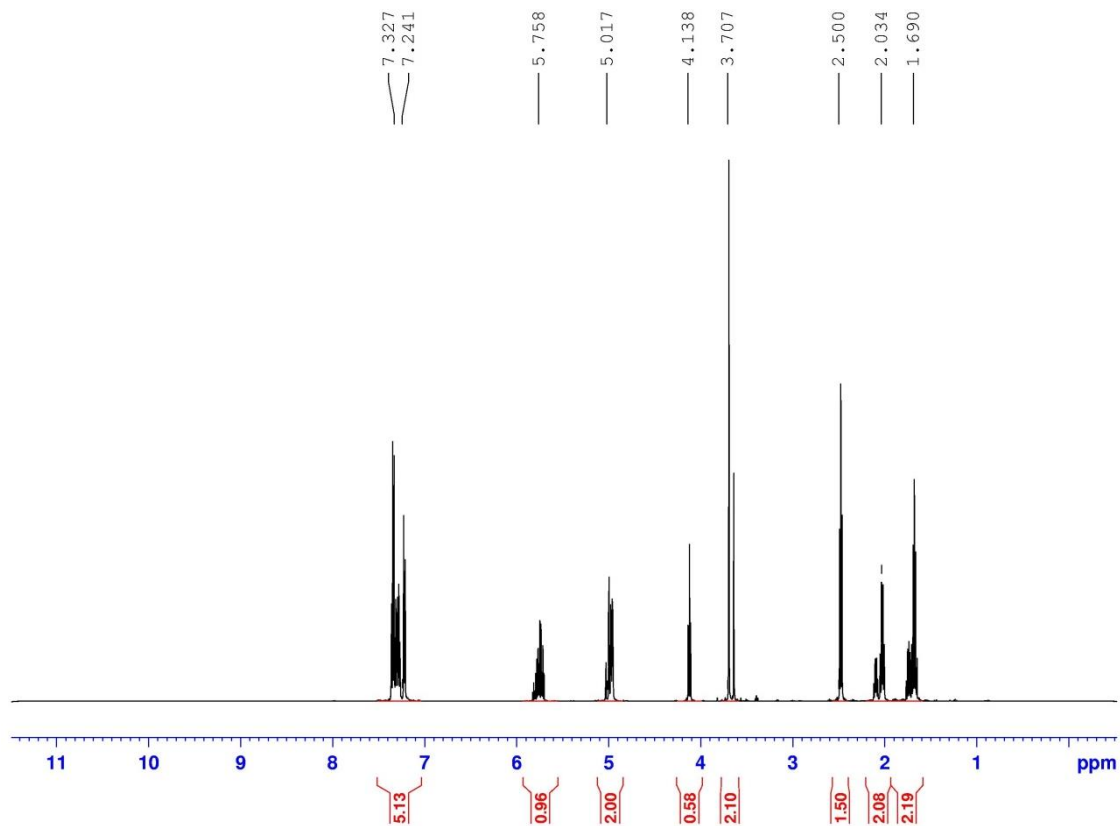
Figure 10.65 [1]H Spectrum of 1-phenyl-6-hepten-2-one
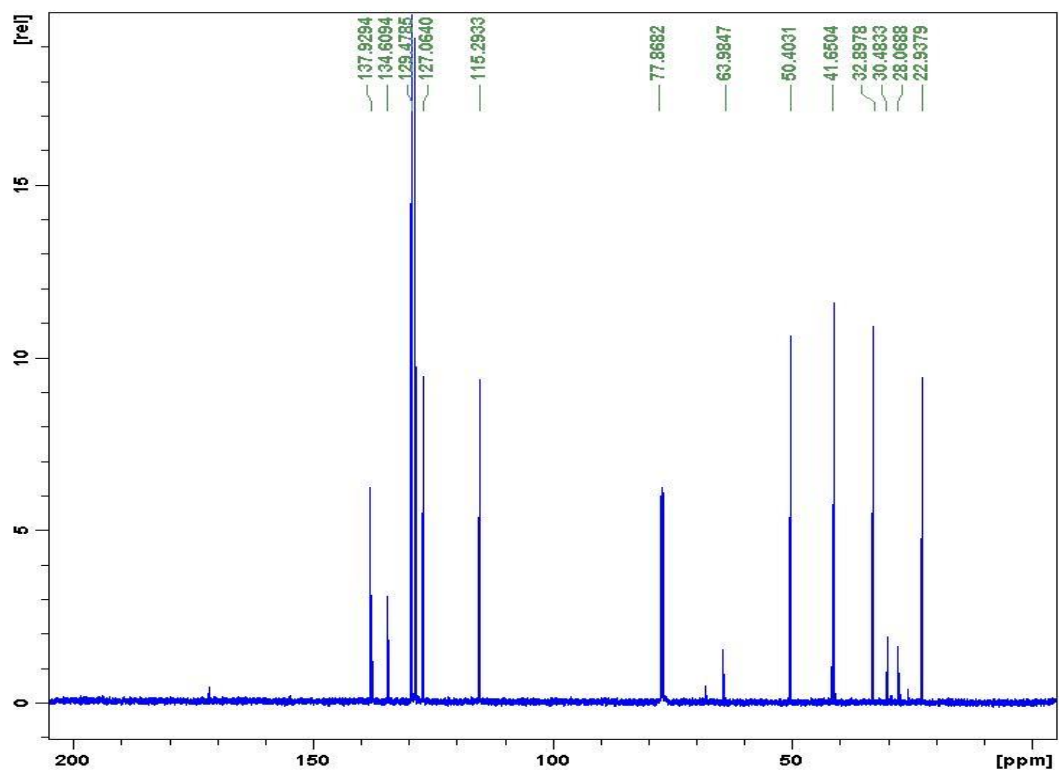
Figure 10.66 ^{13}C Spectrum of 1-phenyl-6-hepten-2-one
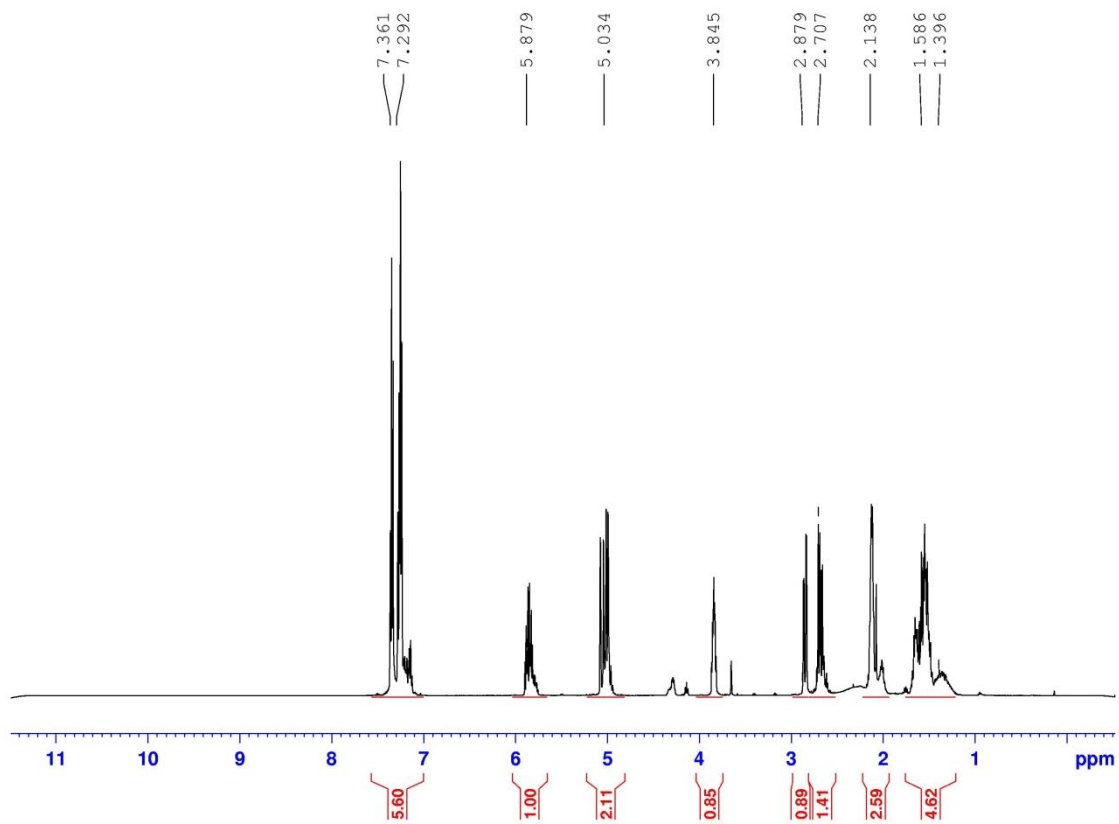
Figure 10.67 [1]H Spectrum of 1-phenyl-6-hepten-2-ol.
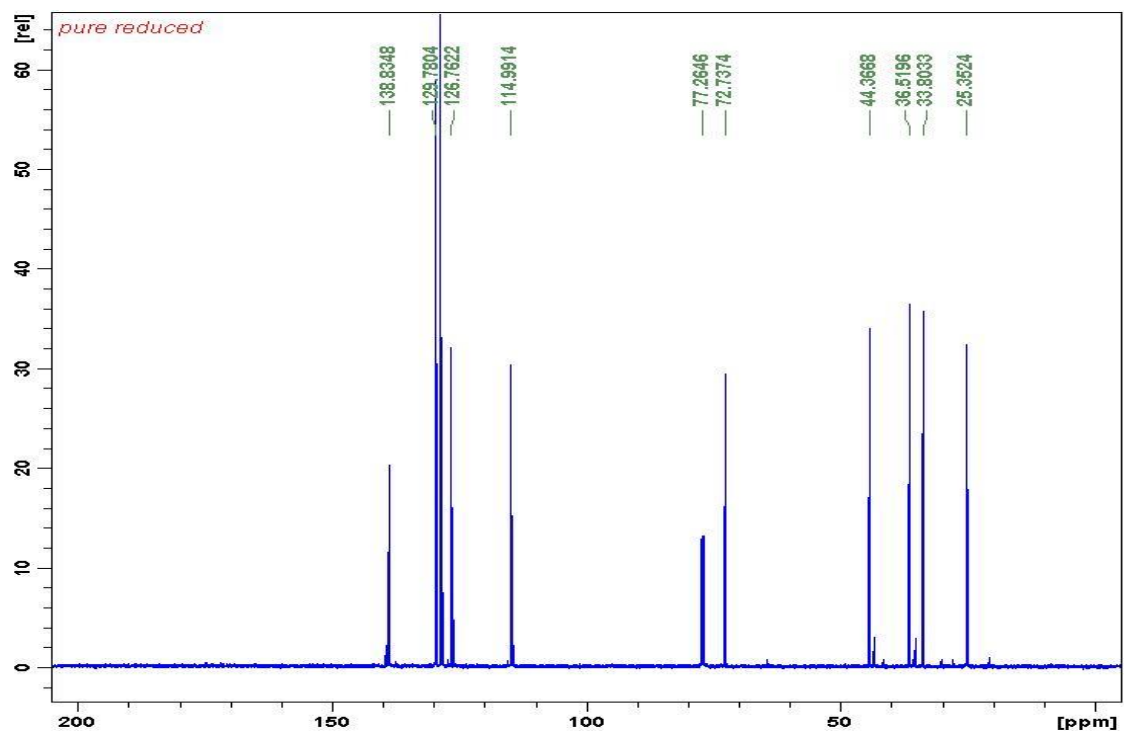
Figure 10.68 ^{13}C Spectrum of 1-phenyl-6-hepten-2-ol.
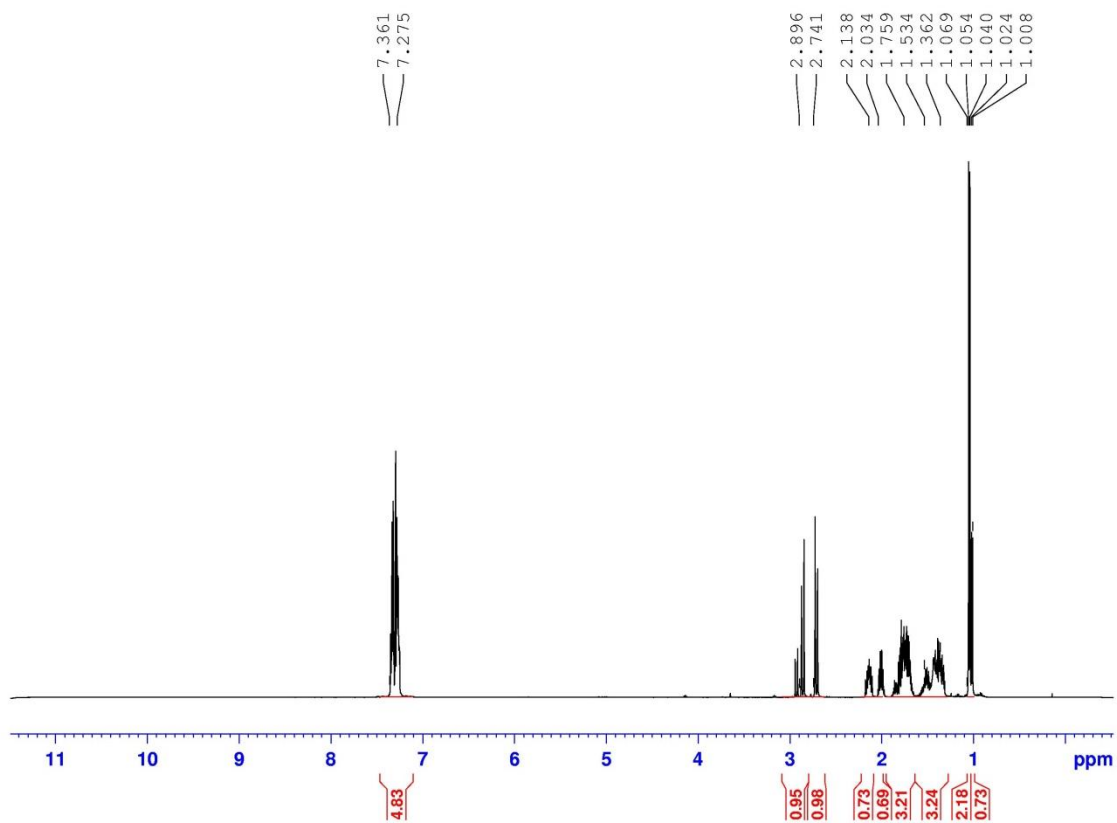
Figure 10.69 ^{1}H Spectrum of Cyclopentanol, 2-methyl-1-(phenylmethyl)-
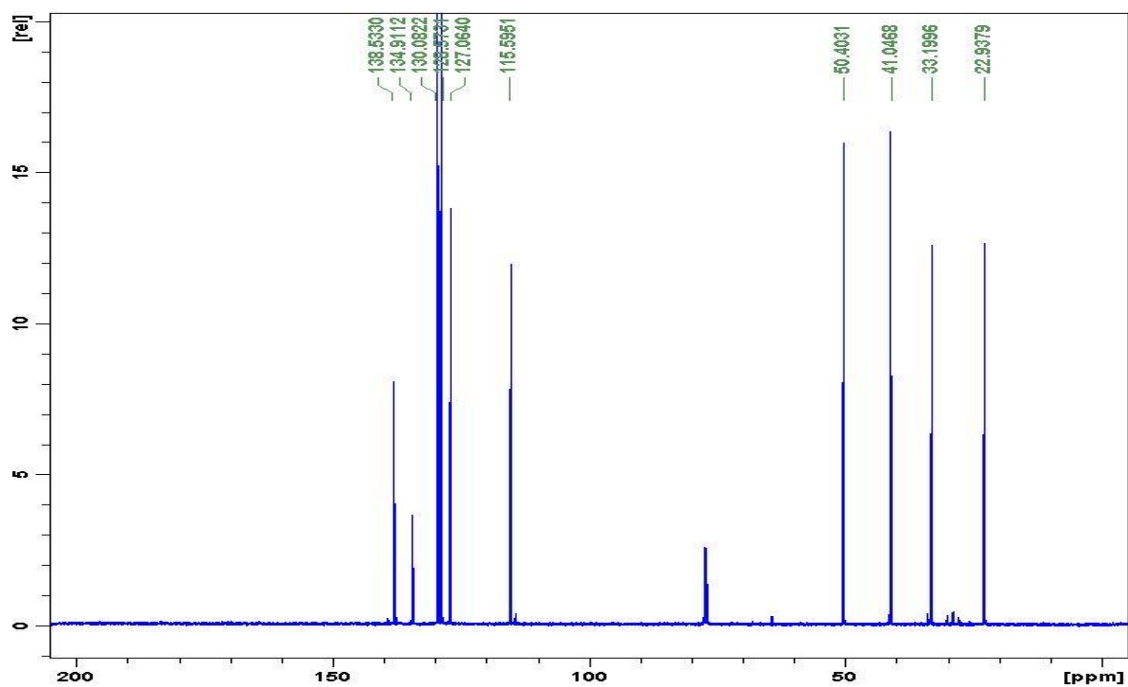
Figure 10.70 ^{13}C Spectrum of Cyclopentanol, 2-methyl-1-(phenylmethyl)-
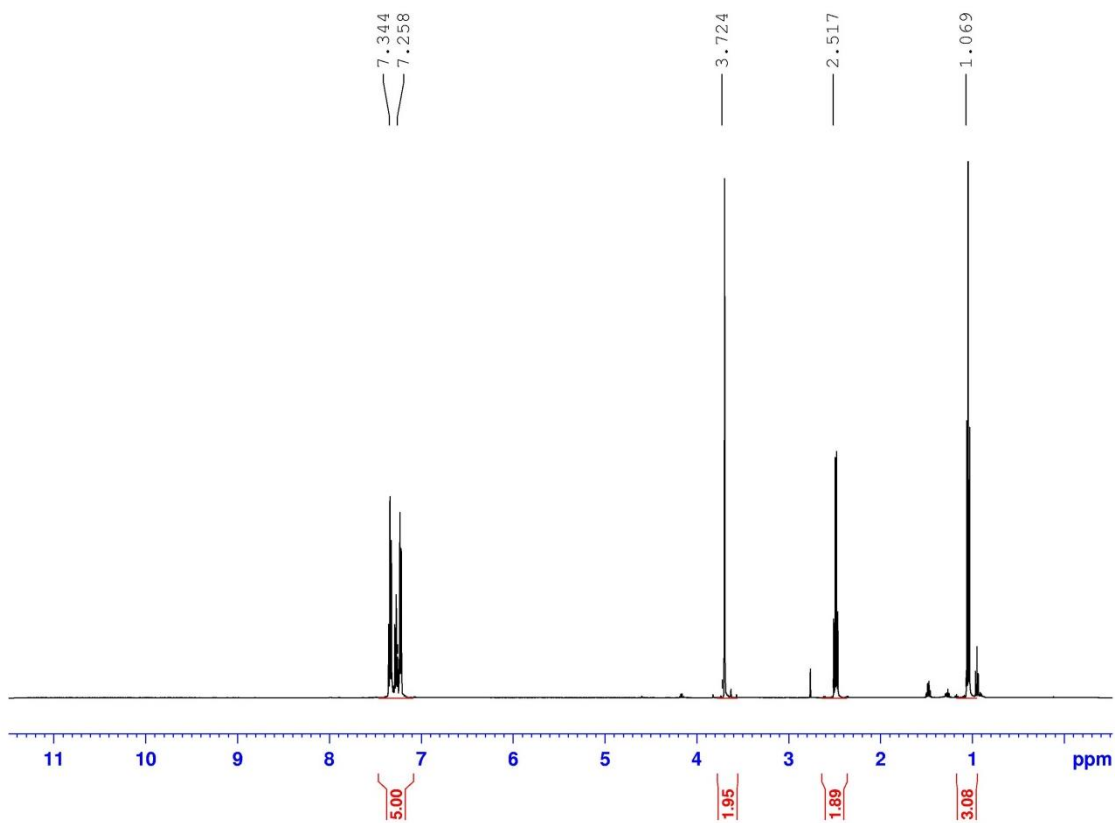
Figure 10.71 [1]H Spectrum of Benzylethylketone
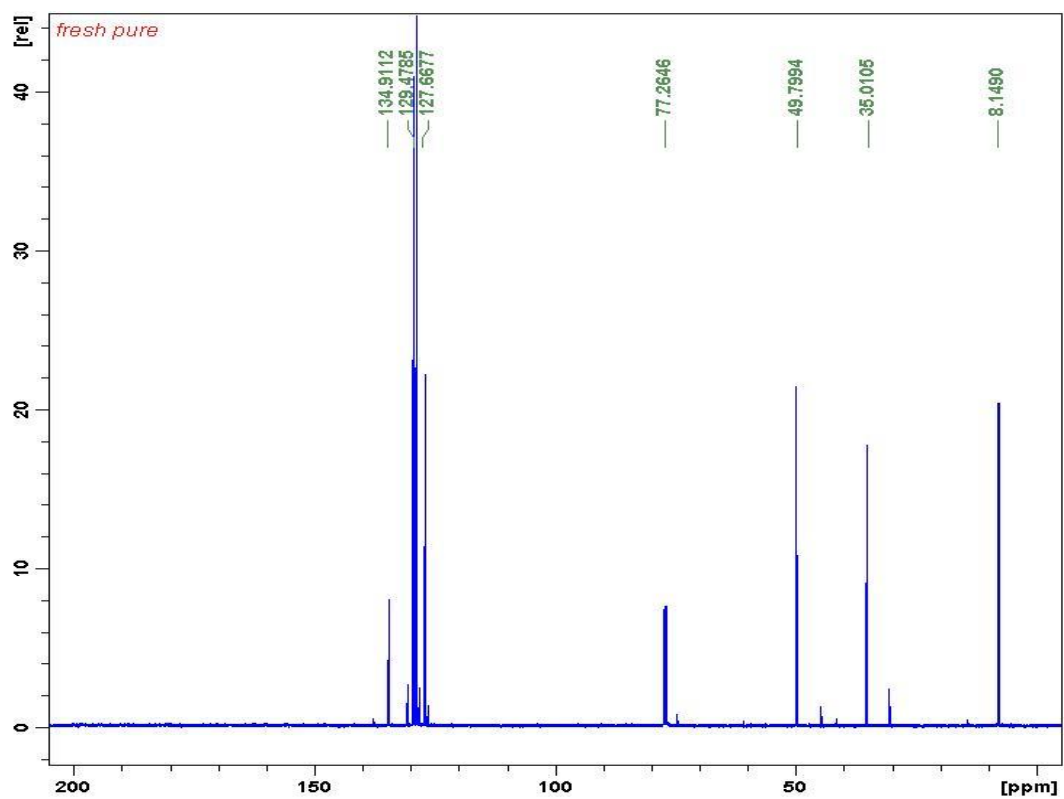
Figure 10.72 ^{13}C Spectrum of Benzylethylketone
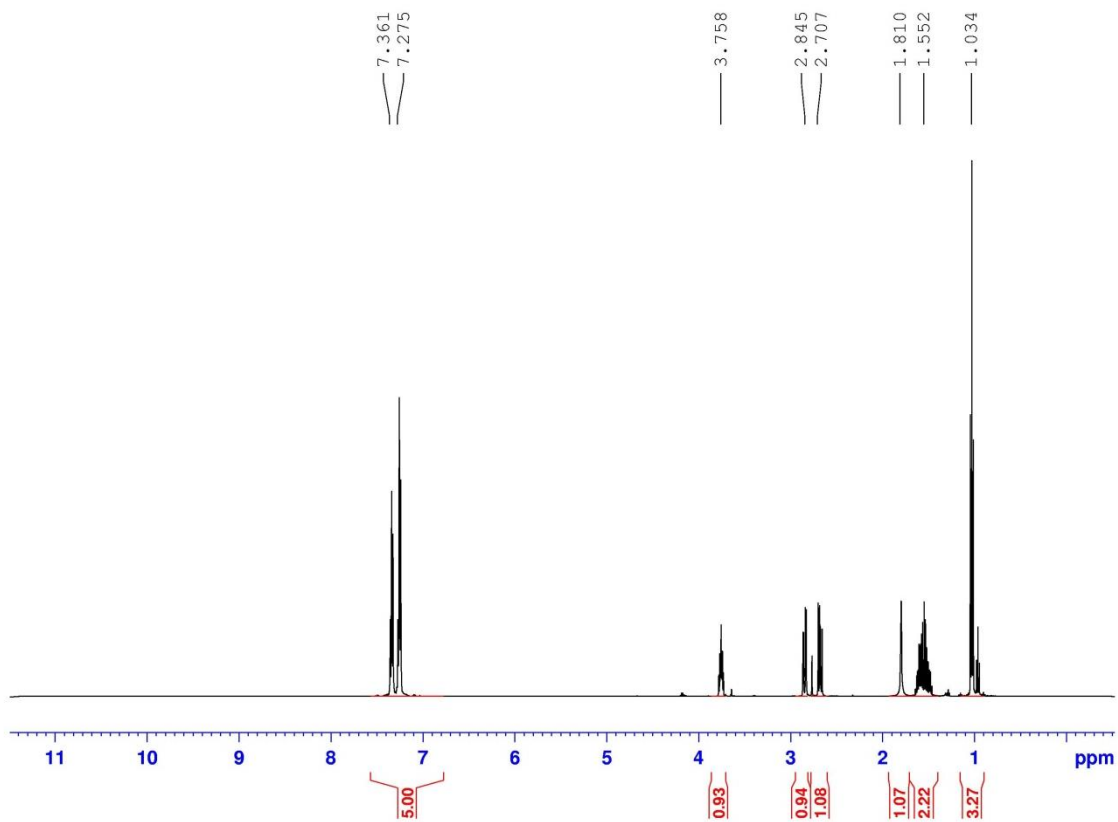
Figure 10.73 ^{1}H Spectrum of Benzeneethanol, α-ethyl-
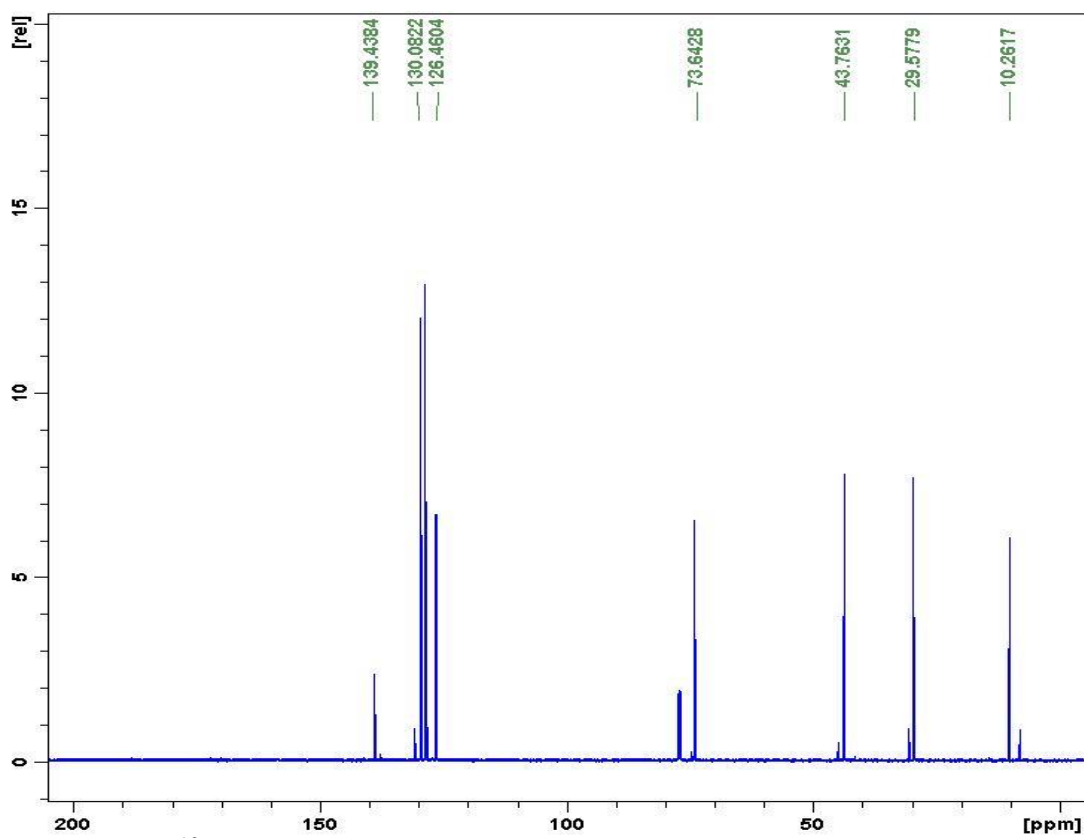
Figure 10.74 ^{13}C Spectrum of Benzeneethanol, α-ethyl-

O-H BDFE = 108.0 kcal/mol   C-H BDFE = 34.1 kcal/mol

Bond-weakening of at
least at least 73.9 kcal/mol
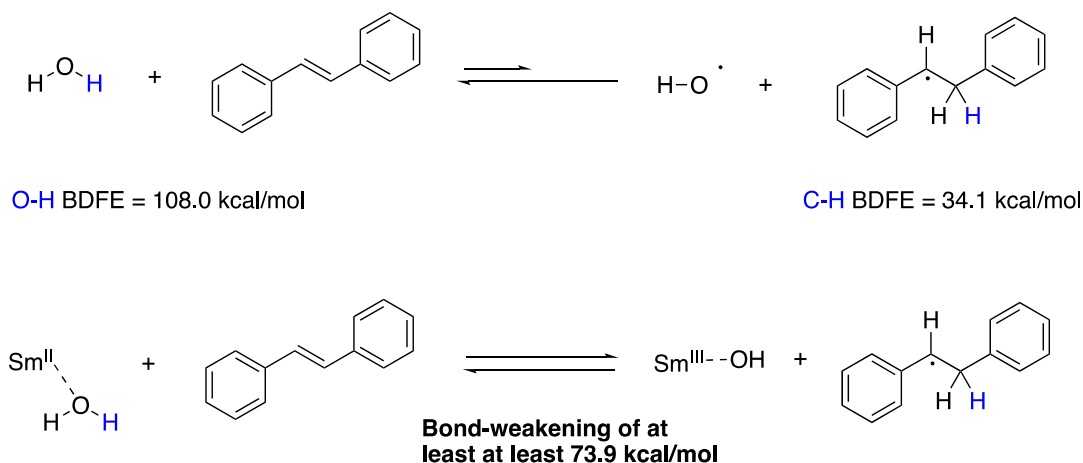
Figure 10.75 SmI_2-Induced Bond Weakening

Computational Methods

Gaussian09(1) programs were used for the calculations with the APF-D(2) hybrid DFT(3) method and the 6-311+g(2d,p) basis set(4,5). Solvation values were calculated using the polarizable continuum model with integral equation formalism. IEFPCM(6,7), with tetrahydrofuran as the solvent. The geometries and frequencies were calculated with uapfd/6-311+g(2d,p) opt=(calcfc,tight) int=(ultrafine,acc2e=12)pop=npa. scrf=(iefpcm,solvent=thf) was added to the route section for solvation. Natural-population analysis(8) was obtained by including pop=npa. opt = tight was not used for trans stilbene.

1) Gaussian 09, Revision D.01,
 M. J. Frisch, G. W. Trucks, H. B. Schlegel, G. E. Scuseria,
 M. A. Robb, J. R. Cheeseman, G. Scalmani, V. Barone, B. Mennucci,
 G. A. Petersson, H. Nakatsuji, M. Caricato, X. Li, H. P. Hratchian,
 A. F. Izmaylov, J. Bloino, G. Zheng, J. L. Sonnenberg, M. Hada,
 M. Ehara, K. Toyota, R. Fukuda, J. Hasegawa, M. Ishida, T. Nakajima,
 Y. Honda, O. Kitao, H. Nakai, T. Vreven, J. A. Montgomery, Jr.,
 J. E. Peralta, F. Ogliaro, M. Bearpark, J. J. Heyd, E. Brothers,
 K. N. Kudin, V. N. Staroverov, T. Keith, R. Kobayashi, J. Normand,
 K. Raghavachari, A. Rendell, J. C. Burant, S. S. Iyengar, J. Tomasi,
 M. Cossi, N. Rega, J. M. Millam, M. Klene, J. E. Knox, J. B. Cross,
 V. Bakken, C. Adamo, J. Jaramillo, R. Gomperts, R. E. Stratmann,
 O. Yazyev, A. J. Austin, R. Cammi, C. Pomelli, J. W. Ochterski,

R. L. Martin, K. Morokuma, V. G. Zakrzewski, G. A. Voth,
P. Salvador, J. J. Dannenberg, S. Dapprich, A. D. Daniels,
O. Farkas, J. B. Foresman, J. V. Ortiz, J. Cioslowski,
and D. J. Fox, Gaussian, Inc., Wallingford CT, 2013

2)A. Austin, G. Petersson, M. J. Frisch, F. J. Dobek, G. Scalmani, and K. Throssell, "A density functional with spherical atom dispersion terms", *J. Chem. Theory and Comput*. **8** (2012) 4989.
3) R. G. Parr and W. Yang, *Density-functional theory of atoms and molecules* (Oxford Univ. Press, Oxford, 1989).
4)A. D. McLean and G. S. Chandler, "Contracted Gaussian-basis sets for molecular calculations. 1. 2nd row atoms, Z=11-18," *J. Chem. Phys.*, **72** (1980) 5639-48
5)K. Raghavachari, J. S. Binkley, R. Seeger, and J. A. Pople, "Self-Consistent Molecular Orbital Methods. 20. Basis set for correlated wave-functions," J. Chem. Phys., 72 (1980) 650-54.
6)E. Cancès, B. Mennucci, and J. Tomasi, "A new integral equation formalism for the polarizable continuum model: Theoretical background and applications to isotropic and anistropic dielectrics," *J. Chem. Phys.*, **107** (1997) 3032-41.
7)J. Tomasi, B. Mennucci, and R. Cammi, "Quantum mechanical continuum solvation models," *Chem. Rev.*, **105** (2005) 2999-3093.
8)A. E. Reed, R. B. Weinstock, and F. Weinhold, "Natural-population analysis," *J. Chem. Phys.*, **83** (1985) 735-46.

In the table below, E+ZPE, G, & H, energies are in hartree particle. S is in Cal/Mol.

	E+ZPE	G	H	S
Gas Phase Calculations:				
H2O	-76.374696	-76.392334	-76.370917	45.076
OH radical	-75.692588	-75.709512	-75.689283	42.575
Hydrogen atom		-0.502246	-0.512900	-0.499886 27.392
2-methylcyclohexanone_eq	-348.847541	-348.879659	-348.838652	86.306
2-methylcyclohexanone_eq radical	-349.389217	-349.422140	-349.379894 88.913	
2-methylcyclohexanone_eq radical anion	-348.826843	-348.859586	-348.817917 87.700	
2-methylcyclohexanone_ax	-348.844584	-348.876726	-348.835702	86.341
2-methylcyclohexanone_ax radical	-349.387464	-349.420281	-349.378149	88.674
2-methylcyclohexanone_ax radical anion	-348.818905	-348.851720	-348.809914 87.987	
2-methyl cyclohexol_eq	-350.032024	-350.064081	-350.022779	86.928

2-methyl cyclohexol_eq radical   -349.389217   -349.422139   -349.379894
88.913
2-methylcyclohexol_ax   -350.029000   -350.060899   -350.019802   86.497
2-methylcyclohexol_ax radical   -349.387464   -349.420281   -349.378149
88.674
methylhydrindanol   -466.643147   -466.677983   -466.631694   97.422
methylhydrindanol radical   -465.989134   -466.024853   -465.977454   99.758
1-butene-2-cyclohexanone   -465.424182   -465.462486   -465.411753
106.778
1-butene-2-cyclohexanone radical   -465.966074   -466.005187   -465.953177
109.464
Trans-stilbene   -540.177797   -540.217439   -540.165532
109.247
Trans-stilbene radical   -540.744960   -540.785356   -540.732508
111.230
==
PCM Calculations(solvent=THF):

H2O   -76.380974   -76.398617   -76.377194   45.089
OH radical   -75.696673   -75.713599   -75.693368   42.579
Hydrogen atom   -0.502264   -0.512918   -0.499903
27.392
2-methylcyclohexanone_eq   -348.852987   -348.885114   -348.844102
86.315
2-methylcyclohexanone_eq radical   -349.393018   -349.425926   -349.383709
88.854
2-methylcyclohexanone_eq radical anion   -348.899453   -348.931703   -348.890764
86.164
2-methylcyclohexanone_ax   -348.850399   -348.882596   -348.841493
86.508
2-methylcyclohexanone_ax radical   -349.391452   -349.424291   -349.382115
88.767
2-methylcyclohexanone_ax radical anion   -348.895682   -348.928011   -348.886913
86.498
2-methyl cyclohexol_eq   -350.036210   -350.068318   -350.026907   87.155
2-methyl cyclohexol_eq radical   -349.393018   -349.425926   -349.383709
88.854
2-methylcyclohexol_ax   -350.033146   -350.065101   -350.023902   86.711

2-methylcyclohexol_ax radical   -349.391452   -349.424291   -349.382115
88.767

methylhydrindanol   -466.646367   -466.681173   -466.634914   97.359

methylhydrindanol radical   -465.992379   -466.028134   -465.980623
99.994

1-butene-2-cyclohexanone   -465.430770   -465.469018   -465.418344
106.653

1-butene-2-cyclohexanone radical   -465.970854   -466.009939   -465.957985
109.346

Trans-stilbene   -540.183009   -540.223175   -540.170732   110.375

Trans-stilbene radical   -540.749605   -540.790462   -540.737131   112.245

==

OH radical + H_atom → H2O   (gas)

ΔH = -75.689283 -0.499886 -(-76.370917) = 0.181748   627.5095 x 0.181748 = 114.0 kcal/mol

ΔG = -75.709512 -0.512900 -(-76.392334) = 0.169922   627.5095 x 0.169922 = 106.6 kcal/mol

OH radical   + H_atom → H2O   (iefpcm,thf)

ΔH = -75.693368 -0.499903 -(-76.377194) = 0.183923   627.5095 x 0.183923 = 115.4 kcal/mol

ΔG = -75.713599 -0.512918 -(-76.398617) = 0.172100   627.5095 x 0.172100 = 108.0 kcal/mol

==

2-methylcyclohexanone_eq + H_atom → 2-methyocyclohexanone_eq OH radical   (gas)

ΔH = -348.838652 -0.499886 -(-349.379894) = 0.041356   627.5095 x 0.041356 = 26.0 kcal/mol

ΔG = -348.879659 -0.512900 -(-349.422140) = 0.029581   627.5095 x 0.029581 = 18.6 kcal/mol

2-methylcyclohexanone_eq + H_atom → 2-methyocyclohexanone_eq OH radical (iefpcm,thf)

ΔH = -348.844102 -0.499903 -(-349.383709) = 0.039704   627.5095 x 0.039704 = 24.9 kcal/mol

ΔG = -348.885114 -0.512918 -(-349.425926) = 0.027894   627.5095 x 0.027894 = 17.5 kcal/mol

methylcyclohexanone_eq → methylcyclohexanone_eq O radical anion   (gas)

ΔH = -348.838652 -(-348.817917) = -0.020735   627.5095 x -0.020735 = -13.0 kcal/mol

ΔG = -348.879659 -(-348.859586) = -0.020073   627.5095 x -0.020073 = -12.6 kcal/mol

methylcyclohexanone_eq → methylcyclohexanone_eq O radical anion (iefpcm,thf)
ΔH = -348.844102 -(-348.890764) = 0.046662   627.5095 x 0.046662 = 29.3 kcal/mol
ΔG = -348.885114 -(-348.931703) = 0.046589   627.5095 x 0.046589 = 29.2 kcal/mol

2-methylcyclohexanone_eq   NPA = -0.564(gas) -0.609(iefpcm,thf)
2-methylcyclohexanone_eq OH radical   NPA = -0.708(gas) -
0.726(iefpcm,thf)
2-methylcyclohexanone_eq O radical anion NPA = -0.717(gas) -0.889(iefpcm,thf)
==
2-methylcyclohexanone_ax + H_atom → 2-methyocyclohexanone_ax OH radical (gas)
ΔH = -348.835702 -0.499886 -(-349.378149) = 0.042561   627.5095 x 0.042561 = 26.7 kcal/mol
ΔG = -348.876726 -0.512900 -(-349.420281) = 0.030655   627.5095 x 0.030655 = 19.2 kcal/mol

2-methylcyclohexanone_ax + H_atom → 2-methyocyclohexanone_ax OH radical
(iefpcm,thf)
ΔH = -348.841493 -0.499903 -(-349.382115) = 0.040719   627.5095 x 0.040719 = 25.6 kcal/mol
ΔG = -348.882596 -0.512918 -(-349.424291) = 0.028777   627.5095 x 0.028777 = 18.1 kcal/mol

methylcyclohexanone_ax → methylcyclohexanone_ax O radical anion (gas)
ΔH = -348.835702 -(-348.809914) = -0.025788   627.5095 x -0.025788 = -16.2 kcal/mol
ΔG = -348.876726 -(-348.851720) = -0.025006   627.5095 x -0.025006 = -15.7 kcal/mol

methylcyclohexanone_ax → methylcyclohexanone_ax O radical anion (iefpcm,thf)
ΔH = -348.841493 -(-348.886913) = 0.045420   627.5095 x 0.045420 = 28.5 kcal/mol
ΔG = -348.882596 -(-348.928011) = 0.045415   627.5095 x 0.045415 = 28.5 kcal/mol

2-methylcyclohexanone_ax   NPA = -0.564(gas) -0.612(iefpcm,thf)

2-methylcyclohexanone_ax OH radical   NPA = -0.712(gas) - 0.731(iefpcm,thf)

2-methylcyclohexanone_ax O radical anion NPA = -0.751(gas) -0.910(iefpcm,thf)

==

2-methylcyclohexol_eq radical + H_atom → 2-methylcyclohexol_eq   (gas)

ΔH = -349.379894 -0.499886 -(-350.022779) = 0.142999   627.5095 x 0.142999 = 89.7 kcal/mol

ΔG = -349.422139 -0.512900 -(-350.064081) = 0.129042   627.5095 x 0.129042 = 81.0 kcal/mol

2-methylcyclohexol_eq radical + H_atom → 2-methylcyclohexol_eq   (iefpcm,thf)

ΔH = -349.383709 -0.499903 -(-350.026907) = 0.143295   627.5095 x 0.143295 = 89.9 kcal/mol

ΔG = -349.425926 -0.512918 -(-350.068318) = 0.129474   627.5095 x 0.129474 = 81.2 kcal/mol

==

2-methylcyclohexol_ax radical + H_atom → 2-methylcyclohexol_ax   (gas)

ΔH = -349.378149 -0.499886 -(-350.019802) = 0.141767   627.5095 x 0.141767 = 89.0 kcal/mol

ΔG = -349.420281 -0.512900 -(-350.060899) = 0.127718   627.5095 x 0.127718 = 80.1 kcal/mol

2-methylcyclohexol_ax radical + H_atom → 2-methylcyclohexol_ax   (iefpcm,thf)

ΔH = -349.382115 -0.499903 -(-350.023902) = 0.141884   627.5095 x 0.141884 = 89.0 kcal/mol

ΔG = -349.424291 -0.512918 -(-350.065101) = 0.127892   627.5095 x 0.127892 = 80.3 kcal/mol

==

methylhydrindanol radical + H_atom → methylhydrindanol   (gas)

ΔH = -465.977454 -0.499886 -(-466.631694) = 0.154354   627.5095 x 0.154354 = 96.9 kcal/mol

ΔG = -466.024853 -0.512900 -(-466.677983) = 0.140230   627.5095 x 0.140230 = 88.0 kcal/mol

methylhydrindanol radical + H_atom → methylhydrindanol   (iefpcm,thf)

ΔH = -465.980623 -0.499903 -(-466.634914) = 0.154388   627.5095 x 0.154388 = 96.9 kcal/mol

ΔG = -466.028134 -0.512918 -(-466.681173) = 0.140121   627.5095 x 0.140121 = 87.9 kcal/mol

==

1-butene-2-cyclohexanone + H_atom → 1-butene-2-cyclohexanone radical   (gas)

ΔH = -465.411753 -0.499886 -(-465.953177) = 0.041538   627.5095 x 0.041538 = 26.1 kcal/mol

ΔG = -465.462486 -0.512900 -(-466.005187) = 0.029801   627.5095 x 0.029801 = 18.7 kcal/mol

1-butene-2-cyclohexanone + H_atom → 1-butene-2-cyclohexanone radical (iefpcm,thf)
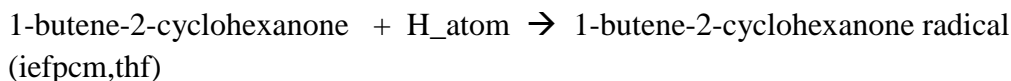
ΔH = -465.418344 -0.499903 -(-465.957985) = 0.039738   627.5095 x 0.039738 = 24.9 kcal/mol

ΔG = -465.469018 -0.512918 -(-466.009939) = 0.028003   627.5095 x 0.028003 = 17.6 kcal/mol
===
trans-stilbene + H_atom → trans-stilbene radical (gas)
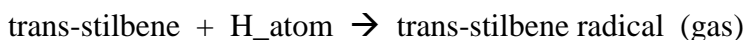
ΔH = -540.165532 -0.499886 -(-540.732508) = 0.067090   627.5095 x 0.067090 = 42.1 kcal/mol

ΔG = -540.217439 -0.512900 -(-540.785356) = 0.055017   627.5095 x 0.055017 = 34.5 kcal/mol

trans-stilbene + H_atom → trans-stilbene radical (iefpcm,thf)

ΔH = -540.170732 -0.499903 -(-540.737131) = 0.066496   627.5095 x 0.066496 = 41.7 kcal/mol

ΔG = -540.223175 -0.512918 -(-540.790462) = 0.054369   627.5095 x 0.054369 = 34.1 kcal/mol

10.5 Alternative Hydrogen Atom Transfer Promoters for Reductions of SmI_2
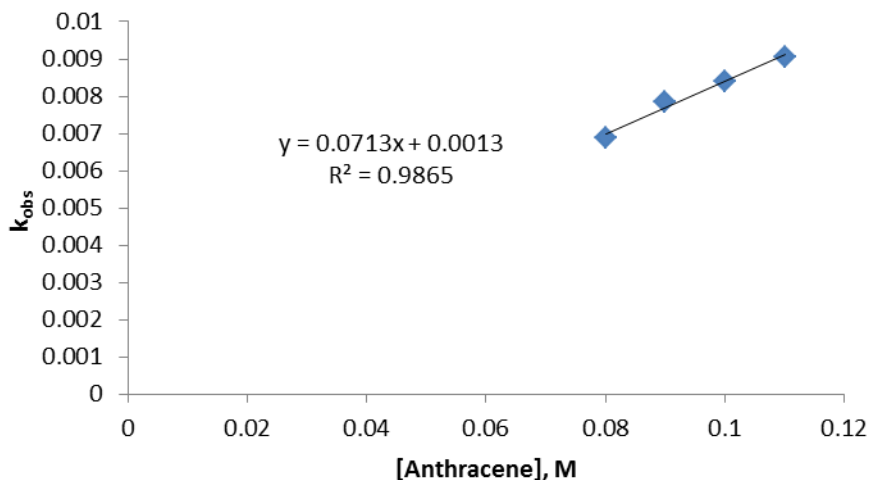
Figure 10.76 Rate order of anthracene with SmI2-DMAE.
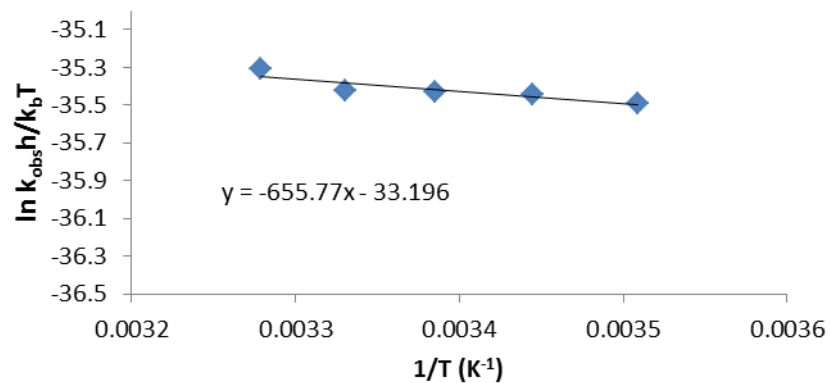
Figure 10.77 Sample Eyring of anthracene with SmI2-DMAE with 10mM SmI$_2$, 120mM Anthracene, 50mM DMAE measured over 12-32°C at 560nm
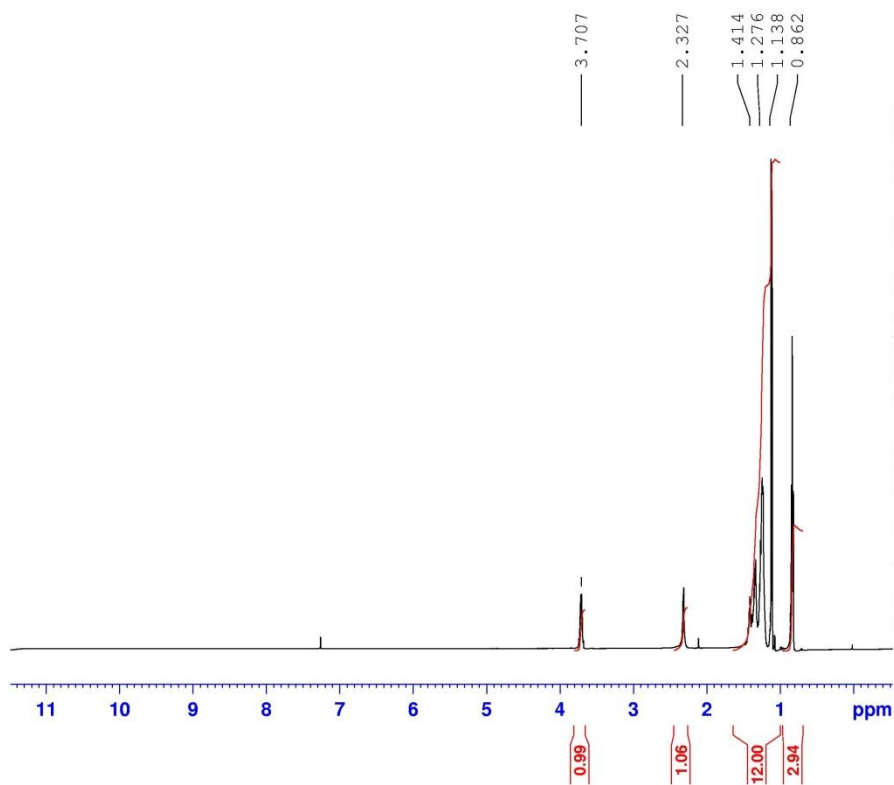
Figure 10.78 ^{1}H NMR Spectra of 2-Heptanol.
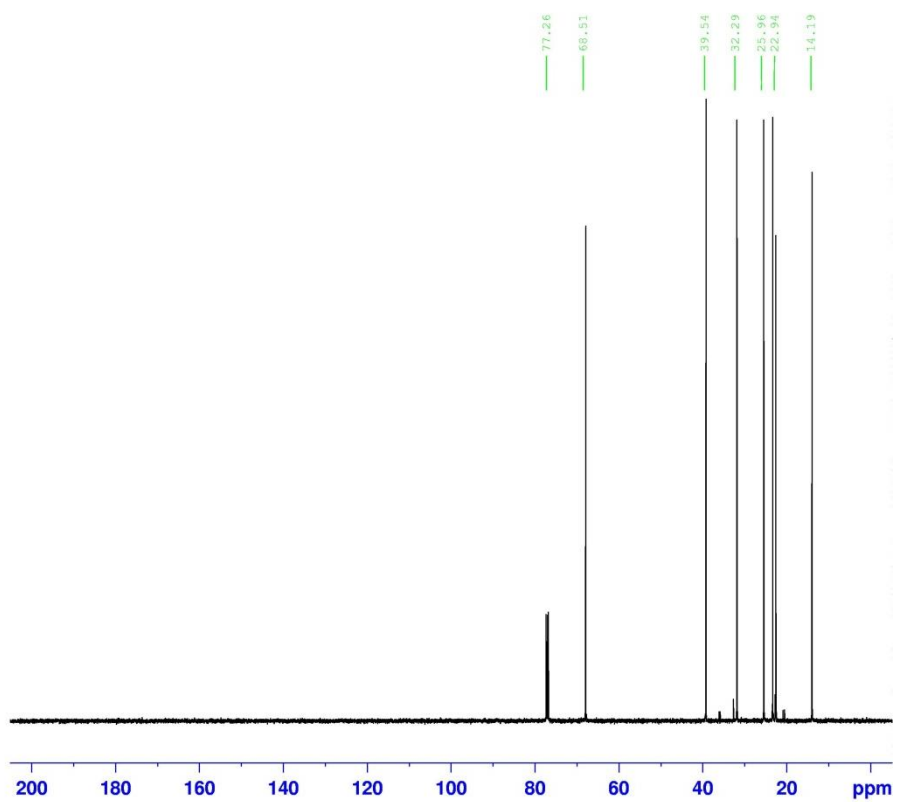
Figure 10.79 ^{13}C NMR Spectra of 2-Heptanol.
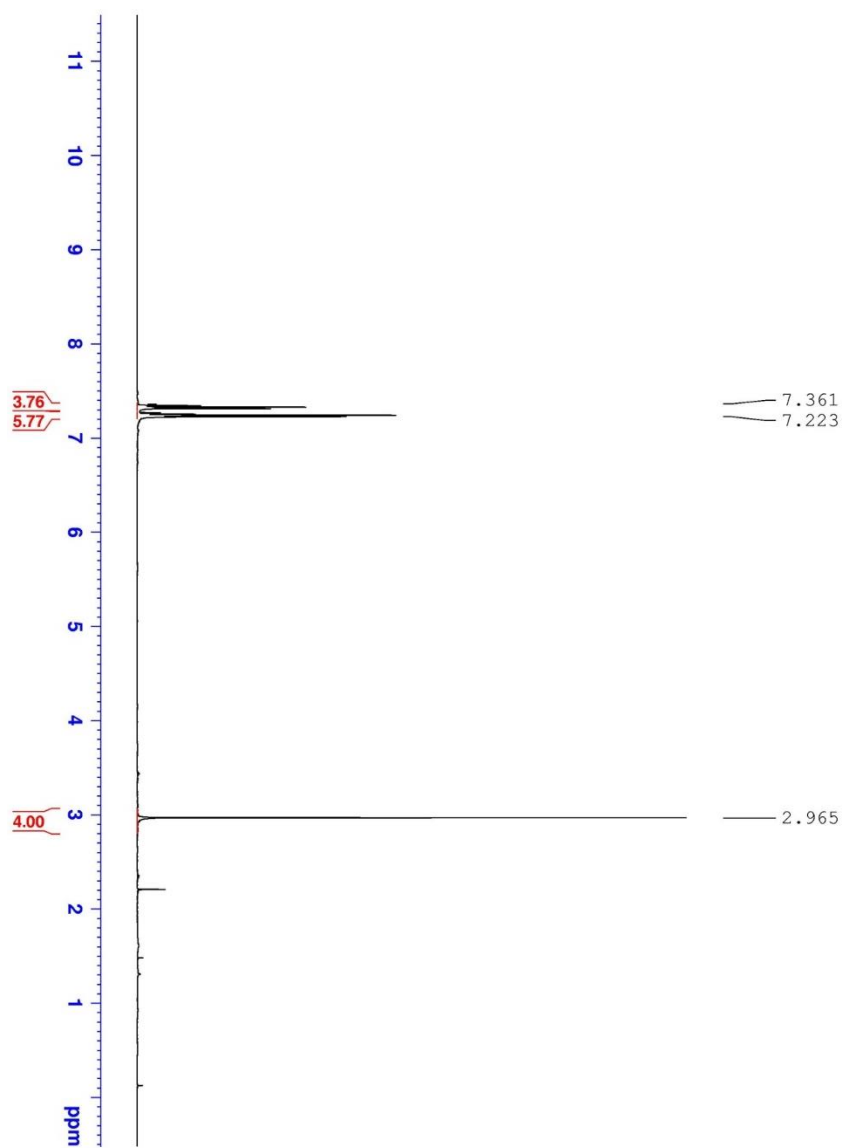
Figure 10.80 ^{1}H NMR Spectra of bibenzyl.
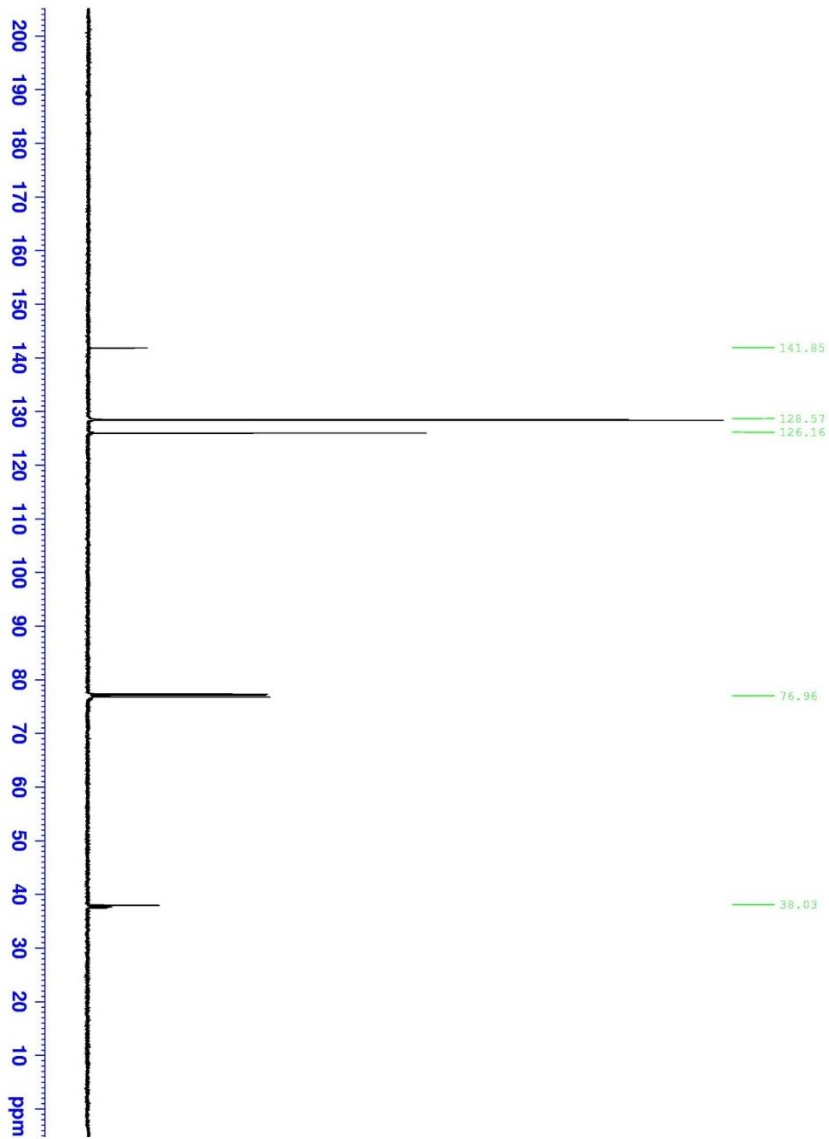
Figure 10.81 ^{13}C NMR Spectra of bibenzyl.
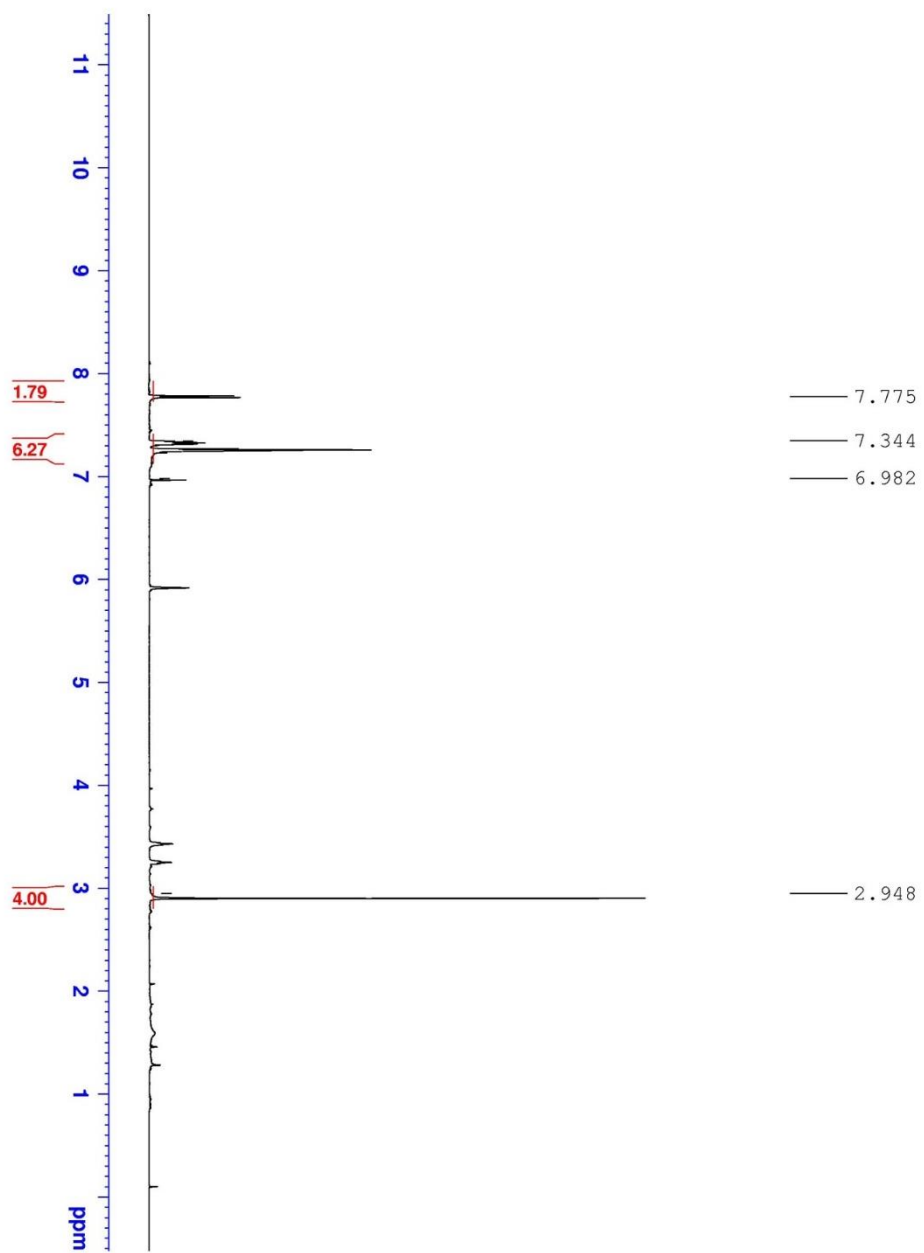
Figure 10.82 ^{1}H NMR Spectra of 9,10-dihydrophenanthrene.
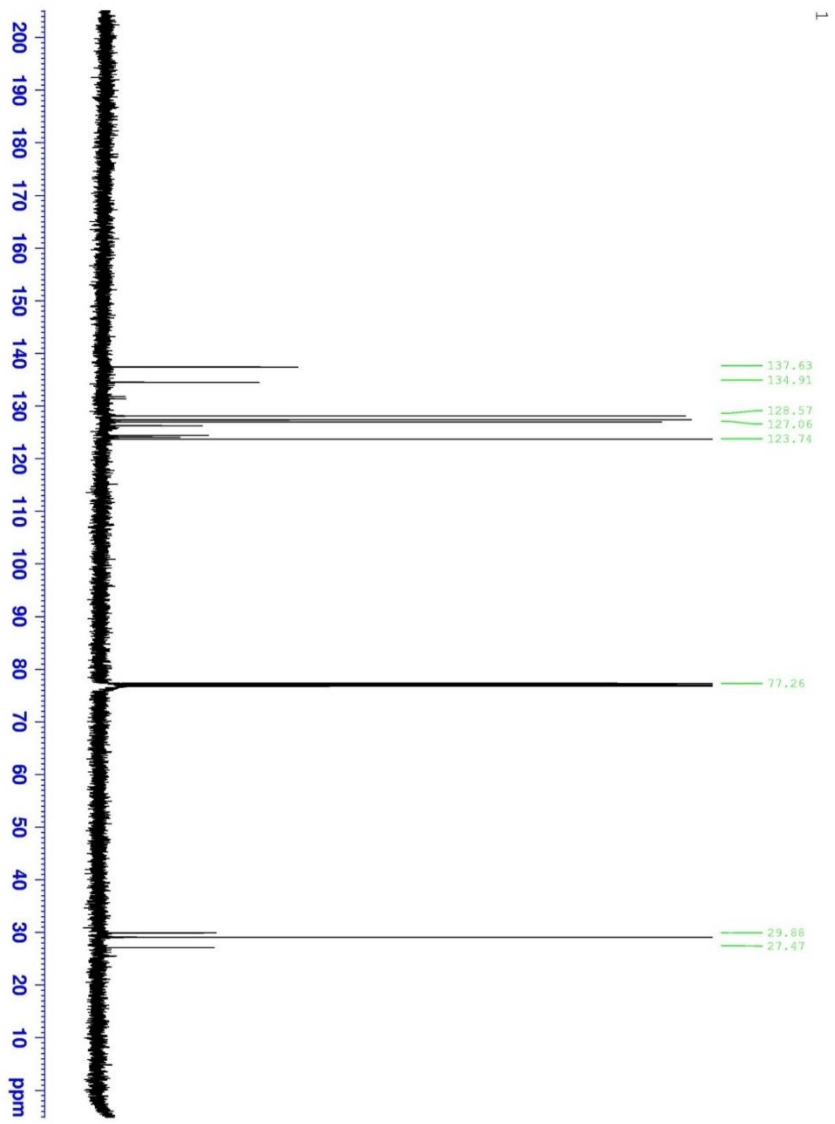
Figure 10.83 ^{1}H NMR Spectra of 9,10-dihydrophenanthrene.
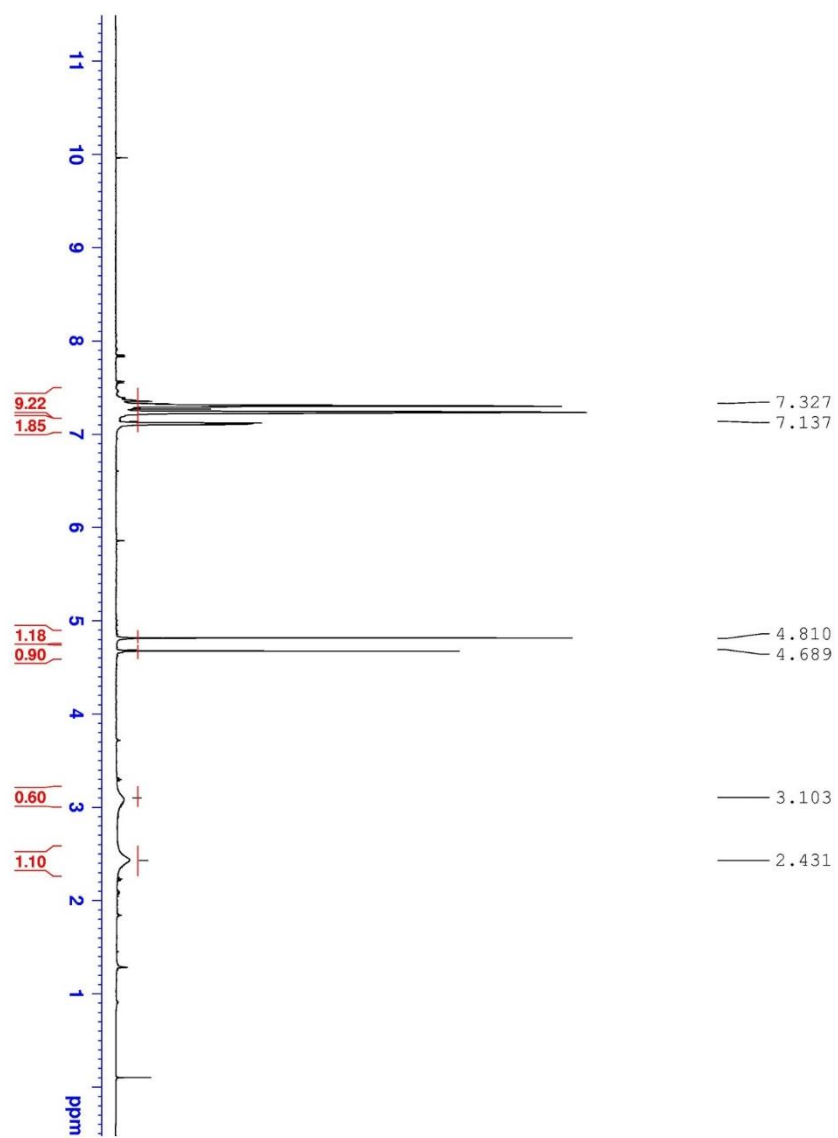
Figure 10.84 [^1]H NMR Spectra of hydrobenzoin.
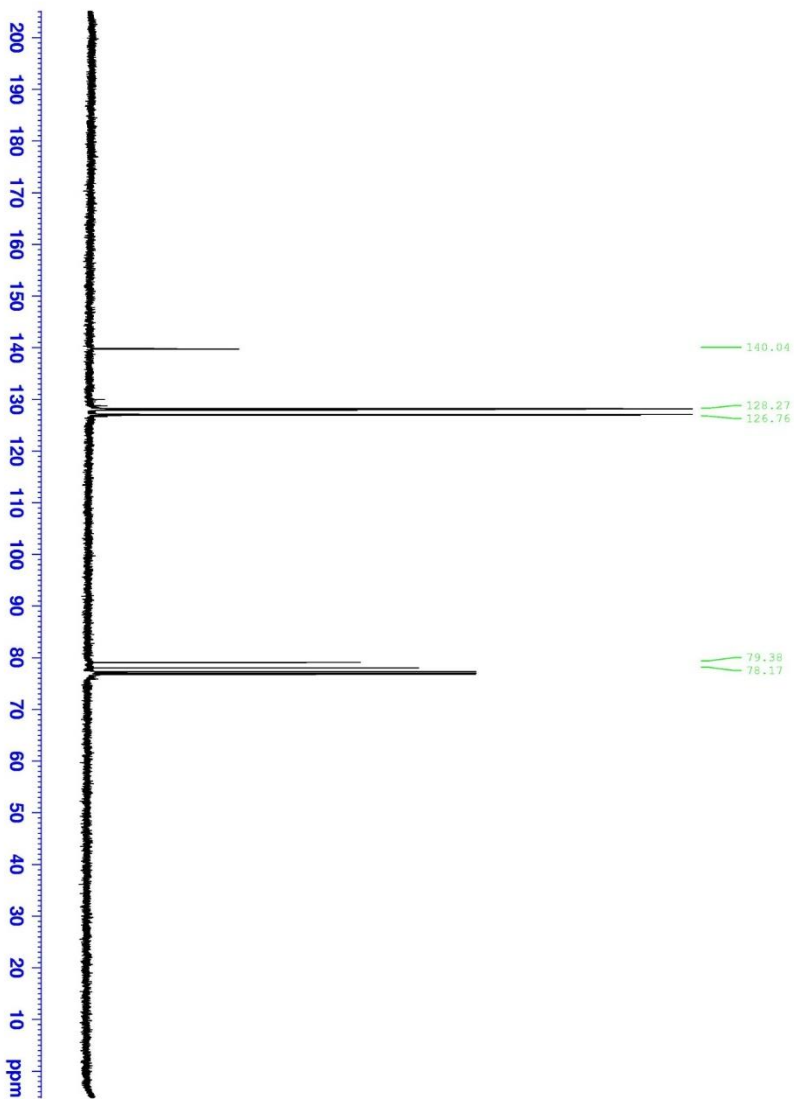
Figure 10.85 ^{13}C NMR Spectra of hydrobenzoin.
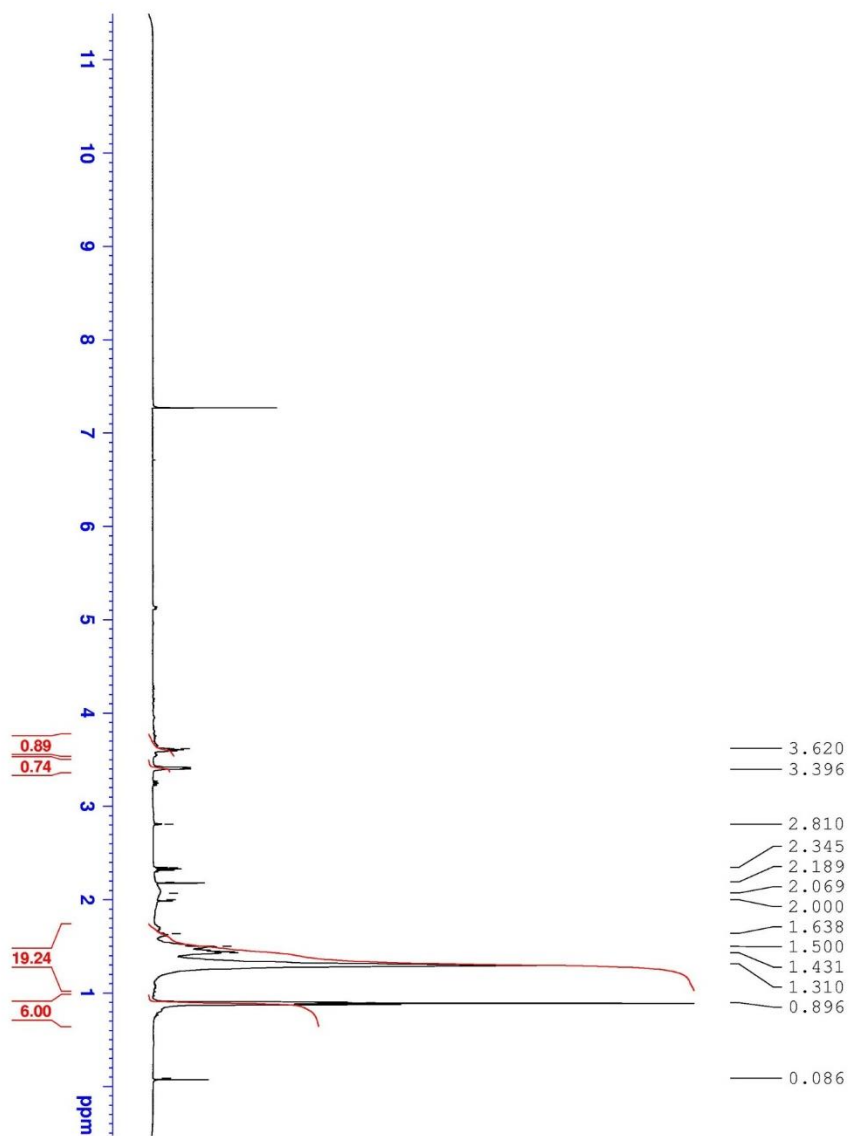
Figure 10.86 ^{1}H NMR Spectra of 7.8-tetradecanediol
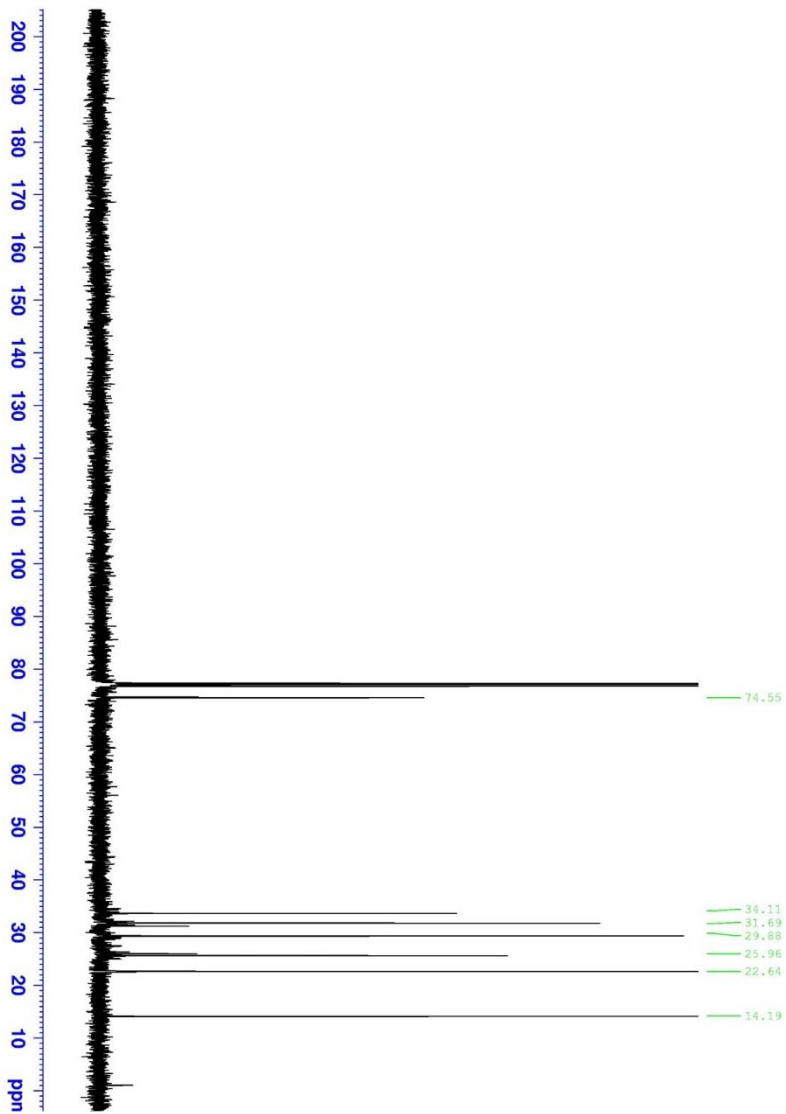
Figure 10.87 ^{13}C NMR Spectra of 7,8-tetradecanediol.
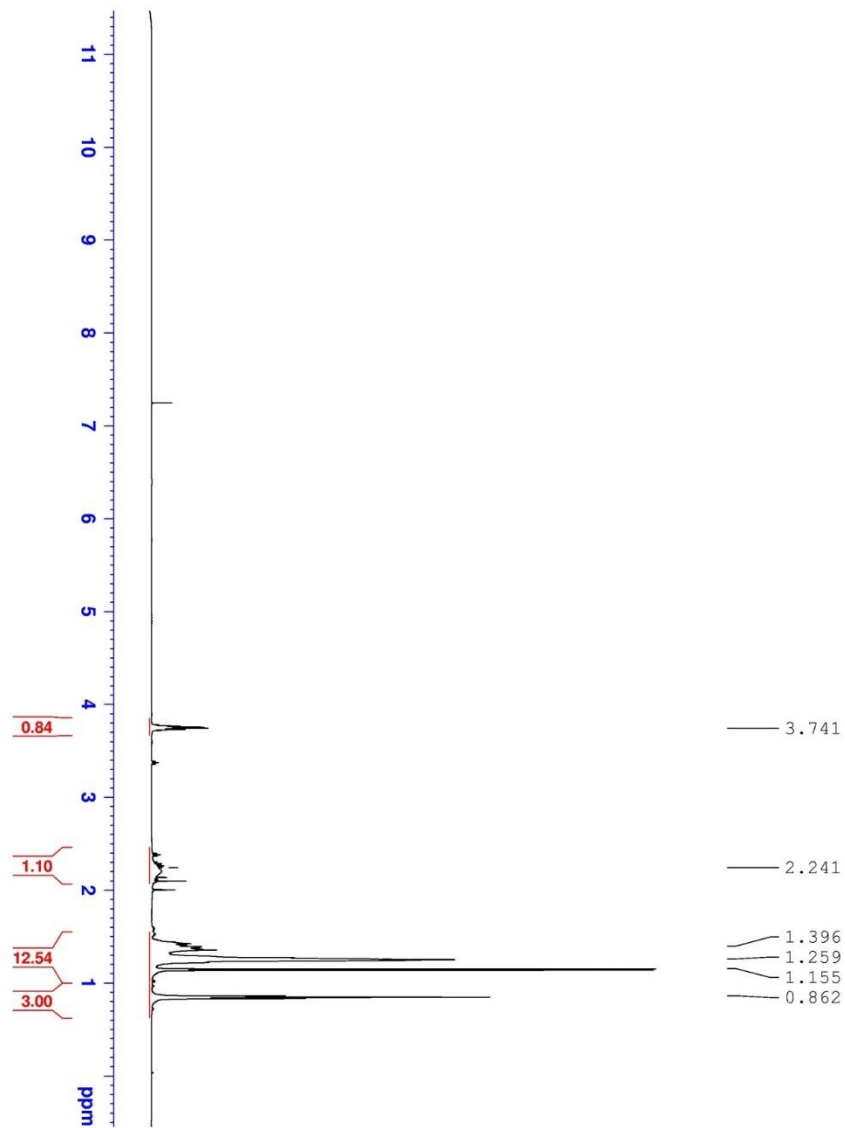
Figure 10.88 ^{1}H NMR Spectra of 2-octanol.
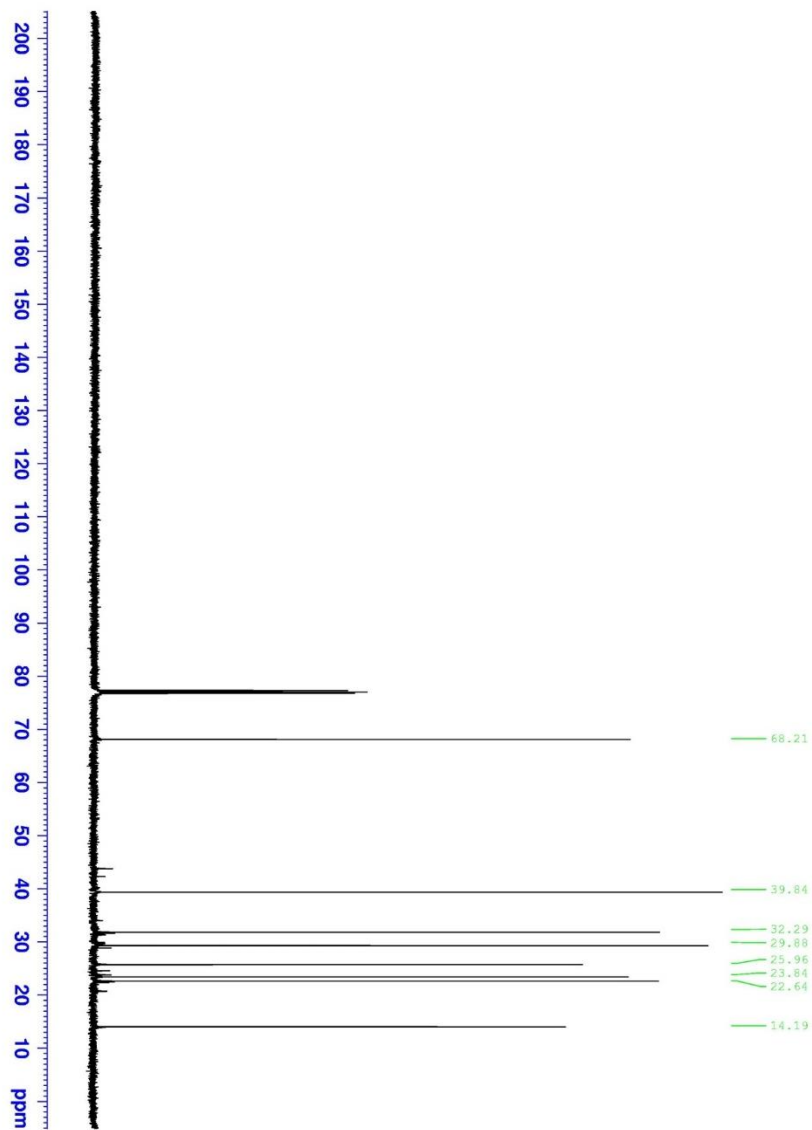
Figure 10.89 ^{13}C NMR Spectra of 2-octanol.
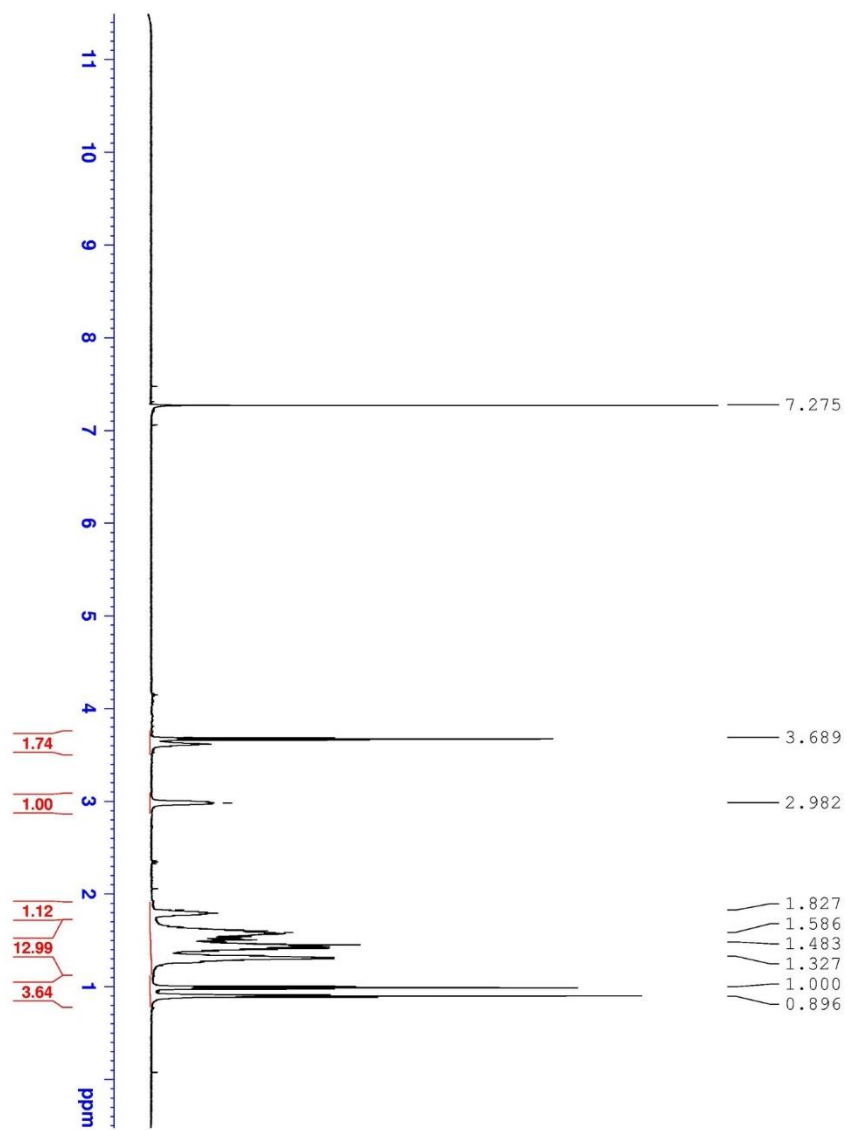
Figure 10.90 ^{1}H NMR Spectra of 1,5-decanediol.
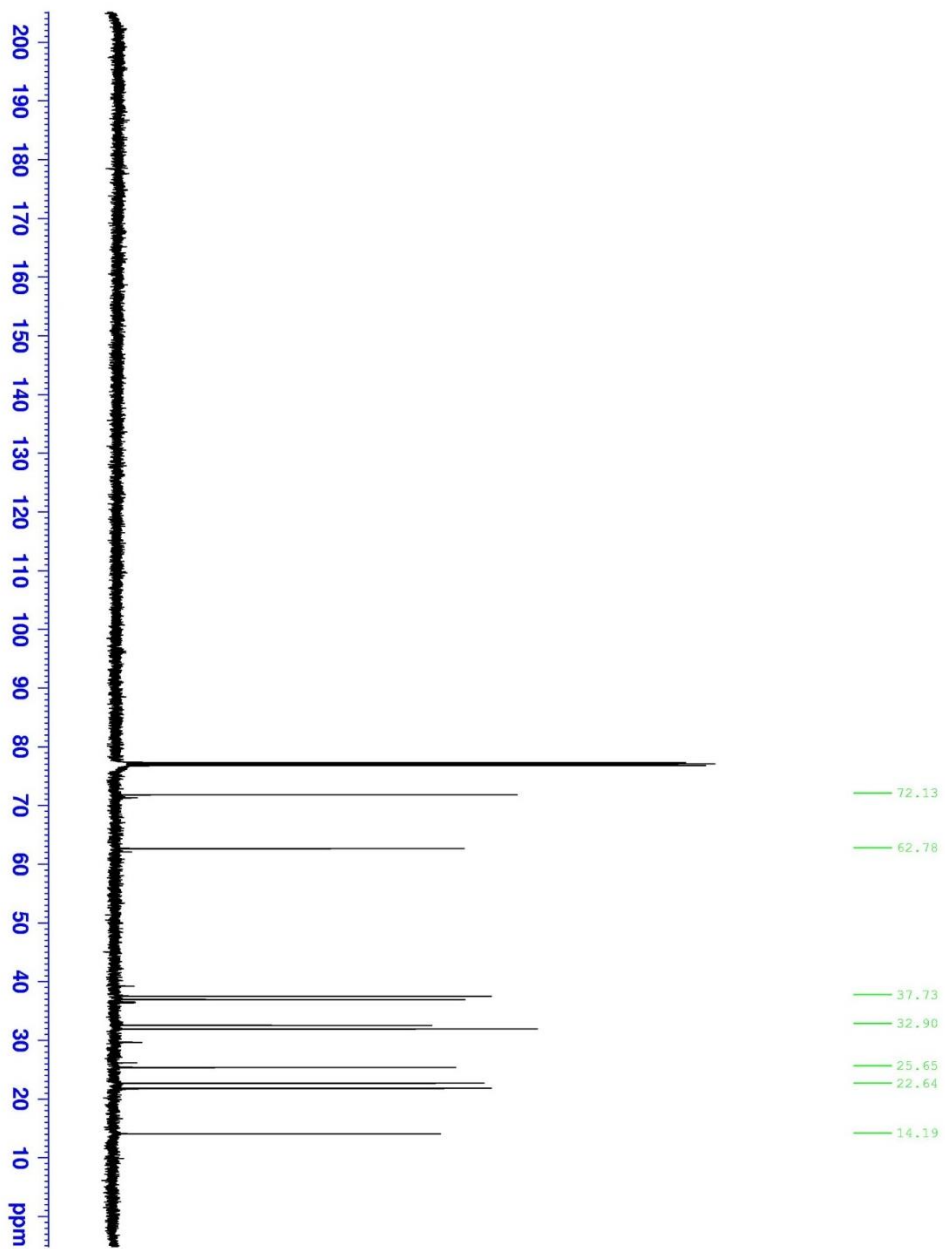
Figure 10.91

^{13}C NMR Spectra of 1,5-decanediol.
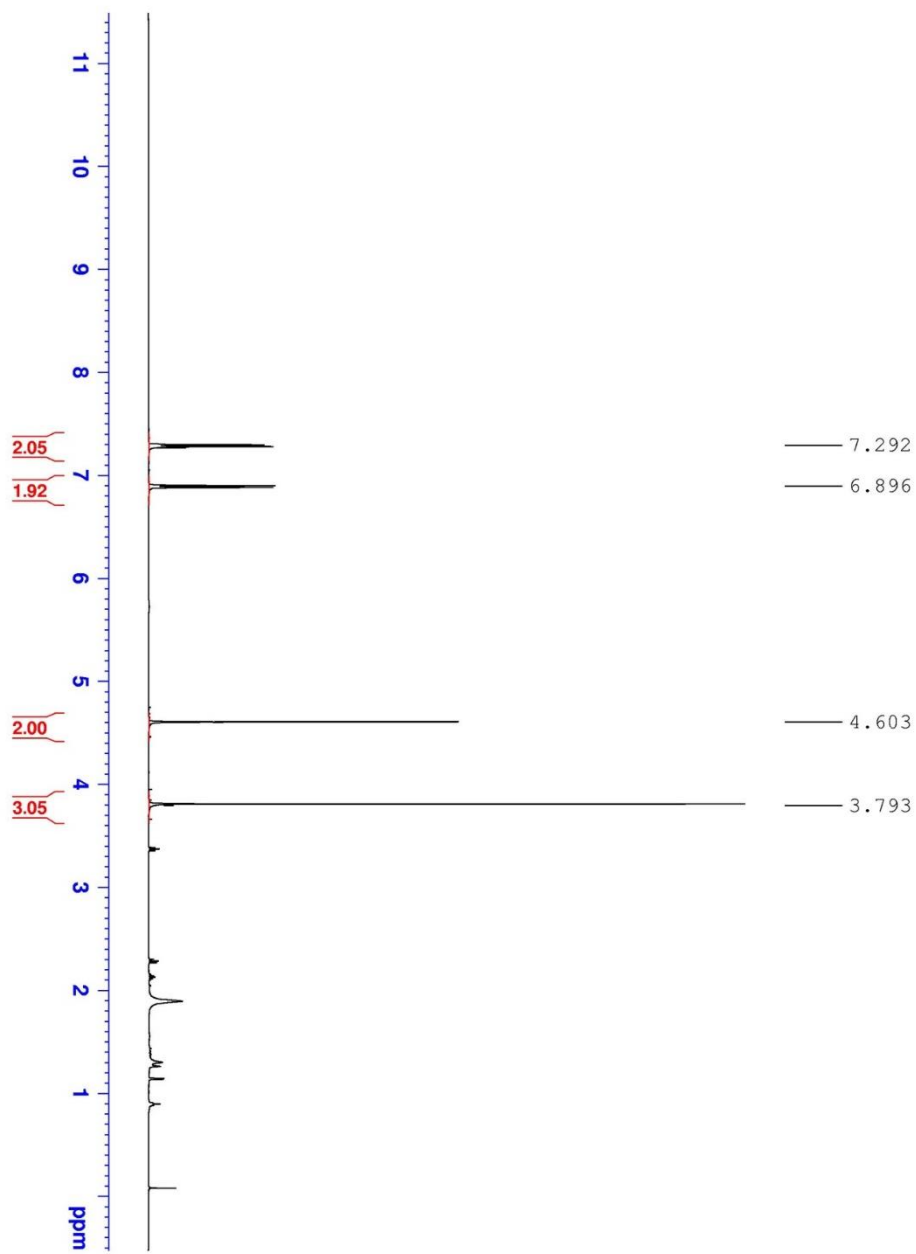
Figure 10.92 ^{1}H NMR Spectra of 4-methoxybenzylalcohol.
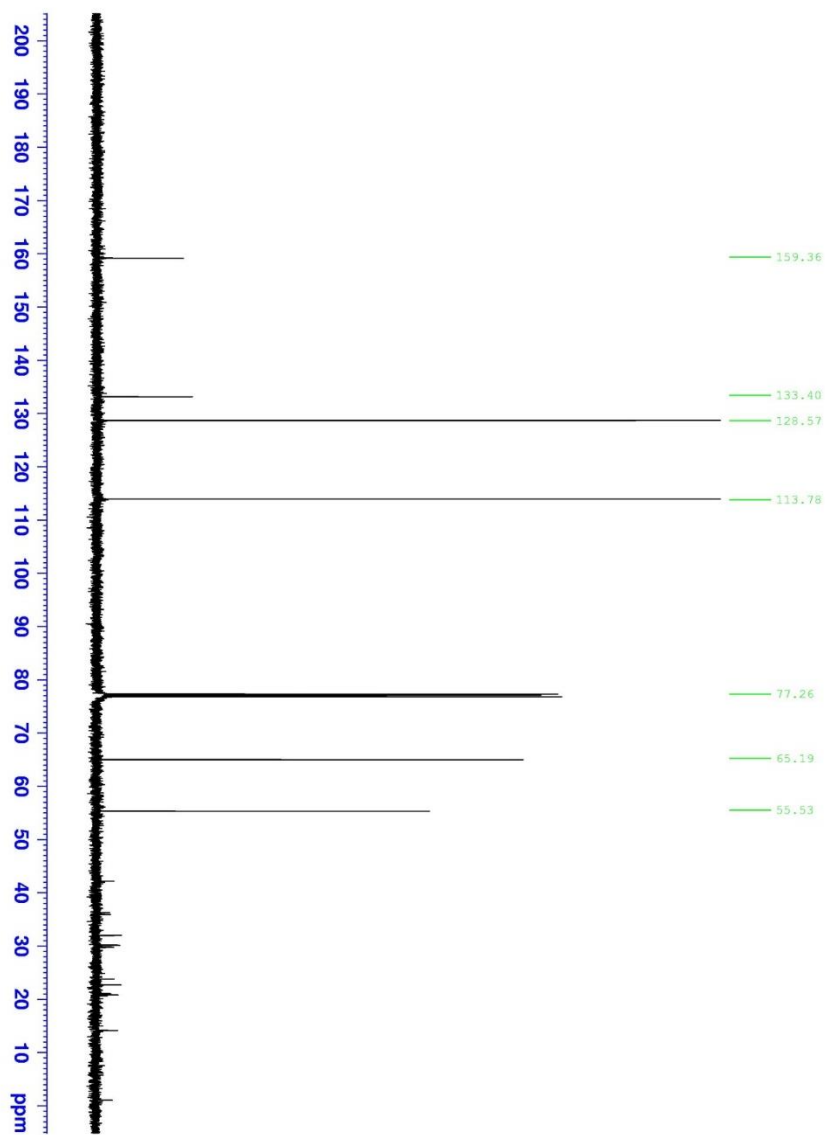
Figure 10.93 ^{13}C NMR Spectra of 4-methoxybenzylalcohol.
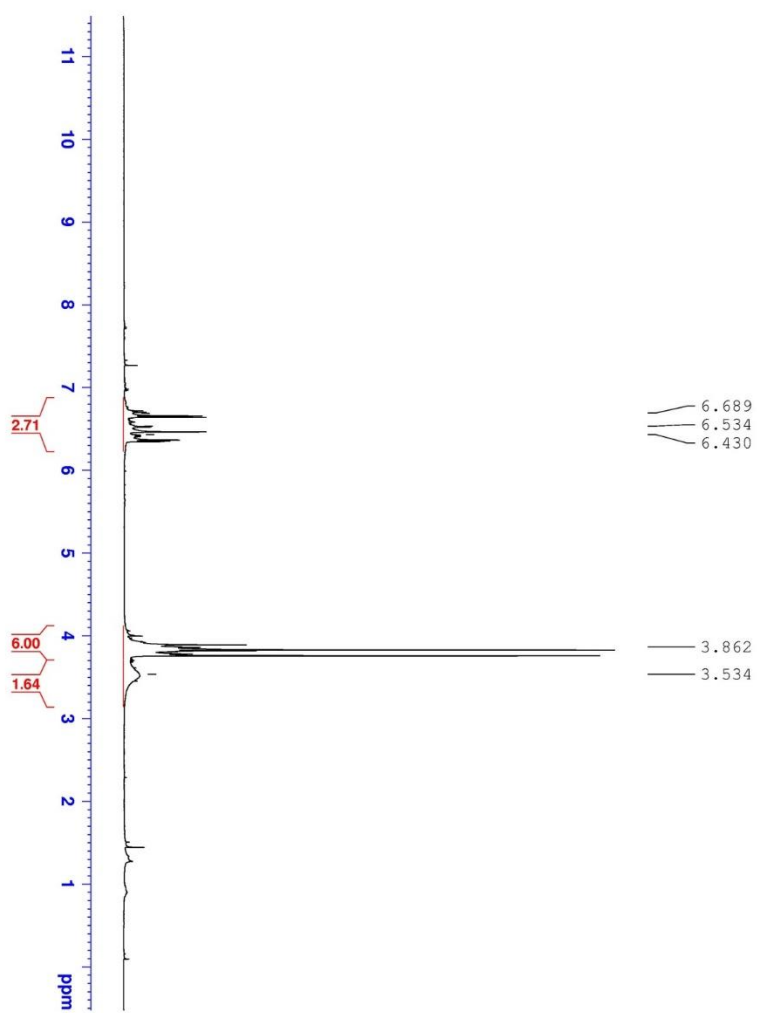
Figure 10.93 ^{1}H NMR Spectra of 2,4-dimethoxyaniline.
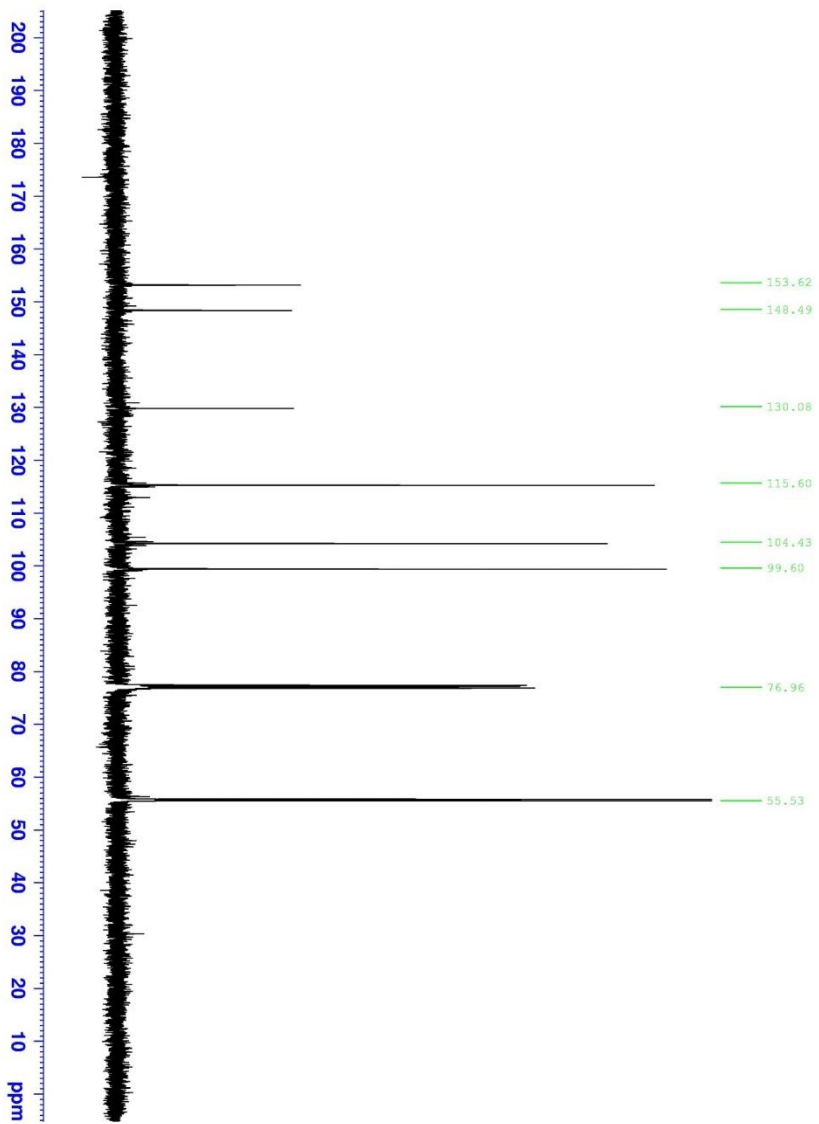
Figure 10.94 ^{13}C NMR Spectra of 2,4-dimethoxyaniline.
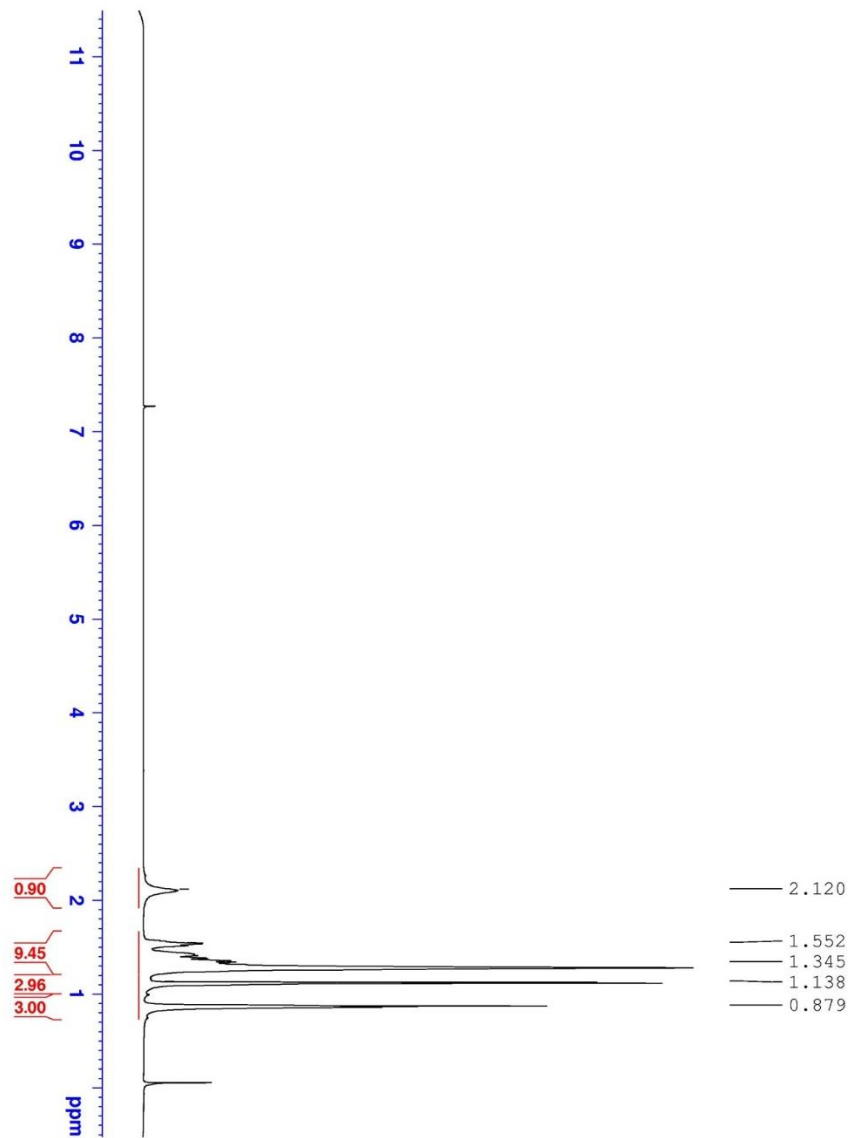
Figure 10.95 ^{1}H NMR Spectra of 7,8-dimethyl-7,8-tetradecanediol.
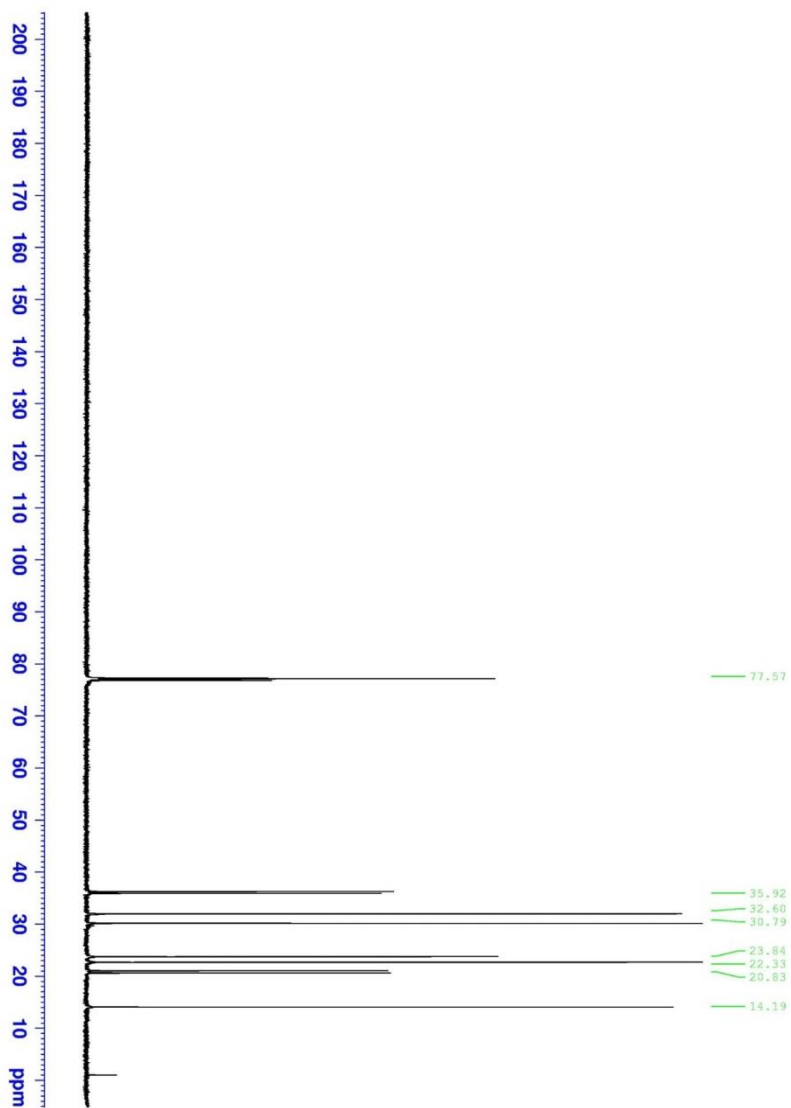
Figure 10.96 ¹³C NMR Spectra of 7,8-dimethyl-7,8-tetradecanediol.

10.5 Computational Methods

Gaussian09(1) programs were used for the calculations with the APF-D(2) hybrid DFT(3) method and the 6-311+g(2d,p) basis set(4,5). Solvation values were calculated using the polarizable continuum model with integral equation formalism. IEFPCM(6,7), with tetrahydrofuran as the solvent. The geometries and frequencies were calculated with uapfd/6-311+g(2d,p) opt=(calcfc,tight) int=(ultrafine,acc2e=12)pop=npa. scrf=(iefpcm,solvent=thf) was added to the route section for solvation. Natural-population analysis(8) was obtained by including pop=npa.

1) Gaussian 09, Revision D.01,

M. J. Frisch, G. W. Trucks, H. B. Schlegel, G. E. Scuseria,
M. A. Robb, J. R. Cheeseman, G. Scalmani, V. Barone, B. Mennucci,
G. A. Petersson, H. Nakatsuji, M. Caricato, X. Li, H. P. Hratchian,
A. F. Izmaylov, J. Bloino, G. Zheng, J. L. Sonnenberg, M. Hada,
M. Ehara, K. Toyota, R. Fukuda, J. Hasegawa, M. Ishida, T. Nakajima,
Y. Honda, O. Kitao, H. Nakai, T. Vreven, J. A. Montgomery, Jr.,
J. E. Peralta, F. Ogliaro, M. Bearpark, J. J. Heyd, E. Brothers,
K. N. Kudin, V. N. Staroverov, T. Keith, R. Kobayashi, J. Normand,
K. Raghavachari, A. Rendell, J. C. Burant, S. S. Iyengar, J. Tomasi,
M. Cossi, N. Rega, J. M. Millam, M. Klene, J. E. Knox, J. B. Cross,
V. Bakken, C. Adamo, J. Jaramillo, R. Gomperts, R. E. Stratmann,
O. Yazyev, A. J. Austin, R. Cammi, C. Pomelli, J. W. Ochterski,
R. L. Martin, K. Morokuma, V. G. Zakrzewski, G. A. Voth,
P. Salvador, J. J. Dannenberg, S. Dapprich, A. D. Daniels,
O. Farkas, J. B. Foresman, J. V. Ortiz, J. Cioslowski,
and D. J. Fox, Gaussian, Inc., Wallingford CT, 2013

2)A. Austin, G. Petersson, M. J. Frisch, F. J. Dobek, G. Scalmani, and K. Throssell, "A density functional with spherical atom dispersion terms", *J. Chem. Theory and Comput*. **8** (2012) 4989.

3) R. G. Parr and W. Yang, *Density-functional theory of atoms and molecules* (Oxford Univ. Press, Oxford, 1989).

4)A. D. McLean and G. S. Chandler, "Contracted Gaussian-basis sets for molecular calculations. 1. 2nd row atoms, Z=11-18," *J. Chem. Phys.*, **72** (1980) 5639-48

5)K. Raghavachari, J. S. Binkley, R. Seeger, and J. A. Pople, "Self-Consistent Molecular Orbital Methods. 20. Basis set for correlated wave-functions," J. Chem. Phys., 72 (1980) 650-54.

6)E. Cancès, B. Mennucci, and J. Tomasi, "A new integral equation formalism for the polarizable continuum model: Theoretical background and applications to isotropic and anistropic dielectrics," *J. Chem. Phys.*, **107** (1997) 3032-41.

7)J. Tomasi, B. Mennucci, and R. Cammi, "Quantum mechanical continuum solvation models," *Chem. Rev.*, **105** (2005) 2999-3093.

8)A. E. Reed, R. B. Weinstock, and F. Weinhold, "Natural-population analysis," *J. Chem. Phys.*, **83** (1985) 735-46.

In the table below, E+ZPE, G, & H, energies are in hartree particle. S is in Cal/Mol.

	E+ZPE	G	H	S
Gas Phase Calculations:				
Hydrogen atom	-0.502246	-0.512900	-0.499886	
27.392				
Pyrrolidone	-286.378947	-286.407714	-286.372634	
73.833				
Pyrrolidone radical	-285.712597	-285.742224	-285.706306	
75.597				
N-methylacetamide	-248.298722	-248.329585	-248.291127	
80.942				
N-methylacetamide radical	-247.635250	-247.666187	-247.627815	
80.761				
Anthracene	-539.022617	-539.056793	-539.012186	
93.882				
Anthracene radical	-539.591462	-539.628608	-539.580404	
101.455				
Phenanthrene	-539.031261	-539.066187	-539.020832	
95.458				
Phenanthrene radical	-539.582274	-539.619371	-539.571137	
101.517				

Trans-stilbene   -540.177797   -540.217434   -540.165532
109.237

Trans-stilbene radical   -540.745002   -540.786629   -540.732357
114.227

PCM Calculations(solvent=THF):

Hydrogen atom   -0.502264   -0.512918   -0.499903
27.392

2-Pyrrolidone   -286.388164   -286.416893   -286.381873
73.705

2-Pyrrolidone radical   -285.721192   -285.750781   -285.714913
75.492

N-methylacetamide   -248.307550   -248.337718   -248.300011
79.361

N-methylacetamide radical   -247.641198   -247.672190   -247.633722
80.961

Anthracene   -539.027046   -539.061910   -539.016611
95.340

Anthracene radical   -539.595870   -539.632953   -539.584817
101.311

Phenanthrene   -539.035877   -539.070960   -539.025405
95.877

Phenanthrene radical   -539.586812   -539.624231   -539.575648
102.251

Trans-stilbene   -540.183009   -540.223175   -540.170732
110.375

Trans-stilbene radical   -540.749714   -540.788732   -540.737972
106.833

===

2-pyrrolidone radical + H_atom → 2-pyrrolidone   (gas)

ΔH = -285.706306 + (-0.499886) – (-286.372634) = 0.166442   627.5095 x 0.166442 = 104.4 kcal/mol

ΔG = -285.742224 + (-0.512900) - (-286.407714) = 0.152590   627.5095 x 0.152590 = 95.8 kcal/mol

2-pyrrolidone radical + H_atom → 2-pyrrolidone (iefpcm,thf)
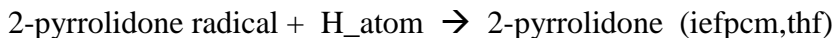
ΔH = -285.714913 + (-0.499903) – (-286.381873) = 0.167057   627.5095 x 0.167057 = 104.8 kcal/mol

ΔG = -285.750781 + (-0.512918) – (-286.416893) = 0.153194   627.5095 x 0.153194 = 96.1 kcal/mol

==

N-methylacetamide radical + H_atom → N-methylacetamide   (gas)

ΔH = -247.627815 + (-0.499886) – (-248.291127) = 0.163426   627.5095 x 0.163426 = 102.6 kcal/mol

ΔG = -247.666187 + (-0.512900) – (-248.329585) = 0.150498   627.5095 x 0.150498 = 94.4 kcal/mol

N-methylacetamide radical + H_atom → N-methylacetamide   (iefpcm,thf)
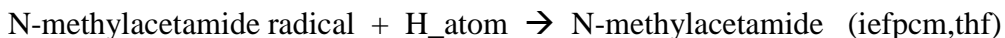
ΔH = -247.633722 + (-0.499903) – (-248.300011) = 0.166386   627.5095 x 0.166386 = 104.4 kcal/mol

ΔG = -247.672190 + (-0.512918) – (-248.337718) = 0.152610   627.5095 x 0.152610 = 95.8 kcal/mol

==

anthracene + H_atom → anthracene radical (gas)
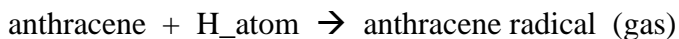
ΔH = -539.012186 -0.499886 -(-539.580404) = 0.068332   627.5095 x 0.068332 = 42.9 kcal/mol

ΔG = -539.056793 -0.512900 -(-539.628608) = 0.058915 627.5095 x 0.058915 = 37.0 kcal/mol

anthracene + H_atom → anthracene radical (iefpcm,thf)

ΔH = -539.016611 -0.499903 -(-539.584817) = 0.068303 627.5095 x 0.068303 = 42.9 kcal/mol

ΔG = -539.061910 -0.512918 -(-539.632953) = 0.058125 627.5095 x 0.058125 = 36.5 kcal/mol

==

phenanthrene + H_atom → phenanthrene radical (gas)
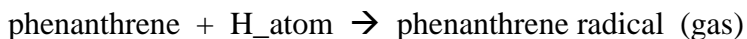
ΔH = -539.020832 -0.499886 -(-539.571137) = 0.050419 627.5095 x 0.050419 = 31.6 kcal/mol

ΔG = -539.066187 -0.512900 -(-539.619371) = 0.040284 627.5095 x 0.040284 = 26.3 kcal/mol

phenanthrene + H_atom → phenanthrene radical (iefpcm,thf)
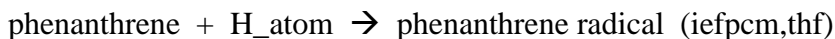
ΔH = -539.025405 -0.499903 -(-539.575648) = 0.050340 627.5095 x 0.050340 = 31.6 kcal/mol

ΔG = -539.070960 -0.512918 -(-539.624231) = 0.040353 627.5095 x 0.040353 = 25.3 kcal/mol

==

trans-stilbene + H_atom → trans-stilbene radical (gas)
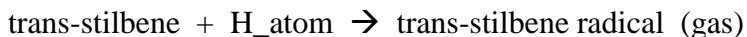
ΔH = -540.165532 -0.499886 -(-540.732357) = 0.066939 627.5095 x 0.066939 = 42.0 kcal/mol

ΔG = -540.217434 -0.512900 -(-540.786629) = 0.056295 627.5095 x 0.056295 = 35.3 kcal/mol

trans-stilbene + H_atom → trans-stilbene radical (iefpcm,thf)

324

ΔH = -540.170732 -0.499903 -(-540.737972) = 0.067337   627.5095 x 0.067337 = 42.3 kcal/mol

ΔG = -540.223175 -0.512918 -(-540.788732) = 0.052639   627.5095 x 0.052639 = 33.0 kcal/mol

===

10.6 Solvent-Dependent Substrate Reduction by {Sm[N(SiMe₃)₂]₂(THF)₂}: Elucidating the Role of Solvent Coordination in Sm(II) Chemistry
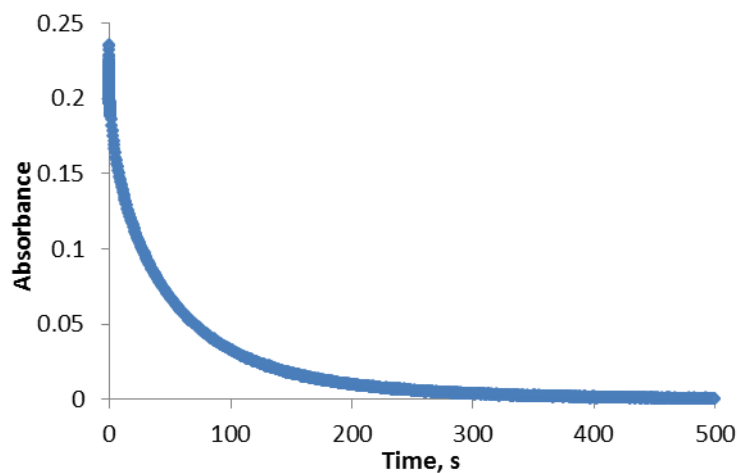
Figure 10. 97. Sample decay of 5mM {Sm[N(SiMe₃)₂]₂(THF)₂}, 50 mM 1-Bromododecane in THF at 15 °C, 400nm
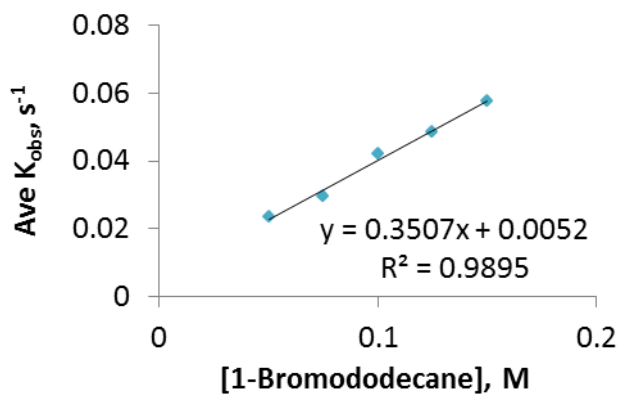
Figure 10. 98. Sample rate dependence of 50 mM 1-Bromododecane in THF at 15 °C, 400nm
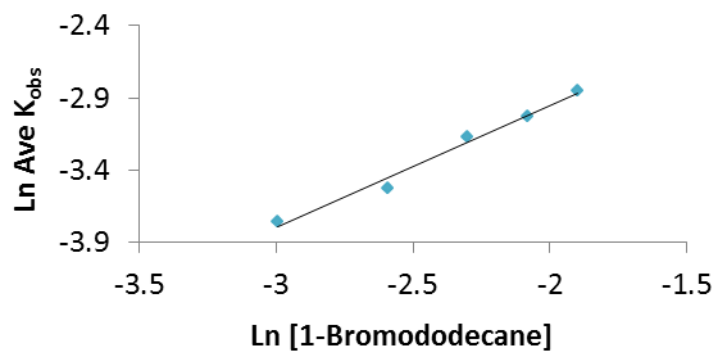
Figure 10. 99 Sample rate order plot of 1-Bromododecane in THF at 15 °C, 400nm
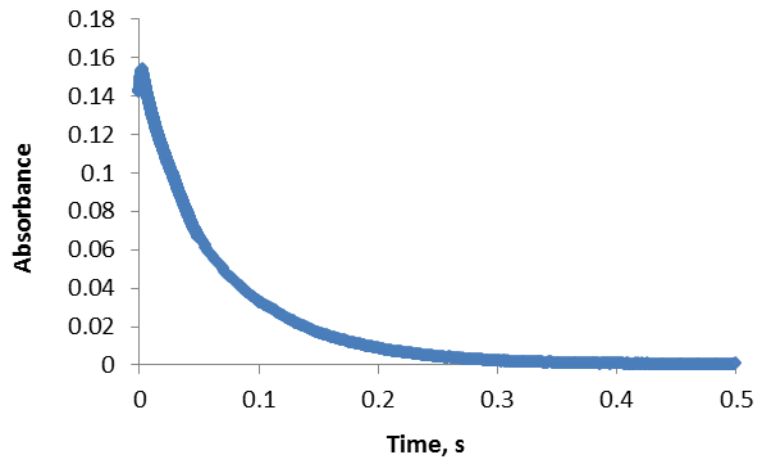
Figure 10.100 Sample decay of 5mM {Sm[N(SiMe$_3$)$_2$]$_2$(THF)$_2$}, 50mM 1-Bromododecane in hexanes at 15 °C, 470nm in hexanes.
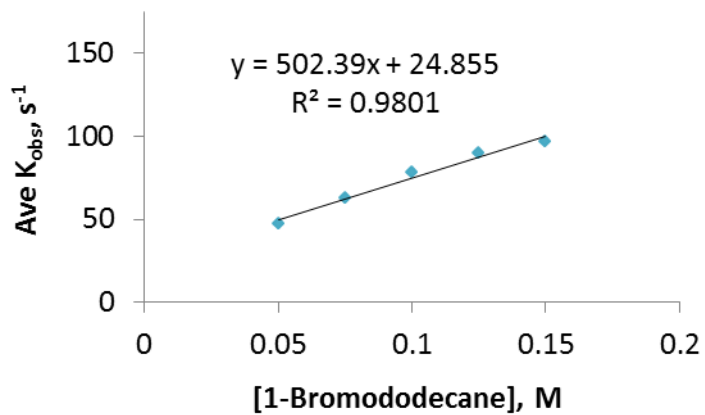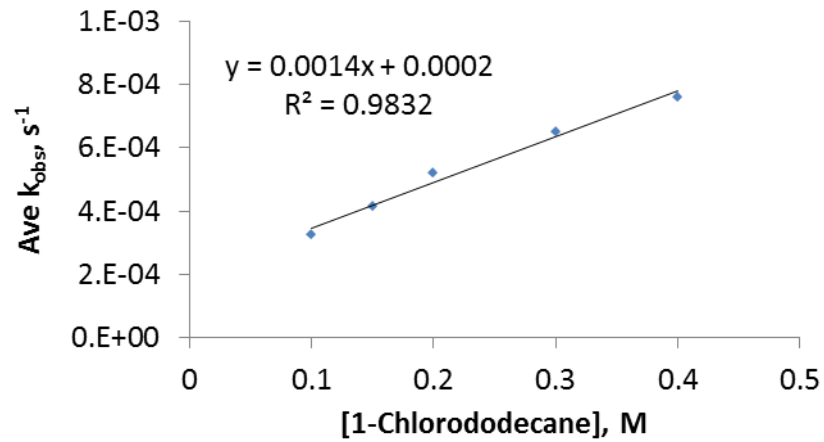

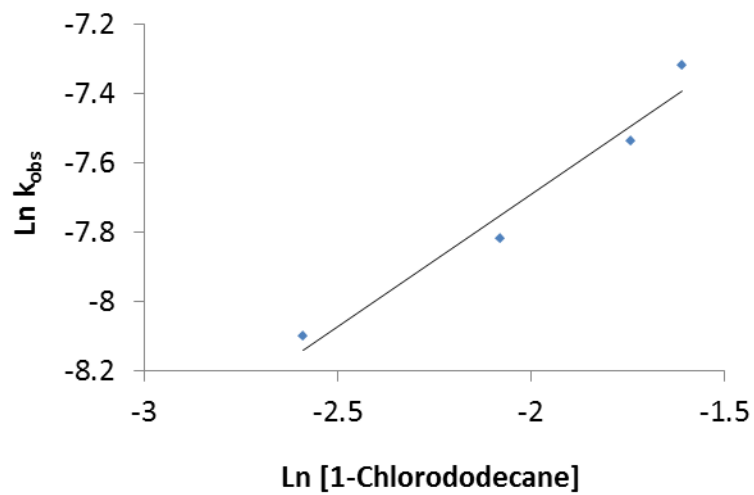**Figure 10.101** Sample rate dependence on 1-Bromododecane in hexanes at 15 °C, 470nm in hexanes.
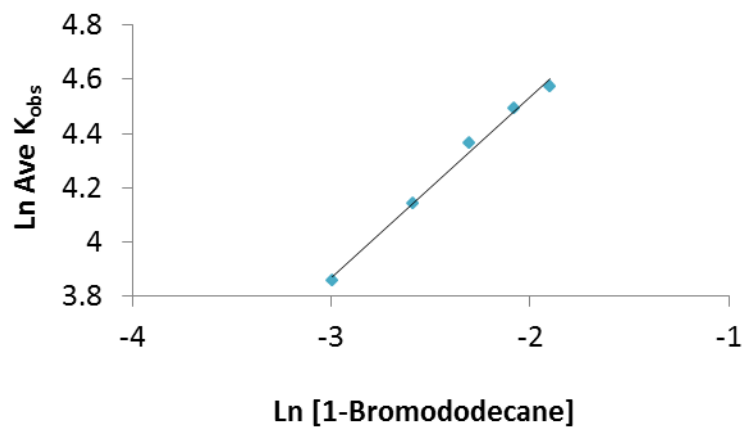
Figure 10.102 Sample rate order of 1-Bromododecane in hexanes at 15 °C, 470nm in hexanes.
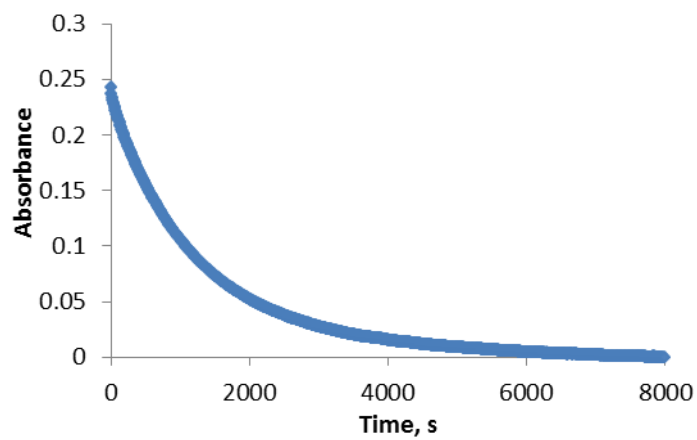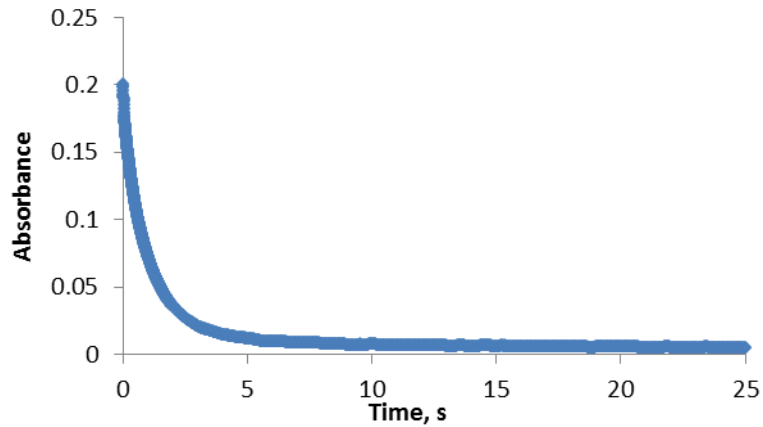

Figure 10.103 Sample decay of 5mM {Sm[N(SiMe$_3$)$_2$]$_2$(THF)$_2$}, 300mM chlorododecane in THF at 15 °C, 400nm.

328

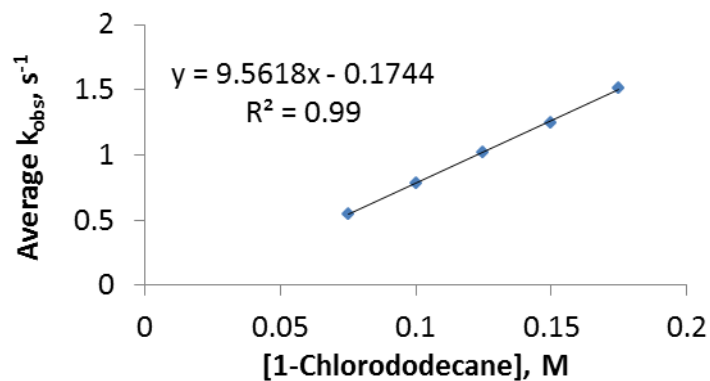**Figure 10.104** Sample plot of rate dependence on 1-chlorododecane in THF at 15 °C, 400nm.

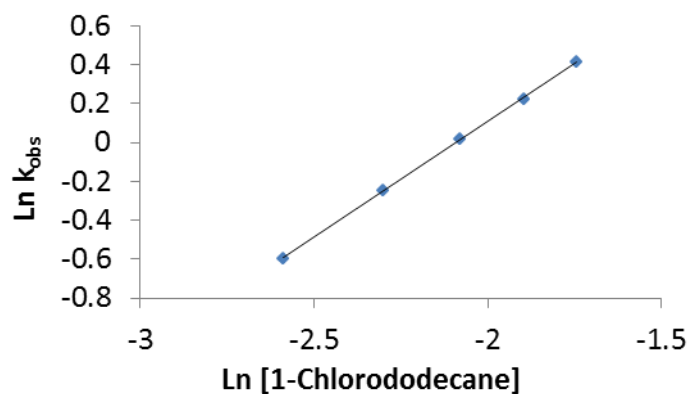**Figure 10.105** Sample plot of rate order of 1-chlorododecane in THF at 15 °C, 400nm.

Figure 10.106 Sample decay of 5mM {Sm[N(SiMe$_3$)$_2$]$_2$(THF)$_2$}, 100mM 1-Chlorododecane in hexanes at 15 C, 470nm.

Rates in hexanes:
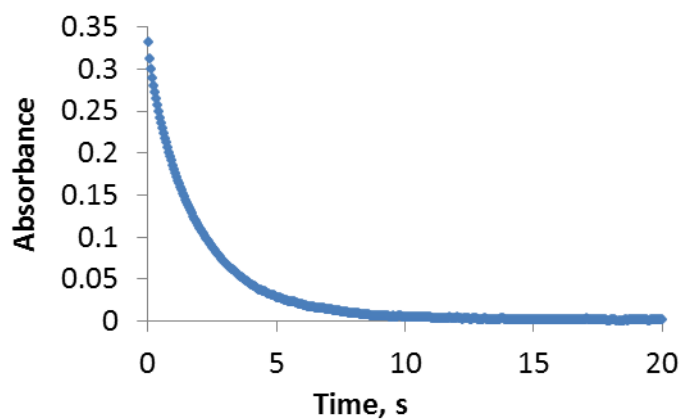

$y = 9.5618x - 0.1744$
$R^2 = 0.99$

Figure 10.107 Sample rate dependence on 1-Chlorododecane in hexanes at 15 C, 470nm.
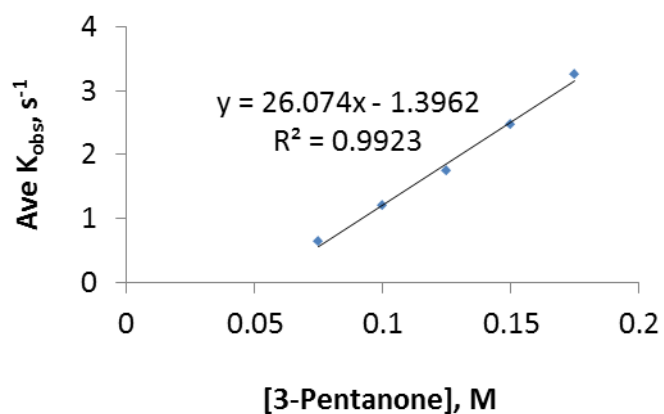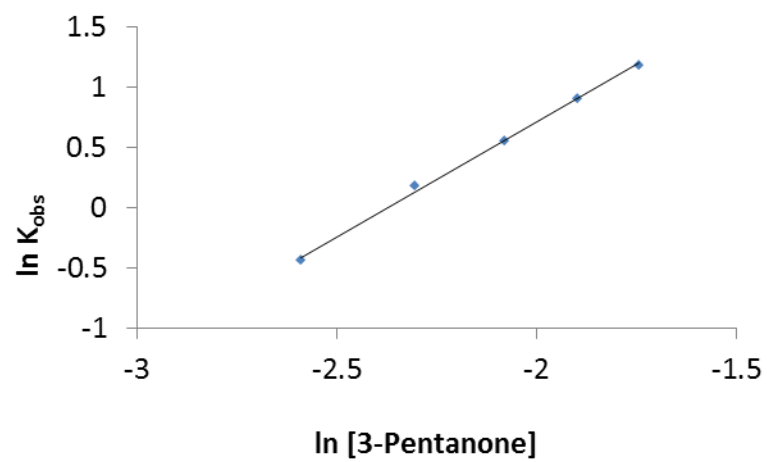
Figure 10.108 Sample rate order of 1-Chlorododecane in hexanes at 15 C, 470nm.

Figure 10.109 Sample decay 5mM {Sm[N(SiMe$_3$)$_2$]$_2$(THF)$_2$}, 75mM 3-Pentanone in THF at 5 °C, 400nm.

Figure 10.109 Sample rate dependence on 3-Pentanone in THF at 5 °C, 400nm.

Figure 10.109 Sample rate order of 3-Pentanone in THF at 5 °C, 400nm.
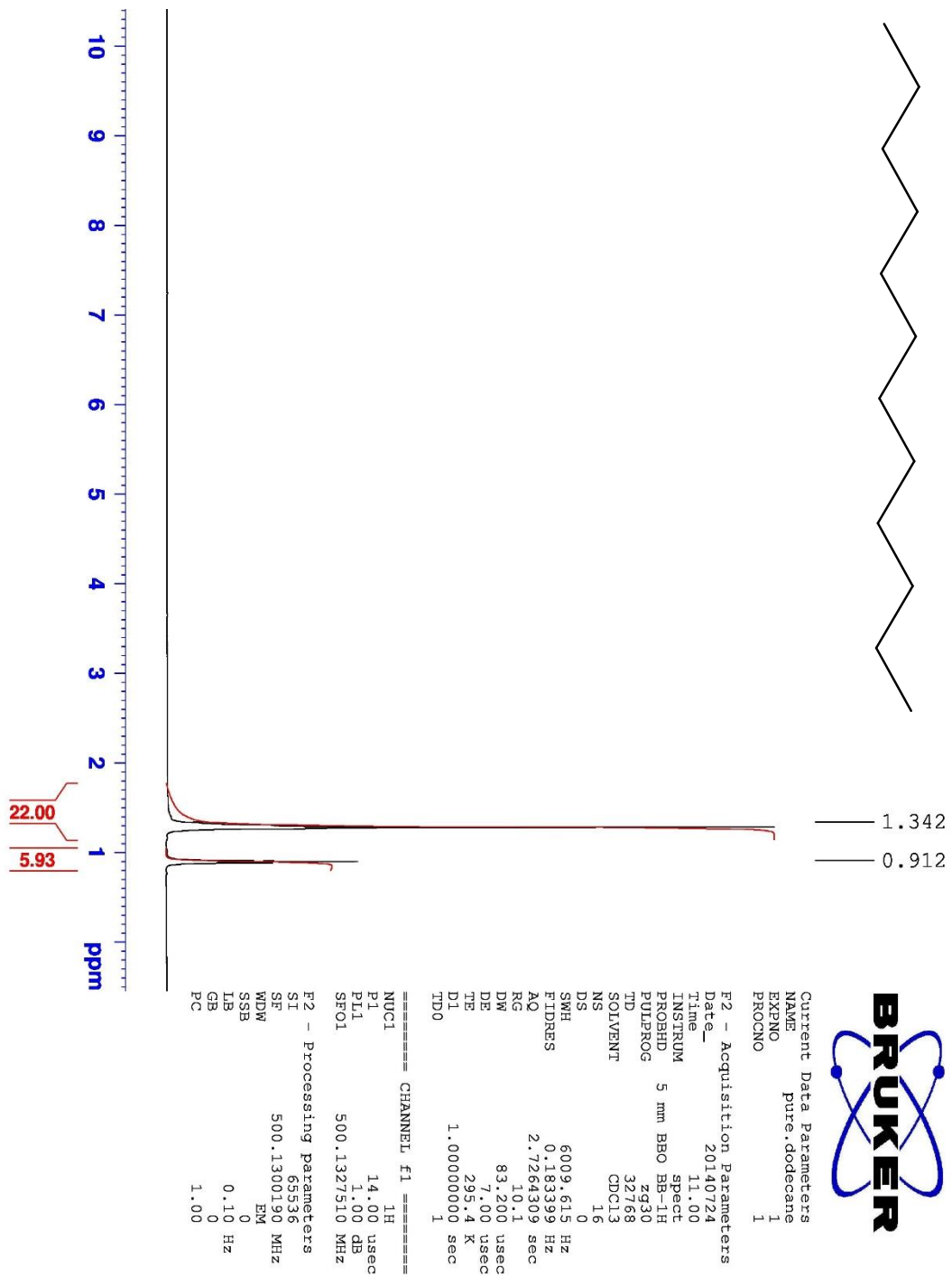
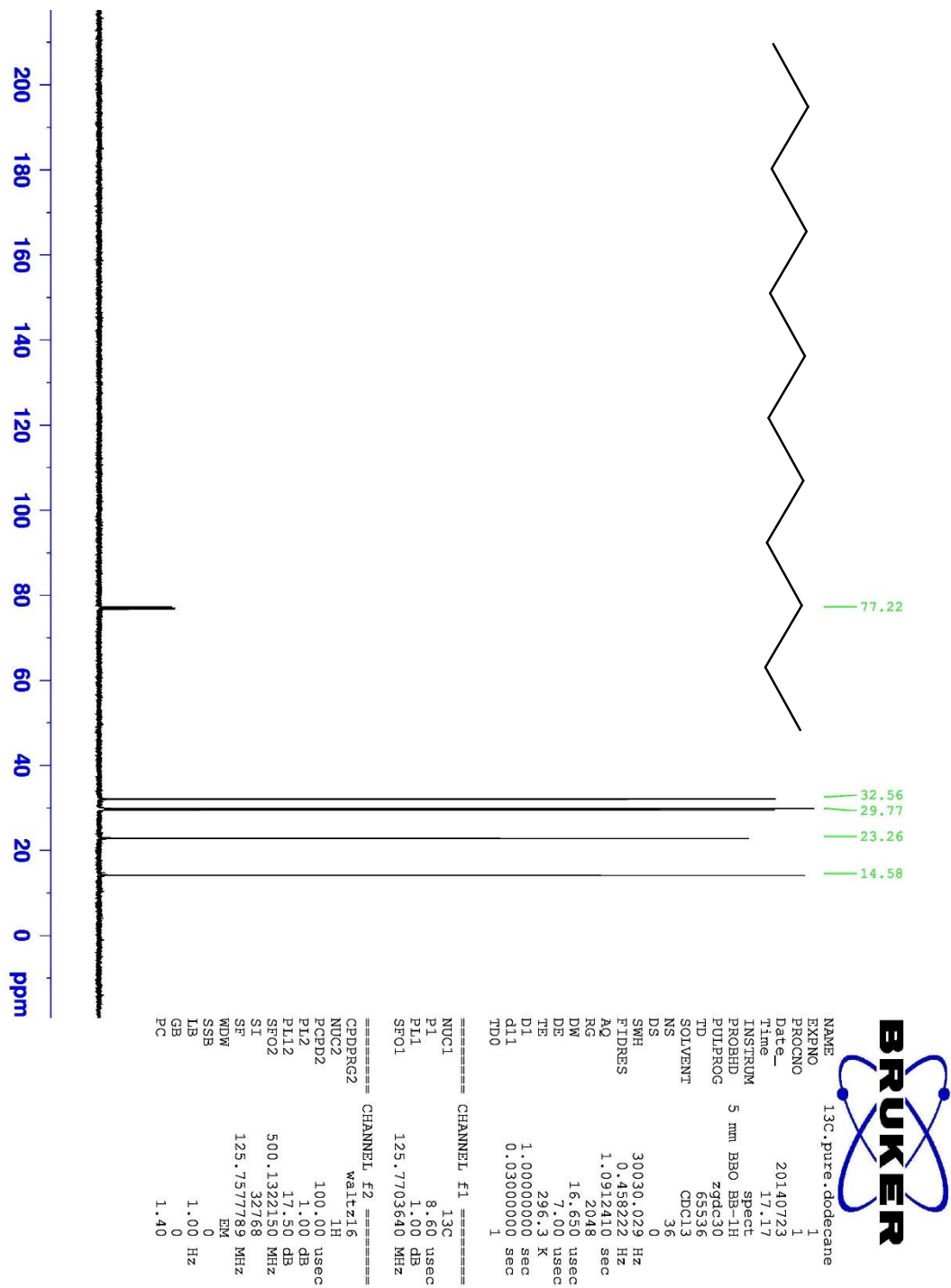**Figure 10.110** ^{1}H NMR Spectrum of *n*-dodecane.

Figure 10.111 ^{13}C NMR Spectrum of *n*-dodecane.
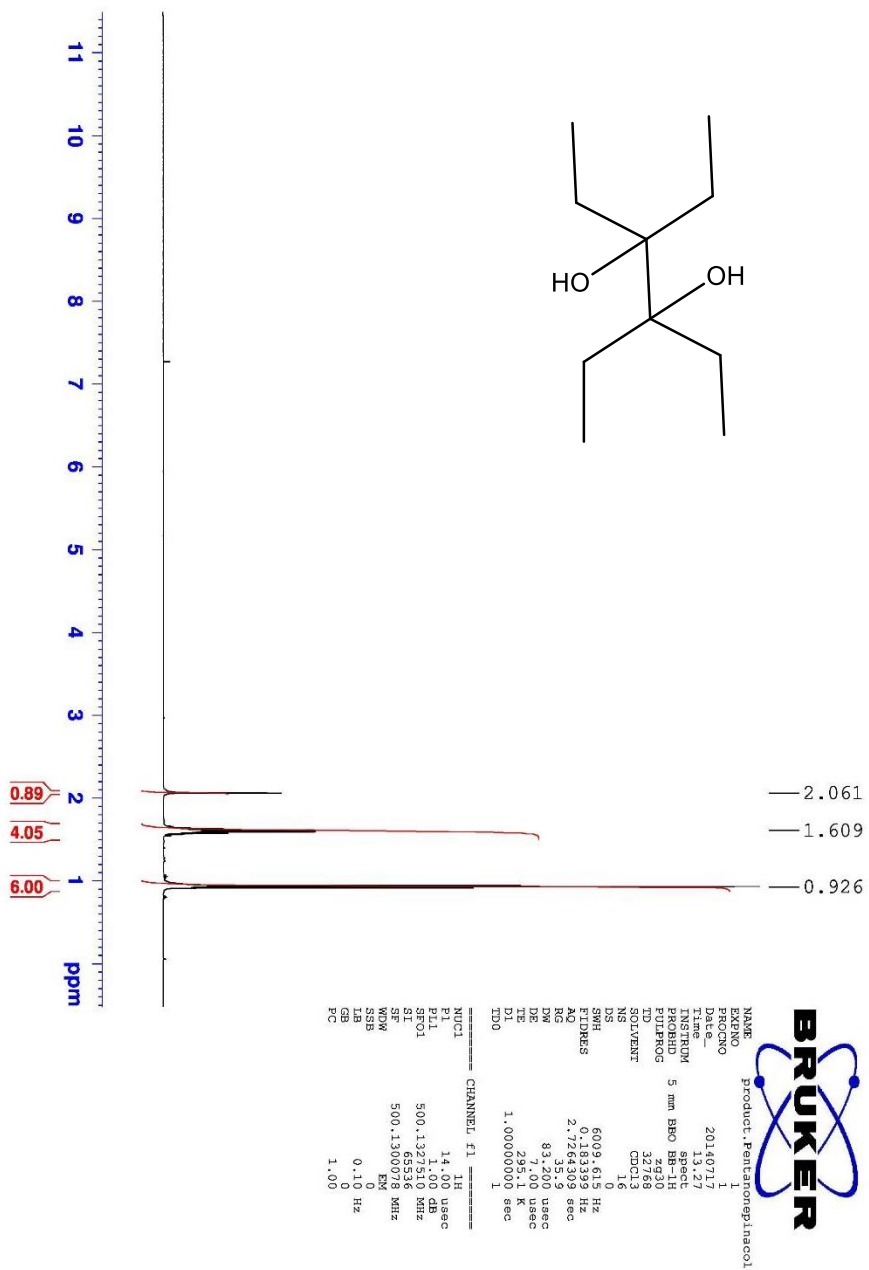
Figure 10.112 ^{1}H NMR Spectrum of 3,4-Diethyl-3,4-hexanediol.

Figure 10.113 ^{13}C NMR Spectrum of 3,4-Diethyl-3,4-hexanediol.

File   : C:\HPCHEM\1\DATA\TVC212\073014-1.D
Operator   : tvc212
Acquired   : 30 Jul 2014 13:52   using AcqMethod SADA4
Instrument :   GC/MS Ins
Sample Name: product.dodecane
Misc Info   :
Vial Number: 1

Figure 10.114 GC-MS of *n*-dodecane.

Figure 10.115 GC-MS 3,4-Diethyl-3,4-Hexanediol.

338

Tesia V. Chciuk

Education
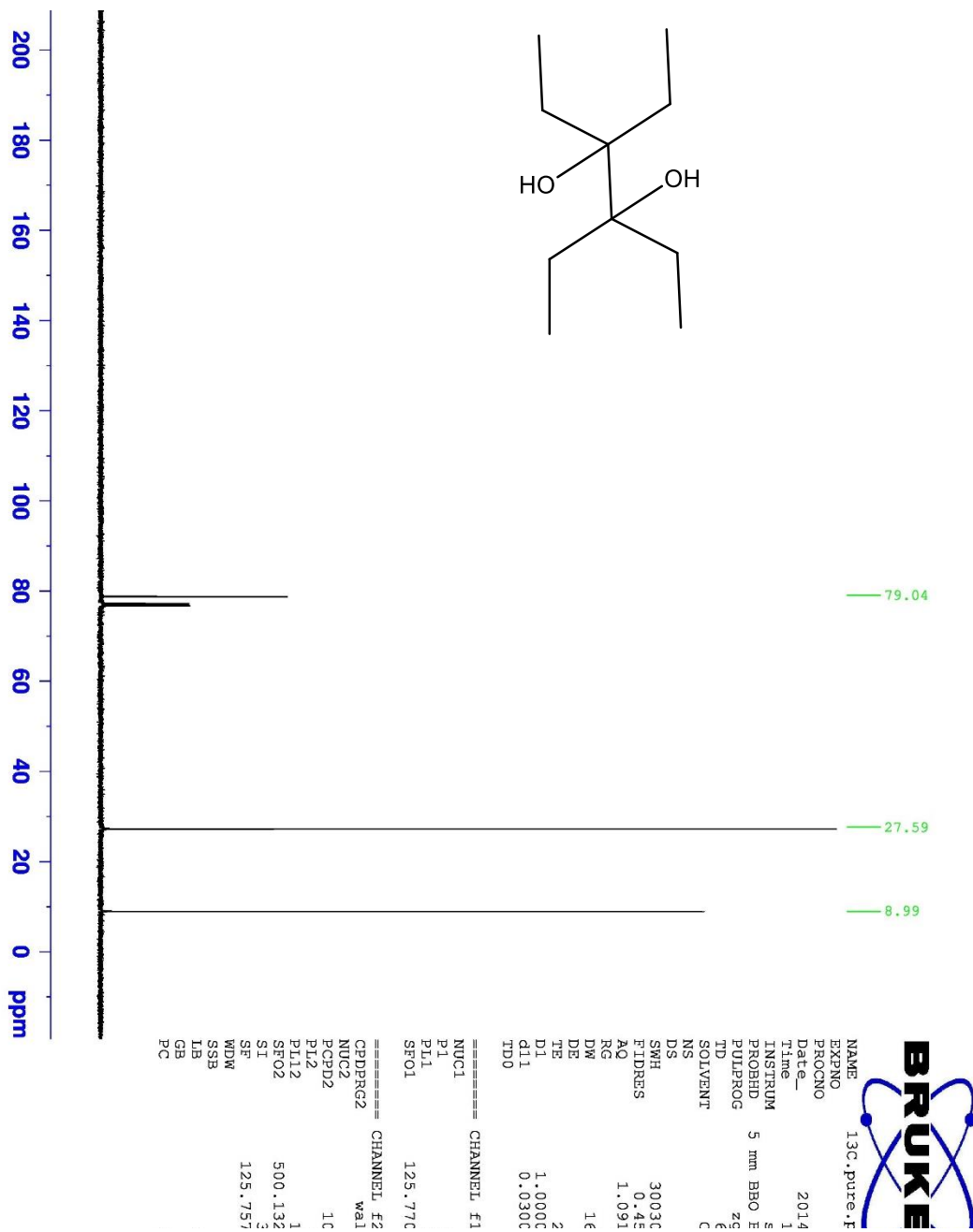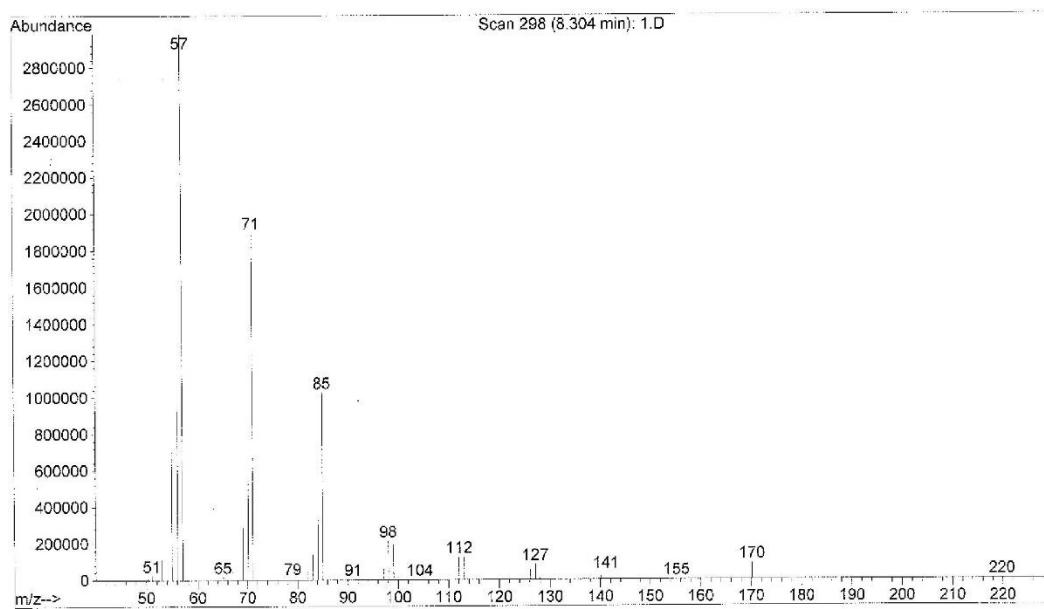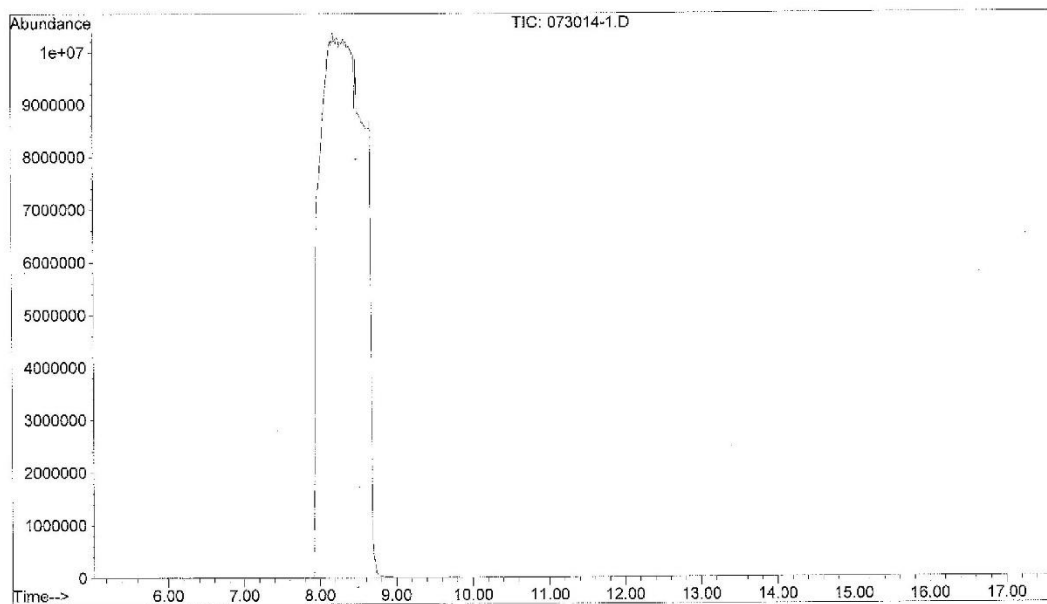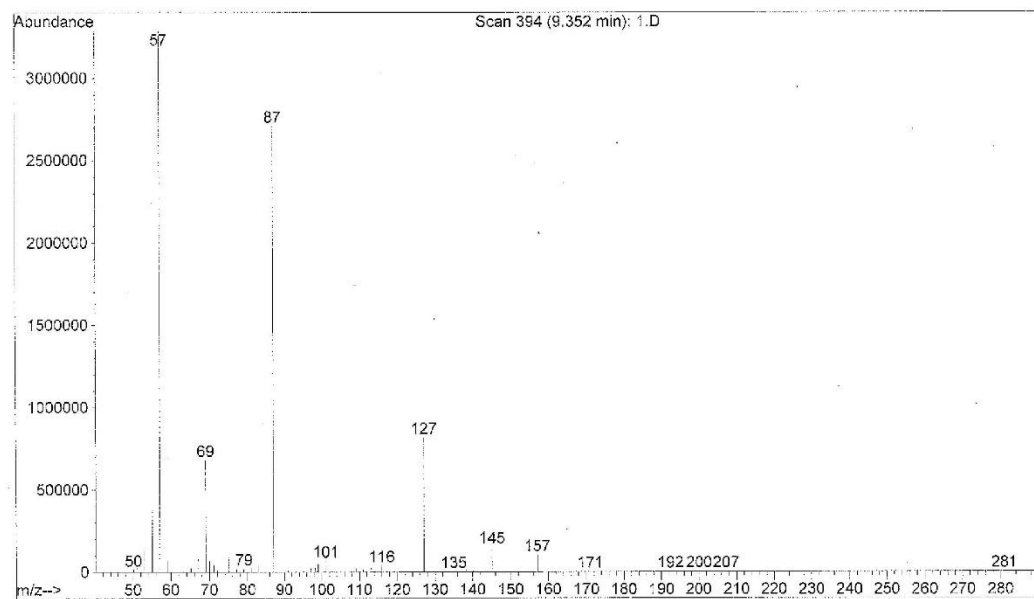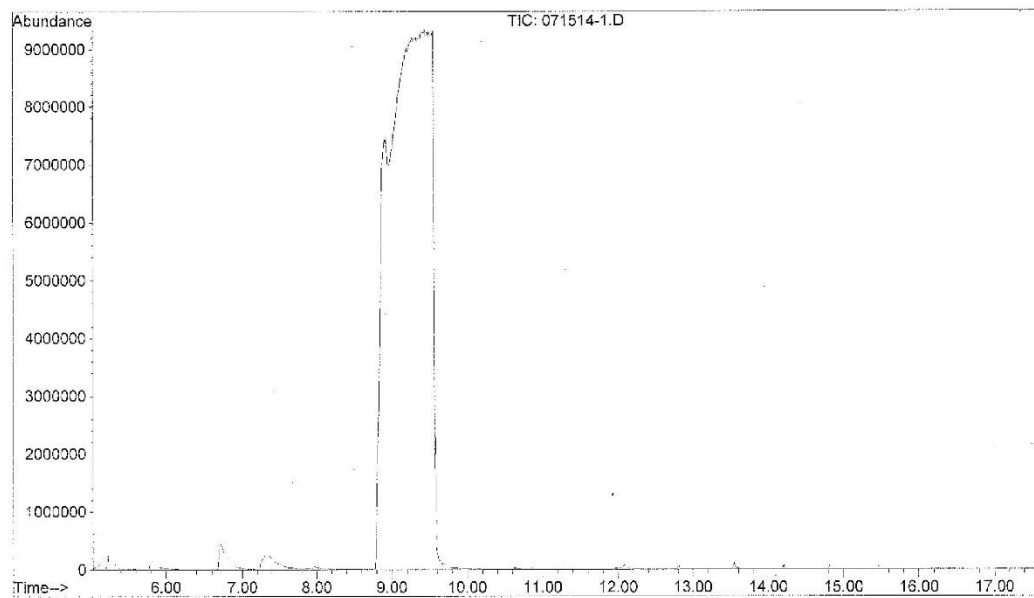
Ph.D., Chemistry (antic. 2017)	Lehigh University	2012-present
M.S., Chemistry	Lehigh University	2012 – 2014
B.S., Chemistry	Cedar Crest College	2005 – 2009

Research Experience

<u>Graduate Research Assistant, Lehigh University</u>

Advisor: Professor Robert A. Flowers, II   2012 – present
Research Focus: *Impact of Solvent and Additive Effects in Sm(II) Chemistry*
- Performed kinetic analyses on Sm(II) reduction systems to elucidate mechanism
- Characterized the impact of solvent choice on reductions with $\{Sm[N(SiMe_3)_2]_2(THF)_2\}$
- Examined the mechanism of proton-coupled electron-transfer in reductions using SmI_2
- Mentored five undergraduate students on research leading to publication
- Instrumentation: GC, GC-MS, NMR (^1H, ^{13}C), Glovebox, Stopped-Flow Spectrophotometry

<u>Undergraduate Researcher, Cedar Crest College</u>   2007-2009

Advisor: Professor John Griswold
Research Focus: *Synthesis and Spectral Properties of* p-*Subst. Benzhydrols via Grignard Rxns*

Awards and Distinctions:

C. Scott Althouse Memorial Fellowship 2016-2017

Industrial Experience

Bethlehem Apparatus Co., Inc.
  Scientific Research Director   January 2012 – September 2012
-Setup a new laboratory facility, ordered equipment, budgeted and implemented early testing protocols for mercury analysis according to EPA methods using GD-MS, ICP-MS, AA.

-Aided in the development of a method to stabilize/retire elemental Hg in a safe and environmentally-friendly fashion

Eos Energy Storage LLC.
  Associate Scientist   August 2009 – January 2012

-Responsible for synthesis of battery components and all phases of electrode, electrolyte, and full cell stability and performance analysis in zinc-air batteries for grid-storage applications.

Publications

Chciuk, T. V.; Li, A. M.; Vazquez-Lopez, A.; Anderson, W. R.; Flowers, R. A. Secondary Amides as Hydrogen Atom Transfer Promoters for Reactions of Samarium Diiodide. *Org. Lett.* **2017**, *19*, 290–293.

Chciuk, T. V.; Anderson, W. R.; Flowers, R. A. Proton Coupled Electron Transfer in the Reduction of Carbonyls by Samarium Diiodide-Water Complexes. *J. Am. Chem. Soc.* **2016**, *138*.

Chciuk, T. V.; Anderson, W. R.; Flowers, R. A. High-Affinity Proton Donors Promote Proton-Coupled Electron Transfer by Samarium Diiodide. *Angew. Chemie - Int. Ed.* **2016**, *55*: 6033-6036.

Chciuk, T. V.; Flowers, II, R. A. Proton-Coupled Electron Transfer in the Reduction of Arenes by SmI_2-Water Complexes. *J. Am. Chem. Soc.* **2015,** *137*: 11526-11531.

Chciuk, T. V.; Boland, B. P.; Flowers, II, R. A. Mechanistic Study of the Samarium Diiodide-N,N-dimethyl-2-aminoethanol Reducing System. *Tetrahedron Lett.* **2015,** *65*: 3212-3215.

Chciuk, T. V.; Hilmersson, G.; Flowers, II, R. A. Solvent-dependent Substrate Reduction by $\{Sm[N(SiMe_3)_2]_2(THF)_2\}$. An Alternative Approach for Accelerating the Rate of Substrate Reduction by Sm(II). *J. Org. Chem.* **2014**, *79*: 9441-9443.

"The Role of Solvents and Additives in Reactions of Samarium Diiodide and Related Reductants" **Chciuk, T.V.**; Flowers, R.A., II. In *Science of Synthesis*; Marek, I., Ed.; Georg Thieme Verlag KG: Stuttgart, 2016; pp. 177–261.

"Use in Organic Synthesis and Catalysis" **Chciuk, T.V.**; Flowers, R.A., II in The Lanthanides and Actinides: Synthesis, Reactivity, Properties and Applications; Natrajan, L. Ed.; Imperial College Press: London, *submitted*.

Publications in Preparation

Chciuk, T. V.; Anderson, W. R.; Flowers, R. A. The Reversibility of Ketone Reduction by SmI_2-H_2O. *Manuscript under review in Angew. Chemie - Int. Ed.*

Chciuk, T. V.; Anderson, W. R.; Flowers, R. A. Coordination is Key: On the Interplay between Substrate and Proton Donor Coordination in Reductions Utilizing Samarium Diiodide. *Manuscript in preparation* for submission to *J. Am. Chem. Soc.*

Patents and Patent Applications

Amendola, S.; Binder, M.; Black, P.; Sharp-Goldman, S.; Johnson, L.; Kunz, M.; Oster, M.; **Chciuk, T.;** Johnson, R. (Eos Energy Storage, LLC). Bifunctional (rechargeable) air electrodes comprising a corrosion-resistant outer layer and conductive inner layer. US Patent No. 8,802,304, August 12, 2014.

Amendola, S.; Binder, M.; Black, P.; Sharp-Goldman, S.; Johnson, L.; Kunz, M.; Oster, M.; **Chciuk, T.;** Johnson, R. (Eos Energy Storage, LLC). Electrically Rechargeable, Metal Anode Cell and Battery Systems and Methods. US Patent App. No. 2015001083, January 8, 2015.

Amendola, S.; Binder, M.; Black, P.; Sharp-Goldman, S.; Johnson, L.; Kunz, M.; Oster, M.; **Chciuk, T.**; Johnson, R. (Eos Energy Storage, LLC). Bifunctional (Rechargeable) Air Electrodes. US Patent App. No. 20130209919, August 15, 2013.

Amendola, S.; Binder, M.; Black, P.; Sharp-Goldman, S.; Johnson, L.; Kunz, M.; Oster, M.; **Chciuk, T.**; Johnson, R. (Eos Energy Storage, LLC). Electrically Rechargeable, Metal-Air Battery Systems and Methods. US Patent App. No. 20130115531, May 9, 2013.

Amendola, S.; Binder, M.; Black, P.; Sharp-Goldman, S.; Johnson, L.; Kunz, M.; Oster, M.; **Chciuk, T.**; Johnson, R. (Eos Energy Storage, LLC). Bifunctional (Rechargeable) Air Electrodes. US Patent App. No. 20120040254, February 16, 2012.

Amendola, S.; Binder, M.; Black, P.; Sharp-Goldman, S.; Johnson, L.; Kunz, M.; Oster, M.; **Chciuk, T.**; Johnson, R. (Eos Energy Storage, LLC). Electrically Rechargeable, Metal-Air Battery Systems and Methods. US Patent App. No. 20120021303, January 26, 2012.

Teaching Experience

CHE 111 Organic Chemistry I Lab Graduate Teaching Assistant   Fall 2012 & Fall 2013

CHE 31 Chemical Equilibrium in Aqueous Systems Lab Graduate Teaching Assistant   Spring 2013

Undergraduate Teaching Assistant (7 different undergraduate-level lab courses) 2006-2009

Departmental Tutor for high school and undergraduate level chemistry courses at both Cedar Crest College and Lehigh University (>15 students)

Conference Presentations

American Chemical Society 249th National Meeting, Denver, CO   March 2015
Elucidating the role of SmI$_2$-water and Glycol in Reductions: Mechanistic Studies of Anthracene Reduction

American Chemical Society 252nd National Meeting, Philadelphia, PA   August 2016

The Role of Coordination in Proton-Coupled Electron-Transfer Reactions Utilizing Samarium Diiodide

Poster Presentations

Division of Organic Chemistry Graduate Research Symposium, Bryn Mawr, PA   July 2016
Proton Coupled Electron Transfer in the Reduction of Carbonyls by Samarium Diiodide-Water Complexes.

Founders Day Research Poster Session, Lehigh University, PA   March 2016
Proton Coupled Electron Transfer in the Reduction of Arenes by Samarium Diiodide-Water Complexes.

Professional Affiliations

-Member of the American Chemical Society (ACS) since 2011.

-Member of the *Association for Women in Science* (*AWIS) since 2015.*